R-12-04

Summary of discrete fracture network modelling as applied to hydrogeology of the Forsmark and Laxemar sites

Lee Hartley, David Roberts
AMEC

April 2013

Svensk Kärnbränslehantering AB
Swedish Nuclear Fuel
and Waste Management Co

Box 250, SE-101 24 Stockholm
Phone +46 8 459 84 00

ISSN 1402-3091
SKB R-12-04
ID 1332762

Summary of discrete fracture network modelling as applied to hydrogeology of the Forsmark and Laxemar sites

Lee Hartley, David Roberts
AMEC

April 2013

Keywords: Hydrogeology, Discrete Fracture Network, Groundwater, Modelling, Transport, Forsmark, Laxemar.

Abstract

The Swedish Nuclear Fuel and Waste Management Company (SKB) is responsible for the development of a deep geological repository for spent nuclear fuel. The permitting of such a repository is informed by assessment studies to estimate the risks of the disposal method. One of the potential risks involves the transport of radionuclides in groundwater from defective canisters in the repository to the accessible environment.

The Swedish programme for geological disposal of spent nuclear fuel has involved undertaking detailed surface-based site characterisation studies at two different sites, Forsmark and Laxemar-Simpevarp. A key component of the hydrogeological modelling of these two sites has been the development of Discrete Fracture Network (DFN) concepts of groundwater flow through the fractures in the crystalline rocks present. A discrete fracture network model represents some of the characteristics of fractures explicitly, such as their, orientation, intensity, size, spatial distribution, shape and transmissivity.

This report summarises how the discrete fracture network methodology has been applied to model groundwater flow and transport at Forsmark and Laxemar. The account has involved summarising reports previously published by SKB between 2001 and 2011. The report describes the conceptual framework and assumptions used in interpreting site data, and in particular how data has been used to calibrate the various parameters that define the discrete fracture network representation of bedrock hydrogeology against borehole geologic and hydraulic data. Steps taken to confirm whether the developed discrete fracture network models provide a description of regional-scale groundwater flow and solute transport consistent with wider hydraulic tests hydrochemical data from Forsmark and Laxemar are discussed. It illustrates the use of derived hydrogeological DFN models in the simulations of the temperate period hydrogeology that provided input to radionuclide transport calculations in the SR-Site safety assessment. Finally, we discuss remaining uncertainties and how these might be addressed by further modelling and the use of additional types of data obtainable from underground investigations.

Contents

1 Introduction

1.1 Context

The Swedish Nuclear Fuel and Waste Management Company, SKB, is responsible for disposing of spent nuclear fuel in a deep geological repository. The permitting of such a repository is informed by assessment studies to estimate the risks of the disposal method to the most affected individuals in any future society. One of the potential risks involves the transport of radionuclides that might be released should any of the disposed canisters be defective to the accessible environment. The transport of radionuclides is governed by groundwater flow and processes such as advection, dispersion, diffusion, and sorption.

SKB has undertaken detailed site characterisation studies in order to assess the potential suitability of two sites, located at Forsmark and Laxemar, for hosting a repository at approximately 500 m depth. The characterisation studies culminated in the production of "Site Descriptive Models" for each site, called SDM-Site Forsmark and SDM-Site Laxemar respectively, which integrate models for geology, thermal properties, rock mechanics, hydrogeology, hydrogeochemistry, bedrock transport properties and a description of the surface system (SKB 2008, 2009). In June 2009 the decision was taken to prepare a licence application for a repository for spent nuclear fuel sited at Forsmark. The Site Descriptive Model for Forsmark served as one of several pieces of information for safety assessment calculations for the potential repository that were conducted as part of the SR-Site project. The application was submitted to the authorities in March 2011 (SKB 2011).

The relevance of hydrogeology to the SR-Site safety assessment calculations and the methodology used in groundwater flow modelling is summarised in Selroos and Follin (2010). Safety assessment calculations were performed for the Forsmark site based on groundwater calculations that considered flow and transport under three different types of hydrological conditions: facility operation period (Svensson and Follin 2010), post-closure temperate climate conditions (Joyce et al. 2010a), and periglacial and glacial climate conditions (Vidstrand et al. 2010a). Safety assessment calculations were not performed for the Laxemar site. However, comparative groundwater flow calculations were made for the same three different types of hydrological conditions: facility operation period (Svensson and Rhén 2010), post-closure temperate climate conditions (Joyce et al. 2010b), and periglacial and glacial climate conditions (Vidstrand et al. 2010b).

A key component of the hydrogeological modelling for all the studies mentioned above has been the development of Discrete Fracture Network (DFN) concepts of groundwater flow through the fractures in the crystalline rocks present at Forsmark and Laxemar. The DFN approach (e.g. Dershowitz 1979, Long et al. 1982, Robinson 1984, Cacas 1989) is one which attempts to explicitly represent the groundwater flows through fractures and considers many of the important observed characteristics of crystalline rock, such as the geometry of fracture patterns, variable connectivity, anisotropy, compartmentalisation and heterogeneity. It is well suited to making direct use and interpretation of the data acquired in the site investigation, and is able to provide statistics of flow and transport around the repository volumes by means of stochastic simulation. For these reasons, the DFN approach underpins all of the hydrogeological modelling performed in support of the site investigation (SDM-Site) and safety assessment (SR-Site) projects.

This report summarises the DFN methodology developed to model groundwater flow and transport at Forsmark and Laxemar. The report summarises how the hydrogeological DFN models were calibrated by simulating single-hole hydraulic tests, cross-hole hydraulic tests and the palaeo-climatic evolution of the chemical composition of groundwater. It also describes how DFN models were used to the safety assessment calculations. This account has involved summarising reports previously published by SKB between 2001 and 2011.

This report also discusses some remaining uncertainties in the groundwater flow modelling and considers how these uncertainties might be addressed by further modelling and the use of additional types of data obtainable from underground investigations. In order to provide a self-contained account of the DFN modelling, some other aspects of the site descriptive modelling, particularly those relating to hydrogeology, geology and transport properties, are summarised in this report. The key references, all published by SKB, on which this synthesis is based are listed in Table 1-1.

Table 1-1. Key references used as the basis for the summary presented in this report.

Discipline	Generic	Forsmark	Laxemar
Summary	(Andersson et al. 1998) Data acquisition. TR-98-02. (Andersson 2003) SDM strategy. R-03-05	(SKB 2008). SDM-Site. TR-08-05.	(SKB 2009). SDM-Site. TR-09-01.
Geology	(Munier et al. 2003) SDM strategy, R-03-07 (Munier 2004) DFN methodology. R-04-66. (Darcel et al. 2009) DFN methodology. R-09-38.	(Fox et al. 2007) Geological–DFN, Stage 2.2. R-07-46.	(La Pointe et al. 2008) Geological–DFN, SDM-Site Laxemar. R-08-55.
Hydrogeology	(Rhén et al. 2003) SDM strategy. R-03-08.	(Follin et al. 2007a) Hydrogeological characterisation, Stage 2.2. R-07-48. (Follin et al. 2007b) Hydrogeological modelling, Stage 2.2. R-07-49.	(Rhén et al. 2008) Hydrogeological characterisation. SDM-Site. R-08-78. (Rhén et al. 2009) Hydrogeological modelling. SDM-Site. R-08-78.
Transport properties	(Berglund and Selroos 2004) SDM strategy. R-03-09	(Crawford J 2008) Transport properties, SDM-Site. R-08-48.	(Crawford and Sidborn 2009) Transport properties, SDM-Site. R-08-94.
Safety assessment calculations	(Gylling et al. 2004) Test of methodology. R-04-45.	(Joyce et al. 2010a) Groundwater flow for temperate conditions, SR-Site. R-09-20.	(Joyce et al. 2010b) Groundwater flow for temperate conditions, SR-Site. R-09-24.

1.2 The discrete fracture network concept

Alternative groundwater flow and transport modelling approaches represent fractures, infer properties and treat scale dependencies in different ways. Three possible conceptual approaches that have been considered within SKB's site investigation programmes (Selroos et al. 2002) are the Continuous Porous Media (CPM), Discrete Fracture Network (DFN) and Channel Network (CN) methods:

- A CPM model of groundwater flow in a fractured rock assumes that, over some representative volume, the fractured rock can be represented as a homogeneous porous medium with groundwater flow governed by Darcy's law. Each element of the model is hydraulically connected to its neighbours, although they may have different hydraulic properties. A CPM model therefore represents the bulk properties of the rock over a specified scale.
- A DFN model of crystalline rock is based on the premise that groundwater flow and transport occur mainly within fractures. A DFN model represents this by assuming that Darcy flow is constrained within fractures, with no flow between fractures except where they intersect one another. Such models allow geometric concepts such as the size, shape and orientation of fractures to be represented explicitly. Hydraulic and transport properties are also described for each fracture (Dershowitz et al. 1998).
- A CN model considers Darcy flow through a network of intersecting one-dimensional channels (see for example Black et al. (2007) or Moreno and Neretnieks (1991)). CN models are often visualised on a regular grid using channels of discrete lengths, however it is possible to distort the network to account for a more realistic geometric understanding of the system. The channels in the CN approach are representative of the regions within fractures where flow-rates are highest. Field observations suggest that fracture surfaces are often uneven and mineralized, with the result that groundwater flow is distributed non-uniformly across the fracture in preferential paths, or channels.

The concepts can also be used in combination. For example, the DFN model can be used to interpret fracture properties, which can then be upscaled to provide element-based properties of an equivalent continuous porous medium (ECPM) representation of the bedrock (Long et al. 1982, Goblet et al. 1994, Renard and de Marsily 1997, La Pointe et al. 1995, Wei and Chakrabarty 1996, Jackson et al. 2000). By doing so, the ECPM approach honours the intrinsic heterogeneity and anisotropy of the underlying fracture network on the scale of resolution of the chosen computational grid, although it does not resolve flow within individual fractures.

The parameterisation of a DFN is essentially a recipe of probability distribution functions for generating stochastic realisations of the fracture network (Munier 2004) since the geometry and hydraulic properties of individual fractures can seldom be determined. Hence, a number of realisations of the fracture system needs to made and the variability between results predicted by individual realisations quantified.

Each of the above concepts has been used by SKB to model groundwater flow at the Äspö Hard Rock Laboratory, which is located near Laxemar (Selroos et al. 2002). The advantages of the DFN concept, compared to the CPM concept, for the purpose of modelling at Forsmark and Laxemar include the ability to:

- Represent flow experiments where the fracture connectivity is thought to be important.
- Predict the equivalent continuous (ECPM) properties of the fracture network system and the scale dependence of those effective properties.
- Predict the effect of the fracture network geometry on the variability in groundwater pathways (such as discharge points, travel times and flow-related transport resistance).
- Estimate groundwater flows at the scale of the deposition holes and deposition tunnels. Such information is necessary in order to predict the likelihood of a flow-carrying fracture intersecting a deposition canister, for example.

Reasons that CPM models might sometimes be chosen in preference to DFN models of flow in crystalline rocks include the relative complexity of the DFN models. Many data are required to characterise fracture systems adequately, and DFN models are typically more computationally intensive than equivalent CPM models. It is not currently practical to model some physical processes within the DFN framework, such as transient coupled flow and salt transport and rock-matrix diffusion, for regional-scale models. However, this issue can be partially addressed by using a DFN model to derive an ECPM model through the process of upscaling discussed in Section 5.

The potential advantages of CN models are that they offer an alternative conceptualisation of flow channelling phenomena within fractures. It is also possible to introduce flow channelling within fractures in the DFN framework, for example by varying the transmissivity within a fracture. This issue is discussed in Section 3.

1.3 The systems approach to hydrogeological site descriptive models

In the conceptual model used for the bedrock hydrogeological modelling of Forsmark (Follin 2008) and Laxemar (Rhén and Hartley 2009), the groundwater system is divided into three different hydraulic domains, as shown in Figure 1-1. These are defined as:

- The Hydraulic Soil Domain (HSD). This domain comprises the regolith (unconsolidated sediments).
- Hydraulic Conductor Domain (HCD). This domain comprises the deformation zones as determined by geological analysis.
- The Hydraulic Rock mass Domain (HRD). This domain comprises the less fractured bedrock outside of the deformation zones and may include so called Minor Deformation Zones (MDZ), i.e. discrete features of significant size yet stochastic in nature. The basis for the HRD delineation is also determined by geological analysis.

The bedrock at each site has been divided into different domains (volumes) according to geological, fracture statistical and hydrogeological characteristics. The division of the bedrock according to hydrogeological characteristics is described in Section 3.3.

In the DFN concept, individual fractures are modelled either deterministically, if their geometric and hydraulic properties are reasonably well constrained by site data, or stochastically for fractures not detected by geophysical techniques or during drilling. Some fractures may be partly determined, e.g. their geometry, but hydraulic properties assigned stochastically where data is lacking or localised. Fracture network models are often at least partly stochastic since it is not possible to determine

the location and extent of each feature in the rock volume of interest. For the stochastic approach, statistical descriptions of specific characteristics of the fracture system are required, and realisations of a DFN model that exhibit the same statistics as the physical system are used for simulation. Realisation dependent uncertainty corresponds to a lack of knowledge of the precise fracture location and geometry.

The DFN modelling approach that was adopted combines a deterministic representation of the geometrical properties of the HCD with a stochastic representation of the HRD. The flow and transport properties of the HSD were studied using a CPM approach in the context of the near surface hydrology (Bosson et al. 2008, 2009). The repository was designed to avoid placing canisters containing spent nuclear fuel within a certain distance of deformation zones (the HCD). This report focuses on the properties of the HRD, where any waste canisters would be deposited.

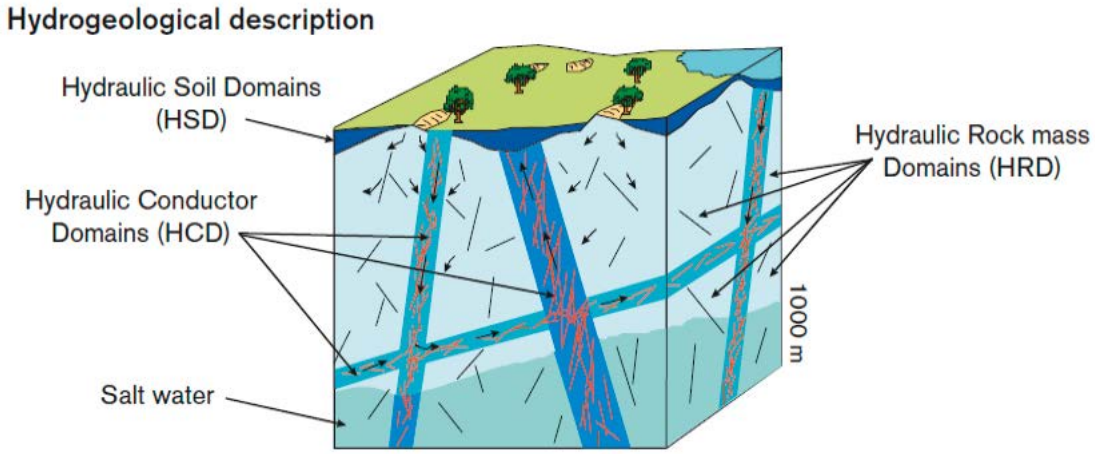

Figure 1-1. *Illustration showing the division of the crystalline bedrock and the regolith into three hydraulic domains, HCD, HRD and HSD (reproduced from Rhén et al. 2003).*

2 Available site data

2.1 Data requirements

A large investment in data collection (site, field, airborne, in situ experiments, and laboratory analysis) is necessary to acquire sufficient information to develop, parameterise, and perform confirmatory testing of the hydrogeological site description, and in particular the characterisation of the bedrock components (HCD and HRD) in terms of Hydrogeological DFN (Hydro-DFN) models. In particular site-specific data at Forsmark and Laxemar have been used to:

- **Justify or motivate the conceptual model.** Examples of this include the choice of model to describe the intensity-size distribution of fractures and the treatment of flow channelling.
- **Directly parameterise parts of the model.** Data such as the intensity of fracturing were used directly as input parameters in Hydro-DFN modelling.
- **Provide calibration targets.** Some parameters used in the Hydro-DFN models, such as parameters relating to the transmissivity and size distributions of fractures, could not be measured directly through experiments. The values of such parameters were found by calibration, i.e. comparing the results of models using different assumptions with the measured values of related quantities, and adjusting the parameters as necessary to improve the consistency between observations and numerical simulation.
- **Provide confirmatory testing of the Hydro-DFN.** The development of the Hydro-DFN models was achieved primarily with data obtained from single-borehole hydraulic tests. In order to determine if the models could be reliably applied to larger scale problems, a series of confirmatory tests were developed which compared the results of large scale hydraulic tests and other measurements with predictions which relied on the Hydro-DFN models.

This chapter provides an overview of the types of data used in the Hydro-DFN models developed for the Forsmark and Laxemar sites. The uses made of each of these data are discussed later in this section.

2.2 Site locations

Forsmark and Laxemar are both on the south-eastern Swedish coast on the Baltic Sea, as shown in Figure 2-1. The Forsmark site is located in the northern part of the province of Uppland within the municipality of Östhammar, about 120 km north of Stockholm. The investigated candidate area is located along the shoreline of Öregrundsgrepen. The candidate area is approximately 6 km long and 2 km wide.

The Laxemar site is located in the province of Småland, approximately 320 km south of Stockholm, within the municipality of Oskarshamn and immediately west of the Oskarshamn nuclear power plant. The eastern-most part of the investigation area includes the Simpevarp peninsula which hosts the power plants and the Central interim storage facility for spent nuclear fuel (Clab). The island of Äspö, below which the Äspö Hard Rock Laboratory is located, is found three kilometres northeast of the central parts of Laxemar. The Laxemar site covers approximately 12.5 km^2 (excluding Simpevarp).

Both the Forsmark and Laxemar sites consist of crystalline bedrock that belongs to the Fennoscandian Shield. The bedrock was formed approximately $1.9–1.8 \cdot 10^9$ years ago during the Svecokarelian orogeny. Both sites have been affected by ductile and brittle deformation. Söderbäck (2008) provides a detailed description of the geological evolution of the Fennoscanian Shield in south-eastern Sweden up to the Quaternary period.

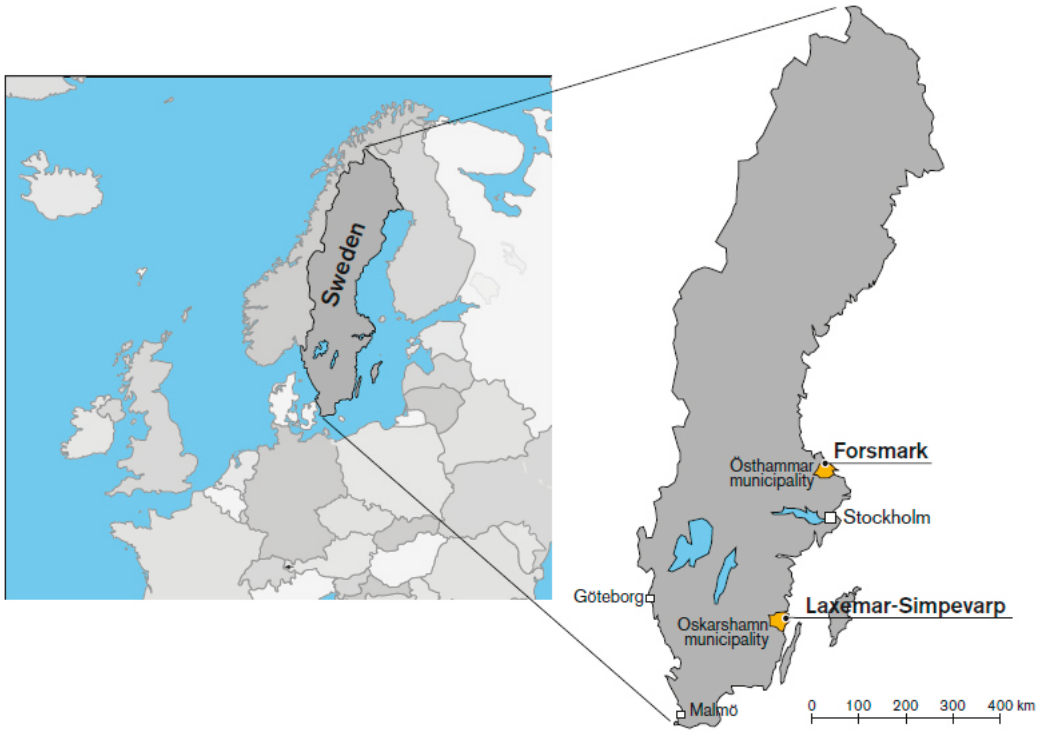

Figure 2-1. *The locations of the Forsmark and Laxemar sites.*

2.3 Geophysical data from surface investigations

Geophysical mapping was used to inform the structural models of deformation zones in the Forsmark and Laxemar sites. The geophysical data collected includes magnetic data, reflection seismic data and refraction seismic data. Magnetic data included both fixed-wing airborne geophysical data, which were collected predominantly by the Geological Survey of Sweden, and similar helicopter airborne data with higher resolution.

Approximately 40 km of high resolution surface reflection seismic data were generated along fifteen profile lines at Forsmark. Borehole seismic data were subsequently acquired and used to construct local-scale geological models in combination with borehole mapping data (Rhén et al. 2006). Reflection seismic data were acquired in 1999 (Bergman et al. 2001) and 2004 (Juhlin et al. 2004) in the Laxemar site. In 2004, approximately 9.9 km of high resolution seismic data were acquired along three separate profiles.

Refraction seismic data in the Forsmark site were acquired during older investigations (1970–1982) in connection with the construction of the nuclear power plant and SFR, and more recently (2004–2006) inside and adjacent to the targeted area during the site investigation programme.

2.4 Fracture data from boreholes

Three types of boreholes were drilled during the site investigations, comprising core-drilled boreholes, percussion-drilled boreholes and shallow boreholes through the regolith (also designated soil boreholes). The geological information provided by core drilling is superior in comparison with percussion drilling, which crushes the rock meaning that no cores can be recovered. Cored boreholes are slim, with diameter of approximately 76 mm. The borehole length and inclination vary; the most important boreholes to hydrogeological characterisation were drilled approximately one kilometre long.

Fracture intersections with a borehole are identified during borehole logging using the so-called Borehole Imaging Processing System (BIPS), a down-hole video camera system which, together

with inspection of the drill core or, for percussion boreholes, drill cuttings, is used to provide a so-called "Boremap" mapping of core- and percussion-drilled boreholes. The orientation of identified geological structures is calculated by processing of the images (SKB 2005a).

Each mapped fracture is first documented as "Broken" or "Unbroken" – depending on how it is found in the core. Each fracture is then classified as "Sealed", "Open" or "Partly open" and with a judgement of how certain the geologist is of this classification: "Certain", "Probable" or Possible". In more detail:

1. Each mapped fracture is first documented as "Broken" or "Unbroken", depending on how it is found in the core. If the fracture splits the core it is mapped as broken, otherwise unbroken.
2. If an aperture is seen in BIPS and the core is unbroken, the fracture is mapped as partly open. If an aperture is seen in BIPS and the core is broken the fracture is mapped as open. The aperture is mapped in BIPS and is intended to represent an approximate mean aperture (mean aperture as seen on the borehole wall, may not have much to do with hydraulic aperture). If no aperture is seen in BIPS and the core is unbroken, then it is mapped as sealed.
3. Sometimes when the core is broken no aperture is seen in BIPS. If the core pieces fit badly the aperture is set to 0.5 mm and the fracture is mapped as open and probable. If it is a good fit between the pieces and the surfaces are not fresh, the aperture is set to 0.5 mm and the fracture is mapped as open and possible. If there is a good fit between the pieces and the surfaces are fresh, the aperture is set to 0 mm and the fracture is mapped as sealed.

2.5 Outcrop data

Both the Forsmark and Laxemar sites have regions of outcropping bedrock in which fracture traces are apparent. At Forsmark natural outcrops have been augmented by the areas cleared for the drill sites. Measurements of fracture traces have the advantage over boremap data in that it is potentially possible to infer information about the size distribution of the fractures and their relative terminations, along with fracture intensity based on trace length per unit area, P_{21}, and orientations of steeply dipping fractures. However, it is not possible to classify outcropping fractures as "Sealed", "Open" or "Partly open". Various interpretations and corrections are necessary before deriving the fracture size distribution from the discrete outcrop fracture trace data. This involves accounting for the influence of fracture segmentation, the irregular topography of the outcrop surface and the finite size of the outcrop, as discussed in Darcel et al. (2009), Fox et al. (2007) and La Pointe et al. (2008).

Fractures can be grouped in sets according to their orientations. It is thought that the creation of fractures in orientation sets is related to the deformation history of the rock. One indicator of the deformation history is gained through fracture termination analysis. Fracture termination analysis describes how fractures belonging to one orientation set interact with fractures belonging to a different orientation set. Fracture terminations are described through the use of a matrix. The values in the matrix give the percentages of fractures in a given set which are judged to terminate against fractures from another set. The fracture termination percentages can be interpreted to suggest the order in which the fractures belonging to different orientation sets were created. Fracture termination relationships have been studied in outcrops at Forsmark and Laxemar in Fox et al. (2007) and La Pointe et al. (2008). More important evidence on the deformation history was gained from the mineralogical record, both from outcrop and cored boreholes. For example, different generations of fracture minerals have been recognised at Forsmark and the relative time relationships of these have had a bearing on establishing the geological evolution of the site (Söderbäck 2008). The occurrences of fracture minerals along different sets of deformation zones have been addressed in Stephens et al. (2007).

The rock stress conditions in the upper bedrock are different to those found at depth, in particular at Forsmark (Glamheden et al. 2007, Martin 2007). Therefore it is possible that the distributions of fracture orientation and size are different for outcropping fractures compared to those at depth. Independent methods of assessing the distributions of fracture orientation and size at depth have been developed using borehole data, as discussed in Section 4.

2.6 Single borehole hydraulic test data

2.6.1 Shallow boreholes

Shallow single-hole investigations have been carried out with the aim of characterising the bedrock surface, providing input to the HSD model of the regolith and establishing the level and seasonal variations in the water table. Most of these boreholes were terrestrial, but some were drilled through sea or lake sediments into the underlying till. In the Forsmark site about 70 boreholes (SFM-holes) were drilled in the regolith. In the Laxemar site around 40 near-surface boreholes (SSM-holes) were drilled. The use of the data in the HSD modelling are described in Bosson et al. (2008, 2009).

2.6.2 Flow logging

Three different types of flow logging investigations have been carried out:

- **PFL-f (Posiva Flow Logging):** A long duration (around one week) abstraction test where difference flow logging at presumably steady-state flow allows inflows to be measured with high spatial resolution, i.e. 0.1 m.
- **PSS (Pipe String System):** A short duration (20–30 minutes) injection test between a double-packer system on three scales of support, 5 m 20 m and 100 m.
- **HTHB** (Swedish abbreviation for Hydraulic Test System for Percussion Boreholes): An impeller flow logging technique based on a few hours abstraction.

Percussion-drilled boreholes have been characterised with the HTHB method predominantly. Most of the cored boreholes have been characterised hydraulically with both the PFL-f method and the PSS method in order to allow for consistency checks between the two methods. The three test methods have different characteristics. In particular, there are significant differences between the PFL-f and PSS methods in terms of field operation, borehole intervals tested, scale of influence of rock tested, and measurement threshold (detection limit) compared with the HTHB method (Follin et al. 2007a).

The PFL-f method

The PFL-f method is a geophysical logging device developed to detect continuously flow-conducting fractures in sparsely fractured crystalline bedrock by means of difference flow logging. The PFL-f method is designed to detect individual fracture flows along the borehole with a spatial resolution of 0.1 m (although when various potential borehole length errors are summed the overall accuracy is c ±0.2 m). The flow-conducting features detected with the PFL-f method are called flow anomalies, or PFL-f anomalies. Flows measured by the PFL-f method have been assigned to individual fractures identified in the boremap (then called PFL-f fractures). The methodology for the association of a flow measured by the PFL-f method to a fracture is described in, for example, Wikström et al. (2008).

The PFL-f tool includes a flow sensor, which uses the thermal dilution method or the thermal pulse method (Pöllänen et al. 2007), within a 1-m long test section that is moved stepwise 0.1 m. This means that if several flow-conducting fractures intersect a borehole within the test section their flows would be summed and assigned to a single fracture. The test section is hydraulically separated from the rest of the borehole by rubber disks. The PFL-f measurements are based on around one week of abstraction pumping where the entire borehole acts as a line sink. The hydraulic test configuration would imply that a cylindrical, steady-state flow regime prevails (see Follin et al. 2011 for a discussion of this issue).

The implications of effectively assuming that the PFL-f count of fractures in a 0.1 m interval is less than or equal to one is discussed with respect to the SFR site near Forsmark in Öhman and Follin (2010). It was estimated that this assumption might lead to an underestimate of the flow-conducting fracture intensity by 16% for an interval size of 0.2 m. Methodological changes were suggested which could avoid this inconsistency in future work. The estimates above were for near-surface rocks, with significantly higher fracture intensity than at Forsmark and Laxemar. Thus, the implications in the sparser flow system at depth are likely to be more limited.

The detection limit of the PFL-f method varies depending on the in situ conditions. Examples of disturbing conditions are floating drilling debris and gas bubbles in the borehole water, or high flows rates

(above about 30 L/min) along the borehole. As a rule of thumb, the lower detection limit of the flow meter device used is approximately 30 mL/h ($8.3 \cdot 10^{-9}$ m^3/s) for the thermal dilution method. The upper detection limit is 300 L/h (8.3 10^{-5} m^3/s). Typically a drawdown of 5-10 m is used implying a range of transmissivities measured between about 10^{-9} to 10^{-5} m^2/s. However, for borehole intervals with PFL-f measured flows at or above the upper detection limit, tests were repeated with a lower drawdown of c 0.5 m to 1 m, giving an upper range of transmissivity of c $2 \cdot 10^{-4}$ m^2/s. If a fracture is flow-conducting at a rate below the lower detection limit it does not count in the PFL-f statistics. Hence the detection limit is an important modelling parameter. A cylindrical, steady-state flow regime prevails around each test interval. The interval is thought to be small enough to characterise the flow from individual fractures. By combining the PFL-f method with boremap data, the orientation of the flow-conducting fracture can be assessed, as described in Forsmark et al. (2008) for example. The maximum uncertainty in position along the borehole of the PFL-f method is approximately ± 0.2 m.

The potential for flow-conducting fractures to "short circuit" the borehole above and below the rubber discs is minimised since the borehole is a line sink. Problems with the rubber discs may arise however, for example when there are cavities in borehole diameter or large axial flows in the borehole below the test interval. The flow-rate of isolated fractures or isolated clusters of fractures connected to the pumped borehole cannot be investigated; that is, only connected hydraulically open fractures with a sufficient flow-rate can be detected and analysed.

If a radial, steady-state flow regime of known radius of influence is assumed, transmissivity values associated with individual flow-conducting fractures can be calculated using Thiem's equation (see, for example, de Marsily 1986). Assuming t.hat the ratio of the radius of influence divided by the borehole radius is 500 leads to the relationship that transmissivity, $T \approx Q/s$, where Q is the flow-rate, s is the drawdown and the fraction is called the specific capacity (m^2/s). Formally the validity of this approximation would require fracture transmissivity to be homogeneous and not to be intersected by the wider fracture network within the radius of influence. Since the actual flow geometry, skin effects (i.e. localised changes in fracture hydraulic properties around a borehole due to damage, induced stress changes or debris during drilling), and radii of influence are unknown, transmissivity values should only be taken as indicating orders of magnitude. Calibration of the Hydro-DFN models was based on simulations to match the recorded distributions of specific capacity, as discussed in Section 4.6. For a drawdown of 10 m, as typically used, the lower detection limit corresponds to the ability to detect fractures with transmissivities above c 1 10^{-9} m^2/s.

Approximately 9,475 m of core in 12 core-drilled boreholes were mapped by the PFL-f method during site investigations at Forsmark (up to data-freeze stage 2.2) (Follin 2008). 16,456 m of core in 45 core-drilled boreholes were mapped by the PFL-f method during site investigations at Laxemar (up to data-freeze stage 2.3) (Rhén and Hartley 2009).

Data acquired through the PFL-f method has a fundamental role in the development of the Hydro-DFN models, as discussed in Section 4.

PSS flow logging

The PSS (Pipe String System) measurements apply a test approach known as constant-head injection within a test section length defined by the spacing between a pair of inflatable packers (double-packer system). PSS measurements have been run with different test section lengths. The test section lengths and injection periods used in the site investigations were 5 20 and 100 m with corresponding injection times 20 20 and 30 minutes, respectively. The evaluation of the flow-time envelope was made after 20–30 minutes of injection, which means that the duration of the PSS measurements is much shorter than for the PFL-f measurements.

The accuracy of the flow-rate measurements depends on the actual flow-rate. As a rule of thumb, the lower detection limit of the PSS flow meter device used is approximately 60 mL/h ($1.7 \cdot 10^{-8}$ m^3/s), defining the measurement limit for flow. The upper limit for pumping is about 40 L/min. First the tests employing 100 m test sections were performed. For 100 m test-sections showing flow-rates above the measurement limit for the flow, tests with 20 m test sections were performed. Subsequently, the tests with a test section length of 5 m were performed for those 20 m test sections showing flow-rates above the measurement limit for flow.

The PSS method has test sections which might be so long that several conductive fractures are investigated simultaneously. Their individual contribution or geometry cannot be inferred by this method. Furthermore, the flow regime (linear, radial, and spherical) and the state of flow (steady-state or transient) cannot be assumed with confidence, because the tested section acts like one or several point sources. Hence the flow regime and the state of flow must be analysed and evaluated using the entire flow-time envelope, preferably using time-derivates of the pressure. There is the potential for locally connected fractures short-circuiting the borehole above and below the inflatable packers, in particular at locations where the fracture intensity is high.

A transmissivity of the test section is estimated assuming steady state flow using Moye's equation (Moye 1967). When assuming transient flow conditions the evaluation of transmissivity is made for the first acting radial part of the flow-time envelope using type-curve interpretation methods. If no acting radial part exists, the test section transmissivity value is calculated using linear or spherical flow models (Enachescu and Rahm 2007, Ludvigson et al. 2007). For a typical injection pressure corresponding to 20 m head, the detection limit means transmissivities of borehole sections above approximately $7 \cdot 10^{-10}/9 \cdot 10^{-10}/1 \cdot 10^{-9}$ m^2/s are observed for test scales 5/20/100 m, respectively.

The majority of the skin factors inferred from transient analyses of the PSS tests performed were negative. This suggests that the cored boreholes generally increased the connectivity of the near-field fracture system.

The transmissivity of some isolated fractures, or isolated clusters of fractures, connected to the test section may also be measured; that is, it is not only the connected hydraulically open fractures that are detected and analysed. The hydraulic diffusivity of the more compartmentalised parts of the fracture network is also investigated (Follin et al. 2011).

HTHB flow logging

The HTHB method has been applied to percussion drilled boreholes. Percussion-drilled boreholes at Forsmark and Laxemar have a larger diameter than core drilled boreholes, of approximately 140 mm, and are generally not deeper than 200 m. The HTHB method is based on pumping and flow logging in an open borehole. The borehole transmissivity is determined after a few hours of pumping and the individual flow contributions along the borehole are determined by means of a cumulative impeller flow-log. The practical detection limit varies; at Forsmark, a common value of transmissivity observed is about $1 \cdot 10^{-6}$ m^2/s. The method was used to provide transmissivity measurements of deformation zones, HCD, in the upper bedrock to augment PFL and PSS tests in HCD.

2.7 Interference test data

Hydraulic interference tests involve pumping water to or from a borehole or tunnel and monitoring, over time, the pressure responses in packed off sections of other boreholes at some distance from the pumping borehole or tunnel.

Interference tests during the site investigations have been performed in a number of boreholes. They provide an indication of the hydraulic connectivity and properties of the rock on scales larger than those investigated using single-hole tests. Interference tests were chosen as being appropriate for model testing and calibration when the number of observation sections is fairly large, the pumping durations relatively long and the tests situated in areas of interest. In particular, interference tests which meet these criteria have been conducted by pumping HFM14 at Forsmark (Follin et al. 2007b), and by pumping HLX28 and HLX33 at Laxemar (Rhén et al. 2009).

In addition to the cross-borehole interference tests, the Äspö Hard Rock Laboratory (Äspö HRL), situated below the Äspö island north-east of the Laxemar local model area, has recorded drawdown data in surrounding boreholes, as well as tunnel inflow data.

2.8 Hydrogeochemical data

The spatial distribution of some of the hydrogeochemical components of the groundwater is thought to be strongly linked to the evolution of the groundwater flow system, and therefore the hydrogeochemical data can provide insights in to the flow system. In particular, changes in the chemical composition of groundwater in the Forsmark and Laxemar sites are caused by the infiltration of waters with glacial, marine and meteoric origins, as determined by the topographic and climate evolution of the sites. It has been suggested that an understanding of the chemical evolution of groundwater throughout time is a powerful tool to predict the future development of groundwater flow and its chemical composition, see for example OECD/NEA (1993) and Bath and Lalieux (1999)

The bedrock hydrochemistry of the Forsmark site is described in detail in Laaksoharju et al. (2008). The bedrock hydrochemistry of the Laxemar site is described in Laaksoharju et al. (2009) and the hydrochemistry of surface water and shallow groundwater is discussed in more detail in Tröjbom et al. (2008). The hydrochemistry data consists of measurements of major ions, isotopes, and porewater data with samples taken from boreholes. The major ions considered in the groundwater flow model are Br, Ca, Cl, HCO_3, Mg, Na, K and SO_4. The two isotope ratios of interest to hydrogeology are δ^2H and $\delta^{18}O$.

The development of conceptual models of groundwater chemistry at Forsmark and Laxemar, and attempts to model the evolution of the groundwater chemistry since the last glacial episode at each site, are described in Section 6.6.

2.9 Tracer test data

SKB has performed in situ tracer tests at several locations in Sweden, as discussed by Löfgren et al. (2007) and Hjerne et al. (2010). Tracers tests are a potential way of establishing values for transport parameters pertinent to groundwater advective velocity, sorption, diffusion and dispersion, as discussed in Crawford (2008) and Crawford and Sidborn (2009). Tracer tests can also be used to verify fracture network connectivity. Tracer tests conducted by SKB have been performed at Studsvik research centre area, Finnsjön test site, the Stripa mine, Äspö Hard Rock Laboratory (Äspö HRL), as well as the Forsmark and Laxemar sites as part of the site investigation programme.

The tracer tests that have most relevance for the transport properties used in the site descriptive modelling consist of multiple well tracer tests and a series of single well injection withdrawal tests (SWIW). SWIW tests are also commonly referred to as “push-pull” tests in the scientific literature since the method involves a pulse injection of a tracer into a packed-off borehole section followed by pumping withdrawal in the same section.

Two multiple well tracer tests were performed at Forsmark and reported in time for relevance to the SDM modelling (Wass and Andersson 2006, Lindquist et al. 2008). The first test took the form of a large scale pumping test with non-sorbing tracer release from packed-off sections in three boreholes in an approximately radially converging flow configuration. The other tracer test was made in a two well, weak dipole configuration over a substantially shorter distance within a deformation zone using a mix of both sorbing and non-sorbing tracers. The main purpose of the former investigation was to test connectivity of the fracture zone for confirmation of the hydrogeological flow model. The second tracer test was also intended to partially validate the hydrogeological model over the Forsmark candidate area, but also was intended to test the transport characteristics of the rock for comparison with data obtained from the laboratory transport properties investigations using drill core material.

Two multiple well tracer tests were performed in Laxemar in time for the SDM modelling. The first test took the form of a pumping test with non-sorbing tracer (Rhodamine WT) injection, with withdrawal at a distance of roughly 260 m (Gustafsson and Ludvigson 2005). The second test was carried out by non-sorbing tracer (uranine) injection in a soil well with withdrawal at a distance of 204 m.

Six SWIW tests have been performed at both the Forsmark and Laxemar sites in different types of structure, at different depths and transmissivity ranges with the aim of characterising the transport properties of a variety of flow-conducting features typical of those which might be encountered in the vicinity of a repository.

The various tracer test data were generally assessed positively against criteria concerning the utility of tracer tests in site characterisation, as listed in Löfgren et al. (2007). These criteria referred to the confirmation of flow connectivity, the qualitative confirmation of retention and the confirmation of process understanding (Crawford 2008). The modelling evaluations were also considered to support the abstraction of lumped transport parameters, with the caveat that the retardation processes observed may not scale simply to safety assessment timescales (Crawford 2008).

3 Model development and use of data

This chapter begins by briefly describing in Section 3.1 the geological classification of the bedrock that provides the framework in which the hydrogeological model is developed. As described in Section 1.3 the hydrogeological site descriptive model follows a systems approach starting with the large-scale hydraulic conductor domains (HCD) model, as described in Section 3.2, and then sub-dividing the remaining bedrock into appropriate hydraulic rock domains (HRD), as described in Section 3.3, based on a synthesis of the geological description of fracture domains and the observed hydrogeological characteristics of the bedrock.

3.1 Geological bedrock classification

3.1.1 Definition of rock domains

The geological classification of the bedrock starts with the definition rock domains based on lithology. The identification of rock domains was initiated at the surface and then extended to the subsurface based rock units identified in the single hole interpretations of the cored boreholes. These are defined on the basis of

- Composition, grain size and texture of the dominant rock type.
- Degree of bedrock homogeneity.
- In the case of Laxemar – Strong ductile structural overprinting (high frequency of ductile shear zones).

The resulting definitions rock domain distributions at the surface are shown in Figure 3-4 for both sites and on the scale of the local model areas.

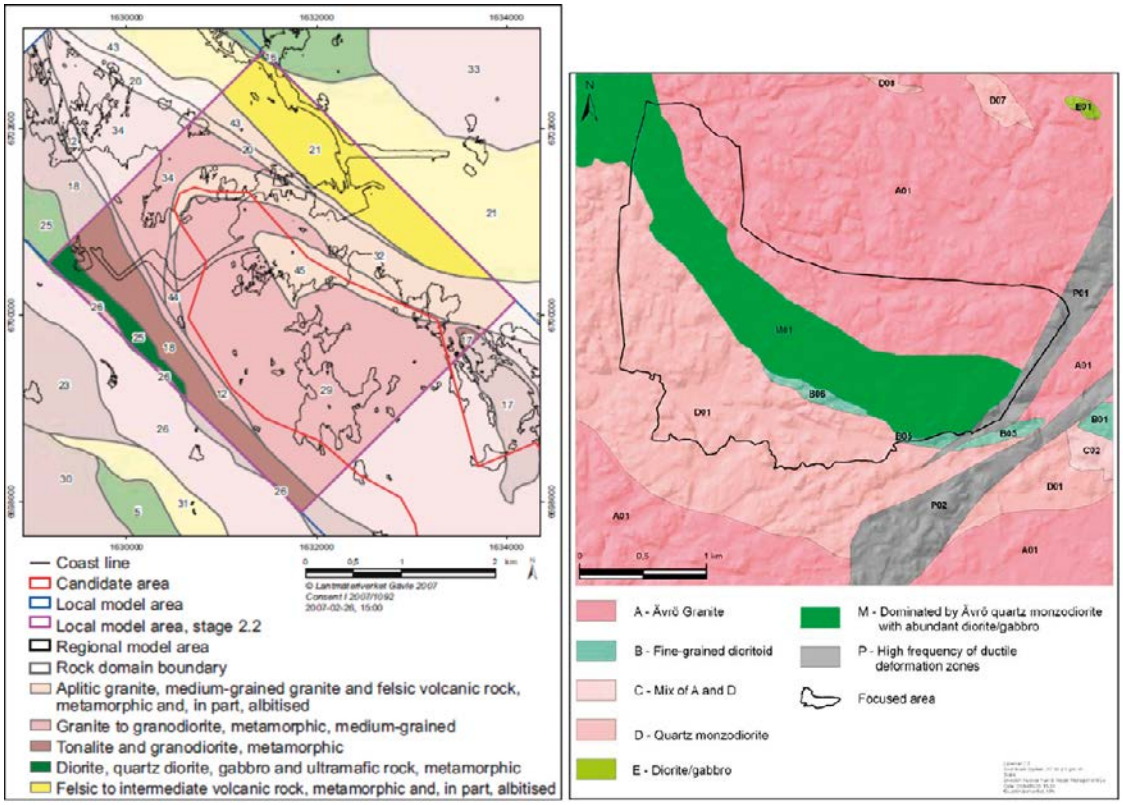

Figure 3-1. *Illustrations of the rock domains at the surface of the local model areas for Forsmark (left) (SKB 2008) and Laxemar (right) (SKB 2009).*

3.1.2 Definition of deformation zones

The next step in the geological classification is the identification of deformation zones, which are defined as essentially tabular structures along which there is a concentration of brittle, ductile or combined brittle and ductile deformation. The interpretation of the deformation zones involves constructing a three-dimensional deterministic structural model based on the integrated evaluation of geophysical data (airborne magnetic data, high-resolution ground magnetic data, seismic reflection data), the identification of possible deformation zones in the single-hole interpretation of cored and percussion boreholes, and the interpreted geological framework of the deformation history of the site. Interpretation of geophysical data resulted in a lineament map of the regional model areas comprising lineaments longer than 1,000 m; these constituting the basis for the site descriptive models of deformation zones (Rhén et al. 2006). An important aim of the modelling work was to attain a similar degree of resolution for a geological entity throughout the volume selected at a particular modelling scale (Munier et al. 2003). Lineaments identified were thought to generally correspond to deformation zones. Percussion drilling was used to intersect some of the potential deformation zones associated with the lineaments in order to confirm them as deformation zones. The borehole intercept data was used to develop a "single-hole geological interpretation", providing a synthesis of all geological and geophysical data from a borehole, essentially a one-dimensional geo-model for the individual borehole. The geometric mapping of deformation zones is described in Stephens et al. (2007) for Forsmark, and Wahlgren et al. (2008) for Laxemar. The deformation zones provide the geometrical framework for describing the hydraulic conductor domains, as described in Section 3.2.

3.1.3 Definition of fracture domains

In order to describe the brittle aspects of the rock domains the rock is divided into deformation zones and the rock mass outside them can be further subdivide into fracture domains. Fracture domains provide a large-scale conceptual framework for describing spatial heterogeneity in rock fracturing. The identification of fracture domains was motivated by the concept that different deformation histories in different rock volumes would be indicated by variations in fracture intensity or orientation statistics. The goal being to find rock volumes with fracture characteristics such that the variability between volumes is larger than the variability within volumes (after Munier et al. 2003), in line with standard geologic practice. As such, fracture domains should form the basic divisions over which spatial heterogeneity in rock fracturing is characterised; these domains may not necessarily correspond to the limits of other geologically-significant volumes such as the rock domains. The identification and description of fracture domains also provides a basis for the stochastic modelling of fractures and minor deformation zones, i.e. the Geo-DFN.

The fracture domains were defined on the basis of the following considerations:

1. The structural context of the rock mass blocks between the deformation zones.
2. Fracture mineralogy.
3. The rock domain model.
4. Changes in fracture orientations and their relation the conceptual model for the deformation history of the site.
5. The relative intensity of different fracture sets.
6. Stress state.
7. Hydrogeochemistry.

At Forsmark the tectonic lens was recognised as a key structural feature (indicated approximately be the red line showing the candidate area in Figure 3-4) in which the bedrock is less affected by ductile deformation within surrounding belts of high ductile strain. It was recognised that an area in the upper part of the bedrock contains an increased frequency of sub-horizontal to gently dipping, open and partly open fractures. A systematic assessment of the variation in the frequency of particularly open and partly open fractures with depth contributed to the division of the bedrock between deformation zones into fracture domains (SKB 2006a, Olofsson et al. 2007). The allocation of a borehole section to a particular fracture domain was carried out as a working hypothesis for the subsequent statistical modelling of fractures and minor deformation zones at the site. Furthermore, on the basis of these borehole data,

a 3D geometric model for four of the six fracture domains (FFM01, FFM02, FFM03 and FFM06) inside the tectonic lens was constructed (Olofsson et al. 2007) and analysed in the Geo-DFN modelling of Fox et al. (2007). The configuration of these fracture domains is shown in Figure 3-2.

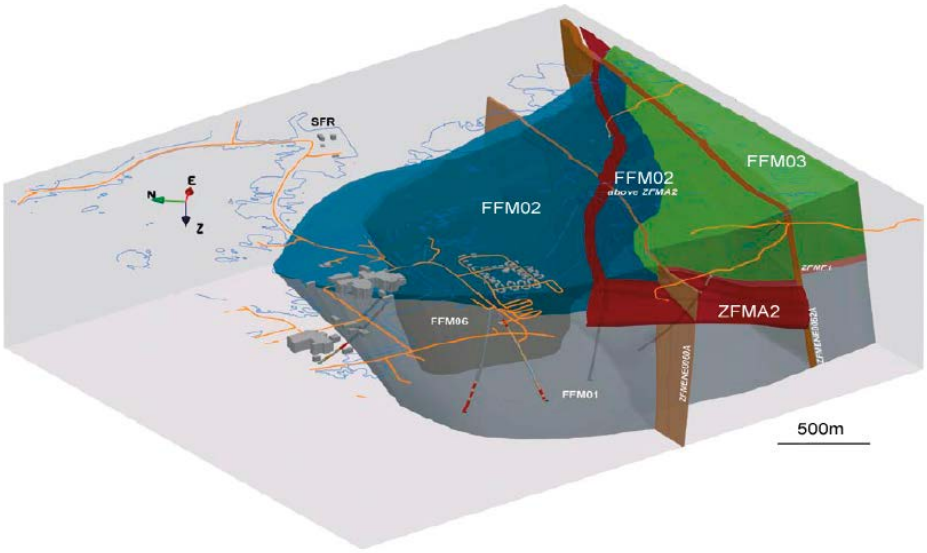

Figure 3-2. *Three-dimensional view towards ENE showing the relationship between fracture domains (FFM) and deformation zones (ZFM) at Forsmark. (Olofsson et al. 2007).*

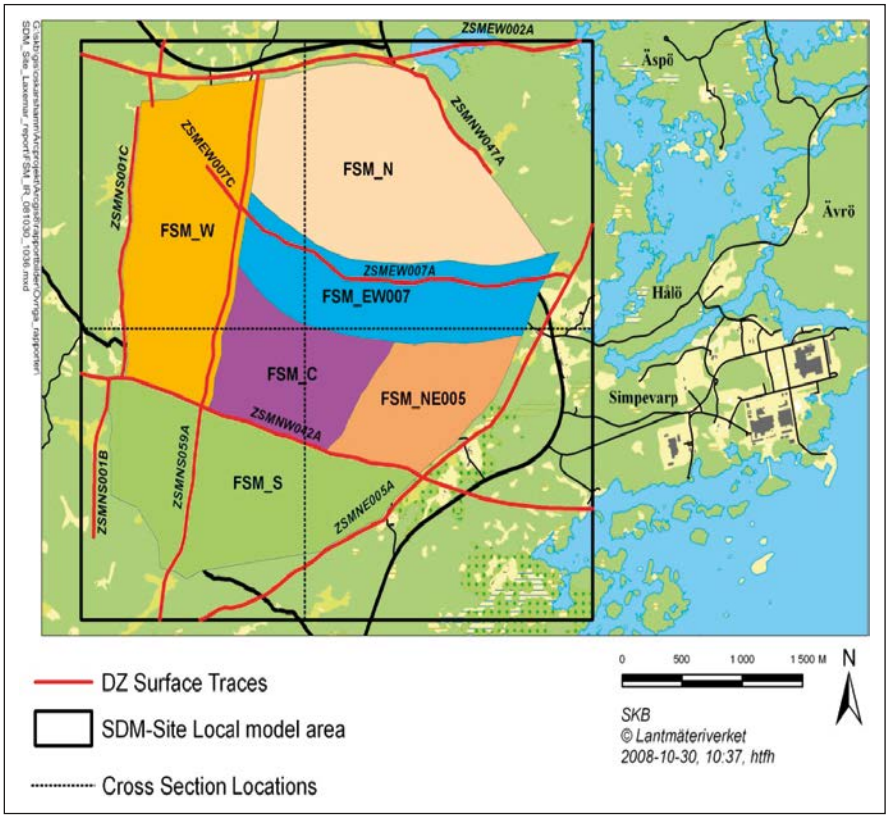

Figure 3-3. *Illustration of the SDM-Site Laxemar fracture domain (FSM) model and key deformation zones (ZSM), based on La Pointe et al. (2008).*

At Laxemar, the fracture orientation set definitions do not change significantly across the local model domain. Rather, the relative intensity of fracture sets and the locations of deformation zones are used to delineate domains showing similar fracture intensity trends. Fracture domains were identified by first examining fracture orientation data from boreholes, outcrops, and trenches for spatial trends in orientation. Tentative fracture domains were hypothesised by combining observed intensity patterns with potential volume boundaries (regional and local deformation zones from the deformation zone model) and an understanding of the deformation history and tectonics in the Laxemar-Simpevarp region. The relative intensities of the fracture sets that are defined are used to confirm and finalise the fracture domain definitions, as shown in Figure 3-3.

3.2 Development of the HCD model

Deformation zones are envisaged as being composed of swarms of smaller fractures, as indicated in Figure 3-5. Hydrogeologically they are characterised by an overall transmissivity for the structure, which is calculated for each borehole intercept by summing the interpreted transmissivity measurements between the upper and lower bounds of the deformation zone interval, as determined in the single-hole geological interpretations. This approach implies that the hydraulic thickness is assumed to be equal to the geological thickness. The heterogeneity in the in-plane transmissivity of a given deformation zone was studied by means of a combination of PSS and PFL-f single-hole tests at different locations in the zone. At Forsmark, the overall fracture frequency in the HRD is about one third that found in the HCD, whereas for open and partly open fractures the figure is closer to one quarter suggesting that fractures are less likely to be open in the HRD. Taken as a whole, the intensity of flow-conducting fractures in the HRD is roughly 20% of that in the HCD. It may be noted from Figure 3-5 that the width of zones is defined to include the damage zone. This renders a wider zone than just the core, potentially capturing more flow measurements within the zones, but spreading the total flow-rate over a wider volume.

An exponential model for the depth dependency of the in-plane deformation zone transmissivity was interpreted in Follin et al. (2007a, b) for Forsmark and Rhén et al. (2008) for Laxemar. There are few HCDs with well characterised hydraulic properties such that they have individual transmissivity versus depth trend functions, requiring that most of the HCDs be described using generalised depth dependencies. The HCDs at Laxemar were divided into four main categories based on orientation and size. The assignment of hydraulic properties to the different deformation zones modelled was then based on depth trend regression analyses of single-hole transmissivity data acquired at a number of deformation zone intercepts. In the case of several measurements at different locations in the same zone, the geometric mean of the calculated values was used as an effective value. At Forsmark a local conditioning of the resulting depth trend was applied (Follin et al. 2007b), as described in Section 6.2. The resulting HCD models are shown in Figure 3-4.

Initially a “deterministic base case” was defined with a deterministic prescription of transmissivity within deformation zones. Significant spatial variability in transmissivity was evident within zones at both sites based on hydraulic tests performed in the same zone. A conceptual model for lateral heterogeneity in transmissivity was developed with normally distributed variation in log (T) about the interpreted depth trend (see Follin et al. 2007a, Section 9.2 and Rhén et al. 2008, Section 4.1.2). To test and illustrate this interpretation numerically, a series of variant simulations were sampled a spatially varying transmissivity across zones by adding a log-normal random deviate to the exponent. The transmissivity model assumed a nugget covariance model for the lateral spatial variability, which was conditioned on measured transmissivity data. Since the heterogeneity away from the measurement boreholes is undetermined, this required a stochastic approach using several model realisations.

The transport apertures were calculated by assuming a relationship between the transport aperture and the assigned effective transmissivity of the deformation zones (see Section 3.3.10). In the groundwater flow modelling, values of the kinematic porosity were calculated from the ratio between the transport aperture and the geological thickness. The values of flow-wetted surface area were based on Terzaghi corrected intensity values (Terzaghi 1965) obtained from PFL-f measurements within the HCDs (Follin et al. 2007b, Rhén et al. 2008).

Rhén et al. (2008) estimated the storage coefficient as a function of the transmissivity for HCDs from a large number of interference tests at Laxemar. Follin et al. (2007b) estimated the storage coefficient as a function of the transmissivity for HCDs from interference tests at Forsmark. These relations were used for initial assignment of the storage coefficient when modelling the interference tests, as described in Section 6.4.

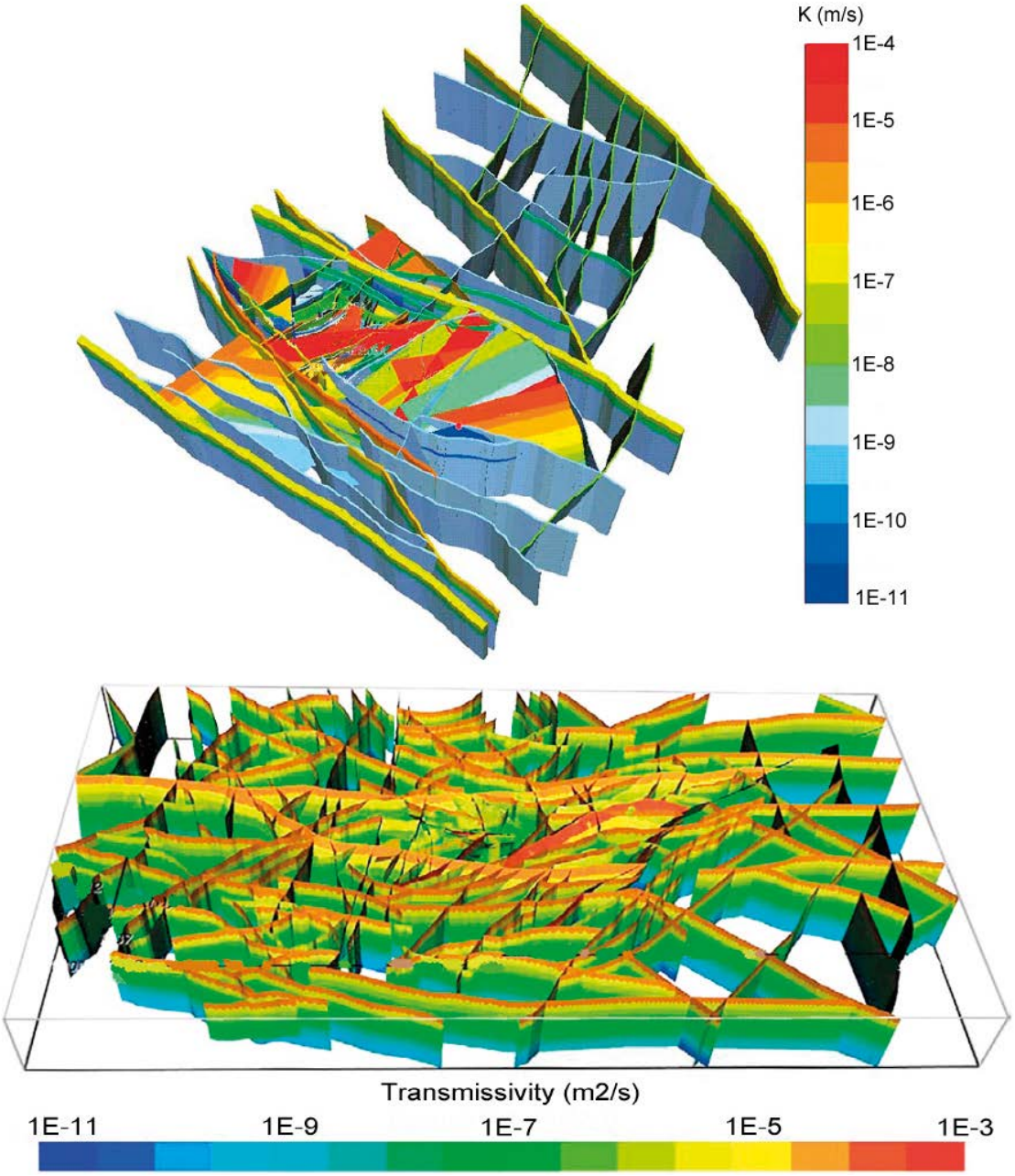

Figure 3-4. *The deterministic base case HCD model at Forsmark (top) (Follin et al. 2007b). The regional-scale deformation zones are coloured by the hydraulic conductivity within the zones and drawn as volumes to show their assigned hydraulic width. The depth dependency is clearly apparent. The deterministic base case HCD model at Laxemar, coloured by transmissivity (bottom) (Rhén et al. 2008).*

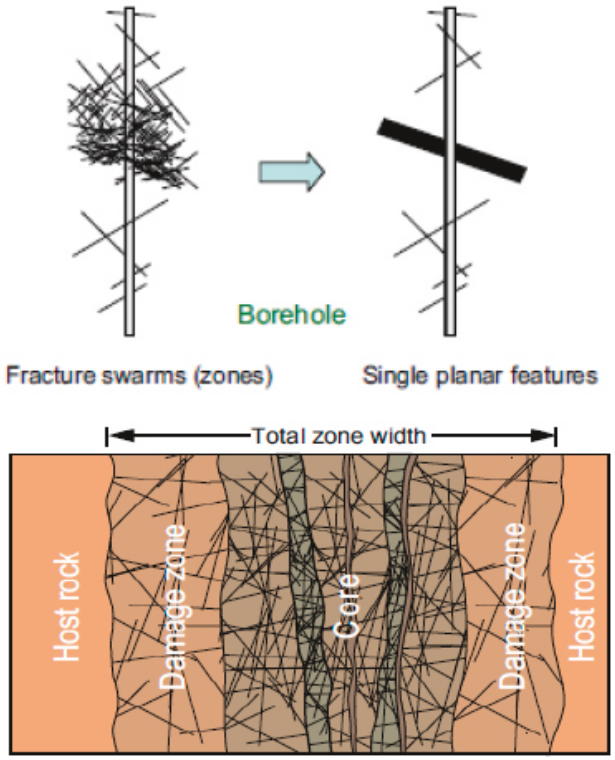

Figure 3-5. *Top figure: The fracture data between the upper and lower bounds of a deformation zone interval are combined to form a single planar feature. In the same fashion, all hydraulic data in the interval are also combined in the hydrogeological modelling, to form a single in-plane transmissivity value. (From Follin et al. 2007b). Bottom figure: Illustration of the typical fracturing associated with faults (note the definition of the zone includes the damage zone).*

3.3 Development of the HRD model

Fractures can be modelled either stochastically, or deterministically if their position and properties are known with reasonable confidence. In the modelling of Forsmark and Laxemar the geometric properties of the Hydraulic Conductor Domains (HCD) were modelled deterministically, and their hydraulic properties were modelled either stochastically or deterministically. Fractures belonging to the Hydraulic Rock mass Domain (HRD) were generally modelled entirely stochastically. For stochastically modelled fractures each property is sampled from probability distributions representing: orientation, frequency, size, spatial distribution, and transmissivity (Dershowitz et al. 1998). The details of the assumptions made regarding the properties of stochastically modelled fractures in the HRD are described in this section, and summarised in Subsection 3.4.

Using SKB's terminology, a DFN model of the geometric properties of the set of all of the fractures in the rock, including both sealed and open fractures, is a geological DFN (Geo-DFN) model, see Table 1-1.

A fracture also has hydraulic properties as well as geometric properties. In particular, some fractures, or regions within fractures, have the potential to conduct flow. Other fractures, or regions within fractures, cannot conduct flow, for example because they are tightly sealed by fracture surface asperity contact or annealed by precipitation of minerals.

In the Hydro-DFN models, an open fracture is assumed to conduct flow if it is connected as part of a percolating network. Open fractures might be interpreted as representing the hydraulically open portions within otherwise sealed fractures. In this sense they might crudely represent heterogeneous flow channelling within larger fractures. To be more precise, the properties of the open fractures are intended to characterise the statistical properties of the hydraulically open regions within otherwise sealed fractures. An alternative approach is to explicitly model individual fractures and assign hydraulically open and sealed areas to those fractures, see Hartley et al. (2011), for example.

The intensity of open fractures is less than or equal to the intensity of all fractures. This defines a key relationship between the Geo-DFN and Hydro-DFN, and can be used as a check on the consistency between the two different types of DFN models, as discussed in Section 4.5.

It should be noted that for the rest of this report we use the term "intensity" as a short-hand for the unbiased definition of intensity as "fracture surface area per unit volume" intensity, P_{32}. However, because this is difficult to determine, practically it has to be estimated from linear measures of fracture intensity along boreholes. However, measurements along a borehole preferentially detect fractures orthogonal to the borehole compared to those at an oblique angle. This can bias estimates of fracture intensity, such as frequency or stereographic concentration contour plots, heavily in favour of fractures orthogonal to the borehole. To compensate for this bias, estimates of fracture intensity are accumulated in terms of a weighted sum, rather than a simple count, with a geometrical weighting factor calculated and applied to each fracture measured. This weighting is used in calculating statistics such as the corrected linear fracture intensity when comparing between different borehole orientations, or can be applied to concentration plots for identifying fracture sets. The process used is called Terzaghi correction (Terzaghi 1965). In the analysis of fracture data a maximum weight of 7 was used so as to avoid over sensitivity to observed steep angled fractures.

Establishing the fracture surface area intensity of the set of open fractures is a key issue in development of the Hydro-DFN models. The decisions in the Forsmark and Laxemar models were based on the statistical analysis of the Boremap data classification of factures as "sealed" or "open" and "partly open" with an associated confidence, and are discussed in Section 3.3.4. Uncertainty in this classification was addressed through model variants.

For open fractures, the geometric properties are supplemented with the hydraulic properties of transmissivity, storativity and transport aperture to complete the specification necessary for a Hydro-DFN model.

3.3.1 Definition of hydraulic rock domains (HRD)

For the purposes of hydrogeological modelling the rock mass was sub-divided into hydraulic fracture domains (HRD). The basis for this subdivision was strongly linked to the geological framework, i.e. the fracture domains. However, for fracture domains where there was either very limited data, or where there the differences in the hydraulic data (e.g. orientation or intensity of PFL-f fractures) between adjacent domains were not considered statistically significant, then the merging of fracture domains, or drawing analogies between them, was considered. The main driver for making such judgements is a practical one – the need to have sufficient hydraulic measurements, mainly PFL detected fractures (a few hundred, say), within each HRD to calibrate a Hydro-DFN model specific to that domain.

For Hydro-DFN modelling of Forsmark (Follin et al. 2007a), the treatment of the HRD was as follows:

- A HRD comprising fracture domains FFM01/FFM06. These fracture domains were merged since FFM06 has a similar structural context to FFM01, below zone A2 and FFM02, it is distinguished from FFM01 by slight differences in lithology, but has limited borehole data compared to FFM01.
- A HRD representing fracture domain FFM02 that is situated close to the surface directly above FFM01/06.
- A HRD representing fracture domain FFM03 above zone A2 to the south east of the candidate area.
- A HRD representing fracture domain FFM04 which forms a relatively thin band of rock bordering the southwest side of the candidate area, but had limited data, and so was characterised by analogy to FFM03.
- A HRD representing fracture domain FFM05 which forms a relatively thin band of rock bordering the north and northeast sides of the candidate area, but had limited data, and so was characterised by analogy to FFM03.
- A HRD for all the rock mass outside FFM01-06. This was not characterised directly by the site investigations at Forsmark. For the purposes of the SDM and SR-Site its bulk hydraulic properties were described on the basis of water supply well yield and from earlier investigations at Finnsjön (Follin et al. 2007b).

With this approach there was sufficient hydraulic data to construct a Hydro-DFN model for the first three HRD described above, whereas the last three HRD were described based on either analogy or in terms of just bulk hydraulic (i.e. continuous porous medium rather than DFN description) properties.

An important hydrogeological characteristic observed at Forsmark was a strong variation in the intensity of PFL-f features with depth. Part of this depth trend is captured by the location of fracture domain FFM02 above FFM01/FFM06 with higher intensity of sub-horizontal fractures, and likewise further to the south east the more fractured FFM03 above FFM01/FFM06, see Figure 3-2. There still remains a significant depth trend within FFM01/FFM06 that exists from about –100 m to the base of the geological model, and within FFM03 that extends from groundwater to the base of the geological model. For Hydro-DFN modelling purposes this depth trend was represented by further sub-dividing the HRD into depth zones and assigning different fracture intensity values and transmissivity distributions within each depth zone. The HRD of FFM01/FFM06 was eventually divided into three depth zones: above –200 m, –200 to –400 m and below –400 m (Follin et al. 2007a). FFM03 was split into two depth zones: above –400 m and below –400 m. FFM02 is limited to approximately the top 200 m of bedrock, and so a depth trend within this narrower range is less important, and so was modelled as a single volume.

For Laxemar the orientations of open and PFL-f fractures did not show appreciable variation between the fracture domains shown in Figure 3-3. In particular, the fracture domains in the south bore very similar fracture characteristics, e.g. orientations and PFL-f fracture intensities. Because borehole data was limited in FSM_NE005 and FSM_S, then these fracture domains were merged with FSM_C into a single HRD resulting in the following four HRD (as shown in Figure 3-6) (Rhén et al. 2008):

- HRD_EW007 corresponding to FSM_EW007.
- HRD_N corresponding to FSM_N.
- HRD_W corresponding to FSM_W.
- HRD_C corresponding to a combination of FSM_C, FSM_NE005 and FSM_S.

At Laxemar there was also trend in hydraulic properties with depth, evident as both a reduction in intensity of PFL-f fractures and transmissivity with depth. Therefore, for modelling purposes the parameterisation of the Hydro-DFN was defined according to four depth zones for each HRD (Rhén et al. 2008):

1) DZ1: from ground surface down to –150 m.
2) DZ2: from –150 to –400 m.
3) DZ3: from –400 to –650 m.
4) DZ4: below –650 m.

An example of the variation in intensity of PFL-f fractures with depth is shown in Figure 3-7.

3.3.2 Minor Deformation Zones

Deformation zones with trace length shorter than 1,000 m were called Minor Deformation Zones (MDZ) and were geologically assessed in Munier and Hökmark (2004), Stephens et al. (2008) and Wahlgren et al. (2008) for Forsmark and Laxemar respectively. In the conceptual model underlying the development of the hydrogeological DFN, each minor deformation zone was generally considered to be a single feature in the overall distribution of features. Minor deformation zone were therefore included in the hydrogeological DFN model as stochastic features. Therefore, within a simulation of the hydrogeological DFN model it was not possible to identify explicitly whether or not a particular feature is a minor deformation zone. However, it was expected that the minor deformation zones were probably among the larger features in the size distribution. Some 28 minor deformation zone were treated deterministically (as HCDs) at Forsmark (Stephens et al. 2008, Follin et al. 2007b) with further 43 called “possible deformation zones” (PDZ) considered to be shorter than one kilometre that were handled as part of the stochastic modelling. Within SR-Site the sensitivity to including four of these PDZ that had associated PFL-f measurements and extended below –150 m was quantified in variant calculations (Joyce et al. 2010a). MDZ were modelled deterministically be geology at Laxemar. However, they were analysed hydraulically, resulting in some 24 minor deformation zone were treated deterministically (as HCDs) in Laxemar hydrogeological modelling (Rhén et al. 2008).

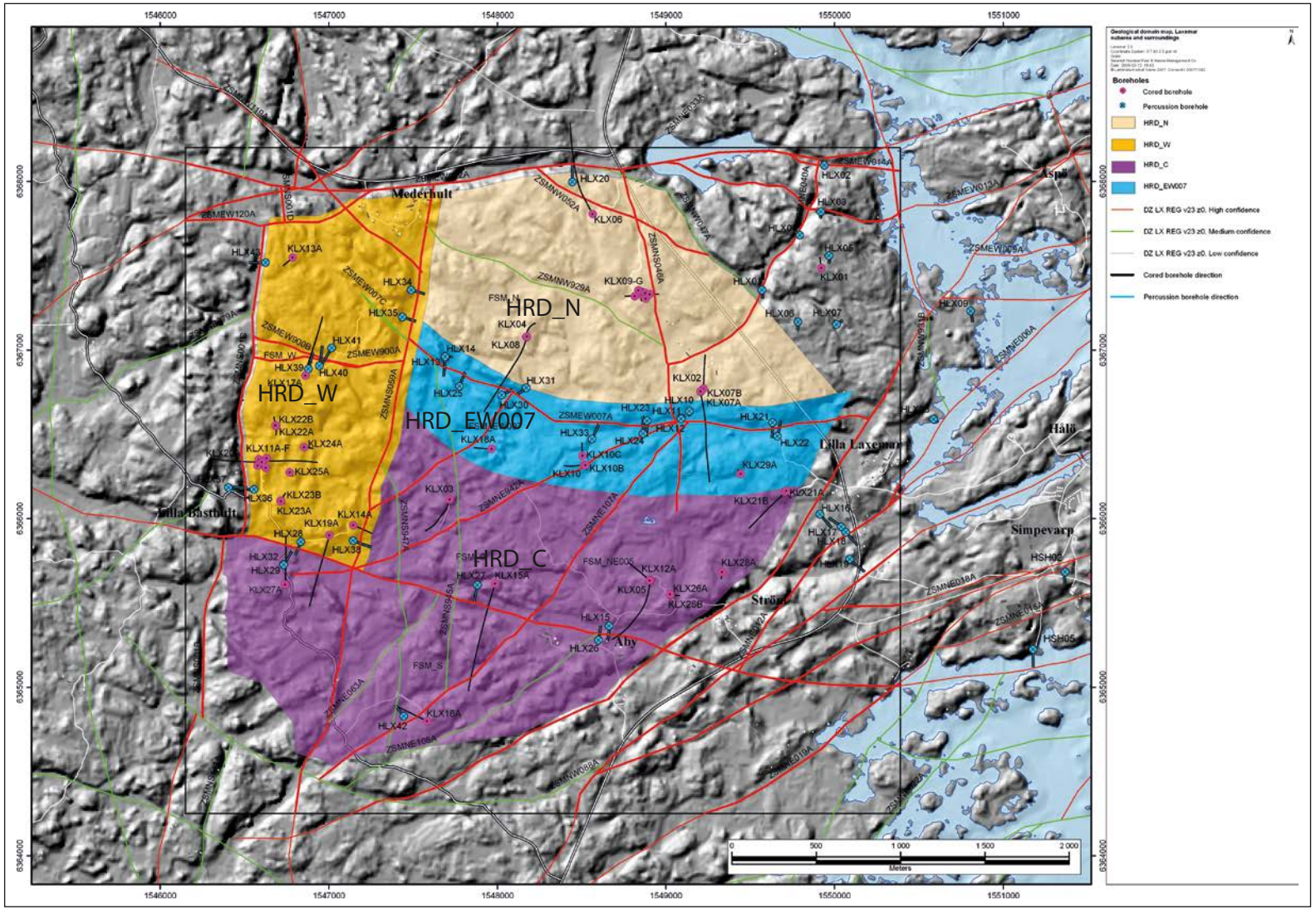

Figure 3-6. *Hydraulic Rock Domain model of Laxemar. (After Rhén et al. 2008, Figure 9-48).*

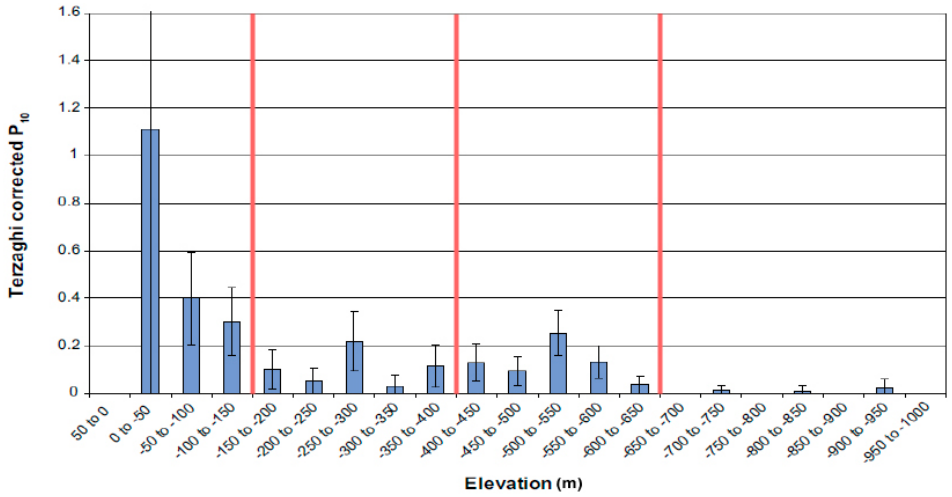

Figure 3-7. *Variation of the Terzaghi-corrected fracture intensity for PFL-f fractures with elevation for the fully characterised sections of boreholes penetrating fracture domain FSM_C, Laxemar. The depth zones are indicated by red lines.*

The treatment of each MDZ was as follows:

- The features that lie within an MDZ were merged into a single effective hydraulic feature in the statistics that are used to define the hydrogeological DFN model for each HRD. Therefore, this single MDZ feature represents the combined effect of their hydrogeological properties. The Intensity of fractures in the associated HRD was consequently reduced slightly.
- Each MDZ was assigned an orientation of the effective planar feature that it represents, based on interpretation on analysis of the Boremap data. All MDZs were assumed to be open for the purposes of calculating the intensity of open fractures.
- If an MDZ contained any PFL-f features then it was hydrogeologically significant. It was assigned a transmissivity which was the sum of the transmissivities of the PFL-f features that it contained. It contributed to the measured intensity of PFL-f fractures only as a single feature.
- If an MDZ did not contain any PFL-f features then it only contributed to the intensity of open fractures.

3.3.3 Fracture shape

Although isolated fractures are in theory likely to be elliptical in shape, there are mechanical reasons to suppose that the actual fracture shapes may tend towards being equant, as the mechanical layering present in sedimentary rocks which promotes non-equant fracture shape is far less well-developed in the crystalline rocks of the Fennoscandian Shield. Further, intersections, truncation, shear and geologic evolution in general distort the idealisation of elliptical fractures. In any case, there is not sufficient data to characterise fracture shape at Forsmark or Laxemar. In the Geo-DFN, stochastic fractures have been assumed to be circular discs, while deformation zones comprise tabular groups of adjoining polyhedral-shaped fractures. In the Hydro-DFN, square shaped stochastic fractures are used instead simply because of the numerical implementation used. Triangulated surfaces are used to represent the geometry of the HCD. For consistency, the fracture size distributions used in the Hydro-DFN modelling are presented here and elsewhere in terms of the radii of circular fractures of equivalent area. It is considered that the difference between square and circular fractures of the same area in terms of network connectivity is minor in light of other uncertainties, see for example Yi and Tawerghi (2009). Fractures in the HCD, which are modelled deterministically, are comprised of triangulated surfaces. Fracture shape is discussed further in Section 8.3.6.

3.3.4 Concepts for fracture openings

The identification of open fractures in the core drilled boreholes using a combination of BIPS and core characterisation is described in Section 2.4.

An open fracture is considered to be a fracture which would conduct flow if it were connected within a percolating network. Various ways of identifying the intensity of open fractures are possible. For the Forsmark modelling, the open fractures were identified as those which are open or partly open, regardless of confidence: this set is here abbreviated to OPO. For the Laxemar modelling, two cases were considered: In one case the set of open fractures was identified as those which are open or partly open, regardless of confidence (i.e. OPO); In the other case the additional constraint was included that the confidence had to be either certain or probable, giving a subset of OPO denoted as OPO-CP. The set of open fractures is a subset of the set of all fractures. Intervals characterised as crush zones were also counted as open features – intervals in the borehole core comprised of crushed rock.

As a simplified comparison of the intensity of open fractures at the two sites some are given here. The Terzaghi corrected intensity of open fractures in FFM01/FFM06 at Forsmark was estimated to be 1.0 m^{-1} above –400 m (effectively limited to depths between –150 m and –400 m as this HRD does not outcrop) and 0.54 m^{-1} below –400 m (Follin et al. 2007a, Chapter 11). For Laxemar, there are two sets of values for HRD_C based on either OPO or (OPO-CP) fractures equal to 2.4 (1.2) m^{-1} between –150 m, 2.2 (0.92) m^{-1} between –400 m and –650 m, and 1.8 (0.8) m^{-1} below –650 m (Rhén et al. 2008, Chapter 10). For the uppermost part of the bedrock, the open intensity of FFM02 at Forsmark is 3.2 m^{-1} can be compared to HRD_C at Laxemar above –150 m, which has a OPO (OPO-CP) intensity of 3.7 (1.8) m^{-1}. It can be seen that open fracture intensities are similar at the two sites above –150 m, but the intensity is significantly less at Forsmark below this depth.

A key resource for the Hydro-DFN models is the assignment of flows measured by the PFL-f method to individual fractures identified in the boremap. By way of comparing the sites, the Terzaghi corrected intensity of PFL-f fractures in FFM01/FFM06 at Forsmark was observed to be 0.07 m^{-1} above –400 m (effectively limited to depths between –150 m and –400 m as this HRD does not outcrop) and 0.005 m^{-1} below –400 m (Follin et al. 2007a, Chapter 10); for HRD_C at Laxemar the value is 0.16 m^{-1} between –150 m, 0.11 m^{-1} between –400 m and –650 m, and 0.008 m^{-1} below –650 m (Rhén et al. 2008, Chapter 10). For the uppermost part of the bedrock, the PFL-f intensity of FFM02 at Forsmark is 0.22 m^{-1} can be compared to HRD_C at Laxemar above –150 m, which has an intensity of 0.56 m^{-1}. Again, this shows how the intensity of PFL-f fractures is considerably lower at Forsmark, and one has to go below –650 m at Laxemar to reach a scarcity inflow similar to that seen at Forsmark below –400 m.

The large reduction in the fracture surface area intensities of those fractures with are observed to conduct flow compared to relative to the super-set of open fractures and is conceptualised as resulting from a proportion of the former not being connected within a percolating network. As discussed in Sections 3.3.7 and 4.5, this assumption is crucial in assessing the intensity-size distribution of the open fractures. This is because the connectivity characteristics of the fracture network are highly sensitive to the intensity-size distribution.

3.3.5 Fracture orientations and set definitions

Stereonet plots showing the orientation of the fractures for each fracture domain were made to understand any clustering of fractures around particular orientations, and therefore guide the definition of appropriate fracture sets. By definition, the fracture domains exclude sections of borehole inside interpreted deterministic deformation zones. Concentration plots were used rather than simple pole plots to identify clustering around particular orientations. For each fracture domain, concentration plots were shown for all fractures, open fractures (with various definitions as described in Section 3.3.4) and PFL-f fractures. Additional pole plots were created showing the orientations of PFL-f fractures with the pole coloured according to interpreted transmissivity. Significant trends in fracture orientation by depth within a fracture domain were not recognised, and so fracture set definitions and orientation distributions were not varied by depth. For the purposes of subdividing fractures into sets, the Geo-DFN used a mix of hard sector and soft sector searching in several steps (Fox et al. 2007; La Pointe et al. 2008). For the Hydro-DFN modelling, hard-sectoring was used to associate each fracture and in particular each PFL-f fracture to a set so as interpret relative intensity and transmissivity statistics between sets. Based on reviewing concentration plots for each fracture domain it was considered adequate to use the same hard sector definitions for all hydraulic rock domains at Forsmark. The same conclusion was drawn at Laxemar, although the set definitions were different between the sites.

At Forsmark, five fracture sets were identified: NS, NE, NW, EW and HZ (Sub-Horizontal), named after the main strike direction (Fox et al. 2007). These were initially defined as hard sectors in the Stage 1.2 Geo-DFN (La Pointe et al. 2005). The same sets remained broadly stable throughout the later Stage 2.2 update for both Geo-DFN and Hydro-DFN. However, since these two update were performed largely in parallel and for different purposes then the actual fitted orientation parameters between the two models differed slightly. The Geo-DFN considered bivariate Fisher (Fisher 1953) and Bingham (Bingham 1974) distributions, however it was these distributions did not provide significantly better statistical fits to the observed data than the univariate Fisher distribution. Hence, for consistency amongst end-users it was decide to use the univariate Fisher distribution throughout Geo- and Hydro-DFN modelling.

Fracture orientations were therefore analysed in terms of a univariate Fisher distribution, with polar angle θ and uniformly distributed azimuthal angle ϕ with respect to a principal orientation vector. The probability density function is given by:

$$f(\theta,\phi) = \frac{\kappa}{4\pi \sinh \kappa} \sin\theta \exp\left(\kappa \cos\theta_0 \cos\theta + \sin\theta_0 \cos(\phi - \phi_0)\right) \quad (3\text{-}1)$$

Where (θ_0, ϕ_0) is the mean pole vector, and the dispersion of the fracture pole distribution is defined by the Fisher concentration parameter, κ.

The orientations distributions used for the Forsmark Hydro-DFN were derived for open fractures only and initially calculated over all fracture domains (Follin et al. 2007a, Table 11-3). Some adjustments to both the hard sectors and orientation distributions were suggested on the basis of concentration plots of PFL-f fractures for the Stage 2.2 update. The primary changes were a redefinition of the NE and NS sets to recognise that sets were more concentrated NE and NNE sets, while true NS was absent (Follin et al. 2007a, Table 11-26). Another important change was that sub-horizontal set became more concentrated with Fisher concentration rising from 8.2 to 15.2. Although only suggested as an alternative orientation model in Follin et al. (2007a), the implication of these changes was a tendency toward a more anisotropic system, which was later found to be an important characteristic of the hydraulic system when performing the hydrogeological confirmatory tests to match cross-hole tests and palaeo-climate evolution in Follin et al. (2007b). The feedback from the confirmatory testing to the Hydro-DFN modelling was adopted in SR-Site (Joyce et al. 2010a), where only the alternative orientation model was utilised.

At Laxemar four fracture sets were called N-S, ENE, WNW and SH (Sub-Horizontal) and again a univariate Fisher distribution was used (Olofsson et al. 2007, La Pointe et al. 2008). For the Hydro-DFN the initial choice of hard sectors was based on the Laxemar 1.2 Geo-DFN model (Hermanson et al. 2005), being based on an analysis of Laxemar 1.2 outcrop data. Appropriate modifications were then made primarily considering the open and PFL-f fractures, although some consideration was also given to concentration plots based on Laxemar 2.3 outcrop data (Rhén et al. 2008, Table 9-2). Different orientation distributions were interpreted for each HRD.

3.3.6 Concepts for fracture intensity scaling, spatial distribution and termination

The concepts of fracture surface area intensity, size, intensity scaling behaviour (Euclidian or fractal), spatial distribution and termination behaviour are inter-related. In the hydrogeological modelling it is the application of these concepts to the set of open fractures that is the focus, as this set of fractures is the basis of the hydrogeological DFN modelling. However, scaling behaviour is most readily analysed for the set of all fractures in the Geo-DFN (e.g., Fox et al. 2007, La Pointe et al. 2008) using fracture mapping from the variety of scales provided by boreholes, outcrops and lineament maps. This is because the distinction of open fractures from sealed fractures typically can only be attempted using the borehole data. In order to set properties for the open fractures it is necessary to make additional assumptions. We note that the set of connected open fractures have different intensity scaling and spatial distribution characteristics compared to the set of open fractures, as a consequence of the requirement that they form a connected network. For example, Follin et al. (2006) demonstrated that when fractures were generated according to a Poissonian point-process, then when isolated fractures are removed, the spatial distribution of the remaining connected fractures is fractal. This is a general characteristic where the size distribution includes fractures

smaller than the average fracture spacing. Small fractures are then less likely to be connected, such that connected fractures tend to cluster around the larger fractures, leading to fractal characteristics. The result is also illustrated here in Section 4.5.

The spatial distribution of fractures describes how fracture centres are distributed. For example fracture centres might be distributed independently, that is, by a Poisson point process, or they might be clustered together. There are many different ways in which the clustering could be organised depending on the stress history and mechanical properties of the rock mass.

Fracture intensity scaling refers to the observation that the measured intensity of fracturing depends on the scale of the observation. The spatial distribution of fractures controls how fracture intensity varies with scale. Certain types of spatial models imply that fracture intensity will increase, remain the same or decrease as a function of scale. Fracture intensity which changes with scale is characteristic of fractal clustering of fractures. Intensity scaling behaviour is important to quantify, as the scale at which fracture data are obtained might not be the scale at which it is used for subsequent modelling or calculations.

Fracture termination behaviour can be interpreted to imply a non-Poissonian distribution of fracture centres, depending on the method envisaged for the creation of each successive fracture set. For example, fracture termination behaviour might be simulated by generating a proportion of fractures so that they terminate against another fracture set. It is possible to envisage other implementations of a fracture termination model, for example by clipping fractures where they intersect. This would however also affect the fracture size distribution.

A theoretical model for fracture scaling based on simple fracture growth concepts and the interaction between fractures as they grow was explored by Davy et al. (2010). They identify two regimes: a dilute regime where fractures grow independently; and a dense regime where they grow until terminating so that small fractures do not cross larger ones. For the dense regime, fractures sizes are shown to follow a power-law determined by the fractal dimension (between 2 and 3 in three dimensions, and typically limited to the range 2.7 to 3 based on analysis of outcrop and lineament maps) and a dimensionless geometric factor depending on the number of sets and orientation of fractures. Small fractures are in the dilute regime and the largest fractures are in the dense one. The transition occurs at a scale which decreases with increasing fracture intensity. Based on analysis of outcrop and lineaments at Laxemar and Forsmark (Darcel et a. 2009) suggest this transition occurs for fractures of radius about 0.5 to 5 m, with a self similar model, k_r=3, applying at larger scales.

Fracture termination behaviour

Fracture termination relationships have been studied in outcrops at Forsmark and Laxemar in Fox et al. (2007) and La Pointe et al. (2008). Fox et al. (2007) estimated different sequences of fracture set creation for the two fracture domains studied at Forsmark (see Table 3-1). They found that the total percentage of termination against any other fracture set varied between 32% and 82%. At Laxemar, fracture termination relationships suggest that the N-S set appears to have formed earliest, while the three remaining sets formed later (La Pointe et al. 2008). The relative chronology of the ENE and WNW sets could not be distinguished from the termination relations. At Laxemar, the total percentage of termination against any other fracture set was found to vary between 28% and 47% for the suggested termination relationship averaged over all fracture domains (see Table 3-2). The fracture termination analysis described in Fox et al. (2007) and La Pointe et al. (2008) applies to the set of all fractures, as the data is obtained from outcrop traces. It is possible that the sets of open fractures at depth would have different fracture termination behaviour.

Fracture intensity scaling

The scaling behaviour of the intensity of all fractures, i.e. the tendency for the measured intensity to depend on the observation scale, has been characterised by the scalar mass dimension, D_m. The mass dimension of a fractal data set is given by the equation (e.g. Fox et al. 2007, Chapter 3):

$$N(r) = \rho r^{D_m} \tag{3-2}$$

where ρ is a constant, r is the scale, D_m is the mass dimension, and $N(r)$ is the intensity at the scale r. $N(r)$ is measured as the number of fractures observed within the sample space, and has dimension equal

to one over the Euclidean dimension. For Euclidean dimension 1.0, e.g. along a borehole, then $N(r)$ is the number of fractures along a line of length r. For Euclidean dimension, 2.0, e.g. outcrop, then $N(r)$ is the number of fracture traces contained within a circle of radius r. For Euclidean dimension 3.0, e.g. a rock volume, then $N(r)$ is the number of fracture planes contained within a sphere of radius r.

Euclidean scaling behaviour is characterised by a mass dimension equal to the Euclidean dimension. A Euclidean scaling model for fracture intensity would be characterised by a linear, first order relation between the number of fractures in a volume of rock and the volume itself: Doubling the volume would lead to a doubling of the number of fractures. A Poisson point spatial model implies Euclidean scaling. If the mass dimension is less than the Euclidean dimension then it implies a fractal scaling behaviour. For example, if fracture traces on an outcrop are clustered around points then there will be circles with high numbers of traces within small circles, while for large circles the number of tracers is just an overall average. If one measures the mass dimension from the slope of a line through the distribution of numbers of fracture traces within circles of different radius against their radius on a log-log plot, ignoring circles without any traces, then one gets a gentler slope than for a homogenous distribution of fracture centres.

There are two sources of data for estimating the mass dimension of fracture intensity at Forsmark and Laxemar: outcrops and boreholes (Fox et al. 2007, La Pointe et al. 2008). The borehole data consist of the positions of fractures along the borehole. Borehole data offer the possibility to calculate the mass dimension over scales approaching the length of the borehole. A disadvantage of using borehole data is that they quantify the scaling behaviour in a particular direction; it is possible that other directions may have a different scaling exponent or model. Unless boreholes are drilled in several directions, the three-dimensional scaling behaviour may not be well characterised by analyses of borehole fracture data. Outcrops allow for a two-dimensional characterisation. While this added dimension provides insight into the scaling behaviour, it is limited to the scale of the outcrops, which are of the order of a few tens of metres for the outcrops studied at Forsmark and Laxemar; and is limited to the top surface of the bedrock, not necessarily representing scaling behaviour at depth.

At Forsmark, analysis of outcrop and borehole data (Fox et al. 2007) led to the suggestion that a fractal mass dimension of about 1.9 in 2D (i.e. Euclidean dimension of 2.0) might be appropriate up to a scale of approximately 20–30 m. At scales greater than 30 m, the fracture intensities were thought to scale in a Euclidean manner.

Table 3-1. Termination matrix based on all fractures mapped on outcrops for FFM02, Forsmark. (After Fox et al. 2007, Table 4-80).

	Terminates Against				
Target Set	**NE**	**NS**	**NW**	**EW**	**Bulk Termination**
NE	0	7.3%	19.5%	11.1%	38.0%
NS	26.9%	0	18.7%	12.7%	58.2%
NW	33.2%	5.9%	0	11.5%	50.7%
EW	35.1%	9.4%	19.5%	0	64.0%

Table 3-2. Termination matrix based on all fractures mapped on outcrops (all fracture domains) in Laxemar. (After La Pointe et al. 2008, Table 4-57).

	Terminates Against				
Target Set	**ENE**	**N-S**	**WNW**	**SH**	**Bulk Termination**
ENE	0	25.5%	12.2%	6.5%	44.3%
N-S	11.8%	0	11.6%	4.5%	27.9%
WNW	14.1%	26.9%	0	6.0%	46.9%
SH	13.2%	20.7%	12.1%	0	46.0%

The analyses of the mass dimension from both borehole and outcrop data at Laxemar (La Pointe et al. 2008) suggest that a Euclidean scaling model best characterises the scaling of fracture intensity at scales greater than 10 m to 30 m and possibly at smaller scales. However, the data do not conclusively rule out fractal scaling at larger scales, because fracture data from outcrops are limited to scales not much greater than 30 m, and although the cored boreholes offer data records longer than 30 m, they do not adequately test fracture intensity scaling in all directions. The apparent fractal or non-Euclidean aspect of fracture intensity in boreholes at scales below a few tens of metres could be due to artefacts in the mass dimension calculation methodology. Analysis in La Pointe et al. (2008) suggest that the calculation of the mass dimension introduces an artefact due to the censoring of data below a size threshold, in this case the borehole diameter.

The mass dimension analysis described in Fox et al. (2007) and La Pointe et al. (2008) applies to the set of all fractures. It is possible that the sets of open fractures would have different scaling behaviours. Furthermore it is known that, for an infinite system at the percolation threshold, the set of connected open fractures in the DFN models would have a fractal spatial distribution (Bour and Davy 1998).

Hydrogeological DFN modelling assumptions

A Poissonian spatial model has been adopted to describe the open fractures, on the basis of the geological argumentation in favour of this distribution for all fractures on the scale of tens of metres. It should be noted that this does not imply that the distribution of flow-conducting fractures also exhibits a Poissonian spatial structure, as fractal clustering of flow-conducting fractures can arise spontaneously in a fracture system if it is close to the percolation threshold (see Bour and Davy 1998, Follin et al. 2006, and Section 4.5).

For simplicity there was no attempt to honour the fracture termination relationships between fracture sets in the modelling described in this report. The assumption of a Poisson point spatial model, without modification to allow for fracture termination behaviour, means that fracture intensity follows Euclidean scaling. It follows that the fracture intensity-size relationship can be considered independently of observation scale, leading to the tectonic continuum hypothesis described in 3.3.7.

3.3.7 Concepts for fracture intensity and fracture size

The intensity of fracturing can be measured and expressed in several ways usually depending on the method by which fractures are mapped. The main measures of intensity are defined as:

- P_{10} [m^{-1}] – average fracture frequency along a borehole or scan-line in rock.
- P_{21} [m/m^2] – average fracture trace length per unit area of rock, for example on an outcrop or lineament map.
- P_{32} [m^2/m^3] – average fracture surface area per unit volume of rock.

The first two of these are used commonly to collate field data since they can be computed readily. However, both are subject to bias introduced by the orientation in which a measurement is made relative to the orientation of fractures. Hence the process of Terzaghi correction (Terzaghi 1965) is used. P_{32} is often considered an unbiased fracture intensity statistic, although it is difficult, if not impossible, to measure in the field directly. It is used to parameterise and characterise fracture intensity in models because of its independence of how you sample fracture data by means of boreholes or traceplanes. In practice, P_{32} is of estimated by the Terzaghi corrected value of P_{10}, $P_{10,corr}$ (Dershowitz and Herda 1992). It should be noted, however, that the value of P_{32} is dependent on fracture size, whereas the Terzaghi correction method is not (Darcel et al. 2004; Follin et al. 2005, Davy et al. 2006).

In order to model the intensity of fractures with sizes comparable to the borehole radii to the size of the regional deformation zones the so called tectonic continuum hypothesis has been used (Fox et al. 2007, Darcel et al. 2009). This hypothesis states that a single fracture population extends in size over a very large scale range; for example, from meters to kilometres. In the tectonic continuum model, the fractures in outcrop with traces on the scales of meters are part of the same fracture population as lineaments or deformation zones with traces on the scale of kilometres. This model allows for the combination of data sets at multiple scales, but rules have been set up to avoid double-counting, cf. Figure 3-3.

Evidence for the applicability of the tectonic continuum concept comes from analysis of fracture trace lengths, as measured on outcrops at the smallest scale, through regional lineaments up to the largest lineaments with lengths of several kilometres 10 km (Fox et al. 2007, Darcel et al. 2009). Examples of such analyses of the tectonic continuum concept are shown in Figure 3-8 and Figure 3-9 for Forsmark (Fox et al. 2007), presented as area-normalised size-intensity observations for the sub-vertical north-east set and the sub-horizontal set. Here, plots are shown for fracture domain FFM02 since this domain outcrops within the tectonic lens and was used as the basis for intensity-size distributions of deeper fracture domains FFM01 and FFM06 that form the candidate volume. These plots show collate intensity-size distributions for the deformations zones (DZ) models within the geological local model area (clipped) and the regional model area (Regional), lineaments interpret from ground magnetic surveys, linked lineaments from the outcrop surveys AFM001264 and AFM100201, Geo-DFN models of the outcrop traces (P_{32} Fit to Trace Data), and the interpreted tectonic continuum intensity-size model (TCM).

A power-law fracture size distribution is inherently scale invariant which is conceptually consistent with the tectonic continuum hypothesis. The key parameters for a power-law fracture size distribution, measured in terms of the radius r of a disc, are the shape parameter (k_r) and the location parameter (r_0). The distribution, $f(r)$, is defined as

$$f(r) = \frac{k_r r_0^{k_r}}{r^{k_r+1}}, \tag{3-3}$$

where $r_0 \le r < \infty$, $r_0 \ge 0$, and $k_r \ge 0$. If P_{32} $[r > r_0]$ denotes the fracture surface area intensity of all fractures larger than the location parameter then the intensity of fractures larger then r_1 is:

$$P_{32}[r > r_1] = P_{32}[r > r_0]\left(\frac{r_0}{r_1}\right)^{(k_r-2)} \tag{3-4}$$

For practical reasons it is often necessary to generate a truncated distribution of fracture sizes $r_{min} \le r < r_{max}$. The upper limit corresponds with a typical censoring limit for the size of smallest deformation zones interpreted in the SDM, c 564 m (i.e. 1 km trace length), while the lower limit is controlled by numerical limits on how many fractures can be generated and stored by the software used. For the Hydro-DFN modelling performed to interpret the PFL tests in boreholes at the two sites, r_{min} was set to 0.28 m in volumes immediately surrounding the boreholes, but increased to 2.24 m further away so as to make simulations tractable (Follin et al. 2007a, Rhén et al. 2008) The intensity within the size interval $r_{min} \le r < r_{max}$ is given by:

$$P_{32}[r_{min}, r_{max}] = P_{32}[r > r_0]\left(\frac{(r_{min})^{(2-k_r)} - (r_{max})^{(2-k_r)}}{(r_0)^{(2-k_r)}}\right) \tag{3-5}$$

The probability that a fracture of a given size, intersects any plane (for example the outcrop surface) is linearly proportional to the size (La Pointe 2002). In other words, larger fractures have a higher probability of intersecting a plane than do smaller ones. Hence, the trace patterns observed in outcrop or in lineament patterns are biased in that they preferentially record the trace of the larger fractures. An equation that describes the power-law distribution of trace lengths can be used to describe the shape parameter of the parent radius distribution by simply adding 1.0 to the trace length shape parameter (La Pointe 2002).

In the models applied at Forsmark and Laxemar, it has been assumed that the set of open fractures can be characterised with a power-law size distribution. The value of r_{max} has been set to 564 m (the radius of a disk with the same area as a square fracture of side 1,000 m). 1,000 m was chosen as an appropriate limit for the minimum size of deterministic structures as a fair balance between model resolution and modelling efforts in identifying deformation zones within the geological local model volume, to ensure a homogeneous resolution of structures throughout the entire model volume. To honour the assumption, or conceptual model, called “tectonic continuum”, all smaller stochastically modelled structures need to have a maximum size that correspond to the minimum size of the deterministic features. The location parameter, r_0, was generally assumed to be equal to the radii of the core drilled boreholes used in obtaining fracture intensity from BIPs and core description, that is $r_0 = 0.038$ m. This provides a lower limit on the size of fractures measured. Model variants have been developed with different location parameter values to understand the sensitivity of the models to this parameter (see Section 4.5). The minimum fracture size, r_{min}, was set as close as practical to

r_0, based on considerations of simulation run times and memory use. For the Hydro-DFN modelling performed to interpret the PFL tests in boreholes, r_{min} was set to 0.28 m in a cylinder of radius 2.83 m surrounding the axis of the borehole, and the P_{32} for $0.28\ m \le r < 564\ m$ was calculated from Equation 3-5 with P_{32} $[r > r_0]$ estimated from the measured values of $P_{10,corr}$ for open fractures. Outside of this cylinder fractures were generated in the size range $2.24\ m \le r < 564\ m$ with P_{32} for this size range again calculated from Equation 3-5. This nesting of the scale of fractures generated is necessary to include small metre scale fractures around the borehole that can provide additional connections between larger fractures and the borehole, while avoiding generating metre scale fractures over volumes that typically of side 1 km. In sensitivity tests it was found that including the fractures $0.038\ m \le r < 0.28\ m$ made little difference to the calculation of inflows to a borehole as such small fractures were rarely connected.

The motivation for the assumption of a tectonic continuum with a power-law intensity-size distribution comes from the analysis of all fractures in the Geo-DFN (Fox et al. 2007, La Pointe et al. 2008, Darcel et al. 2009). For hydrogeological purposes it is the set of open fractures that are of interest, but these constitute a subset of the fracture network considered in the Geo-DFN. The consequence, therefore, of the assumption of tectonic continuum is that the size distribution of open fractures is also likely follow a power-law distribution, although it is conceivable that the exponent may be different if the likelihood a fracture is open is correlated to size. Hence, it is a working assumption in the hydrogeological DFN modelling that open fractures also follow a power-law size distribution. The borehole core mapping and PFL-f method have been used to estimate the fracture surface area intensity of open fractures and flow-conducting fractures, respectively. In simulations, the intensity of flow-conducting fractures is critically sensitive to the intensity-size distribution of the open fractures; this allowed calibration of the intensity-size distribution of the open fractures, as described in Section 4.5.

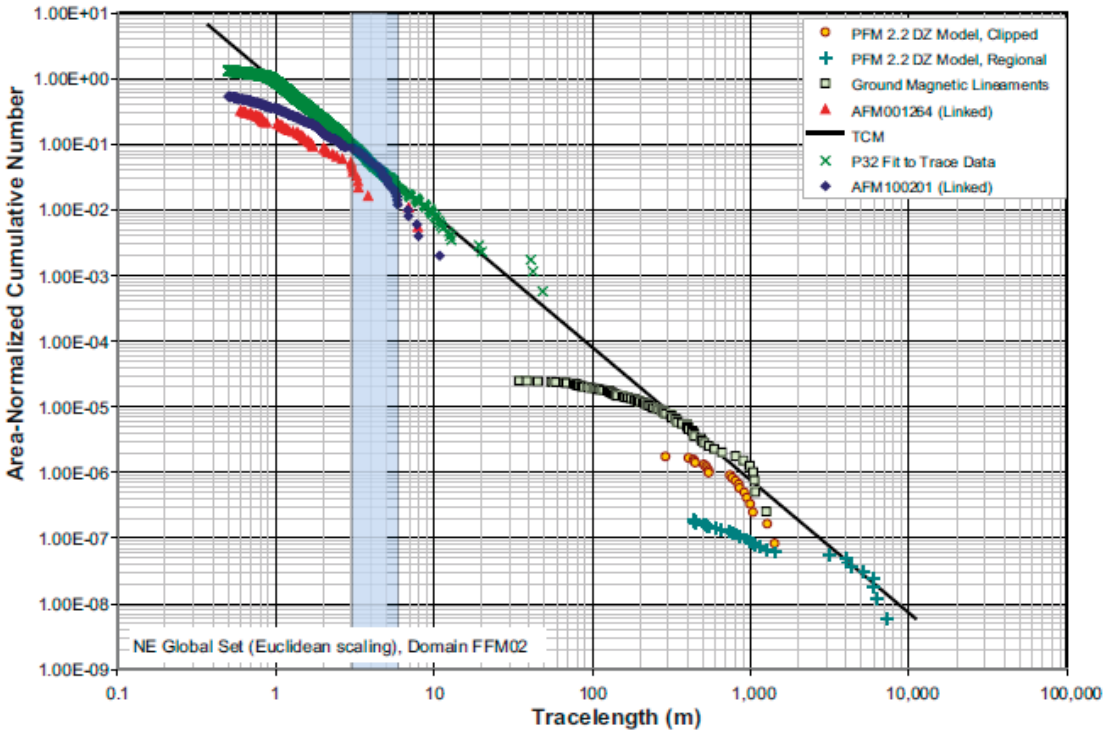

Figure 3-8. *Example of fracture size distributions interpretation from Forsmark (After Fox et al. 2007, Figure 6-10). The fit is for the north-east set within fracture domain FFM02 that outcrops inside the tectonic lens and provided the basis for the size distribution in the deeper FFM01/FFM06 as well. The first 3 data series in the legend are either deformation zones or lineaments; AFM data is from two outcrops; TCM is a tectonic continuum model fit.*

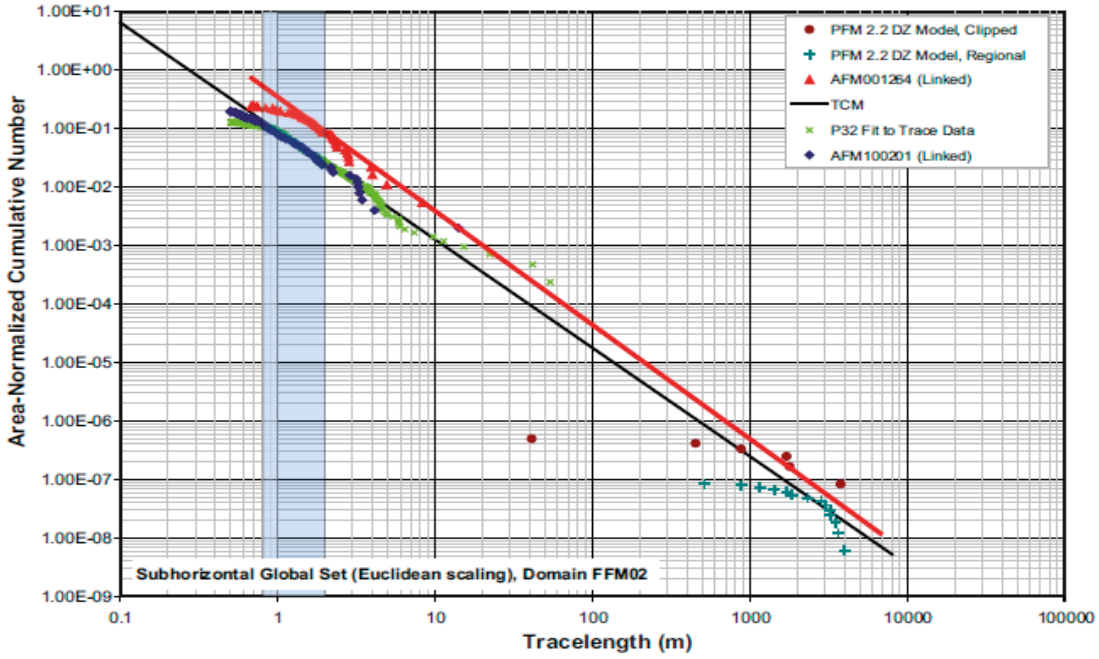

Figure 3-9. *Example of fracture size distributions interpretation from Forsmark (After Fox et al. 2007, Figure 6-24). The fit is for the sub-horizontal set (bottom) within fracture domain FFM02 that outcrops inside the tectonic lens and provided the basis for the size distribution in the deeper FFM01/FFM06 as well. The first 2 data series in the legend are either deformation zones or lineaments; AFM data is from two outcrops; TCM is a tectonic continuum model fit.*

3.3.8 Fracture network connectivity and hydraulic properties

Although fracture transmissivities at Forsmark and Laxemar can be estimated from the PFL-f tests in the core drilled boreholes, this requires an additional set of assumptions. For each PFL-f fracture identified, the changes in inflow to the borehole and head after several days of pumping relative to conditions prior to pumping are calculated. A transmissivity value is interpreted for the PFL-f measurement based on an assumed radius of influence of 19 m (see Section 2.6.2). The choice of 19 m reflects that tests are performed over several days, and hence should represent an effective transmissivity of the whole fracture intersected, and possibly adjoining parts of the network, but 19 m is otherwise arbitrary. It was chosen for convenience in evaluating hydraulic tests, as parts of Thiem's equation (Thiem 1906) cancel out with this assumption, leading to transmissivity equal to the measured specific capacity. Consequently, the interpreted values of transmissivity should not be viewed as necessarily the transmissivity of an individual fracture, or the transmissivity of the fracture local to the borehole intersect. They are more indicative of the effective transmissivity over a larger scale. In other words, the evaluated PFL-f transmissivities are effective values, representing the total specific capacity for the flow-paths between the tested borehole interval and surrounding constant head boundary. The distance to the hydraulic bottleneck or head boundary cannot be deduced directly from data.

It is considered preferable to use flow simulations where fracture transmissivity is treated as a fitting parameter and the calibration criterion is that specific capacity is reproduced in the simulated inflow (see Follin et al. 2007a, Rhén et al. 2008, Frampton and Cvetkovic 2010) as examples of such calibration). The benefit of this method is that it circumvents relying on assumptions of flow dimension, yet honours borehole data in terms of flow. Furthermore, network scale flow channelling effects, as distinct from flow channelling within a single fracture, arise naturally due to fracture connectivity issues. The effects of within-fracture variability relative to those of fracture-to-fracture variability were investigated by Painter (2006) using DFN simulations within in-plane variability (a simple multi-Gaussian random space function model was applied). It was found that within-fracture aperture variability has little effect on field-scale transport because it is overwhelmed by the much larger fracture-to-fracture variability. The effect of in-plane variability was quantified as a reduction in transport related flow resistance of 50% at the low end of the distribution and about 15% in the median.

Flow channelling within fractures

It is known that preferential flow-paths can develop within fractures, or at their intersections. They arise because fracture surfaces can be uneven and mineralised, resulting in groundwater flow and contaminant concentrations that are distributed non-uniformly across a fracture. Flow channels arising at the intersection of crossing or terminating fractures have been suggested as possible conduits for preferential flow and transport in fractured rock (NRC 1996). Observations of increased flow at fracture intersections in tunnels constructed in crystalline rock have been reported (Abelin et al. 1990, 1991, 1994, Neretnieks 1994), and observations of such flow features have also been documented at the Forsmark site by Carlsson and Olsson (1977) who studied inflow to tunnels in the vicinity of the nuclear power plant.

A concern for hydrogeological interpretation is that if flow channels are narrow, and sparsely distributed within individual fractures, the frequency of flow-conducting fractures in the rock could be underestimated during flow logging due to the low probability of intersection with a borehole. This has been referred to as a Type 1 flow censoring effect (Crawford 2008). Even if hydraulic testing successfully detects the nearby presence of a flow conduit, the borehole is unlikely to intersect it directly and therefore the effective transmissivity of the structure may be underestimated. This has been referred to as a Type 2 flow censoring effect (Crawford 2008). Flow censoring effects are illustrated in Figure 3-10.

Within DFN models fractures are typically represented as homogeneous planar structures. This description reasons that flow at the scales of interest can be adequately represented by the assignment of an effective transmissivity value for a single fracture that represents the overall flow-rate through the fracture over its area. This approach is used because flow channelling within fractures is both difficult to characterise and computationally expensive to simulate. The absence of flow channelling within factures in the Hydro-DFN models has the potential to bias the predictions of these models, and must therefore be assessed.

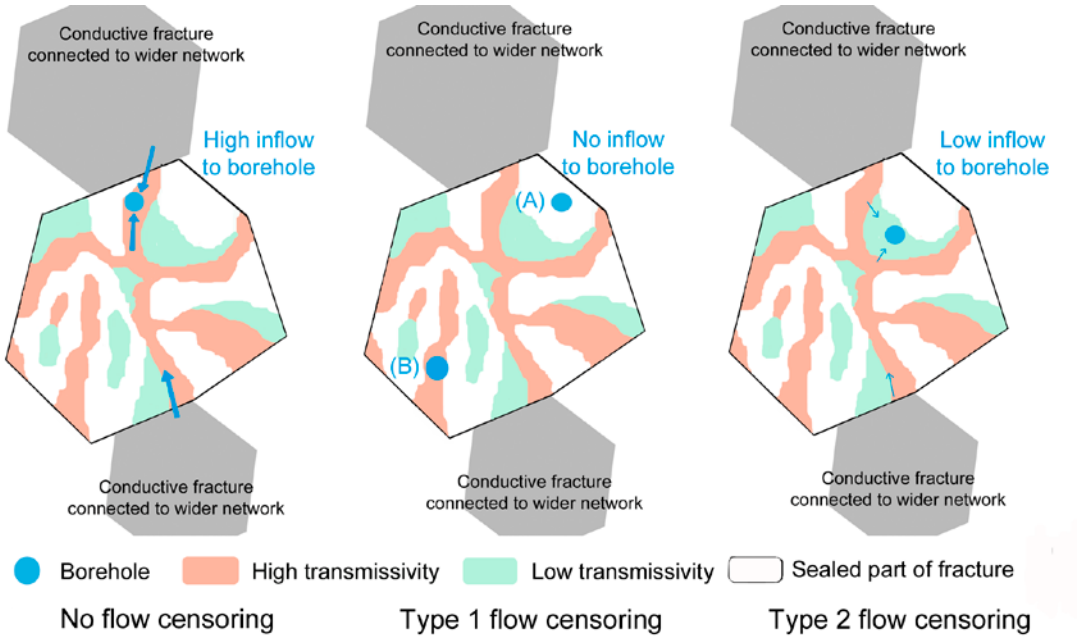

Figure 3-10. *An illustration of different types of flow censoring possible when hydraulic testing is applied to a fracture with variable hydraulic aperture. During PFL-f testing pumping leads to inflows to the borehole, indicated by blue arrows. In type 1 flow censoring the flow-conducting path is not detected at all, either because the borehole intersects a sealed area of the fracture (A), or because the borehole intersects a hydraulically isolated area (B). In type 2 flow censoring the flow-conducting path is detected, but the effective transmissivity of the flow-conducting path is underestimated. (After Crawford 2008).*

The potential biases that uncertainties about flow channelling within fractures could introduce to the Hydro-DFN models therefore include the following:

1. The flow channels within fractures could be so narrow, of the order of a few centimetres width, that their frequency might be underestimated when using borehole logging methods (a Type 1 flow censoring effect).
2. If hydraulic testing successfully detects the nearby presence of a flow conduit, the borehole is unlikely to intersect it directly and therefore the transmissivity of the structure may be underestimated (a Type 2 flow censoring effect).
3. Even assuming the above points are not significant, it is possible that the Hydro-DFN model predictions of distributions related to the safety assessment, such as advective travel time, flow-related transport resistance, and equivalent flux at the release point (see Section 7), might still be biased by neglecting in-plane heterogeneity or fracture intersection zones.

These issues have been addressed through a combination of arguments. Points (1) and (2) have been quantified through generic scoping calculations and analysis of pressure responses to hydraulic tests in boreholes as discussed below. The work undertaken to address point (3) includes modelling studies of both in-plane heterogeneity in transmissivity, and of the influence of fracture intersection zones, as discussed in Section 7.6.

Concerns about Type 1 flow-censoring have been considered in detail in the report for transport properties at the Forsmark site (Crawford 2008), where it was concluded that most flow-conducting features should be identifiable from borehole investigations even in the presence of highly channelised flow arising due to surface asperity contacts. The reason for this is that fracture planes need to support a certain level of in-plane connectivity in order for flow to exist at all in sparsely fractured rock. Further, it was found by simulations that for fractures with percentages of area which is sealed due to surface contact of up to 30%, then the fractures should be sufficiently well connected hydraulically that detection of in-plane flow channels is almost certain, provided that the borehole at least partially intersects a hydraulically open region of the fracture and assuming fracture filling materials do not fill the pore space. For surface contact fractions of approximately 40% and upwards hydraulically isolated areas could occur, reducing the chance by the same percentage of a positive identification depending upon where the borehole intersects the fracture plane in relation to the flow-conducting area. This means that the true frequency of flow-conducting fractures could be approximately 1.6 times (1/0.6) that estimated from the PFL-f data. This was thought likely to be an overestimate, as a borehole can partially intersect a hydraulically open region and still register a positive detection of a flow-conducting feature.

Fractures become essentially non-conductive for surface contact fractions above about 50%, which is the theoretical percolation limit for 2D bond networks (Kesten 1980). This analysis assumed that the longest correlation length for hydraulic aperture variation is substantially less than the size of the fracture under consideration. The actual measurement bias will depend upon the effective correlation length for hydraulic aperture variation in relation to the borehole diameter. The more transmissive fractures were thought likely to be the least compressed, and should therefore exhibit small surface area contact fractions (Crawford 2008). The least transmissive fractures were likely to exhibit greater a degree of surface contact, meaning that a larger biasing effect for fractures belonging to the lower end of the transmissivity spectrum might be expected. Therefore Crawford (2008) considered that although Type 1 flow censoring effects are probably present, they were not expected to have a significant impact on the more transmissive fractures within the HRD.

Concerns about Type 2 flow-censoring have been addressed through analysis of hydraulic tests in boreholes. Generalised radial flow analysis of PSS hydraulic responses in packed off borehole sections at Forsmark (Follin et al. 2011) suggests that most flow-conducting features (70–90%) are associated with flow dimensions greater than 1.5, although a significant minority (10–30%) exhibit smaller flow dimensions characteristic of approximately linear flow channelling. This result is generally consistent with the notion of a hydraulically well connected flow space within the fractures that have been measured.

Generalised radial flow analysis of PSS hydraulic responses in packed off borehole sections at Laxemar (Rhén et al. 2008) suggests that greater than 90% of flow-conducting features on a 5 m test scale are associated with flow dimensions greater than 1.5. Only a limited number of test sections gave indications of approximately linear flow channelling. In the transient analyses reported by Rhén

et al. (2008), approximately 20% of the 5 m test sections gave indications of positive skin effects or recharge boundaries which could be interpreted as strongly transmissive flow channels embedded in less transmissive features (that is, where the borehole happens to intersect a less transmissive region of the flow space). It is therefore not possible to strictly rule out Type 2 flow censoring effects in the available hydrogeological data set, although it appears likely that this only influences a minority of identified features. Based on this reasoning it is speculated that network-scale flow channelling effects probably dominate, although the other more localised flow channelling effects described above are also likely to be present in Laxemar and cannot be completely discounted.

Network scale flow channelling

Network scale flow channelling refers to the tendency of heterogeneous fracture networks to exhibit poor hydraulic connectivity and form preferential flow-paths on the scale of the fracture network itself. When there are large contrasts between transmissivities of individual fractures comprising the network, groundwater flow will tend to seek out the path of least hydraulic resistance. Network scale flow channelling processes of this kind are taken to include both regional flow channelling within deformation zones in the HCD, as well as on the scale of local fracture clusters within the HRD. The modelling procedure described in this report simulates flow channelling phenomena on the network scale. These arise naturally as a consequence of the modelling methodology because of fracture connectivity issues.

The flow properties of crystalline rock are determined by both the fracture network connectivity and the hydraulic properties of the fractures. This is because in sparsely fractured rock the connectivity between fractures, as well as the upstream fracture transmissivity, might be the constraining factor for flow. Hence the treatment of both fracture connectivity, which is governed by the geometric properties of the open fractures, particularly the intensity-size distribution, and the hydraulic properties, cannot be constrained independently unless additional assumptions are made. The conceptual model of network scale flow channelling effectively determines the emphasis placed on network connectivity (involving geometric properties) versus transmissivity (hydraulic properties) in simulating sparse flow networks.

In order to separate fracture connectivity issues from the fracture hydraulic properties the measured intensity of PFL-f fractures has been equated with the simulated intensity of open fractures which are part of a percolating network: These fractures are called “connected open fractures”. The conceptual model therefore has a geometric interpretation of flow-conducting fractures, meaning that the geometric properties of the open fractures can be considered without reference to the hydraulic properties. Once the geometric properties are determined, the hydraulic properties can be addressed through a subsequent stage of the model calibration process.

Equating the intensity of connected open fractures with the intensity of PFL-f fractures in the simulations of the single-hole hydraulic tests is an important part of the conceptual model. It means that the experimental detection lower limit of specific capacity in the PFL-f method of approximately 10^{-9} m^2/s is integral to the Hydro-DFN models. In light of this, the interpretation given to the set of fractures described by the Hydro-DFN model should be revised, perhaps to ‘the hydraulically open portions within an otherwise sealed fracture which, when in the context of a PFL-f hydraulic test, have the potential to yield specific capacities above the experimental detection limit’. The potential to use alternative methodologies, where the interpretation of the potentially flow conducting fractures would not be linked to the experimental detection limit of the PFL-f test, are discussed in Section 8.3.

The exclusion from the Hydro-DFN model of fractures which would lead to PFL-f measurements below the detection limit on specific capacity has the potential to under-estimate the number of flow-conducting fractures. The effects on repository performance measures such as initial flux around a deposition hole and flow-related transport resistance is estimated in Section 7.1. In the upper bedrock the greater intensity of high transmissivity flow-conducting fractures means that the distributions of specific capacity are well characterised, and this is not thought to be a significant issue. It is thought that the total flow-rates to boreholes are well constrained because the highest inflows are detected by the PFL-f and PSS methods. These conclusions are supported by observations during the construction on the ONKALO facility in Finland. During investigations at Olkiluoto, construction of underground facilities has allowed a reduced detection limit of the PFL-f method. This is due to an effectively

increased drawdown when operating at depth from tunnels at atmospheric pressure. The reduction in the detection limit led to more flow-conducting fractures being observed at depth, but the total inflows were comparable to those measured from surface-based boreholes (Hartley et al. 2011).

Size-transmissivity distributions

Within the Hydro-DFN model, transmissivities are specified stochastically for each individual fracture within the HRD. The transmissivity distribution is allowed to vary between fracture domains, by depth zone and by orientation set. Because of the uncertainties in the values estimated from flow logging tests, transmissivity distributions for the set of open fractures are estimated as part of a calibration process, where the single-hole PFL-f tests are modelled explicitly. Uncertainties in the transmissivity distributions are addressed through the use of three alternative relationships between transmissivity and fracture size, as indicated in Table 3-3.

The three transmissivity relationships considered are:

- "Correlated" – the fracture transmissivity is directly related to the fracture radius.
- "Semi-correlated" – the fracture transmissivity is related to the fracture radius, but subject to some variability.
- "Uncorrelated" – the fracture transmissivity is not related to the fracture radius, but does exhibit variability around an average value.

Arguments exist for assuming a correlated model. One such argument is the support-scale for hydraulic tests, where a high transmissivity value could imply a large influence radius. Conversely small values could either imply a short influence radius, or else in-plane variability with the borehole intersecting a relatively closed part of the fracture. Another argument is that there exist geologic observations on weak correlation between trace length and maximum visible aperture. The width of deformation zones is also larger for large zones (Stephens et al. 2007), and it seems plausible that the same should hold for large fractures. The uncorrelated model is considered to have little physical basis in light of the arguments above. The most realistic model is perhaps some kind of semi-correlated model, but this involves additional assumptions about how it should be parameterised.

The semi-correlated and uncorrelated cases have typically been truncated at $\pm 2\sigma$ to avoid stochastic generation of transmissivities with very high or low values, where σ is the standard deviation of the Logarithm of the transmissivity (see Table 3-3). An additional check on the plausibility of transmissivity parameters was to calculate the maximum transmissivity that would be expected for a stochastic fracture and ensure this did not significantly exceed the maximum transmissivity measured in the deterministically interpreted deformation zones (HCD). The maximum transmissivity was calculated based on the size of the largest stochastic fracture, r = 564 m, for the correlated and semi-correlated models, and adding two standard deviations for the semi-correlated and uncorrelated models. This ensures that when the hydrogeological DFN model is applied on the regional-scale no anomalously high transmissivities are generated compared to field data.

Table 3-3. Transmissivity parameters used for all sets when matching measured PFL flow distributions. (After e.g. Follin et al. 2007a, Table 11-16).

Transmissivity relationship	Description	Relationship	Parameters
Correlated	Power-law relationship	$\log(T) = \log(a\, r^{b})$	a , b
Semi-correlated	Log-normal distribution about a power-law correlated mean	$\log(T) = \log(a\, r^{b}) + \sigma_{\log(T)}\, N(0,1)$	a , b, $\sigma_{\log(T)}$
Uncorrelated	Log-normal distribution about a specified mean	$\log(T) = \mu_{\log(T)} + \sigma_{\log(T)}\, N(0,1)$	$\mu_{\log(T)}$, $\sigma_{\log(T)}$

3.3.9 Fracture storage properties

Specific storage properties for the crystalline rock of the HRD were difficult to assess directly from hydraulic tests. Rough estimates could be obtained from rock mechanical parameters (Rhén et al. 2008). An alternative approach was to use the relation between hydraulic feature transmissivity and the storage coefficient estimated for the HCD based on analysis of interference test data. There were however no storage coefficient data from tests in the transmissivity range < $1 \cdot 10^{-7}$ m^2/s at Laxemar. This makes the assessment of the storage coefficient uncertain for low-transmissivity features in the hydrogeological DFN models. The fracture storage properties are therefore estimated by calibration to the interference test data at both Forsmark and Laxemar.

3.3.10 Fracture transport properties

Solute transport in fractured rock is thought to occur primarily along advective flow-paths within fractures and deformation zones. Matrix diffusion coupled with sorption was identified as the main retardation process that limits the rate at which solutes are transported along these flow-paths.

The parameters used to model transport depend on the model concept being used in the simulations (that is, a DFN or CPM model concept). However, a key variable is the transport aperture of the fractures, e_t, which is assumed to follow a power-law in fracture transmissivity:

$$e_t = a \cdot T^b \tag{3-6}$$

For SDM-Site Forsmark, the Hydro-DFN models assume a=0.46, b=0.5 (Follin 2008). For SDM-Site Laxemar the Hydro-DFN models assume a=0.404, b=0.705 (Rhén et al. 2009). In Crawford (2008), estimates of the advective transport time were made using a macroscopic cubic law based upon the Hagen-Poiseuille equation for flow in a parallel plate slit, as well as a macroscopic quadratic law based upon a previous study by Uchida et al. (1994). Two further variants have been proposed in Rhén et al. (2008) based upon site specific data for Laxemar as well as previous work described in Rhén et al. (1997).

For a DFN model concept, advective travel time through a fracture network is calculated as

$$t_r = \sum_f \frac{e_{tf} w_f \delta l}{Q_f}, \tag{3-7}$$

where δl is a step length along a path through the fracture network taking f steps, each between a pair of fracture intersections, e_{tf} is the fracture transport aperture, w_f is the flow width between the pair of intersections, and Q_f is the flow-rate between the pair of intersections in the fracture. The other important transport property is the flow-related transport resistance which determines both the amount of retention of radionuclides by sorption on the surface of fractures and the diffusive exchange of solutes in fractures with the adjoining rock matrix, and is defined as

$$F_r = \sum_f \frac{2 w_f \delta l}{Q_f}, \tag{3-8}$$

having units of time over length.

Consequences of the uncertainty in the transport aperture are considered in Crawford (2008) and Crawford and Sidborn (2008). A review of the relationships between transport and hydraulic apertures, along with a summary of results from cross-hole tracer tests with conservative tracers, are given in Hjerne et al. (2010).

Modelling solute transport and the effects of rock matrix diffusion on the evolution of groundwater composition have generally been performed using the ECPM approach (see Chapter 5). This requires additional transport parameters including flow wetted fracture surface area per unit volume of rock and kinematic porosity which can be derived from the underlying description of a fracture network (see Chapter 5), in addition to matrix porosity, matrix diffusion length and effective diffusivity.

The values of flow wetted surface were defined as uniform within a given hydraulic rock domain and depth zone. These were estimated from measured average Terzaghi corrected intensity, $P_{10,corr}$, of flowing fractures detected by the PFL-f method, as $2 \cdot P_{10,PFL,corr}$, although other values were tried to illustrate the sensitivity to this parameter (see Rhén et al. 2009, Section 9.1.4, for example).

For the ECPM approach, the kinematic porosity is conceived as the fluid volume available within the connected fracture system, and hence is derived based on the description of the connected fracture system and transport aperture defined in the underlying Hydro-DFN model, as described in Section 5.1. For a given finite-element grid, the kinematic porosity in ECPM flow and transport models have been calculated element-by-element by upscaling the underlying Hydro-DFN calculated as the total connected fracture volume divided by the element volume (see Chapter 5). In this way the kinematic porosity is spatially varying according to the realisation of the Hydro-DFN model generated. The fracture volume for an individual fracture is calculated as the fracture area within an element multiplied by the transport aperture of the fracture. Although this approach provides a direct link between the assignment of kinematic porosity in the ECPM model and the underlying Hydro-DFN model, it relies on several approximations, including that the full fracture surface area contributes to advection and that the contribution to porosity of fractures below the truncation of fracture sizes in the regional DFN model is not significant.

For the SDM-Site, SR-Can and SR-Site hydrogeological modelling of Forsmark a matrix porosity value of $3.7 \cdot 10^{-3}$ was used (see Hartley et al. 2006b, Follin et al. 2008a, Joyce et al. 2010a), while Crawford (2008) collates laboratory sample measurements with median values for various rock classifications between c 2-3 10^{-3} over all samples and c 5 10^{-3} for strongly altered rock in deformation zones. For the SDM-Site modelling of Laxemar a matrix porosity value of $8 \cdot 10^{-3}$ was used (see Rhén et al. 2009, Joyce et al. 2010b), while the laboratory measurements collated by Crawford and Sidborn (2009) give median values for different rock types between c 1-4 10^{-3} outside of deformation zones, and 2-8 10^{-3} inside deformation zones. The relative importance of the kinematic porosity and matrix porosity depends on the timescales considered. Over long time scales, solutes have time to access at least some of the diffusion accessible porosity by rock matrix diffusion. Hence, the influence of both types of porosity on solute transport needs to be quantified.

The rate of diffusive transport in the rock matrix is determined by: the intrinsic diffusivity of the solute species in the pore water; sorption reactions; geometry of the porous system; and non-partitioning interactions between solutes and mineral surfaces. The resulting solute flux of these processes is measured in terms of the effective diffusivity. Laboratory tests provide estimates of the effective diffusivity in the range 2 10^{-14} to 6 10^{-13} m^2/s at Forsmark (Crawford 2008), and 3 10^{-14} to 6 10^{-13} m^2/s at Laxemar (Crawford and Sidborn 2009). A value of $1 \cdot 10^{-13}$ m^2/s was used for SDM-Site calculations at Forsmark (Follin et al. 2008a), and a value of $1.5 \cdot 10^{-13}$ m^2/s was used for SDM-Site calculations at Laxemar (Rhén et al. 2009). Matrix diffusion length is the maximum penetration distance of the solute into the matrix, and strictly is a dependent parameter equal to the reciprocal of flow-wetted fracture surface area per unit volume of rock (i.e. half the matrix block size). However, since the accurate calculation of rock matrix diffusion for large 3D models can put large demands on computational time and/or storage, then for practical reasons the diffusion penetration length can be truncated according to estimates of diffusion distance for the simulation time if this is shorter half the matrix block size. Such truncations were made for the deep rock, where matrix block sizes were typically several tens of metres (Follin et al. 2008a, Rhén et al. 2009).

In terms of the representation of hydrodynamic dispersion, the ECPM approach represents dispersion by macro-scale spatial variability explicitly by calculating a different permeability for each finite-element based on upscaling an underlying Hydro-DFN model. Hence, solute dispersion on scales larger than the finite-element sizes (20 m was used for the local scale at Forsmark, and 40 m for Laxemar) occurs naturally through the representation of a spatially varying permeability tensor. Therefore, hydrodynamic dispersion only needs to be represented at scales smaller than the finite-elements in order to mimic mixing taking place within the fracture network on the scale of a few tens of metres. Typically the longitudinal dispersion length was set to 75% of the element size and transverse was to 25% of element size (Follin et al. 2008a, Rhén et al. 2009). Such values also ensure numerical stability during long transient simulations, that molecular diffusion c 10^{-9} m^2/s would not suppress on its own.

Slightly different parameters were used in the repository performance assessment modelling to account for anion exclusion. For Forsmark, a preliminary estimate of the effective diffusivity had to be made in the hydrogeological modelling based on an anion exclusion reduction factor of 10 based on suggestion from the SR-Can data report (SKB 2006b). This gave a revised effective diffusivity of $4 \cdot 10^{-15}$ m^2/s (Joyce et al. 2010a). However, estimates of the anion exclusion factor were later revised

to √10 and the analysis of variability revised to give a range of 1×10^{-14}– 1×10^{-13} m^2/s, with the best estimate at 4×10^{-14} m^2/s (SKB 2010a). The revised effective diffusivity for Laxemar was $5\cdot10^{-14}$ m^2/s at Laxemar (Joyce et al. 2010b).

There were two main applications of transport modelling undertaken for SDM-Site and SR-Site:

- Simulate the palaeo-climatic evolution of the groundwaters (see Section 6.6) at Forsmark and Laxemar using the advection-dispersion equation with matrix diffusion. The aim of this modelling was to demonstrate that the hydraulic and transport parameters used allow a reasonable match to the available groundwater chemistry data.
- Predict distributions of quantities of interest as part of the repository safety assessment (see Chapter 7), and estimate some of the uncertainties in these distributions. The quantities of interest included the Darcy flux and equivalent flow-rate at release locations, and advective travel time and flow-related transport resistance along flow-paths (as described in Section 7.1). Transport calculations to determine inputs to the safety assessments have been based upon a particle-tracking approach.

3.4 Summary of the key assumptions

The hydrogeological DFN model of the HRD is a stochastic representation of the open fractures. An open fracture was identified as a hydraulically significant fracture, which would conduct flow if it were connected as part of a percolating network. The following list summarises the main fracture attributes and associated assumptions made in developing the Hydro-DFN model ordered according to importance in the modelling strategy. A different model parameterisation has been developed for each hydraulic rock domain and depth zone.

Fracture intensity scaling, spatial distribution and termination

Euclidean intensity scaling of the open fractures was assumed, with fracture centres generated through a Poisson point process. Fracture termination behaviour was not modelled.

Fracture intensity and fracture size

A tectonic continuum concept was assumed, with the intensity-size distribution of the open fractures assumed to follow a power-law. The power-law parameters were established by calibrating models of the single-hole PFL-f hydraulic tests, as discussed in Section 4.5.

Fracture orientations and set definitions

The open fractures were grouped into sets based on orientation. The definition of the sets was the same for all depth zones and hydraulic rock domains. Sets were characterised by a univariate fisher distribution.

Concepts for the hydraulically significant fractures

The fracture surface area intensity of open fractures was equated with the Terzaghi corrected intensity of fractures classified as open or partly open in the borehole logs. A classification based on open or partly open fractures with a certain or probable appraisal was used as a variant for the Laxemar modelling.

Fracture hydraulic properties

Three different models were assumed to describe the size-transmissivity distribution of the open fractures. The appropriate model parameters were established by calibrating models of the single-hole PFL-f hydraulic tests, as discussed in Section 4.6.

Transport properties

An assumed relationship between transport aperture and transmissivity was adopted based on a collation of tracer test results.

Storage properties

Storage properties (specific storage for ECPM models) were estimated through calibration of regional-scale models against data from hydraulic interference tests.

Fracture shape

The open fractures were assumed to be square. The sensitivity to non-equant fracture dimensions was not tested.

4 Calibration of the HRD model

4.1 Overview of calibration methodology

Calibration of the Hydro-DFN model of the HRD involves defining probability distributions which describe all of the geometric, hydraulic and transport properties for the set of open fractures. This is done for each hydraulic rock domain, depth zone and orientation set.

Using the assumptions described in Section 3, some parameters, such as the orientation distributions and the intensity of open fractures, can be estimated directly from data. Other parameters, such as those relating to fracture intensity-size and size-transmissivity distributions are estimated through an iterative calibration process. The calibration methodology is based on simulation of the PFL-f testing of individual boreholes, followed by a suite of confirmatory testing applied to regional-scale models. The calibration process used can be considered in five consecutive steps:

1) Calculation of the fracture orientation parameters and the intensity of open fractures from boremap data.
2) A consistency check, that is, a confirmation that the estimated geometrical parameters (intensity and orientation distributions) for each fracture set can be used in DFN simulations of open fractures to yield, on average, the measured (Terzaghi corrected) fracture intensity for open fractures, intersecting a borehole.
3) A network connectivity calibration, with the aim of establishing appropriate parameters governing the geometrical connectivity around a borehole. This is done by changing the intensity-size distribution parameters of the open fractures to achieve the observed Terzaghi corrected intensity of PFL-f fractures.
4) A flow calibration using the observed specific capacities reported using the PFL-f method, with the aim of establishing appropriate parameters for the three size-transmissivity models proposed (the transmissivity models are described in Table 3-3).
5) A series of confirmatory tests based on simulations at a regional-scale to establish whether a DFN parameterisation based on data at the borehole-scale could be used to describe flow and transport at the regional-scale. Transport and storage properties were considered at this stage. Some hydraulic parameters were revised.

The first four of these stages are described in this section. The fifth is described in Section 6. The process is summarised in a flow chart, Figure 4-1. Examples of the application of the methodology are presented for FFM01/FFM06 in Forsmark, and HRD_C in Laxemar as these hydraulic domains contain the largest proportion of the candidate volumes at the sites.

The hydraulic rock domains are parameterised in terms of a stochastic DFN model, by calibration against available hydraulic data mainly from the PFL-f tests. The hydrogeological DFN modelling is based on the assumption that:

$$P_{10,all} \geq P_{10,o} \geq P_{10,cof} \geq P_{10,PFL} \quad (4\text{-}1)$$

where $P_{10,all}$ denotes the Terzaghi corrected fracture intensity of all fractures recorded intersecting a borehole. Similarly $P_{10,o}$ and $P_{10,PFL}$ denote the Terzaghi corrected fracture intensity of open fractures and PFL-f fractures intersecting a borehole, respectively. These values can be interpreted directly from the physical measurements such as the boremap and PFL-f data, subject to the assumptions described above. $P_{10,cof}$ denotes the frequency of "connected open fractures"; this is a key property of any Hydro-DFN model, and refers to the intensity of those hydraulically open fractures which form part of a percolating network. The meaning of the different suffixes (all, o, cof and PFL) is illustrated in Figure 4-2.

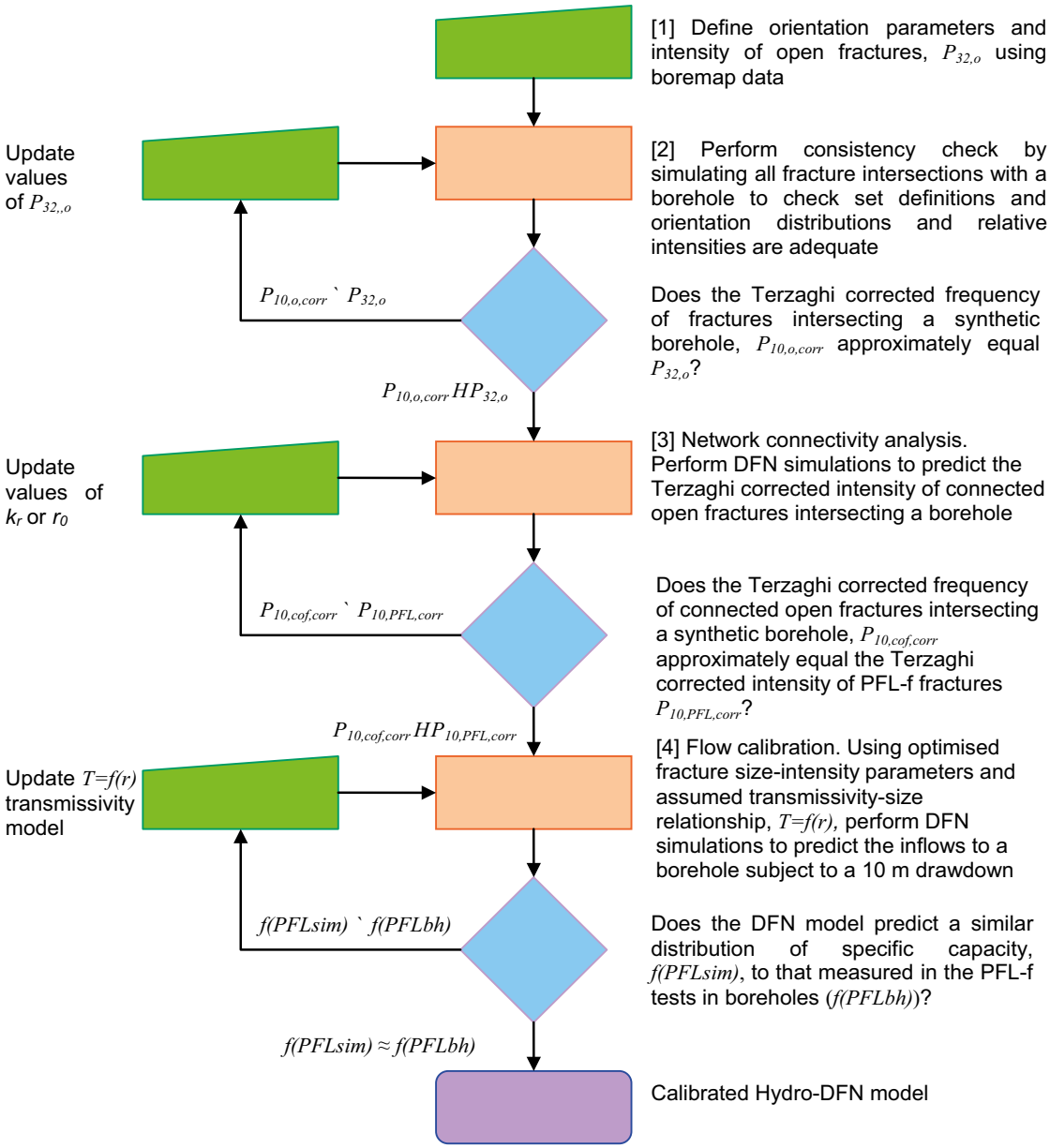

Figure 4-1. *Flowchart showing the process for obtaining optimised Hydro-DFN parameters using an iterative simulation procedure to match the measurements made using the PFL-f method in core drilled boreholes. After Crawford (2008).*

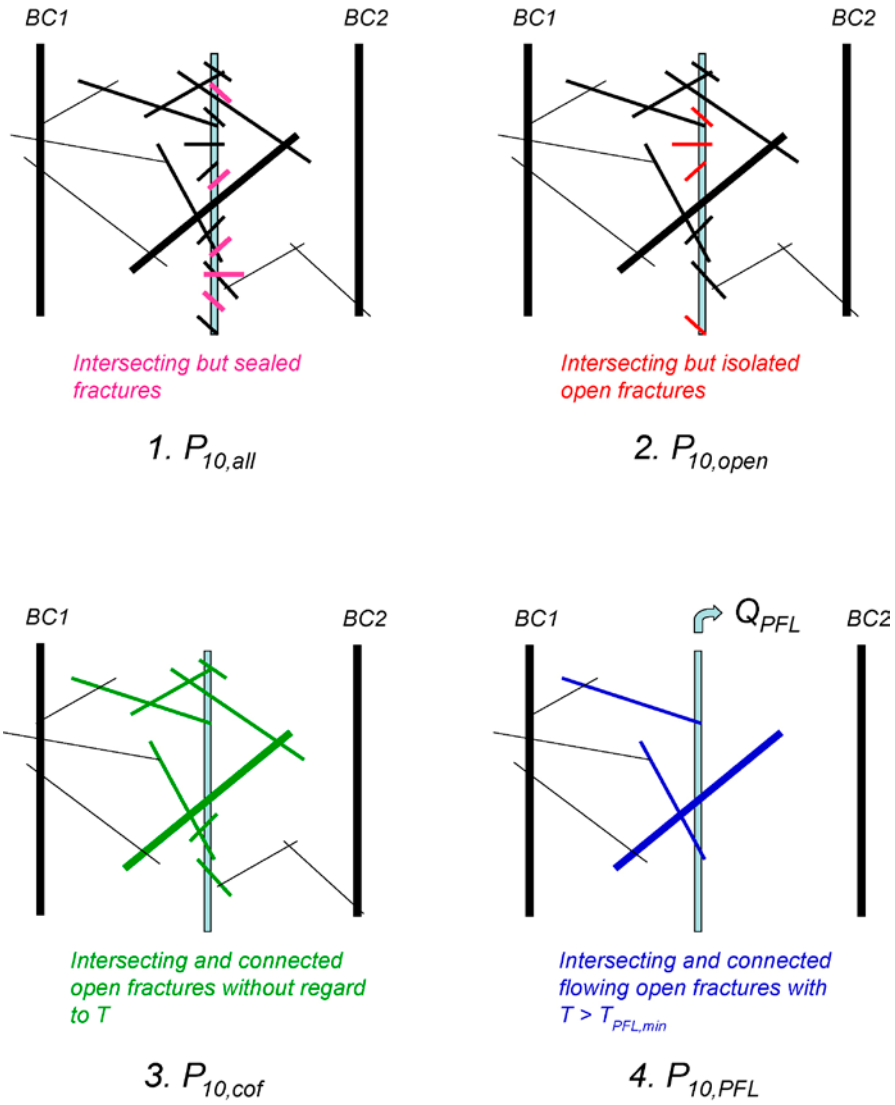

Figure 4-2. *The intensity of 1) All fractures intersecting the borehole, 2) open fractures, 3) connected open fractures (cof) and 4) flow-conducting fractures that have a transmissivity greater than approximately 10^{-9} m^2/s. BC1 and BC2 are constant-head boundary conditions. (After Follin et al. 2007a, Figure 11-1.)*

The hydrogeological DFN model calibration of the fracture intensity-size distribution and the fracture size-transmissivity distribution were based on the simulation of the PFL-f hydraulic tests conducted in individual boreholes. Typically this involved a simulated vertical borehole which was 1,000 m long, inserted through the middle of the model domain, between elevations 0 m and –1,000 m. The model domain extended 400 m in each of the horizontal directions and between elevations 100 m to –1,100 m. The lateral model extension of 400 m was chosen as an approximate average horizontal spacing between regional deterministic deformation zones. The borehole geometry was chosen to represent the deep core drilled boreholes which are typically 1 km long and cased in the upper 100 m. In this way, the results are expected to approximate those for a much larger model domain in which transmissive sub-vertical deformation zones were inserted regularly at a 400 m spacing to provide connectivity and fixed head boundary conditions. This idealised vertical column model (see Figure 4-3) was used since it allows a generic stochastic hydrogeological DFN model to be developed for each hydraulic rock domain. Simulation results were analysed in terms of a comparison between the fracture intersections and flow-rates simulated with the borehole data in each of the depth zones. The hydrogeological DFN modelling was undertaken entirely in three dimensions.

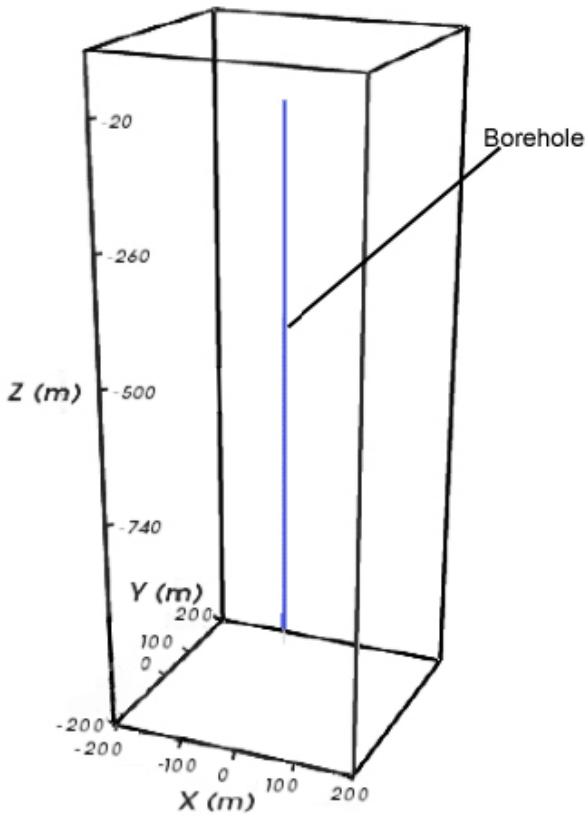

Figure 4-3. *The model domains used to calculate the optimised Hydro-DFN parameters in the SDM Hydro-DFN models, with a vertical synthetic borehole. (After Follin et al. 2007a, Figure 11-5.)*

The Hydro-DFN modelling for SDM-Site is described in Follin et al. (2007a) for Forsmark and Rhén et al. (2008) for Laxemar, both of which were performed using the ConnectFlow software (AMEC 2012a, b, c, d). The development of Hydro-DFN modelling methodology through earlier stages of site investigations at Forsmark are described in Hartley et al. (2005), and in Follin et al. (2006) and Hartley et al. (2006a, 2007) for Laxemar. The work by Follin et al. (2006) was performed using the DarcyTools software (Svensson and Ferry 2010, Svensson et al. 2010).

4.1.1 An elaborated Hydro-DFN methodology

The SDM-site Hydro-DFN models for Forsmark and Laxemar were developed using the methodology summarised above. The hydrogeological modelling was generally performed in two phases. Firstly, analyses of hydraulic measurements in boreholes leading to conceptualisation and parameterisation of the deformation zones and rock mass based on Hydro-DFN modelling (as described in this chapter). Secondly, a numerical implementation of the site hydrogeological model on a regional-scale that was then submitted to a set of confirmatory tests of model parameterisation against cross hole hydraulic tests, head measurements in deep and soil boreholes, and comparisons of simulation results of palaeo-climatic evolution against present-day groundwater composition (see Chapter 6). The SDM-site reporting reflects these two phases in Follin et al. (2007a) followed by Follin et al. (2007b) for Forsmark, and Rhén et al. (2008) followed by Rhén et al. (2009) for Laxemar. If the regional-scale modelling confirmed the validity of the hydrogeological properties derived from the underlying Hydro-DFN, then there was no need to iterate back to the Hydro-DFN phase, which was generally the case at Forsmark. However, for Laxemar it was necessary to significantly reduce hydraulic conductivities derived on the basis of the underlying Hydro-DFN model, and so it motivated some re-evaluation of the Hydro-DFN phase. That is, the Hydro-DFN models failed step (5) of the methodology outlined at the beginning of this section, requiring a re-calibration of the Hydro-DFN models. A second iteration of the Hydro-DFN was not possible within the SDM-Site programme. The regional ECPM modelling suggested that hydraulic conductivity at elevations below –150 m needed to be reduced by a factor of

three to improve the match to measured values of the various chemical tracers and the interference test drawdowns. The implications for the underlying Hydro-DFN being that the fracture network was either too connected or the transmissivity was too high.

In light of these issues, the Hydro-DFN model for Laxemar was re-evaluated as part of the comparisons made between Laxemar and Forsmark in support of SR-Site (Joyce et al. 2010b). Still, the changes required to achieve a self-consistent Hydro-DFN were not large relative to the variability in hydraulic parameters, and so investigations were made as to whether aspects of the methodology or assumptions used in SDM-Site Laxemar (Rhén et al. 2008) could potentially lead to either over-estimating the number of large conductive fractures (corresponding to an under-estimate of the power-law exponent, k_r, in the fracture size distribution) or over-estimating the transmissivity of fractures. As a result the Hydro-DFN methodology was elaborated relative to that described above. Some of the changes are considered generic improvements, while others are specific to particular conditions present at Laxemar. Aspects of this elaborated methodology have been applied in Hydro-DFN modelling of Olkiluoto (Hartley et al. 2011), for example.

The main changes to the methodology are:

1. A selection of boreholes is modelled in their true locations and orientations relative with the HCD model included in the stochastic modelling of the HRD properties. For each HRD, an appropriate set of boreholes needs to be selected that are representative of that domain in terms of having the majority of its length in the domain and extending to at least repository depth within the domain. The significance of this change is that specific deformation zones are effectively controlling the distance from the representative borehole to a specified pressure boundary condition. Since the deformation zones are sometimes closer than the model boundary to the representative boreholes, the calibrated fracture size distribution was found to be shifted slightly towards smaller fractures compared to the original SDM calibration method which did not include deformation zones explicitly. An example of the selection of representative boreholes for each Hydraulic rock domain is shown in Figure 4-4, and a model used in the Hydro-DFN calibration with HCD included is illustrated in Figure 4-5 (cf. Figure 4-3).
2. A greater emphasis was placed on the measured differences in inflow distributions between fracture sets to better resolve hydraulic anisotropy. To address this issue, particular care was taken to calibrate the fracture size-transmissivity relationship for individual sets (at Laxemar the transmissivity distribution of the WNW set aligned parallel to the maximum horizontal stress was distinctly higher than other sets).
3. For the model calibration a maximum Terzaghi correction of 100 was used when calculating $P_{10,o,corr}$ and $P_{10,cof,corr}$. In SDM-Site a maximum correction factor of 7 was used both for data analysis and model calibration (Rhén et al. 2008). This was used to enhance the bias in sampling steeply dipping fractures. There are practical reasons for capping the correction factor for data as it is difficult to accurately record very steep angle fractures in a borehole. For stochastic modelling with statistics calculated over a sizeable ensemble then a higher maximum correction may be appropriate for steeply dipping sets (mean dips for the vertical sets at Laxemar are close to 90°). Tests showed that using this higher maximum correction increased the Terzaghi corrected fracture intensity by up to 20% for some sets, implying that the same corrected intensity of connected open intensity could be matched for a lower intensity of large fractures, essentially allowing k_r to be increased. This issue was also recognised in earlier stages of SDM modelling (see Hartley et al. 2005).

Each of these modifications are generic in the sense they offer a slightly more sophisticated methodology, although the relevance may vary according to site conditions. The first issue may have significance for Forsmark also. The second issue is less relevant to Forsmark because there are less obvious differences in the measured specific capacities between sets (see Follin et al. 2007a, Chapter 11). The third issue also has little relevance to Forsmark as PFL-f fractures are dominated by the sub-horizontal set.

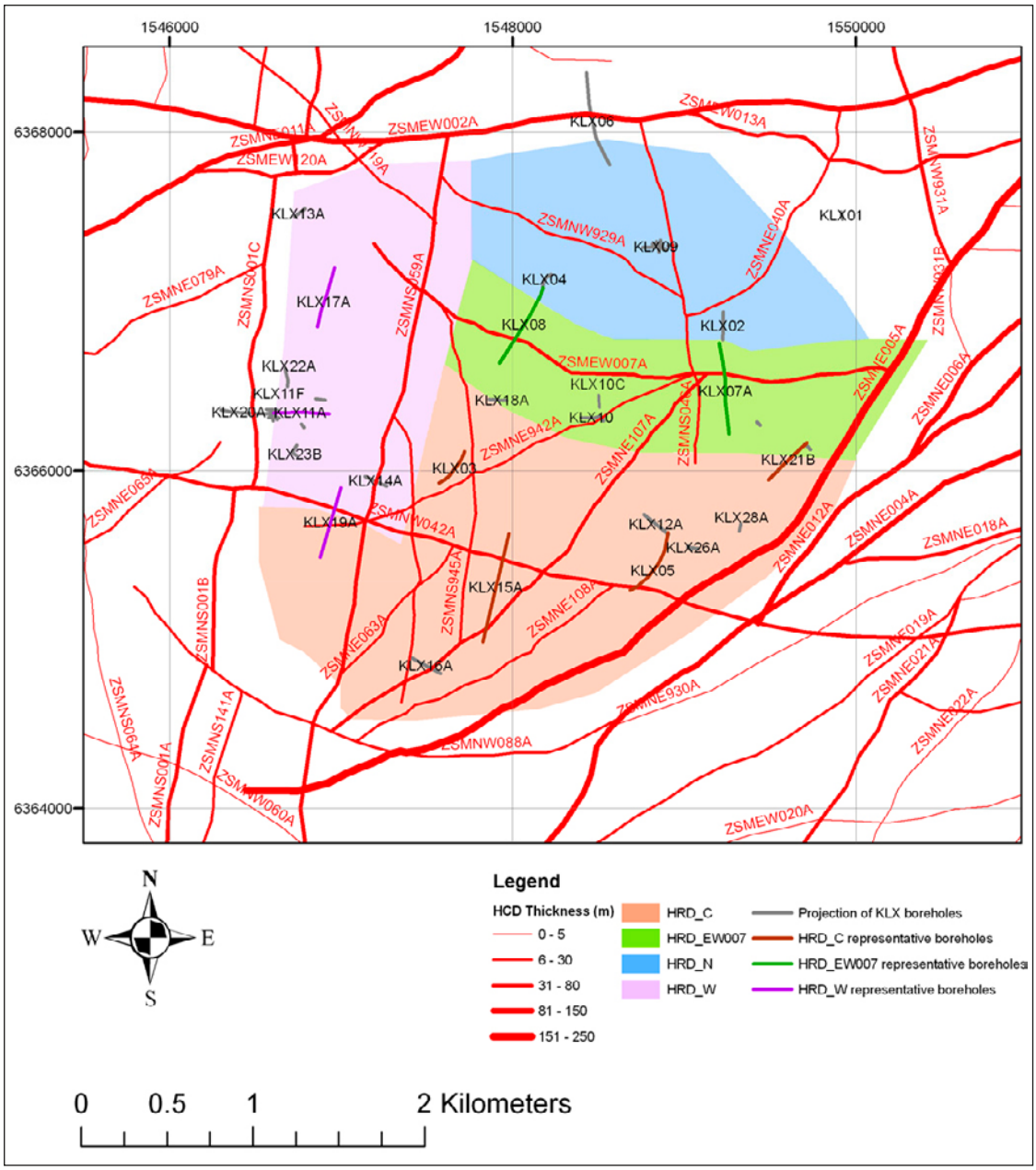

Figure 4-4. *The locations of the representative boreholes used in the Elaborated Hydro-DFN model calibration. A trace of the deformation zones at ground surface is shown in red. The locations of various HRDs at the bedrock surface are indicated. (After Joyce et al. 2010b, Figure 5-1.)*

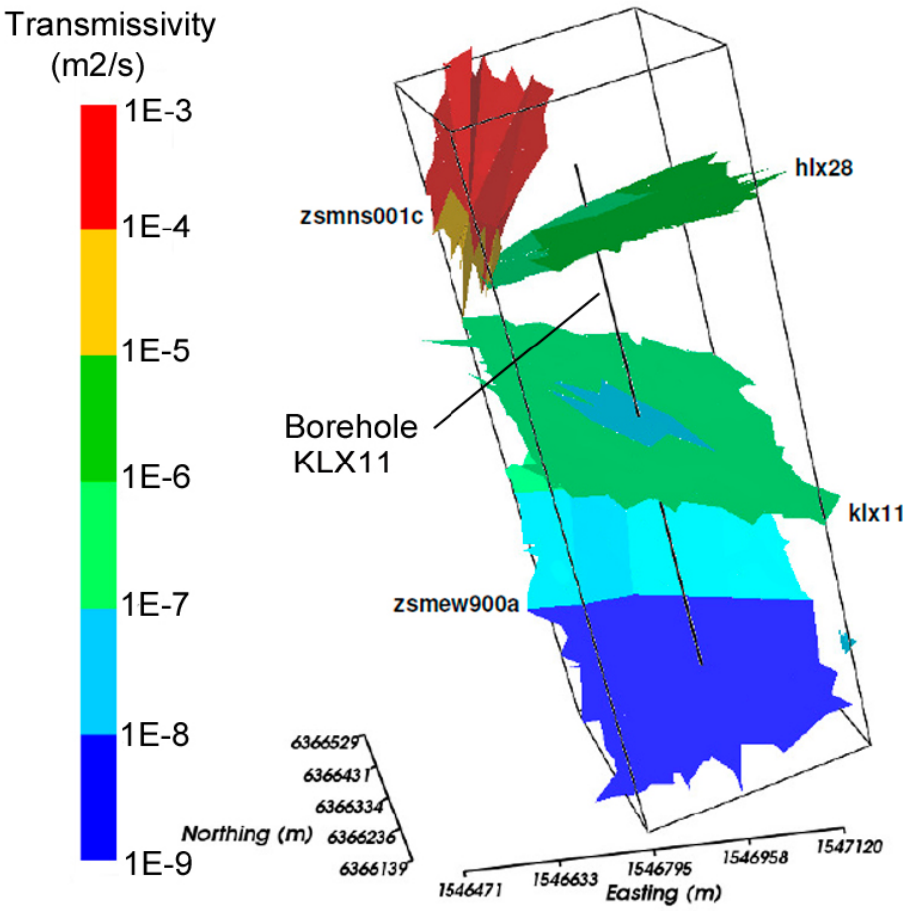

Figure 4-5. *The model domains used to calculate the optimised Hydro-DFN parameters in Elaborated Hydro-DFN for Laxemar, which models the geometry of a representative borehole explicitly (In this case KLX11A). Deterministic deformation zones are also modelled explicitly, and are shown coloured by transmissivity. (After Joyce et al. 2010b, Figure 5-2.)*

4.2 Analysis of fracture orientations

For each fracture set within a hydraulic rock domain, the parameters defining a univariate Fisher distribution (Fisher 1953) (characterised by a mean plunge and trend, together with a Fisher concentration parameter) were assigned for the open fractures. These parameters were assumed not to vary by depth zone. The fitting was done using stereographic methods with Terzaghi weighting. In the initial analyses of fracture orientation distributions for each set at Laxemar the were divided according to the definitions of La Pointe et al. (2005) for the Stage 1.2 Geo-DFN and a fit of Fisher distributions to the set of all fractures (see Follin et al. 2007a, Table 11-3). Recognising changes with the extra borehole data available for Stage 2.2 and comparison of stereographic concentration plots of orientation for the sets of all, open and PFL-f fracture, an alternative orientation model was recommended (see Follin et al. 2007a, Table 11-26). The main changes were a rotation of the NS set toward NNE, and to calculate Fisher orientation parameters on the subset of open fractures since the sub-horizontal set became significantly more concentrated for open fractures relative to all fractures. Eventually, in the SDM-Site regional model confirmatory testing it was determined that this alternative orientation model offered the better explanation of hydraulic anisotropy apparent when trying to match the cross-hole test and palaeo-climatic data (Follin et al. 2007b), and hence was applied in the SR-Site modelling (Joyce et al. 2010a). The parameters for both orientation models are given in Table 4-1.

For Laxemar, the definition of fractures sets was based on the inspection of fracture orientation density plots for open fractures and PFL-f fractures as well for outcrops (Rhén et al. 2008). These definitions were checked for broad consistency with the Geo-DFN (La Pointe et al. 2008) that was developed in parallel. The Fisher orientation parameters for each HRD and set were then obtained

by fitting to the subset of PFL-f data based on the experience from Forsmark described above (i.e. fit to the flowing fracture orientations for the Hydro-DFN modelling). The orientation model used for each HRD is given in Table 4-2.

An example of the stereographic analysis for Forsmark is shown in Figure 4-6. Plots a) –c) are Terzaghi-corrected concentration plots using equal-area lower-hemisphere projection for all, open and PFL-f fractures, respectively. Concentration plots are used rather than simple pole plots to identify clustering around particular orientations. The concentration plotted at a point is a relative concentration equal to the percentage of the number of poles in 1% of the area of the hemisphere around the point. Showing the relative concentration in this way demonstrates how horizontal and NNE-NE sets become successively more pronounced as the fractures are restricted to open and then PFL-f fractures. A similar behaviour is seen at Laxemar, although there it is the sub-horizontal and WNW fractures that become more emphasised when restricting to PFL-f fractures (see Rhén et al. 2008, Figure 9-11).

Fractures are simulated as square features. To avoid vertex orientation bias, the vertices of the fractures are randomised by applying a uniform random rotation around the fracture normal vector.

Table 4-1. Orientation parameters for Forsmark. The left column was used in the Hydro-DFN calibration (Follin et al. 2007a, Table 11-3) based on set definitions from the Stage 1.2 Geo-DFN set definitions. The right hand columns are for the alternative orientation model recommended in (Follin et al. 2007a, Table 11-26).

Set	Orientation model used in F2.2 Hydro-DFN calibration Fisher distribution (trend, plunge), concentration	Alternative model for orientations in FFM01/FFM03/ FFM06 Fisher distribution (trend, plunge), concentration	Alternative model for orientations in FFM02 Fisher distribution (trend, plunge), concentration
1 NS	(87, 2) 21.7	(292, 1) 17.8	(83, 10) 16.9
2 NE	(135, 3) 21.5	(326, 2) 14.3	(143, 9) 11.7
3 NW	(41, 2) 23.9	(60, 6) 12.9	(51, 15) 12.1
4 EW	(190, 1) 30.6	(15, 2) 14.0	(12, 0) 13.3
5 HZ	(343, 80) 8.2	(5, 86) 15.2	(71, 87) 20.4

Table 4-2. Orientation parameters for Laxemar hydraulic rock domains (Rhén et al. 2008).

	(Trend, plunge), Fisher concentration			
Set	**HRD_C**	**HRD_EW007**	**HRD_N**	**HRD_W**
ENE	(155.1, 3.4) 9.6	(162.8, 1.4) 10.7	(342.2, 0.2) 15.8	(340.3, 1.2) 15
WNW	(204, 1.6) 12.0	(25.3, 0.2) 16.4	(209.8, 1.6) 14.6	(208.9, 2.2) 10.9
N-S	(270.2, 8.4) 7.8	(88.9, 3.9) 8.8	(271.3, 3.8) 10.3	(272.8, 12) 11.5
SubH	(46.3, 84.7) 12.0	(138.7, 81.3) 9.7	(238.9, 81.5) 12.7	(277.1, 84.3) 11.1

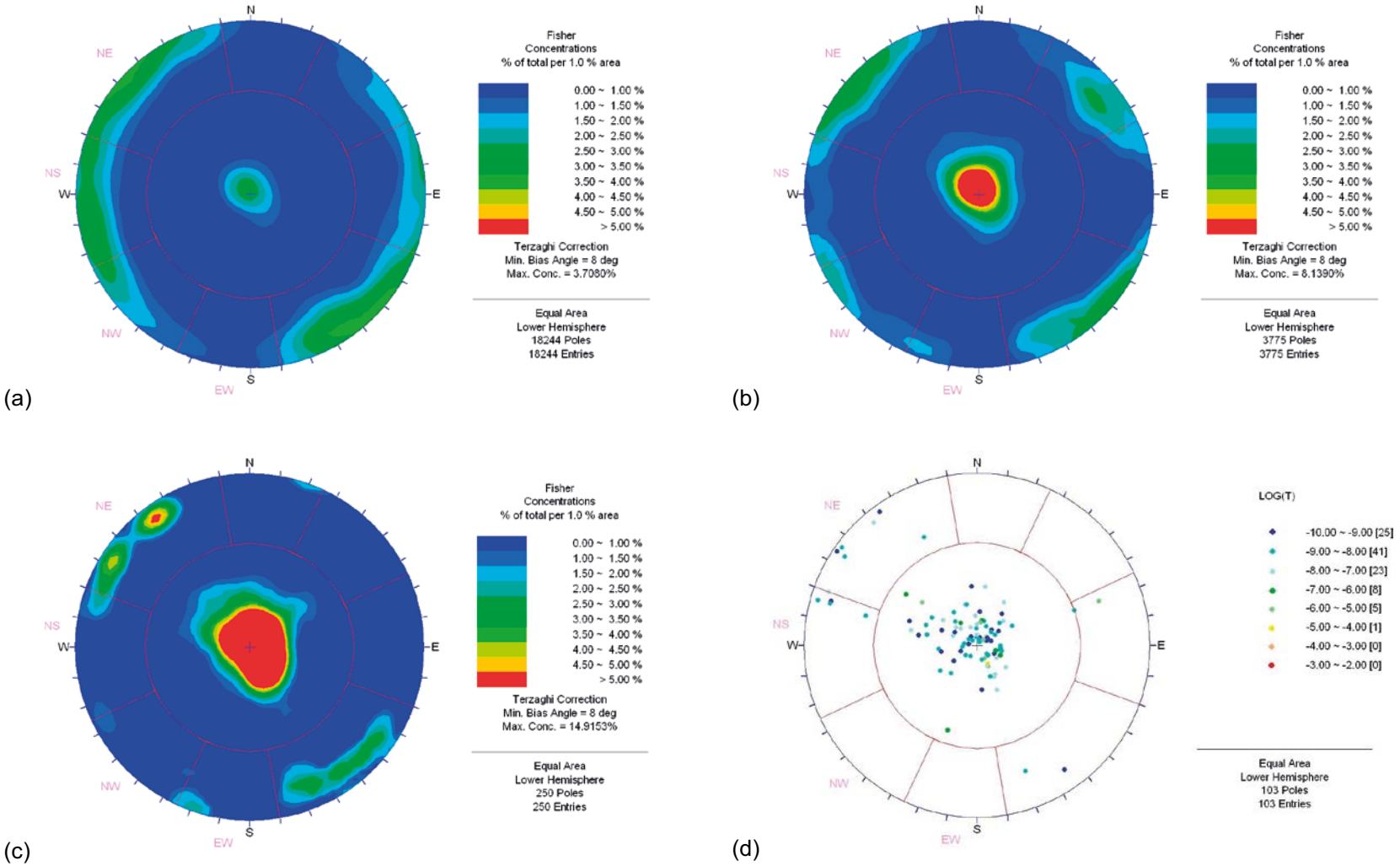

Figure 4-6. *Stereonets for all FFM domains at Forsmark excluding HCD: (a), (b), (c) Terzaghi corrected intensity for all fractures, open fractures and PFL-f features. (d) poles for PFL-f fractures in FFM01 (coloured by transmissivity). (After Follin et al. 2007a, Figures 10-7–10-9, Figure 10-17.)*

4.3 Analysis of hydraulic rock domains and fracture intensity

Another key input Hydro-DFN simulations estimated directly from borehole data is the intensity of open fractures. Strictly, the input required in the simulations is the surface area intensity, P_{32}, but this is estimated from the borehole data as the Terzaghi corrected linear intensity, $P_{10,o,corr}$. The validity of this estimate along with the interpreted fracture orientations were then tested in the step described in the next section.

The open fracture intensity was calculated for each hydraulic domain and fracture set, but also by depth zone since there was generally found to be a gradual reduction in open fracture density with depth at both sites. A summary of open fracture intensity by hydraulic domain and depth zone are shown in Figure 4-7 and Figure 4-8, for Forsmark and Laxemar, respectively. Figure 4-7 illustrates the strong depth trend in fracture intensity at Forsmark within the candidate area. FFM02 actually represents the uppermost 150 m of bedrock in the candidate area with open fracture intensity above 3 m^2/m^3, while FFM01/FFM06 (essentially the bedrock between c –100 m and –400 m) has an intensity c 1 m^2/m^3, falling to c 0.5 m^2/m^3 below –400 m. FFM03 to the south-east has a lesser trend with depth. Figure 4-8 shows Laxemar has a similar OPO intensity c 3 m^2/m^3 near-surface reducing to c 1 m^2/m^3 at depth.

At Laxemar, the relevance of the characterisation of fractures as being open for modelling water-conducting fractures was considered. Open or partly open were appraised with a varying degree of confidence (certain, probable or possible). Of all open fractures only 40% were recorded as being certain or probable (OPO-CP), which if this subset contained all water-conducting fractures it would imply a significantly lower fracture intensity would be appropriate to the hydrogeological system than the set of open fractures as whole (OPO). In fact, it was found that about 73% of PFL-f fractures were contained within OPO-CP fractures, and this fraction varied over the large range from 33% to 95% for individual boreholes (see Rhén et al. 2008, Table 9-9). It was concluded that it was uncertain whether to use fracture intensity based on all open fractures (OPO) or the significantly lower intensity based on OPO-CP fractures. Hence, both derivations of fracture intensity were tested in the Hydro-DFN modelling. In order to calibrate both models to the same connectivity and flow characteristics measured by the PFL-f measurements it was found that the OPO had a higher open fracture intensity, but higher power-law exponent, k_r, while the OPO-CP case had lower intensity with lower k_r.

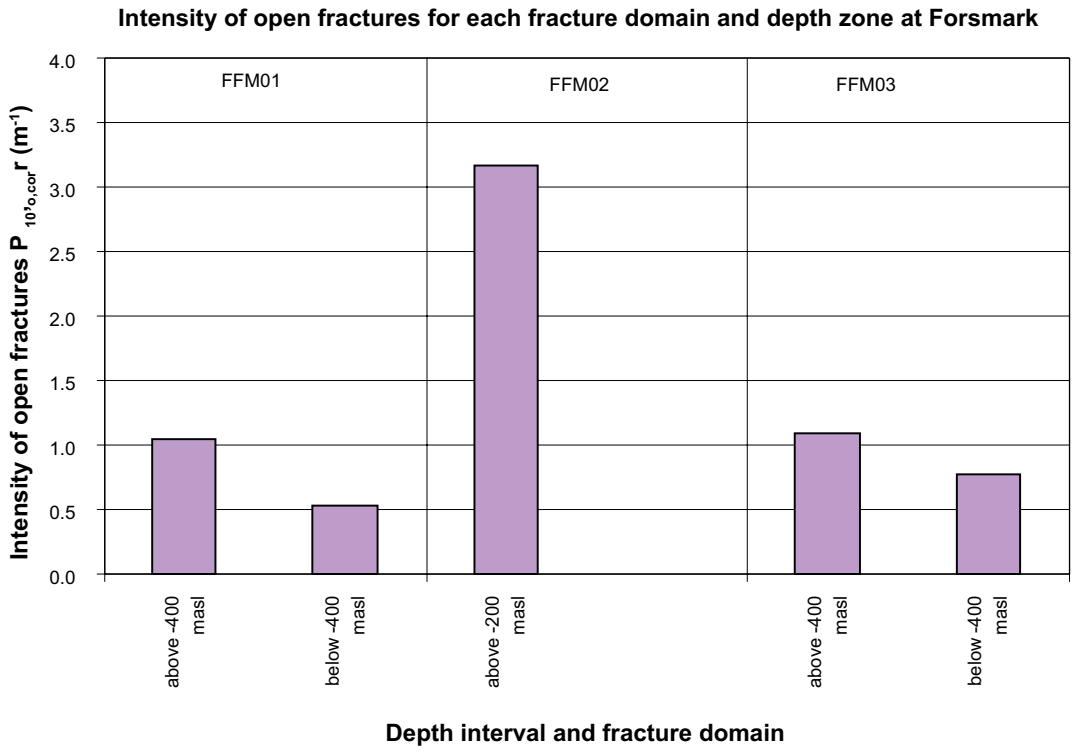

Figure 4-7. *The intensity of open fractures assumed in the initial model for Forsmark, by hydraulic rock domain and depth zone. (Based on Follin et al. 2007a, Chapter 11.)*

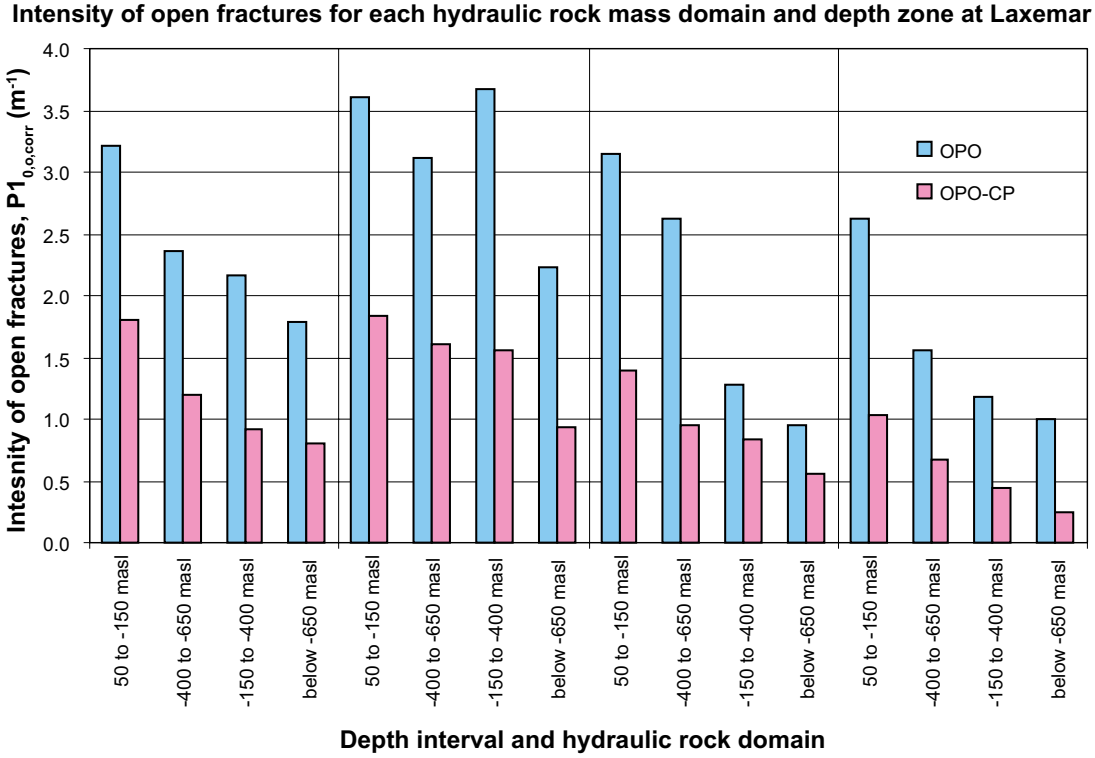

Figure 4-8. *The intensity of open fractures used in the initial modelling for Laxemar, by hydraulic rock domain and depth zone. (Based on Rhén et al. 2008, Chapter 9.)*

The implications for the hydraulic system were that the OPO case had fewer large fractures and more variability in equivalent hydraulic conductivity on the 100 m scale than the OPO-CP case. This increased variability more consistent with the variability seen in the 100 m PSS interval measurements was taken as an indicator that OPO case was more representative and hence used in the base case, and the OPO-CP case was treated as a variant in subsequent calculations. The geometric characteristics of the OPO case were found to have a preferential effect on the matching process, as discussed in Section 4.5. For the Forsmark, OPO fractures were used to derive the open fracture intensity as input to the Hydro-DFN modelling.

4.4 Consistency check

A Terzaghi corrected value of the intensity of open fractures, $P_{10,o,corr}$, was used as the initial estimate of P_{32}. Simulations of the intensity of open fracture intensity in a borehole were then compare with measured average $P_{10,o}$ for each fracture set. This consistency check was the second step (see Figure 4-1) of the calibration process: A check that the geometrical parameters for each fracture set can be used in DFN simulations of open fractures to yield, on average, the measured fracture intensity for open fractures. A reasonable match would be expected provided the orientations and fracture intensity represent the data adequately and hence this step largely a check the data analysis and simulation procedure have been performed proficiently. Any discrepancies would either indicate errors in the process or a poor representation of distributions measured, which might require either use of alternative orientation models and distributions or some fine-tuning of P_{32}.

For the modelling of both Forsmark and Laxemar, a set of four illustrative cases was used initially to explore sensitivities to the power-law size parameters. The cases considered were:

1) Small k_r and r_0, (2.6 and 0.038 m).
2) Large k_r and r_0, (2.9 and 0.282 m).
3) Large k_r and small r_0, (2.9 and 0.038 m).
4) Small k_r and large r_0, (2.6 and 0.282 m).

Fractures were simulated stochastically within the model domain. In order to limit the total number of fractures to make the simulations tractable, the smallest fractures were only generated immediately in the vicinity of the borehole. The centres of fractures with radius $r = r_0$ to r=2.26 m were generated only within a cylinder of radius 2.83 m around the borehole (2.83 m was chosen because the fractures generated were squares not circles).

Fracture centres were generated in a larger region than the model domain, but only their extent in the model domain would be included in the calculations, while their part outside would be effectively removed. The centres of fractures with radius r=2.26 m to r=564 m were generated in a region 500 m larger in each direction than the model domain.

Simulated and measured Terzaghi corrected fracture intensities (for the individual fracture sets and for all sets combined) were compared based on an ensemble over ten realisations of the hydrogeological DFN for each fracture domain or hydraulic domain. The fracture intensities for the simulated realisations were in good agreement with the measured values. The size distribution made little difference to the simulated intensity as expected, as Terzaghi correction does not depend on size, at least not for fractures large than the borehole. Again, the test for different size models was done mainly to check there no basic errors in the simulation procedure. The intensities for the generated realisations were slightly lower than the measured intensities for some sub-vertical sets, but the difference was less than about 15%, which was considered acceptable relative to the variability in intensity between boreholes, the uncertainty in correcting for the borehole trajectories, and the number of realisations performed.

4.5 Analysis of fracture connectivity and size

The intensities of PFL-f features at both Forsmark and Laxemar are much lower than the intensity of open fractures, particularly at depth. The conceptual model assumes that this is primarily a result of the majority of open fractures having limited connectivity. An alternative explanation would be that many of the fractures have low transmissivity. The first interpretation drives an appropriate choice of power-law fracture size distribution to give a connected network consistent with the intensity of PFL-f features. The methodology for obtaining the power-law distribution parameters ensures that the intensity of connected open fractures predicted by the model is, on average, consistent with the observed intensity of PFL-f fractures. This is done by making the assumption that:

$$P_{10,cof,corr} = P_{10,PFL,corr} \tag{4-2}$$

Where $P_{10,cof,cor}$ is the Terzaghi corrected intensity of connected open fractures and $P_{10,PFL,corr}$ is the Terzaghi corrected intensity of PFL-f fractures. If the PFL-f method had a lower detection limit, the intensity of PFL-features might be higher, in which case a different intensity-size distribution would result from the calibration procedure. As discussed in Section 2.6.2, the PFL-f method can only detect specific inflows above approximately $1 \cdot 10^{-9}$ m^2/s. The overall calibration methodology therefore requires that transmissivity assigned to the generated connected open fractures are such that they result in a specific capacity predominantly above the detection limit of the PFL-f method, when the PFL-f tests are simulated.

The approach to network connectivity calibration, step 3) of Section 4.1, is to generate a realisation of open fractures within the specified domain without any borehole present initially. A connectivity analysis was then performed. This was done by first identifying all the intersections between any two fractures and between a fracture and a boundary of the domain. Then fractures that either have no connection via the network to a boundary of the domain, or fractures that have only one intersection (that is, they are "dead-ends") were removed. Hence, the fracture system that remained was the connected open fracture system under in situ conditions, without any enhancements to connectivity that may occur locally around a borehole. Only at this stage was a vertical borehole inserted through the remaining connected network to obtain the simulated intensity of connected open fractures. This procedure avoids retaining, and counting, fractures that form isolated or dead-end connections with the borehole.

However, it also excludes new local connections with the fracture network created when the borehole is drilled. The potential contribution of the borehole to connectivity was investigated as part of the Hydro-DFN modelling for SDM-Site Laxemar (Rhén et al. 2008, Appendix 8). There it was demonstrated that if the effect of the borehole on local connectivity is considered and the minimum fracture

size, r_{min}, is equal to the borehole radius, then the additional clusters of small connected fractures can form around inflow points that may increase the intensity of connected open fractures intersecting the borehole by as much as 50%. Although typically the inflows from these additional small fractures were found to be small, such that they fell below the PFL detection limit c 10^{-9} m^2/s, and hence did not enhance the simulated $P_{10,PFL,\,corr}$. It should be noted however, that additional checks on the connectivity of the network providing inflows to the borehole are made during the flow calibration step 4) described in the next section.

An example of a connectivity analysis is shown in Figure 4-9 for HRD_C in Laxemar. The left hand picture shows all the fractures on a vertical slice and the right hand picture shows the effect of removing isolated and dead-end fractures. This illustrates how by either decreasing intensity of the network with depth and/or increasing the power-law exponent, k_r, then a rapid decrease in connected fracture intensity with depth can be reproduced consistent with the behaviour suggested by the PFL-f data. Making the network sparser reduces the probability that fractures connected, as does shifting the size distribution towards smaller fractures when sparse networks to compound the behaviour.

The values of the power-law intensity distribution parameters (k_r and r_0) are not uniquely constrained by the methodology adopted or the data available. This is because there are two parameters defining the size distribution and only a single constraint in calibration, namely the intensity of PFL-f features. At Forsmark, r_0 was fixed at 0.038 m and k_r varied to match the PFL data. At Laxemar, for a definition of open fractures based on OPO fractures, the case with k_r fixed and r_0 varying had k_r set to 2.9. For OPO-CP fractures, the case with k_r fixed and r_0 varying had k_r set to 2.7. For the Laxemar modelling, several different combinations of power-law parameters were considered in order to allow the sensitivities to these parameters to be quantified in subsequent modelling. For the Laxemar modelling, two different approaches to calibrate the size parameters were followed: in one case r_0 was fixed at 0.038 m. This is the borehole radius, and as such is a definite lower limit for radius of the mapped open fractures. k_r is then varied to match the PFL-f data. In the other case, k_r was held fixed and r_0 varied.

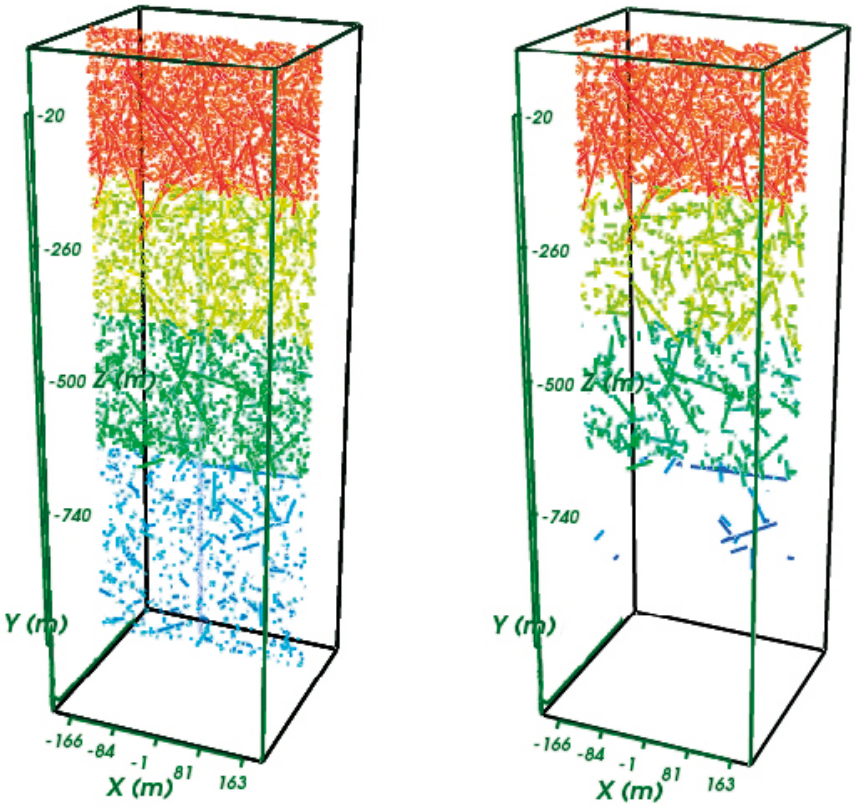

Figure 4-9. *Example of connectivity analysis shown on a vertical (E-W) slice through a DFN simulation of open fractures (this example uses OPO-CP fractures) in HRD_C, Laxemar. Left: a slice through the open fractures generated prior to any connectivity analysis. Right: the same model slice after isolated fractures and dead-ends are removed. The fractures are coloured according to the depth zone in which their centres are generated. (After Rhén et al. 2008, Figure 10-6.)*

There are also additional, physically motivated, constraints on the intensity-size distribution parameters. The geological DFN analysis of outcrops at Laxemar implies an upper limit on r_0 of generally no more than about 0.1 m–1.5 m (La Pointe et al. 2008), depending on fracture domain. Furthermore, for any fracture size interval, the intensity of open fractures must be lower than the intensity of all fractures, as characterised in the Geo-DFN. A constraint that the intensity of open fractures with radius greater than 564 m stipulated by the intensity-size distribution should be consistent with the intensity of mapped deformation zones was imposed, to avoid any conceptual inconsistency. At Laxemar, for the case when r_0 was fixed at 0.038 m and k_r varied, sometimes a low value of k_r would have been required to achieve a match in the upper depth zones at Laxemar, resulting in a physically implausible model. In such instances, k_r was held at 2.2 and r_0 was increased instead.

An iterative approach was used in the calibration of the intensity-size models. A set of intensity-size parameters, as described above, were used as an initial model, and the intensity of connected open fractures predicted by the simulation compared to the intensity of PFL-f fractures measured. For example, if the simulated intensity of connected open fractures were lower than the observed intensity of PFL-f fractures, k_r might be reduced to increase the average length of the fractures, resulting in more connected fractures and a higher simulated intensity of connected open fractures intersecting the borehole. Similarly increasing r_0 would increase the average length of the fractures, resulting in a higher simulated intensity of connected open fractures intersecting the borehole.

At Forsmark it was found that a reasonable match to the PFL-f intensity data could be achieved using intensity-size distributions which varied by fracture orientation set, but the measured variation of open fracture intensity by depth zone was sufficient to reproduce the depth PFL-f intensity without also changing the size distribution with depth. The fit to the data for hydraulic rock domain FFM01/FFM06 is shown in Figure 4-10. The parameters for FFM01 derived based on connectivity analysis for a division of the rock into two depth zones at –400 m is given in Table 4-3. Eventually, for the flow calibration the upper part 400 m of FFM01/FFM06 was subdivided into to give three depth zones: > –200 m, –200 m > z > –400 m, and < –400 m. It should be noted however the bedrock above c –100 m belongs mostly to fracture domain FFM02, with a transition to FFM01 between c –100 m to –200 m.

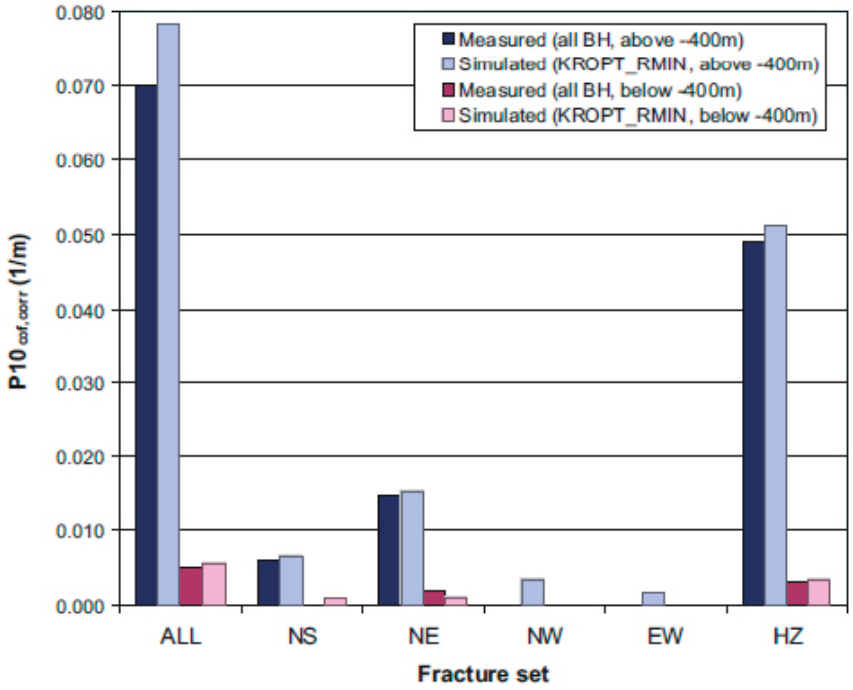

Figure 4-10. *Graphical comparison of measured Terzaghi corrected linear intensities of PFL fractures, $P_{10,PFL,corr}$, for hydraulic rock domain FFM01/FFM06 above and below –400 m for each fracture set with simulation results of connected open fractures, $P_{10,cof,corr}$, for 10 realisations of a vertical borehole for a calibrated power-law size model. (After Follin et al. 2007a, Figure 11-10).*

At Laxemar, for each of the intensity-size variants considered, it was found that the distribution parameters should be varied by depth and orientation set to simulate the PFL-f intensity. The parameters used to fit the PFL-f intensity data for HRD_C and HRD_W are given in Table 4-4 and the fit achieved is shown in Figure 4-11. For the intensity-size variants where r_0 was held constant, it was found that k_r was typically increased with depth, corresponding to decreasing the average fracture size. This seems physically plausible in view of the interpretation of open fractures as the hydraulically open areas within fractures which are capable of supplying inflow above the detection limit during a PFL-f test: As depth increases, so does lithostatic stress, which may close parts of fractures.

Table 4-3. Description of DFN parameters for open fractures in fracture domain FFM01 at Forsmark with depth dependency above and below –400 m elevation (Follin et al. 2007a, Table 11-9).

Fracture domain	Fracture set name	Orientation set pole: (trend, plunge), conc.	Size model, power-law (r_0, k_r) (m, –)	Intensity, (P_{32}), valid size interval: (r_0, 560 m) (m^2/m^3)	Transmissivity model Eq. no, constants T (m^2s^{-1})
FFM01 > –400 m	NS	(87, 2) 21.7	(0.04, 2.60)	0.125	–
	NE	(135, 3) 21.5	(0.04, 2.70)	0.339	
	NW	(41, 2) 23.9	(0.04, 3.10)	0.126	
	EW	(190, 1) 30.6	(0.04, 3.10)	0.083	
	HZ	(343, 80) 8.2	(0.04, 2.42)	0.374	
FFM01 < –400 m	NS	(87, 2) 21.7	(0.04, 2.60)	0.094	–
	NE	(135, 3) 21.5	(0.04, 2.70)	0.163	
	NW	(41, 2) 23.9	(0.04, 3.10)	0.098	
	EW	(190, 1) 30.6	(0.04, 3.10)	0.039	
	HZ	(343, 80) 8.2	(0.04, 2.42)	0.141	

Table 4-4. Description of DFN parameters for OPO fractures in hydraulic domains HRD_C and HRD_W at Laxemar with four depth zones (Rhén et al. 2008, Tables 10-2, 10-3).

		HRD_C		HRD_W	
Depth interval (masl)	Set	Size model, power-law (r_0, k_r)	Intensity, (P_{32}), valid size interval: (r_0, 560 m)	Size model, power-law (r_0, k_r)	Intensity, (P_{32}), valid size interval: (r_0, 560 m)
–150 to 50	ENE	(2.7, 0.038)	0.52	(2.7, 0.038)	0.44
	WNW	(2.5, 0.038)	0.95	(2.5, 0.038)	0.61
	N-S	(2.7, 0.038)	0.54	(2.65, 0.038)	0.54
	SubH	(2.7, 0.038)	1.20	(2.55, 0.038)	1.03
–400 to –150	ENE	(2.8, 0.038)	0.47	(2.7, 0.038)	0.28
	WNW	(2.4, 0.038)	0.55	(2.5, 0.038)	0.38
	N-S	(2.85, 0.038)	0.63	(2.9, 0.038)	0.4
	SubH	(2.8, 0.038)	0.71	(2.7, 0.038)	0.5
–650 to –400	ENE	(2.75, 0.038)	0.38	(2.6, 0.038)	0.17
	WNW	(2.5, 0.038)	0.74	(2.6, 0.038)	0.33
	N-S	(2.85, 0.038)	0.47	(2.6, 0.038)	0.30
	SubH	(2.85, 0.038)	0.58	(2.65, 0.038)	0.38
–1,000 to –650	ENE	(2.85, 0.038)	0.46	(2.8, 0.038)	0.12
	WNW	(2.75, 0.038)	0.73	(2.8, 0.038)	0.09
	N-S	(2.95, 0.038)	0.25	(2.8, 0.038)	0.14
	SubH	(2.9, 0.038)	0.35	(2.8, 0.038)	0.65

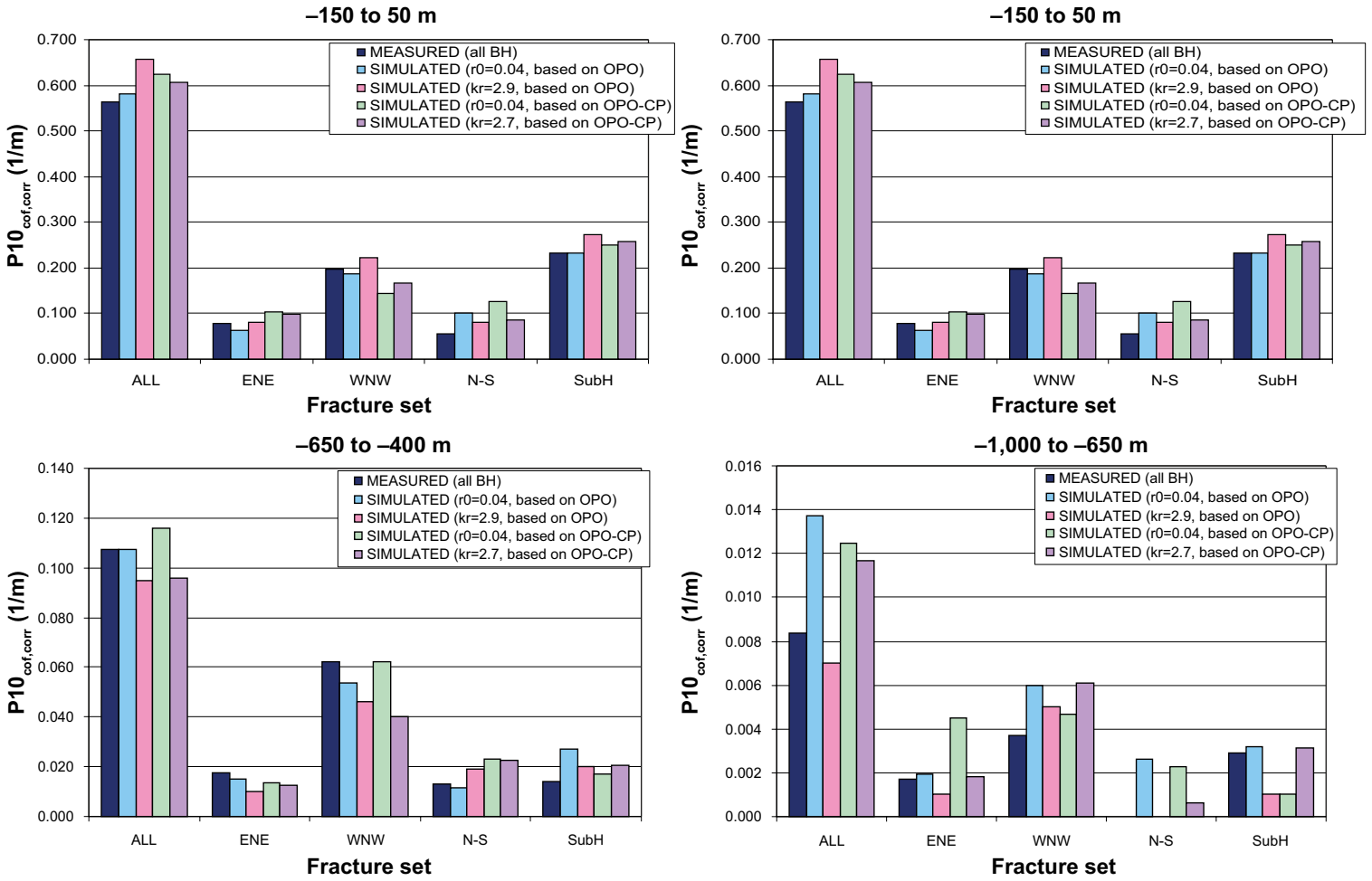

Figure 4-11. *Comparison of the Terzaghi corrected connected open fracture intensities, $P_{10,cof,corr}$ for the individual fracture sets with the measured fracture intensities for PFL-f features for HRD_C, Laxemar. Four geometrical fracture models were considered: k_r fixed with r_0 varying or r_0 fixed with k_r varying, and an input P_{32} based on the intensity of OPO fractures; r_0 fixed with k_r varying or r_0 fixed with k_r varying, and an input P_{32} based on the intensity of OPO-CP fractures. (After Rhén et al. 2008, Figure 10-8.)*

Examples of intensity-size distributions developed through model calibration are shown in Figure 4-12 and Figure 4-13 for Forsmark and Laxemar, respectively, which are compared to the corresponding intensity-size models interpreted from the Geo-DFN modelling. In Figure 4-12 the intensity-size distribution for the 3 depth zones developed in the Hydro-DFN modelling of FFM01/FFM06 are presented along with that for FFM02, corresponding the uppermost part of the bedrock in the candidate area. For all depths the intensity-size distributions for open fractures are below the Geo-DFN consistent with the concept that open fractures are everywhere a subset of all fractures. The same is true in Figure 4-13 for Laxemar, with the exception of depth zone 1 in HRD_C, where fractures greater than approximately 50 m radius are predicted to occur at a slightly higher intensity than is consistent with the Geo-DFN. This discrepancy, amounting to approximately 60%, is within the known uncertainties in the Geo-DFN, as quantified in La Pointe et al. (2008). These figures demonstrate that fracture intensity of open fractures decreases with depth over all size ranges at both Forsmark and Laxemar.

Figure 4-14 illustrates the uncertainty in the intensity-size distribution of open fractures following a calibration on connected open fracture when alternative definitions of open fracture intensity and different approaches to deriving the power-law size model. Here, three variants are shown for depth zone 3, bracketing repository depth, at Laxemar and compare to the Geo-DFN size distribution. Each size model (r_0, k_r) has been calibrated to reproduce a connected open intensity equal to that of PFL-f fractures, $P_{10,cof,corr}=P_{10,PFL,corr}$. It demonstrates that generally the open fractures always have to have a smaller power-law exponent than the Geo-DFN to gain sufficient connectivity, but still the intensity for the two OPO cases is everywhere less than the Geo-DFN. The same is not true for the OPO-CP variant, which requires a higher intensity of large fractures than the Geo-DFN, and so seems less plausible. So, although there is uncertainty in the interpretation of open fractures suitable for describing flow potential at Laxemar, it seems the restriction to only "certain" and "probable" open fractures gives to sparse a hydraulic fracture system to be self-consistent with the geological model of a tectonic continuum model of intensity-size.

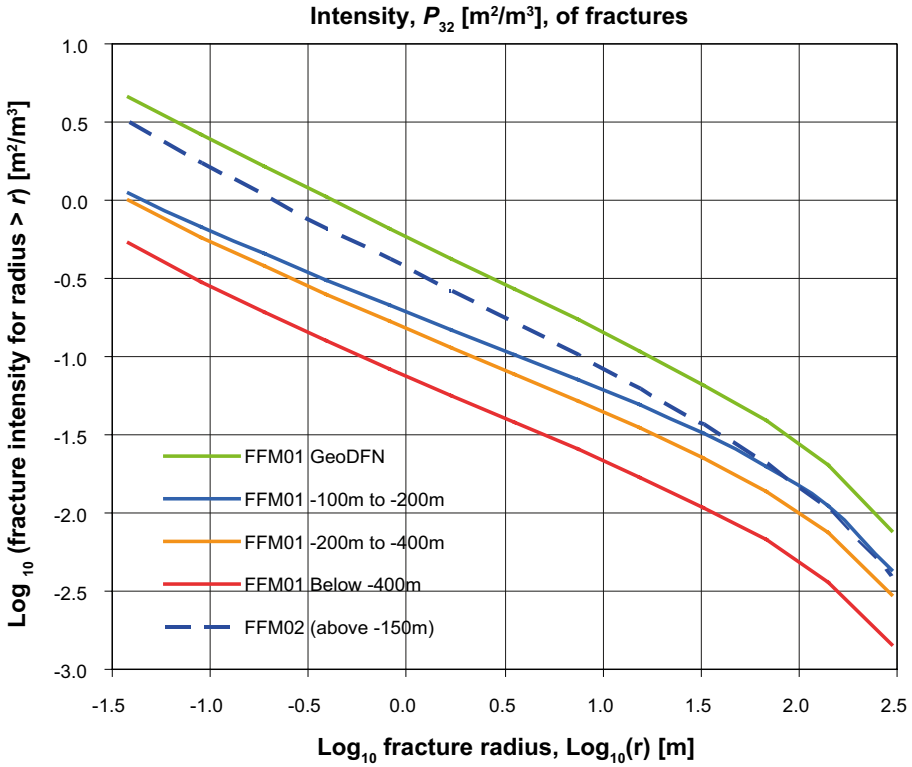

Figure 4-12. *Log-log plot of the intensity-size distributions of open fractures derived through model calibration for FFM01 / FFM06 for 3 depth zones versus the Geo-DFN model for all fractures and depths. The Hydro-DFN intensity-size parameters are from Follin et al. (2007a, Tables 11-20, 11-22), the Geo-DFN intensity-size parameters are from Fox et al. (2007, Table 7-2).*

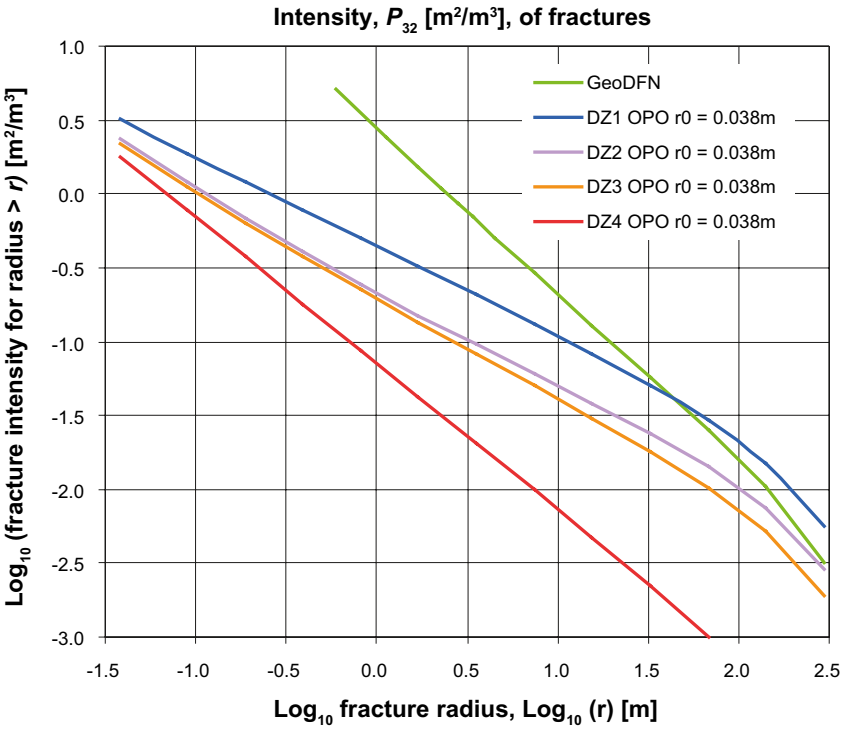

Figure 4-13. *Log-log plot of fracture intensity-size distributions for each of the 4 depth zones (DZ1-4) derived through model calibration for HRD_C (Laxemar) versus the Geo-DFN model for all fractures and depths. The model is based on OPO fractures with r_0 fixed from Rhén et al. (2008, Tables 10-2, 10-3); the Geo-DFN intensity-size parameters are from La Pointe et al. (2008, Section 7.1.2).*

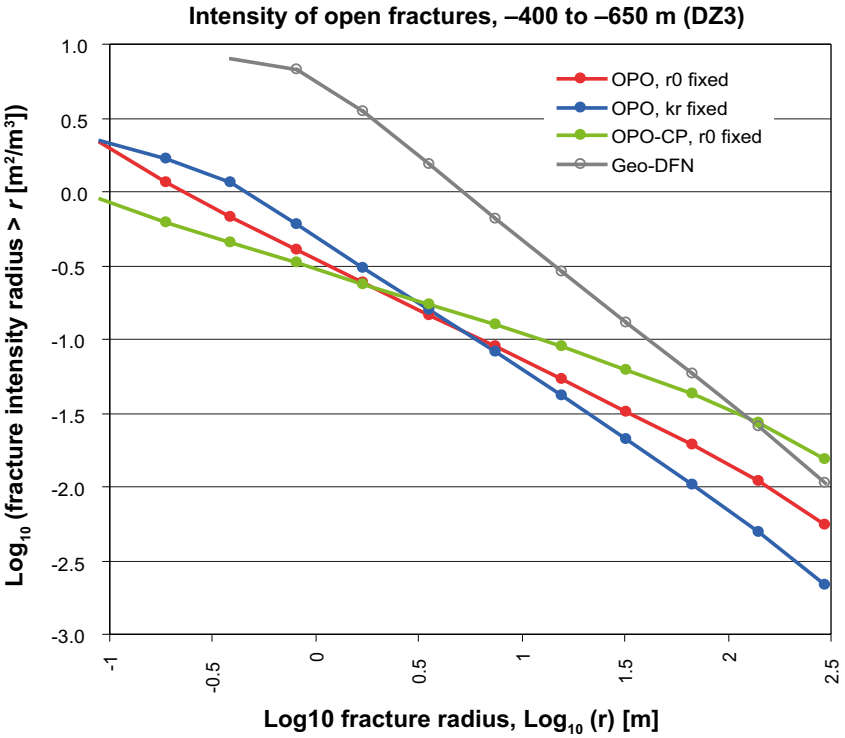

Figure 4-14. *Distributions of open fracture intensity as a function of fracture radius for the three intensity-size variants used in the modelling for HRD_C for Laxemar. The Hydro-DFN intensity-size parameters are from Rhén et al. (2008, Tables 10-2–10-4), the Geo-DFN intensity-size parameters are from La Pointe et al. (2008, Section 7.1.2).*

For sparse networks it is typical that a higher proportion of large fractures are connected than small fractures. This is demonstrated in Figure 4-15 showing the ratio of connected open fractures to open fractures overall as a function of fracture size for each of the depth zones modelled in FFM01/FFM06, Forsmark based on simulations. In particular, it shows open fractures with radii below approximately 1 m are unlikely to be part of a connected network. In order to have a probability of greater than 0.5 of being connected, a fracture must have a radius of greater than approximately 5 m above –400 m, or greater than about 30 m below –400 m.

The consequence of this lack of connectivity in small fractures is revealed in Figure 4-16 in terms of the resulting size distributions of connected open fractures for the three depth zones of FFM01/FFM06 considered in the Hydro-DFN. It suggests a log-normal type size distribution for connected open fractures with mode around 10 m fracture radius above –400 m, and around 50 m below.

A similar behaviour was also found in the size distribution at Laxemar. Here, Figure 4-17 shows the simulated size distributions of connected open fractures in depth zone 3 at Laxemar for three alternative intensity-size variants. Again, all three cases suggest a log-normal type size distribution with a mode of a few metres. Each of these three models are viable alternatives for explaining the occurrence of open and partly open fractures observed in the core logging, and the occurrence of PFL-f features seen in the hydraulic testing. The similarity in the resulting intensity-size distributions of connected open fractures prompts the observation that although the parameterisation of the fracture size distribution is uncertain, constraining the intensity of connected open fractures to equal the intensity of the PFL-f fractures provides strong bounds on the viable parameter combinations. The consequences of alternative viable parameter combinations may only become apparent in subsequent modelling, or as new types of data become available.

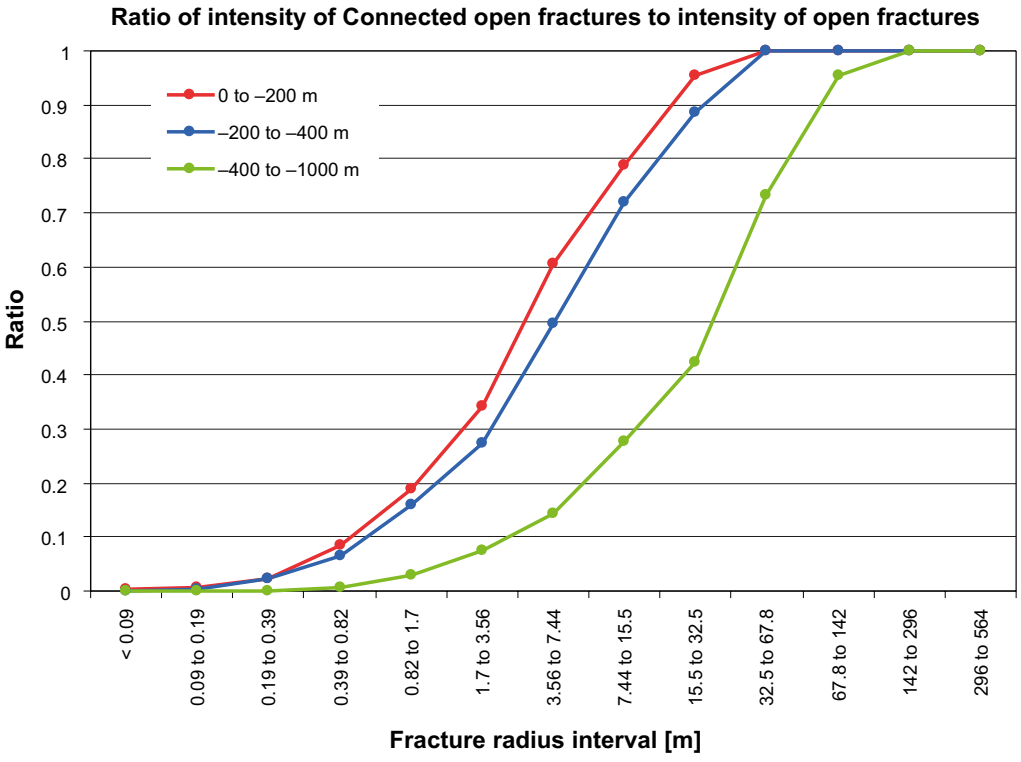

Figure 4-15. *Ratio of the intensity of simulated connected open fractures to open fractures as a function of fracture size for different depth intervals in hydraulic rock domain FFM01/FFM06, Forsmark. The intensities are based on 100 realisations of the models. The top depth zone of FFM01 is mostly limited to elevations between –100 m and –200 m. The Hydro-DFN intensity-size parameters are from Follin et al. (2007a, Table 11-20).*

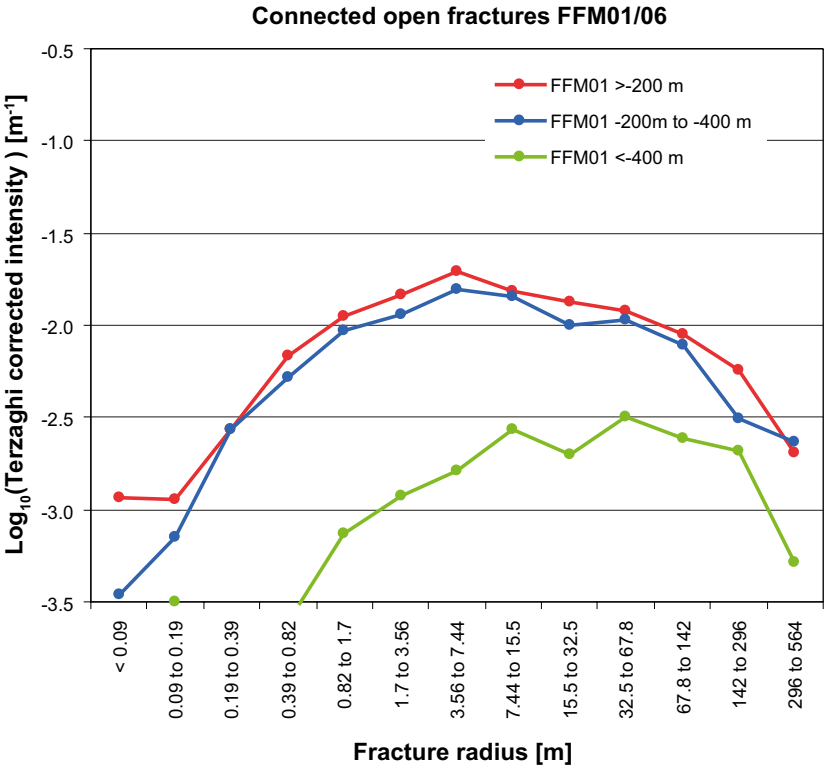

Figure 4-16. *Intensity-size distributions of connected open fractures derived through model calibration for FFM01 / FFM06 for 3 depth zones. The Hydro-DFN intensity-size parameters are from Follin et al. (2007a, Table 11-20).*

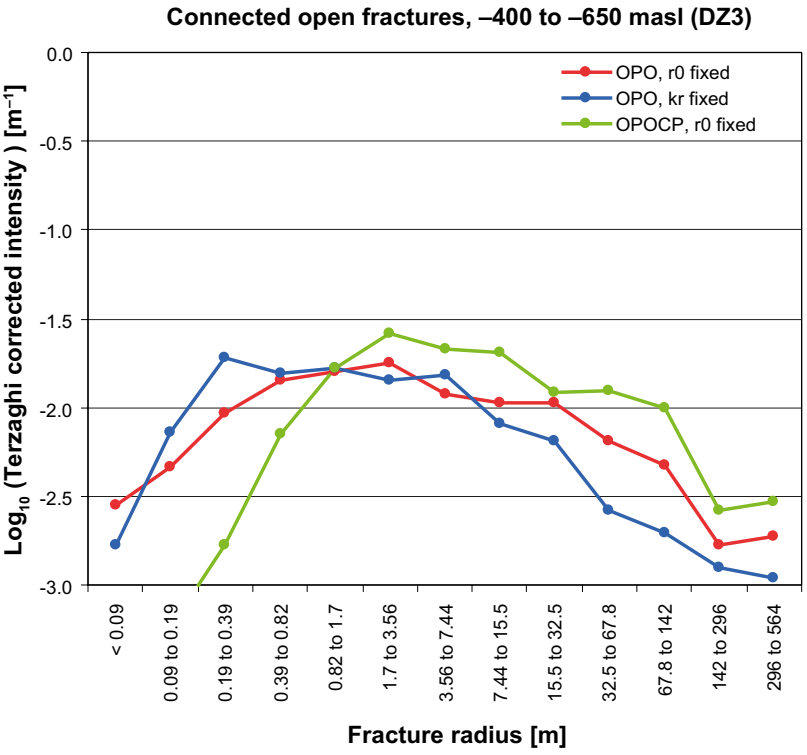

Figure 4-17. *Terzaghi corrected connected open fracture intensity as a function of fracture radius. Results are for the 3 size variants used in the modelling for HRD_C, Laxemar. The results are based on 40 realisations. The Hydro-DFN intensity-size parameters are from Rhén et al. (2008, Tables 10-2–10-4).*

A further characteristic of the generated fracture networks is the spatial variability of fracture intensity as measured within borehole. The amount of variability can vary by length scale and be affected by the underlying variability in the distribution of fractures and also by clustering, i.e. a deviation from Poissonian spatial process. The Geo-DFN analysed fracture spacings for the set of all fractures and concluded a Euclidean scaling model was appropriate at scales large than a few tens of metres as described in Subsection 3.3.6. Hence, the spatial variability in fracture intensity between borehole intervals was investigated on the scale of 50 m intervals to avoid the non-Euclidean scale issues identified on scales less than about 10 m and quantify spatial variability on a typical scale of interest for hydrogeology. On this scale then it is expected that variability in fracture intensity between 50 m borehole sections reflects genuine variability in fracture occurrence rather than an artefact of clustering. It is an underlying assumption of the Hydro-DFN that the set of open fractures also follows Euclidean scaling behaviour, since the set represents a significant proportion of all fractures. However, connected open fractures do not necessarily follow a Euclidean scaling, and in fact due to the tendency for connections to cluster around large fractures in sparse networks, then a fractal scaling behaviour is more likely as demonstrated by Follin et al. (2006).

As a simple illustration of observed and generated variability, Figure 4-18 presents the distribution of Terzaghi corrected (a maximum weight of 7 was used for both model and data) fracture intensity for open fractures in 50 m intervals for SDM-Site Laxemar (Rhén et al. 2008) for both measurements and simulations. Because of the inherent variations in intensity with depth and it is necessary to focus on particular subdomains and then consider the variability within those. The example used is a combination of hydraulic domains HRD_C and HRD_W between –400 m and –650 m were combined to give a reasonable degree of statistical significance. The intensities were summed over all fracture sets. For the model, the appropriate 50 m intervals within 10 realisations of 1 km boreholes were used where the intensity of open fractures was based on the OPO fracture intensity and the r_0 fixed fracture size variant was used. For the data, values were calculated for borehole intervals with the chosen hydraulic domains and depth intervals. Typically 10 realisations were used to provide simulation results as this gave a total simulated length of borehole interval commensurate with amount of data acquired. For practical reasons it was not possible to check the statistical convergence of every simulation result.

The top plot in Figure 4-18 shows that the model does produce some variability on the 50 m scale using a Poisson point process and a power-law size distribution, although the modelled variability is less than that seen in the data, which has some intervals with less than 50 open fractures and some with more than 200. The mode between 50-100 fractures though is the same as expected since the model input P_{32} is based on the measured average Terzaghi corrected intensity. Hence, the model has the correct mean open fracture intensity and some spatial variability, but less than that observed. The model would have to be elaborated to include a description of spatial variability in intensity within each subdomain to reproduce such observations.

The lower figure in Figure 4-18 compares the spatial variability in connected open fracture intensity from the simulations and PFL-f fractures from the hydraulic testing. Here, the model appears to reproduce the variability in connected open fracture intensity, though the data contains some outlying values that are unlikely to be produced in a model. The modelled variability was not produced by design as a calibration target, but seems to arise in any case from the hypothesis of a power-law size distribution and the calibration of connectivity against the observed sparse system of PFL-f fractures.

Perhaps the spatial variability of intensity of classes of fractures is one area for further development in the interpretation and model calibration methodology. However, a main goal of the strategy to first define fracture domains is that the variability within domains should be less than the variability between domains, and so this should not be an overriding issue. Still, spatial variability around the repository volume could be an important consideration in determining favourable volumes for deposition.

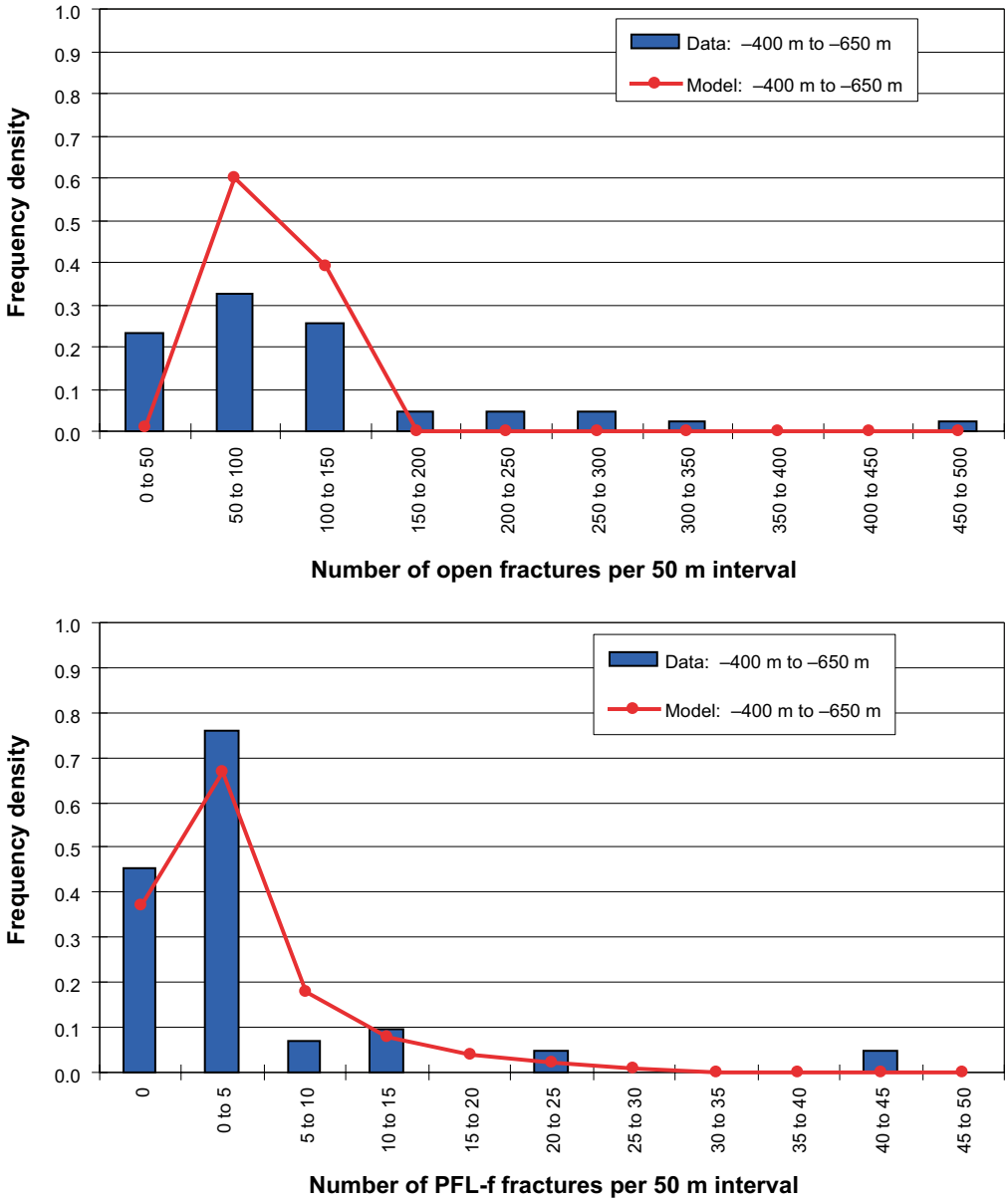

Figure 4-18. *Comparison of distributions of Terzaghi corrected fracture count within 50 m borehole intervals between the borehole intervals within both HRD_C and HRD_W combined, and the results of 10 realisations of HRD_C based on the OPO, r_0 fixed model. Top: Comparison of simulated and observed open fractures. Bottom: Comparison of connected open fractures (simulated) with PFL-f fractures (data). (After Rhén et al. 2008, Figure 10-13.)*

4.6 Calibration fracture transmissivity

The fourth stage of the calibration of the Hydro-DFN model of the HRD is to account for the role of fracture transmissivity in determining the distribution of specific capacity of flow-conducting features detected by the PFL-f method. The parameterisation of the transmissivity relationship within the hydro-geological DFN model is non-unique as assumptions have to be made concerning the relationship of transmissivity to fracture size. Three variants for the relationship of fracture transmissivity to fracture size were considered; uncorrelated, semi-correlated and correlated as described in Table 3-3.

4.6.1 Modelling details

The geometrical model configuration used in the flow simulations was largely the same as for the connectivity simulations described in Section 4.5. There were two minor differences. The first is in the treatment of fracture connectivity around the borehole. For the geometrical connectivity analysis, the connectivity was evaluated without the borehole present, and then the borehole was inserted afterwards to obtain the connected open fracture intensity. In the flow simulations, the borehole was inserted from the start and connectivity was calculated from the intensity of fractures supplying a non-zero inflow to the borehole. The difference is that the borehole itself can create additional connectivity by intersecting parts of the network that would be dead-ends in its absence (some examples can be identified in Figure 4-2 sketch). The approach used for the flow simulations can identify additional fractures not counted in the geometrical connectivity analysis (see Rhén et al. 2008, Appendix 8). Because this effect can have some importance in sparse networks, the approach was to use the size distribution parameters from the connectivity analysis (Section 4.5) as an initial guess from relatively fast geometrical simulations, and then adjust the size parameters if the flow simulations (computationally more intensive) produced a higher connectivity around the borehole. Hence, it is only after this flow calibration step that the size distribution parameters can be finalised. The second difference was to discard fractures smaller than 0.28 m radius to limit simulation times. For sparse networks such small fractures do not contribute significantly to connectivity or flow which was shown to be a relatively minor effect in Rhén et al. (2008, Appendix 8).

Steady-state DFN flow simulations of the PFL-f test configuration are used to predict the distribution of inflows to the boreholes. The idealised boundary conditions used are zero head on the top and sides of the domain, and a drawdown of 10 m along the whole length of borehole. In the field, the drawdown is typically 10 m near the top, but gradually decreases, and hence the normalised specific capacity of flux, Q, divided by drawdown, s, is used for the comparison of inflows. Ten realisations were performed for each simulation case. An example visualisation of the drawdowns predicted by a Hydro-DFN model is shown in Figure 4-19.

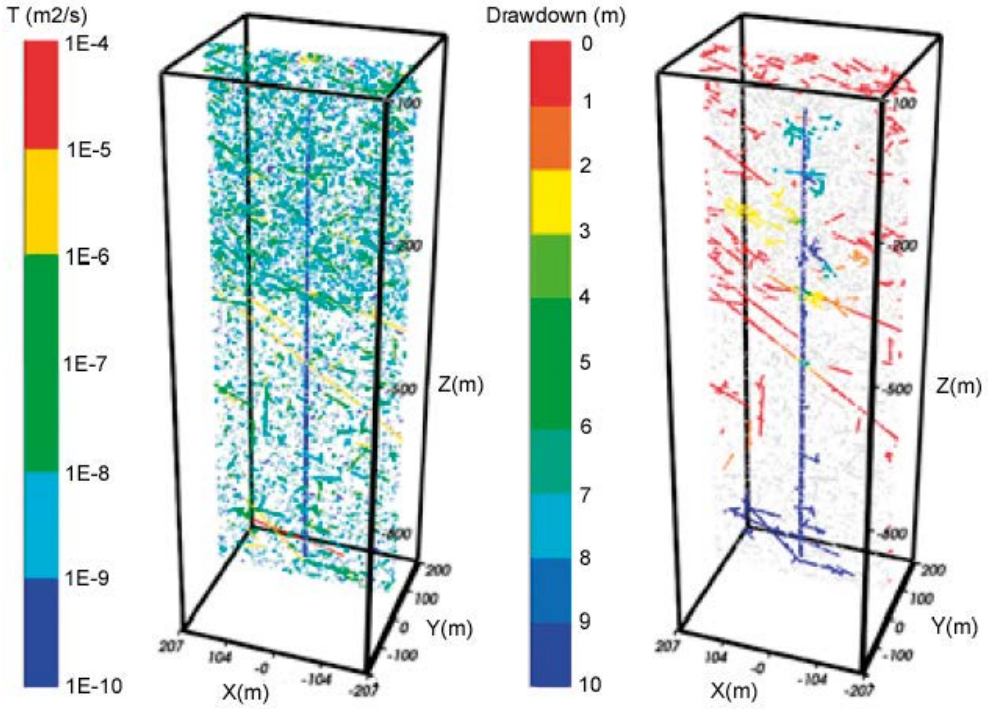

Figure 4-19. *Vertical cross-section through one realisation of the Hydro-DFN model for the semi-correlated model, hydraulic rock domain FFM01/FFM06, Forsmark with different fracture intensity above and below –400 m elevation. Left: all open fractures coloured by transmissivity. The 1 km generic vertical borehole is coloured blue in the middle. Right: all open fractures coloured by drawdown with unconnected fractures coloured grey. (After Follin et al. 2007a, Figure 11-14.)*

4.6.2 Flow calibration

In order to investigate variations with depth, the simulated values of specific capacity, *Q/s,* and the measurements from the PFL-f method, were divided according to the depth zones and used as ensembles to compare the distribution between modelled and measured results. Several calibration targets were used to quantify how well the model simulates the data, including:

1) A histogram of the distribution of specific capacity, *Q/s*, with a bin size of half an order of magnitude. The comparison of the shape of this histogram is quantified by calculating the correlation coefficient between numbers of PFL-f features within each bin. The match was sometimes quantified through the use of correlation coefficients.
2) The sum of specific capacity for the borehole (calculated as an arithmetic average over the realisations).
3) The inflow to 100 m borehole intervals (calculated as a geometric mean over the realisations, as well as standard deviation).
4) The numbers of PFL-f features associated with each fracture set and its distribution of specific capacity. This distribution is quantified in terms of the mean, plus or minus one standard deviation, minimum and maximum of Log(*Q/s*).
5) For the Laxemar modelling, a comparison was made against data from the short interval PSS tests, which largely used a 5 m interval. These were only available for elevations spanning depth zones 2 and 3, and for fewer boreholes than PFL-f data. As a smaller sample size, this data was only used as a confirmatory comparison of the calibrated models. To make a comparison, the simulated flows, *Q/s*, were summed over 5 m intervals to compare with the Moye interpretation (Moye 1967) of the PSS tests, and histograms of modelled and measured distributions compared. As an extra comparison, the number of 5 m intervals within each depth zone that had no detectable flow was calculated as a measure of the frequency of flow-conducting features.

The data statistics were calculated over the ensemble of measurements made in all boreholes for intervals within each depth zone. The statistics (such as total specific capacity and numbers of PFL-f features) were then rescaled according to the thickness of the depth zone divided by the total length of borehole sections measured within that depth zone. For the model, ensemble statistics were calculated over the model realisations. Hence the statistical variability between realisations is used as an analogue of the spatial variability between boreholes. For measures 1, 2 and 4, the comparison is made with statistics based on the PFL-f data. For measure 3, the geometric mean for the data is taken over the 100 m PSS data in intervals not intersected by major deformation zones. For the Forsmark modelling only measures 1, 2 and 4 were used in the calibration.

Terzaghi weighting of the calibration targets was used wherever appropriate. This was done to avoid bias in comparing the simulation of inflows to vertical boreholes with measurements in inclined boreholes, which has particular relevance to Laxemar with the hydraulic importance of the sub-vertical WNW set. Hence, in calibration targets 1, 2 and 4 above, any counts of simulated specific capacity, were weighted by the Terzaghi weight of the associated fracture. For example, in calibration target 4, the Terzaghi weighted count of PFL-f features were compared, which is consistent with the connectivity calibration.

Examples of the alternative types of transmissivity-size relationship developed through model calibration are shown in Figure 4-20 and Figure 4-21 for Forsmark and Laxemar, respectively. Both examples are taken for bedrock appropriate to repository depth. These figures illustrate a characteristic that was found for all subdomains after flow calibration in that although three different transmissivity models are considered, the ranges of transmissivities that each relationship produces are fairly similar for the fractures with radii in the range c 10 m to 100 m (see Follin et al. 2007a, Rhén et al. 2008, Joyce et al. 2010b). Fractures in this size range are thought to be most important in determining the connectivity characteristics of the fracture network, and hence for simulating the inflows in the PFL-f tests. Differences between the three models are only apparent in hydraulic characteristics such as the scaling behaviour of equivalent hydraulic conductivity (i.e. bulk flow scaling) as illustrated in Section 5.2.

Examples of the results of the flow matching procedure are shown in Figure 4-22 for the Laxemar Elaborated Hydro-DFN model of HRD_C, Depth Zone 3 (Joyce et al. 2010b). Parts (a) and (b) of Figure 4-22 relates to calibration target (1), part (c) relates to calibration target (2), part (d) relates to

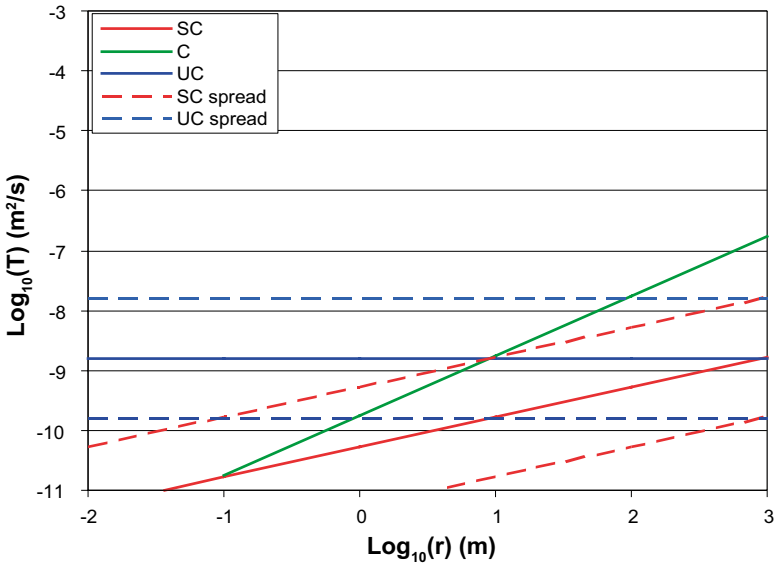

Figure 4-20. *Comparison of the relationships (SC-semi-correlated, C-correlated, UC-uncorrelated; Table 3-3) between fracture transmissivity and fracture size for Sub-horizontal fractures below –400 m in FFM01/FFM06, Forsmark. The plots show the central trend for each relationship together with lines at 1 standard deviation above and below the central trend. Based on parameters given in Follin et al. (2007a, Figure 11-17).*

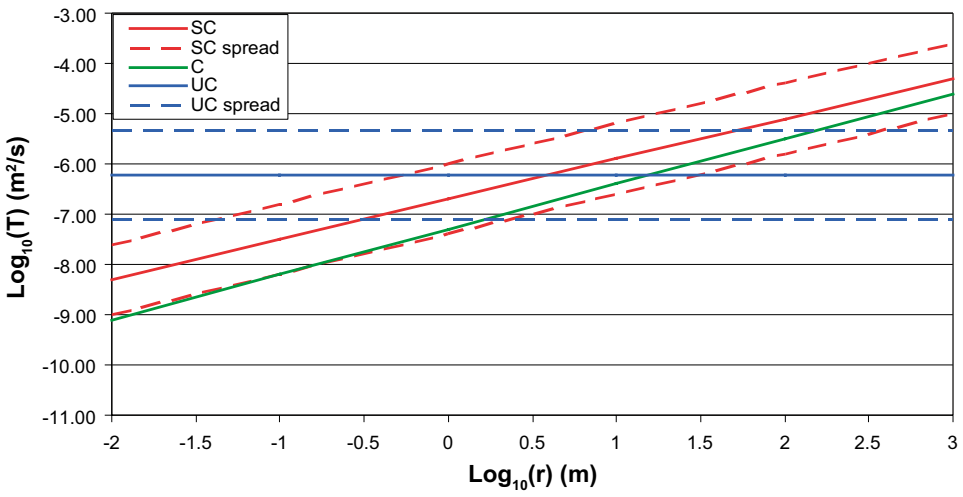

Figure 4-21. *Equivalent plot of fracture transmissivity and fracture size for Sub-horizontal fractures in Depth zone 3 for HRD_C, Laxemar. (Based on parameters given in Joyce et al. (2010b, Appendix E).*

calibration target (3), part (e) relates to calibration target (4) and part (f) relates to calibration target (5). A similar match to the data was obtained for other size-transmissivity variants, and other fracture intensity-size variants at Laxemar. The overall similarity of correlation coefficients obtained by comparing simulated and measured distributions of specific capacity between model variants demonstrates that a consistent level of match to the data was achieved for each variant. This is significant as it means that the PFL-f data is not sufficient to distinguish between any of the size-transmissivity model variants proposed. Additional types of data, possibly from underground investigations, might be necessary to constrain these aspects of the hydrogeological DFN models.

The following provides some insight into how the calibration is performed from a practical sense. Figure 4-20 and Figure 4-21 provide insight into how the parameters in Table 3-3 are adjusted to reproduce the calibration targets. For the correlated model, the transmissivity of c 100 m fractures has to be fixed to reproduce the total flow and flow to 100 m intervals (targets (c) and (d) in Figure 4-22);

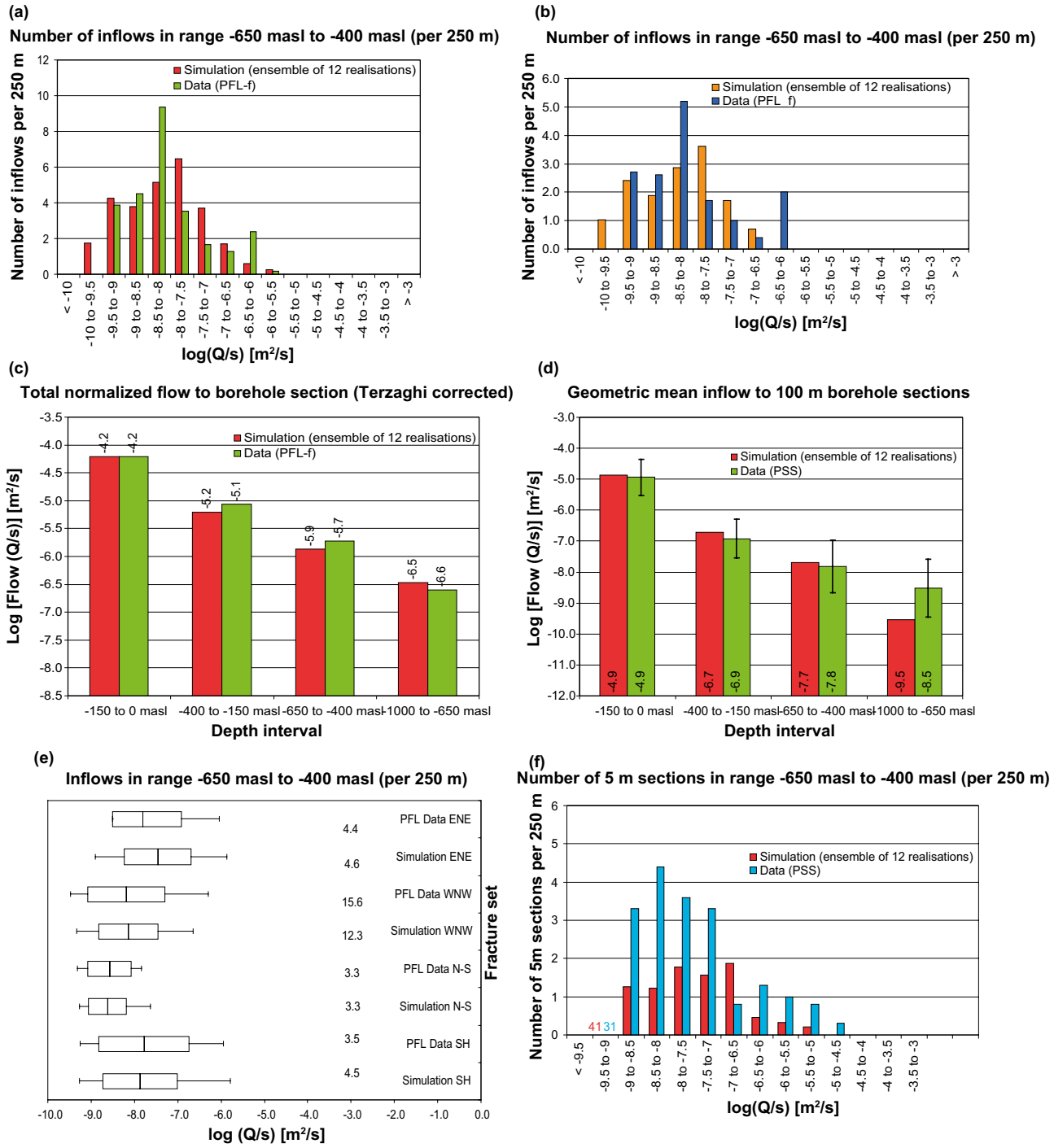

Figure 4-22. *(a) Histograms comparing the distribution of specific capacity for fractures in all sets (b) Histograms comparing the distribution of specific capacity for fractures in the WNW set. (c) Comparison of the sum of specific capacity in to the whole borehole. (d) Comparison of the geometric mean of total specific capacity to 100 m borehole intervals for the PSS data. For the data, the geometric mean is shown as well as the 95% confidence interval in the mean. (e) Bar and whisker plots comparing specific capacity. The centre of the bar indicates the mean value, the ends of the bar indicate ±1 standard deviation, the error bars indicate the minimum and maximum values and the value is the Terzaghi corrected number of flow-conducting features above the PFL-f detection limit. (f) Histogram comparing the distribution of specific capacity in 5 m sections. (After Rhén et al. 2008, Chapter 10.)*

the slope of the size-transmissivity relation is then adjusted to get agreement to the distributions of specific capacity (targets (a), (b) and (e) in Figure 4-22). For the uncorrelated model, the mean of log(transmissivity) has to be fixed to reproduce the total flow and flow to 100 m intervals (targets (c) and (d) in Figure 4-22); the variability in transmissivity is then adjusted to get agreement to the distributions of specific capacity (targets (a), (b) and (e) in Figure 4-22). For the semi-correlated model, the transmissivity of c 100 m fractures has to be fixed to reproduce the total flow and flow to 100 m intervals (targets (c) and (d) in Figure 4-22); both the standard deviation in log(transmissivity) and slope of the size-transmissivity relation are adjusted to get agreement to the distributions of specific capacity (targets (a), (b) and (e) in Figure 4-22); keeping both parameters of similar magnitude to ensure the result can still be described as semi-correlated although the outcome is none unique.

4.6.3 Resulting Hydro-DFN description

The calibrated prescription for a Hydro-DFN representation of fracture domain FFM01/FFM06 for Forsmark as used in the base case model for SR-Site is given in Table 4-5 from Joyce et al. 2010a). Notes this used the alternative prescription for fracture orientation Fisher distribution parameters recommended in Table 11-26 of Follin et al. (2007a).

An equivalent example for Laxemar is given in Table 4-6 for the Elaborated Hydro-DFN representation of the HRD_C hydraulic rock domain.

These two tables in themselves provide a basis for comparing some important characteristics of the hydraulic fracture systems at the two sites:

- At Forsmark open fracture intensity is dominated by the HZ and NE sets with the HZ being more important in the near-surface, with the other 3 sets relatively minor. At Laxemar all 4 sets make a contribution, with SubH dominant near-surface and WNW becoming more important at depth.
- The intensity of open fractures at Forsmark is about one third that at Laxemar. At Forsmark the intensity halves at Forsmark below –400 m, this also occurs at Laxemar, but not until below about –650 m.
- At Forsmark the observed fall-off in PFL intensity with depth could be reproduced with the same size distribution at all depths and explained by the reduction in intensity from relatively low to very low. At Laxemar the network was overly connected unless the fracture size distribution was reduced also.
- Higher transmissivities were generally assigned to the fractures at Laxemar and differences in transmissivities between sets was an important part of the calibration process against PFL data.

Table 4-5. Hydro-DFN parameters for the semi-correlated transmissivity model of FFM01 and FFM06 with depth dependency: above –200 m, –200 m to –400 m and below –400 m RHB 70. (After Follin 2008, Appendix C, using the Alternative orientation parameters).

Fracture domain and depth (m RHB 70)	Fracture set name	Orientation set pole: (trend, plunge), conc.	Size model, power-law (r_0, k_r) (m, –)	Intensity, (P_{32}), valid size interval: (r_0, 564 m) (m^2/m^3)	Transmissivity model T (m^2/s) (a, b, σ) Table 3-4 T (m^2s^{-1})
FFM01/06 > –200	NS	(292, 1) 17.8	(0.038,2.55)	0.073	(6.3×10^{-9}, 1.3, 1.0)
	NE	(326, 2) 14.3	(0.038,2.75)	0.319	
	NW	(60, 6) 12.9	(0.038,3.10)	0.107	
	EW	(15, 2) 14.0	(0.038,3.10)	0.088	
	HZ	(5, 86) 15.2	(0.038,2.42)	0.543	
FFM01/06 –200 to –400	NS	As above	As above	0.142	(1.3×10^{-9}, 0.5, 1.0)
	NE	As above	As above	0.345	
	NW	As above	As above	0.133	
	EW	As above	As above	0.081	
	HZ	As above	As above	0.316	
FFM01/06 < –400	NS	As above	As above	0.094	(5.3×10^{-11}, 0.5,1.0)
	NE	As above	As above	0.163	
	NW	As above	As above	0.098	
	EW	As above	As above	0.039	
	HZ	As above	As above	0.141	

Table 4-6. Description of the Elaborated Hydro-DFN input parameters for HRD_C (Laxemar) with fixed r_0=0.038 m and intensity of open fractures based on OPO. (After Joyce et al. 2010b, Table E-1).

Depth zone (masl)	Set	Orientation set pole: (trend, plunge), conc.	Fracture radius model power-law (k_r, r_0)	Intensity P_{32} (m^2/m^3) of open fractures (r_0, 564 m)	Transmissivity model T (m^2/s) (a, b, σ)
–150 to 0 (DZ1)	ENE	(155.1,3.4), 9.6	(2.70, 0.038)	0.52	SC: ($2\cdot10^{-7}$, 0.7, 0.4)
	WNW	(204,1.6), 12	(2.49, 0.038)	0.95	SC: ($2\cdot10^{-7}$, 0.9, 0.6)
	N-S	(270.2,8.4), 7.8	(2.80, 0.038)	0.54	SC: ($8\cdot10^{-8}$, 0.5, 0.4)
	SubH	(46.3,84.7), 12	(2.59, 0.038)	1.20	SC: ($6\cdot10^{-8}$, 0.7, 0.5)
–400 to –150 (DZ2)	ENE	(155.1,3.4), 9.6	(3.00, 0.038)	0.47	SC: ($6\cdot10^{-7}$, 0.7, 0.9)
	WNW	(204,1.6), 12	(2.44, 0.038)	0.55	SC: ($1\cdot10^{-8}$, 0.5, 0.7)
	N-S	(270.2,8.4), 7.8	(2.91, 0.038)	0.63	SC: ($1\cdot10^{-8}$, 0.7, 0.2)
	SubH	(46.3,84.7), 12	(2.87, 0.038)	0.71	SC: ($3.5\cdot10^{-8}$,1.2,0.9)
–650 to –400 (DZ3)	ENE	(155.1,3.4), 9.6	(2.87, 0.038)	0.38	SC: ($8\cdot10^{-8}$, 0.8, 0.6)
	WNW	(204,1.6), 12	(2.54, 0.038)	0.74	SC: ($3\cdot10^{-9}$, 0.8, 0.6)
	N-S	(270.2,8.4), 7.8	(2.87, 0.038)	0.47	SC: ($6\cdot10^{-9}$, 0.4, 0.4)
	SubH	(46.3,84.7), 12	(3.00, 0.038)	0.58	SC: ($2\cdot10^{-7}$, 0.8, 0.7)
–1,000 to –650 (DZ4)	ENE	(155.1,3.4), 9.6	(2.96, 0.038)	0.46	SC: ($1\cdot10^{-8}$, 0.7, 0.4)
	WNW	(204,1.6), 12	(3.00, 0.038)	0.73	SC: ($3\cdot10^{-7}$, 0.7, 0.4)
	N-S	(270.2,8.4), 7.8	(3.00, 0.038)	0.25	SC: ($1\cdot10^{-8}$, 0.7, 0.4)
	SubH	(46.3,84.7), 12	(2.97, 0.038)	0.35	SC: ($1\cdot10^{-7}$, 0.7, 0.4)

4.7 Summary of identified uncertainties in Hydro-DFN modelling

Uncertainties associated with the groundwater flow and transport modelling in the HRD can be considered in three categories:

1) conceptual uncertainty, representing the conceptualisation of fracture system, and the assumptions made in characterising fracture geometry and hydraulic properties,
2) parameter and distribution uncertainty, which may result from uncertainties in underlying data,
3) stochastic uncertainty, representing spatial variability.

Conceptual uncertainty is understood to concern issues such as the validity of the DFN concept to the bedrock of interest, the assumption of size distribution as a tectonic continuum, and decisions in the DFN modelling methodology such as the assumption that inflows measured by the PFL-f tests are primarily limited by network connectivity. The justification for the modelling strategy pursued here is described in Sections 1.2 and Section 3. Suggestions for work to further investigate conceptual uncertainties are discussed in Section 8.3. An example of the use of model variants to assess the effect of conceptual uncertainty is the use of the stochastic continuum CPM models to predict repository performance statistics at Laxemar (Joyce et al. 2010b).

Here, the key assumptions described in Section 3.4 are re-examined in the context of the methodology applied in the Hydro-DFN model and the conclusion drawn from its application in SDM-Site Forsmark and Laxemar.

Fracture intensity scaling, spatial distribution and termination

A Euclidean intensity scaling of the open fractures was assumed on the basis of the analysis of all fractures performed for the Geo-DFN. The validity of this assumption for open fractures could be tested by analysing the distribution of open fracture spacings in the borehole data. Likewise, the clustering of PFL-f fractures could be analysed and compared with spacing distribution in the simulations. It is apparent from figures such as Figure 4-19 and that the simulated system of connected open fractures is clustered around large fractures when using a power-law size distribution.

In the Hydro-DFN simulations fracture centres and sizes have been generated independently without termination against each other. Including fracture terminations while maintaining overall fracture intensity has the possibility to remove some areas of fractures that would otherwise be dead-ends beyond where they intersect a fracture created earlier in time. As a consequence the density of

fracture intersections for the same fracture surface area could increase. However, any change in concept such as the representation of terminations would require re-calibration of the hydraulic system following the step described in Section 4.1, and the calibration of connectivity in terms of fracture size distribution is likely to restore the network to having similar connectivity characteristics to those derived in SDM-Site Forsmark and Laxemar.

Fracture intensity and fracture size

Similarly the hypothesis of a tectonic continuum concept for intensity-size of open fractures is adopted from the .geology. Alternative log-normal distributions or distinct scales of features were not evaluated. However, some variants models were tested such as considering alternative ways of defining r_0 and k_r based on connectivity analysis was tested for both sites, and at Laxemar alternative definition of open fracture intensity were evaluated basis confidence classifications. For all the variants considered it was possible to adjust the size parameters to simulate the connectivity implied by the PFL-f tests to a similar degree of accuracy. That is to be expected though since the intensity of open fractures measured is everywhere sufficiently sparse that the size distribution can always be adjusted to reduce connectivity to the required level. However, in doing so it can produce connected networks that display characteristics inconsistent with other sorts of information. For example, the Laxemar variants with open fracture intensity based on OPO-CP fractures was problematic in the sense that low k_r values were required to match the PFL-f intensity values, but this meant that the number of large fractures predicted was inconsistent with geology. The different size models derived from connectivity calibration can also strongly affect the scaling behaviour of hydraulic properties, as is discussed in the next chapter.

Results such as those shown in Figure 4-16 and Figure 4-17 illustrate how intensity-size distribution for connected open fractures can be vary different to that from the original distribution of open fractures, often displaying a log-normal type distribution for sparse systems starting from a power-law distribution. Also Follin et al. (2006) showed that the connected open system can follow a fractal spatial distribution due to the clustering of connectivity around large fractures.

Fracture orientations and set definitions

The interpretation of fracture sets appropriate to the Hydro-DFN has typically been performed by analysis of stereonets of the open and PFL-f sets. Generally the sets considered appropriate for water-conducting fractures have been broadly consistent with those interpreted for all fractures in the Geo-DFN models. However, as shown in Figure 4-6 the relative intensities and concentrations of orientations between sets can vary significant between all, open and PFL-f classes of fractures. Therefore, results will be sensitive as to which class of fracture is used as the basis for interpreting orientation distributions. For the Hydro-DFN, it considered that orientations should be interpreted either on the open or PFL-f subsets of fractures. Differences in concentration of orientation within a set affect connectivity of the system. This was found to have moderate importance at Forsmark. Two possible set definitions and orientation distributions were derived: one based on F1.2 set definitions and an alternative (Follin et al. 2007a) based on interpretation of the F2.2 borehole data. During the regional modelling for SDM-site it was found that higher concentration of orientation of the dominant sub-horizontal implied by the alternative orientation model was found to be more representative of the high hydraulic anisotropy apparent when simulating interference tests and the palaeo-climatic evolution. Therefore, in SR-site the alternative orientation model was used.

Concepts for the hydraulically significant fractures

Firstly, defining the subset of fractures that have the potential to contribute to flow and transport has a number of uncertainties. It is generally only possible do so for fractures seen in boreholes, not on outcrop, and still there is a significant uncertainty about the classification of open fractures. For example, at Laxemar only 36% of PFL-f detected flowing fractures belonged to the set of open fractures classified as “certain”, 73% as either “certain” or “probable”, and only when the all open fractures were included were most PFL-f fractures captured. Considering all open fractures (OPO) in the Hydro-DFN modelling amounted to more than doubling the intensity of fractures consider for the hydraulic system than if only the subset of “certain” or “probable” open fractures were modelled (OPO-CP). To investigate this uncertainty, Hydro-DFN modelling was performed for intensities

based on either OPO or OPO-CP intensities with a calibration of connectivity against PFL-f fracture intensity, which required quite different models for intensity-size distribution for the two variants. Only when making sense checks of the calibrated intensity-size distributions against the geological modelling did it become apparent that the OPO-CP model required a higher intensity of large fractures than was evident in geology, and so appeared less plausible, at least not with geological concepts of a tectonic continuum and power-law size distribution.

There are also issues to consider in measuring the intensity of flowing fractures as seen in a borehole. These include the effects on fracture connectivity of the borehole itself; the fact a borehole is a cylinder rather than a scan line, and the effects of the effects of flow censoring due to in-plane heterogeneity. Because the fracture systems considered are generally sparse then it was found that small fractures on the scale of decimetres (or even metres) make a limited contribution to the connected flowing system then radius of the borehole is typically much less than that of connected open fractures. The presence of the borehole has a moderate effect on connectivity as shown in Rhén et al. (2008), and so this effect was considered explicitly within the flow simulations by fine-tuning of the size distribution as necessary. Flow censoring effects due to heterogeneity were not quantified explicitly within SDM-Site. However, it must be emphasised that if concepts are tested with flow restricted to only a portion of the fracture surface area, then other model parameters need to be re-calibrated so to maintain consistency of the resulting connected open system to the measured PFL-f distribution of flow. For example, if flow is restricted to only 50% of fracture surface area then because flow within individual fractures may no longer percolate, then the intensity of open fractures would probably have to be more than doubled and/or the size distribution changed to achieve sufficient connectivity. Such a concept was investigated in Hydro-DFN modelling of Olkiluoto (Hartley et al. 2011), where a model variant denoted "Case C" was tested with then open fracture intensity being taken to be distributed over all fractures, but restricted to only a portion of the area, and the fracture size distribution taken from the corresponding Geo-DFN (Fox et al. 2012). The portion of open area was then used as matching parameter in a connectivity calibration against PFL-f intensity.

Fracture hydraulic properties

Uncertainties associated with hydraulic properties include those arise from the test configuration and detection limit of equipment and the conceptualisation of the high degree of measured variability in flow magnitudes. The two types of hydraulic data PFL-f tests (long duration, short interval, and abstraction) and PSS tests (short duration, longer intervals, and injection) provide a measure of the sensitivity to the test configurations used. For both Forsmark (Follin et al. 2007a, Chapter 4) and Laxemar (Rhén et al. 2008, Chapter 4) consistency between the two types of information was demonstrated with the interpreted values typically falling within an order of magnitude envelope of 1:1 correlation, although a slight bias toward higher values in the PSS data was observed. The Hydro-DFN calibration was mainly focussed on the PFL-f data because of the discrete nature of the measurements lend themselves to interpretation of the hydraulic properties of individual fractures. For example, the differences in properties of different fracture sets can be examined. PSS was data was used in some flow calibration targets such as the geometric mean flow to 100 m borehole section. Sensitivities to assumptions about flow geometry for a pumping borehole were circumvented by calibrating the simulated specific capacity (inflow/drawdown) directly with that measured, rather than comparing interpreted fracture transmissivities.

The detection limit of PFL-f tests of specific capacity c 10^{-9} m^2/s for surface drilled boreholes is typically a few orders of magnitude lower than geometric mean specific capacity values measured in the upper bedrock, and hence is sufficient to detect flow features of any hydraulic significance. At repository depth geometric mean measured values are on the order of 10^{-9} m^2/s at Forsmark (see Follin et al. 2007a, Chapter 11) and at Laxemar on the order of 10^{-8} m^2/s (see Rhén et al. 2008, Chapter 10), and so the detection limit will have an influence on the Hydro-DFN modelling. The Hydro-DFN modelling is essentially only able to calibrate the connected fracture system of fractures with specific capacity above c 10^{-9} m^2/s. Comparison of the role of the detection limits between PFL-f and PSS tests at Forsmark (see Follin et al. 2007a, Section 4.3) suggested similar transmissivity distributions for 5 m intervals above 10^{-8} m^2/s, but PSS suggested c 40% higher intensity of 5 m borehole intervals above 10^{-9} m^2/s. The short duration PSS tests may however, just be detecting finite flow compartments not seen in the PFL tests, and so it can only be concluded there is uncertainty in the intensity of fractures with specific capacity c 10^{-9} m^2/s of a few tens of percent.

During the construction of the ONKALO at Olkiluoto it was possible to run PFL-f tests in tunnel pilot holes ahead of excavation at higher drawdowns giving an effective detection limit on specific capacity of up to 40 times lower, c 2 10^{-11} m^2/s at 400 m depth (Hartley et al. 2011). The results confirmed the intensity of flowing fractures above 10^{-9} m^2/s detected in surface based investigations, but also revealed additional flowing fractures with much lower specific capacity. This implies the possibility for additional connectivity and flow at small scales smaller than the spacing between flowing fractures detected from the surface based investigations, but will have little effect on bulk flow on larger scales.

The variability in specific capacity of fractures observed is in part reproduced in models as a consequence of the stochastic nature of the geometry and connectivity of the fractures essentially giving rise to varying boundary conditions for the flow across individual fractures even without variability in their individual hydraulic properties. Variability in transmissivity between fractures creates addition variability, and these two factors typical have greater affect than variability within fractures (Painter 2006). The precise mix of these effects giving rise to the observed hydraulic variability and the relation to the geometrical properties cannot be inferred. Hence, in the modelling three different assumed size-transmissivity relationships have been considered to quantify the sensitivity to such aspects (see Figure 4-20 and Figure 4-21, for example). Each of these models can provide sufficient variability to reproduce the observed variability in specific capacity. The significance of the relationship between fracture transmissivity and size is seen though in characteristics such the scaling behaviour of equivalent hydraulic conductivity, as is demonstrated in the next chapter. For example the uncorrelated model tends to predict relatively small differences in the geometric mean hydraulic conductivity on the 5 m, 20 m and 100 m scales while the PSS data usually predicts a gradual reduction in mean with test scale. Hence, the uncorrelated model seems less consistent with site data as well as being considered to lack geo-physical motivation, unlike the semi-correlated or correlated models.

Transport and storage properties

The main transport properties of the fracture system of relevance are the transport aperture determining the volume accessed by advection and the fracture surface area determining rock matrix diffusion. The transport aperture was assumed to scale with fracture transmissivity based on collations of tracer tests from various sites (Dershowitz et al. 2003, Hjerne et al. 2010). Consequences of the uncertainty in transport aperture were considered in the equivalent porous medium modelling of palaeo-climatic evolution through sensitivity tests on the kinematic porosity it implies (see Chapter 6.6) and the transport site description (Crawford 2008, Crawford and Sidborn 2009). In fact the evolution of palaeo-climatic had limited sensitivity to transport aperture. Of greater importance was the fracture surface area since rock matrix diffusion since it controls the magnitude of rock matrix diffusion in retarding solute mixing fronts moving through fracture system. The fracture surface area was estimated from the measured intensity of PFL-f fractures. However, there is an uncertainty in how significant is the truncation implied by the PFL detection limit on fracture surface area for rock matrix diffusion. A further issue is how to characterise fracture surface area in deformation zones if for hydrogeology they are described as single tabular features.

Storage properties were only the subject of matching the interference tests discussed in Section 6.4.

Fracture shape

Only the case of square stochastic fractures was considered in the DFN modelling since mechanisms for significantly non-equant fractures were not apparent. It is possible that elongated flow channels in particular directions could exist within fractures. Again, modelling tests of different shapes of channelling within fractures would need to be subject to re-calibration against measure of connectivity and flow distributions.

Stochastic uncertainty refers to the differences between equally plausible realisations of the Hydro-DFN models. This realisation dependent uncertainty might reflect the lack of knowledge of the actual fracture positions, geometries and properties at scales smaller than that of the mapped deformation zones. Stochastic uncertainty is quantified by presenting results for multiple realisations of the Hydro-DFN models.

4.7.1 Testing and application of model variants

The set of model variants considered in SDM-Site uncertainties with respect to:

1. Fracture size model.
2. Fracture size-transmissivity model.
3. Open fracture intensity (Laxemar only).

Where possible these model variants were used to illustrate and quantify the sensitivities of various simulations within SDM-Site and later SR-Site. However, the particular variants used in various modelling tasks varied for practical reasons. This was because some modelling tasks were considerably more expensive in terms of simulation times than others. The set of model variants used are by no means exhaustive, but are considered to cover the key parameter relationships between fracture intensity-size-transmissivity that control the hydraulic connectivity and hydraulic properties of the rock, and hence quantify the sensitivities of the hydrogeological DFN models.

Table 4-7 and Table 4-8 indicate which model variants were developed as fully calibrated DFN models, and which of these were subsequently used for different types of modelling, for Forsmark and Laxemar, respectively.

The types of modelling undertaken once each Hydro-DFN model variant had been calibrated can be considered in three categories: Upscaling to equivalent CPM properties for a representative volume (Block upscaling), confirmatory testing and calculations of interest to the safety assessment (SR-Site).

Block upscaling

The parameters derived through the calibration process are intended for use in modelling flow and transport using a DFN concept. However, a significant part of the hydrogeological modelling within the SDM uses Equivalent Continuous Porous Medium (ECPM) modelling based on upscaling of an underlying DFN model. An ECPM approach is used either to model certain physical processes, such as rock matrix diffusion, which are not implemented in a DFN framework, or where DFN calculations would be too time consuming, for example this would be the case for some regional-scale models. Hence it is interesting to evaluate what kind of upscaled hydraulic properties the hydrogeological DFN models imply. The upscaled properties are calculated for cubes, or blocks, of various sizes, hence the term “block upscaling”. For heterogeneous fracture systems hydraulic properties have a strong dependence on the block scale considered. On the scale of a deposition hole, c 5-10 m, flow and transport depends on the connectivity and transmissivity of individual fractures down to sizes of decimetres or metres, whereas bulk flows on scales of hundreds of metres are controlled by a network system of fractures, and hence some averaging of fracture properties takes place reducing the variability of properties on the larger scale. The results of the block modelling to calculate equivalent hydraulic properties on the 5 m 20 m and 100 m scales are described in Section 5.2. These three scales used since they correspond to the measurement scales for the PSS data, although it should be noted that the bulk flow through a block volume is a different entity to the injectivity at a borehole. Comparisons are also made with characteristics from the PFL-f data.

Confirmatory testing

The Hydro-DFN models developed have been applied to a variety of modelling tasks with the aims of confirming the models provide a description of the groundwater system that is appropriate for regional-scale simulations of flow and transport. This builds confidence that the models are also appropriate for calculations of the repository performance statistics which are used in the repository safety assessment. This confirmatory testing included local conditioning to single-hole hydraulic tests; simulation of groundwater heads; simulation of cross-borehole interference tests; simulation of drawdowns caused by the Äspö HRL at Laxemar and simulation of the palaeo-climatic evolution of the groundwater. Details are given in Section 6.

Safety assessment

To support the understanding and modelling of safety assessment related performance measures similar basic calculations were calculated for both sites (Joyce et al. 2010a, b). However, the hydro-geological models developed for the Forsmark site have been applied to the estimation of repository performance measures. The overall objective was to use these repository performance measures to allow assessment of long-term safety (Selroos and Follin 2010), as discussed in Section 7.

Table 4-7. Description of the variants used to assess parameters and distribution uncertainty which were calibrated as part of the DFN modelling of Forsmark. The use of each model variant in different modelling tasks is indicated with a tick.

P_{32}	Intensity-size power-law distribution parameters	Size-transmissivity model	Block upscaling	Confirmatory tests	Safety assessment
$P_{10,\ opo}$	r_0 = 0.038, k_r varies	Semi-correlated	√	√	√
$P_{10,\ opo}$	r_0 = 0.038, k_r varies	Correlated			√
$P_{10,\ opo}$	r_0 = 0.038, k_r varies	Uncorrelated			√

Table 4-8. Description of the variants used to assess parameters and distribution uncertainty which were calibrated as part of the DFN modelling of Laxemar. The use of each model variant in different modelling tasks is indicated with a tick.

P_{32}	Intensity-size power-law distribution parameters	Size-T model	Block upscaling	Confirmatory tests	Safety assessment	Additional comments
$P_{10,\ opo}$	Open=OPO r_0 = 0.038, k_r varies	Semi-correlated	√	√	√	Re-calibrated for Elaborated Hydro-DFN
$P_{10,opo\text{-}cp}$	Open=OPO-CP r_0 = 0.038, k_r varies	Semi-correlated	√			
$P_{10,\ opo}$	Open=OPO r_0 = 0.038, k_r varies	Correlated	√			
$P_{10,\ opo}$	Open=OPO r_0 = 0.038, k_r varies	Uncorrelated	√			
$P_{10,\ opo}$	Open=OPO r_0 varies, k_r = 2.9	Semi-correlated				HRD_C only

5 Upscaling and equivalent continuous porous medium properties

5.1 Upscaling methodology

In order to assess the implications of the Hydro-DFN models on flow and transport at the regional-scale, it is sometimes necessary for practical reasons to convert the Hydro-DFN models to an equivalent continuous porous medium (ECPM) model with appropriate continuum properties. These reasons include longer computational run times and limitations imposed by which physical processes can be modelled in the DFN representation with discrete fracture network models.

ECPM models have been used for confirmatory testing of the underlying DFN representation by simulating the palaeo-climatic evolution of Forsmark and Laxemar; by modelling borehole interference tests and by predicting groundwater heads in the undisturbed system (i.e. without pumping and prior to construction of a disposal facility). ECPM models, along with composite ECPM/DFN models have been used to calculate repository performance statistics for use in the repository safety assessment.

Defining an ECPM model requires methods (i) to convert the properties of a network of discrete fractures into equivalent continuous porous medium (ECPM) block properties, a process known as upscaling, and (ii) to represent larger scale features such as deformation zones by appropriate properties in a series of continuum blocks (the Implicit Fracture Zone or IFZ method (Marsic et al. 2001). The methods of implementation of the upscaling and IFZ processes using the ConnectFlow code (AMEC 2012c) are described below.

Upscaling a DFN model to give an ECPM model results in a porous media description defined by a spatially varying directional hydraulic conductivity tensor, a kinematic porosity and other transport properties such as the fracture surface area per unit volume. A flux-based upscaling method has been used that requires several flow calculations through a DFN model in different directions (Jackson et al. 2000). Figure 5-1 shows an illustration of how flow is calculated in a DFN model (a 2D network is shown for simplicity). To calculate equivalent hydraulic conductivity for the block shown, the flux through the network is calculated for a linear head gradient in each of the axial directions. Due to the variety of connections across the network, several flow-paths are possible, and may result in cross-flows non-parallel to the head gradient, a phenomenon that occurs in highly heterogeneous porous media (Follin 1992). Cross-flows are a common characteristic of DFN models and can be approximated in an ECPM by an anisotropic hydraulic conductivity. In 3D, ConnectFlow uses six directional components to characterise the symmetric hydraulic conductivity tensor. Using the DFN flow simulations, the fluxes through each face of the block are calculated for each head gradient direction. The hydraulic conductivity tensor is then derived by a least-squares fit to these flux responses for the fixed head gradients (Jackson et al. 2000). The kinematic porosity and fracture surface area per unit volume are treated as scalar quantities in the upscaling calculations.

A refinement of the upscaling methodology is to simulate flow through a slightly larger domain than the block size required for the ECPM properties, but then calculate the flux responses through the correct block size. The reason for this is to avoid over-prediction of hydraulic conductivity from flows through fractures that just cut the corner of the block but that are unrepresentative of flows through the in situ fracture network. The area around the block is known as a ‘guard-zone’, and an appropriate choice for its thickness is approximately one fracture radius. The problem is most significant in sparse heterogeneous networks in which the flux through the network of fractures is affected by ‘bottlenecks’ through low transmissivity fractures. The use of a guard zone was in all block modelling for Forsmark and Laxemar that is presented here in Section 5.2 as the capability was available for upscaling simple cuboid volumes (Jackson et al. 2000). The guard zone approach was extending to upscaling regional Hydro-DFN models for SDM-Site Laxemar (Rhén et al. 2009) and the later safety comparison calculations (Joyce et al. 2010b), and so was also used to provide regional-scale ECPM properties for modelling palaeo-climatic evolution. This facility was not available for regional ECPM modelling in SDM-Site Forsmark, and for consistency was not used in SR-Site (Joyce et al. 2010a). Comparison of regional groundwater flow circulation magnitudes and directions for DFN models and their corresponding upscaled ECPM models are available in Hartley et al. (2011, Chapter 8).

The kinematic porosity, ϕ, for each block is calculated as:

$$\phi = \frac{\sum_f e_t a_f}{V} \tag{5-1}$$

where V is the volume of the block, a_f is the area of each fracture in the block and e_t is the transport aperture of the fracture, which is typically correlated to fracture transmissivity. The summation is over all fractures within the block.

In ECPM models, the deformation zones were represented by modifying the hydraulic properties of any finite-elements intersected by one or more zones to incorporate the structural model in terms of the geometry and properties of zones using the Implicit Fracture Zone (IFZ) method as described in Marsic et al. (2001). In an ECPM model, the methodology is to first create one or more realisations of the stochastic DFN (including the deformation zones to provide connectivity) on the regional-scale and then to convert this to a realisation of the ECPM model (with the deformation zones removed) using the upscaling methodology described above. The ECPM model properties are then modified to incorporate the effect of the deformation zones. The reason for doing it this way was a practical one in that it allowed the sensitivity to the deformation zone properties to be tested independently and quickly without the need to repeat the upscaling methodology for the entire model, which for a large regional model is a substantial operation. It would be possible to test the result of upscaling the Hydro-DFN and deformation zones together to calculate the combined hydraulic conductivities in a single upscaling step and compare to the way which is used in SDM-Site and SR-Site, but this has not been done.

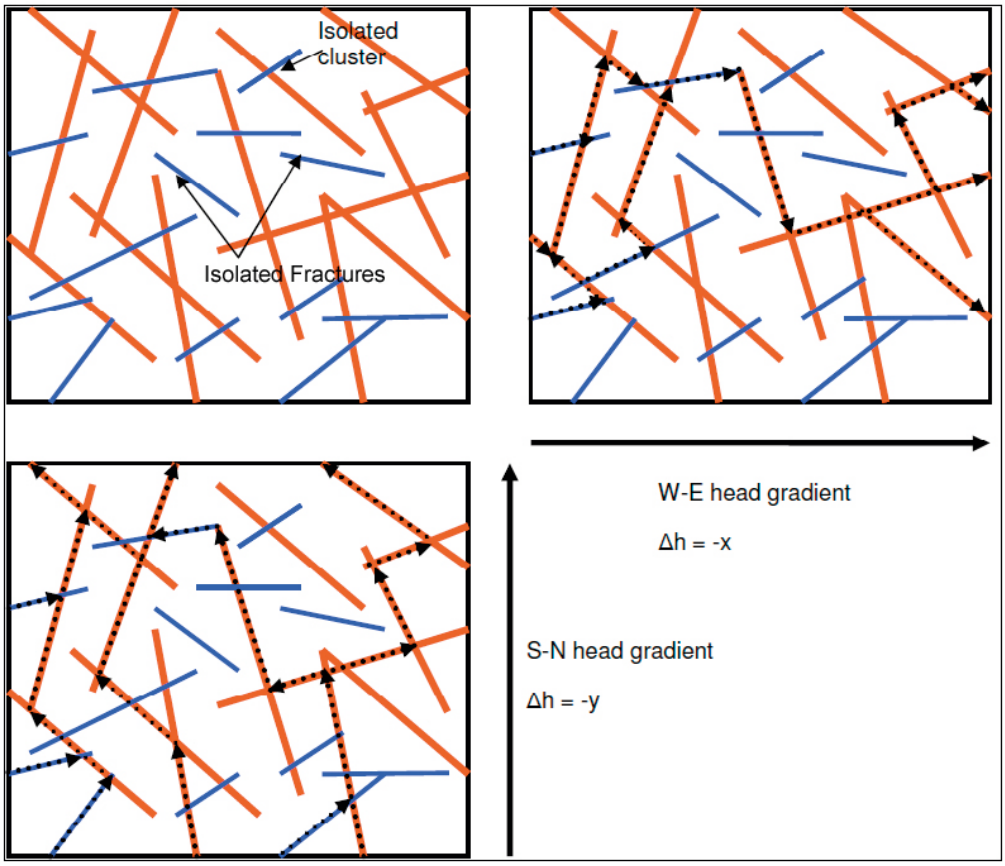

Figure 5-1. *2D illustration of flow through a network of fractures. A random network of fractures with variable length and transmissivity is shown top left (orange fractures are large transmissivity, blue are low). Top right: flow-paths (dotted arrows) for a linear head gradient E-W decreasing along the x-axis. Bottom left: flow-paths through the network for a linear head gradient S-N decreasing along the y-axis. (After Rhén et al. (2008, Figure 10-27.)*

The IFZ method identifies which elements are crossed by a fracture zone and combines a hydraulic conductivity tensor associated with the fracture zone with a hydraulic conductivity tensor for the background stochastic network. For each element crossed by the fracture zone the following steps are performed:

1) The volume of intersection between the fracture zone and the element is determined.
2) The hydraulic conductivity tensor of the background rock is calculated in the coordinate system of the fracture zone.
3) The combined conductivity tensor of the background rock and the fracture zone is calculated in the coordinate system of the fracture zone.
4) The effective hydraulic conductivity tensor that includes the effect of the fracture zone is determined in the original coordinate system.

The methodology is illustrated in Figure 5-2. In 3D, the resultant hydraulic conductivity is a 6-component symmetric tensor in the Cartesian coordinate system. The tensor can be diagonalised to give the principal components and directions of anisotropy. Similarly, combined scalar block-scale porosity is calculated for the element, based on combining the deformation zone porosity and the background block-scale porosity using a weighting based either on the relative volume or on relative transmissibility (total channel flow capacity, which is transmissivity times flow length [m^3s^{-1}]).

The result of this process is to produce a spatial distribution of CPM element properties (hydraulic conductivity tensor, porosity and flow wetted surface [m^2/m^3]) that represent the combined influence of both the deterministic fractures zones and background stochastic fractures. No extra component for matrix conductivity or micro-fracturing is added. However, the stochastic DFN is necessarily truncated in some way, for example based on fracture radius which in consequence means that some elements may not include a connected network of fractures or may only be connected in some directions. To avoid this just being a result of the choice of truncation limit and chance, a minimum block conductivity and porosity is set for any elements that have zero properties following the fracture upscaling and IFZ methods. Appropriate minimum properties were derived by calculating the minimum values seen when the DFN is truncated only at very small fractures relative to the block size, and so are largely free from the truncation effect. A schematic illustration of the process of creating an ECPM model is shown in Figure 5-3 (note the units of flow wetted surface are m^2/m^3).

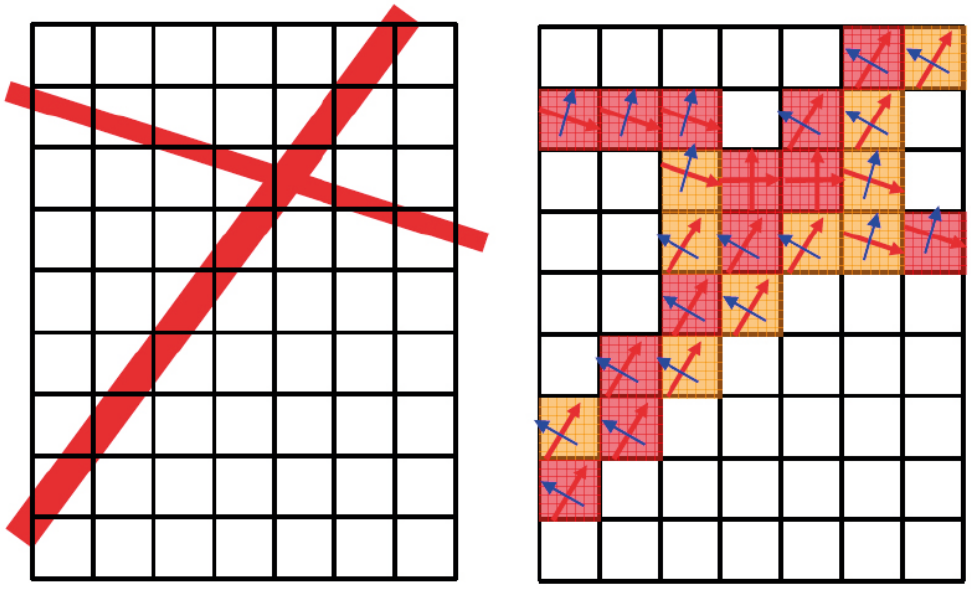

Figure 5-2. *Schematic illustration of the modification of the hydraulic conductivity tensor by the IFZ method. A finite-element grid crossed obliquely by two fracture zones of different thickness (left). (After Joyce et al. (2010a, Figure 3-17.)*

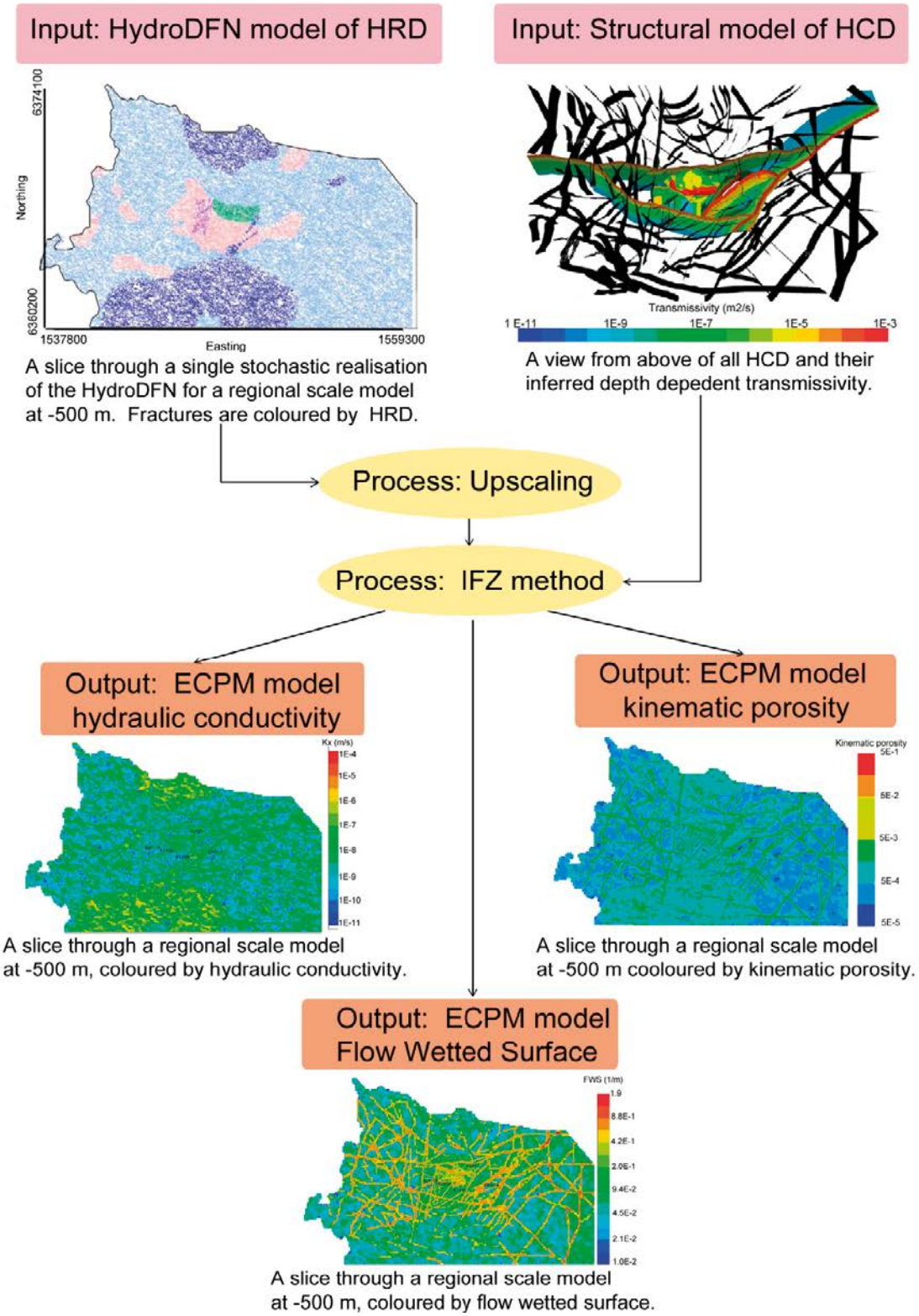

Figure 5-3. *Schematic illustration of the process of creating an ECPM regional-scale model of the Laxemar Simpevarp site from the underlying Hydro-DFN model of the HRD combined with the structural model of the HCD. (Composite of figures from Rhén et al. 2009.)*

An important capability of the ConnectFlow code that was used in the regional-scale modelling was the ability to construct embedded models that integrate sub-models of different types. That is, the model can be split into two different domains: one that uses the CPM concept, and one that uses the DFN concept. This was used to combine a detailed DFN representation near the repository volume, with an ECPM representation of the regional hydrogeological situation. The DFN and CPM sub-models have to be exclusive, that is, the approaches cannot be used simultaneously in any part of the domain. This is different from the situation where discrete fractures co-exist in the same space with a porous medium model of the rock matrix. Internal boundary conditions between the domains ensure continuity of pressure and conservation of mass. On the DFN side of the interface, these boundary conditions are defined at nodes that lie along the lines (traces) that make up the intersections between fractures and the interface surface. On the CPM side, the boundary conditions are applied to nodes in finite-elements that abut the interface surface. Thus, extra equations are added to the discrete system matrix to link nodes in the DFN model to nodes in the finite-element CPM model. By using equations to ensure both continuity of pressure and continuity of mass, a more rigorous approach to embedding is obtained than by simply interpolating pressures between separate DFN and CPM models. The equations used are specified in AMEC (2012a). In order to construct embedded models of the same fractured rock the data used for the DFN and CPM models should be self-consistent. For example, if a repository-scale DFN model is embedded within an ECPM model, then flow statistics on an appropriate scale (the size of the elements in the ECPM model) need to be consistent. This is achieved by the fracture upscaling techniques described above.

To ensure consistency of how larger scale fractures zones are represented when they cross between DFN and CPM models, the fracture zone geometries need to be defined consistently. This is achieved by using the same deformation zone data file for both the DFN and CPM regions of the model. Figure 5-4 illustrates how a large deterministic fracture that crosses between DFN and CPM sub-models can be modelled in such a way as to ensure there is continuity in its representation, and hence in flow, between the regions.

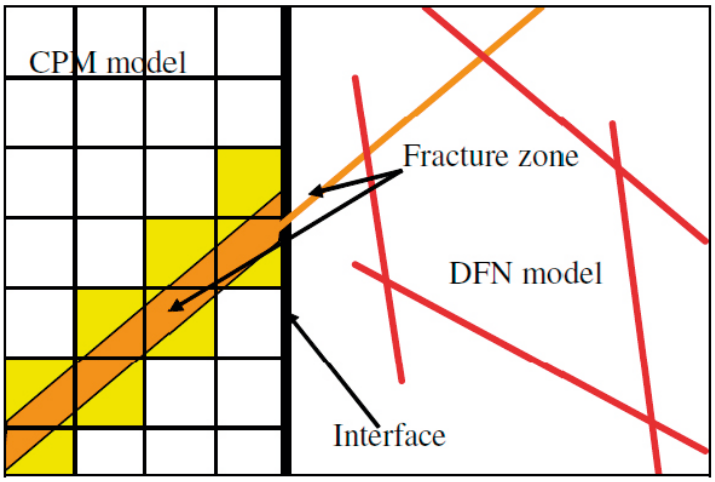

Figure 5-4. *Schematic illustration of continuity of deformation zones (DZs) across a CPM/DFN interface in a ConnectFlow model. The DFN region is to the right with a CPM grid to the left. A few fractures in the DFN region are shown in red and orange. The red fractures may be stochastic, for example. The orange fracture is a deterministic DZ that crosses the interface. On the DFN side it is shown as a plane, while on the CPM side it is drawn with its actual thickness. The elements crossed by the DZs are coloured yellow. Hydraulic conductivity, porosity and flow wetted surface in these elements is modified by the IFZ method to represent the effect of the DZ on flow and transport. (After Joyce et al. 2010a, Figure 3-19).*

5.2 Block upscaling

Upscaling on a regional-scale, where they may be approximately one million elements, can be time consuming. It is therefore useful to evaluate what kind of upscaled hydraulic properties the hydrogeological DFN model variants imply in a simplified setting by evaluating the equivalent properties of a set of blocks of a certain dimension covering a notional volume of rock using the same Hydro-DFN parameters as interpreted for a given site. This exercise also has the potential to reveal differences in the upscaled hydraulic properties between different Hydro-DFN variants or sensitivities to other modelling issues such as truncation of the fracture size distribution. In heterogeneous fracture systems, block scale properties have a strong dependence on the block scale considered.

For each measurement block (MB) scale of interest (5 m 20 m, 100 m), fractures were generated within a volume with side equal to 11 times the length of MB, which was then sub-divided into a 9 by 9 by 9 matrix of contiguous blocks and the ECPM properties calculated for each of these 729 blocks in total. This provided an ensemble over which block property statistics were collated. For each of the 729 contiguous blocks, the domain used for the flow simulation was expanded to 3 times the size of each contiguous block, but only the flux through the central volume equal to the required block size was used to calculate the equivalent hydraulic properties. A connectivity analysis of the network was performed on the scale of the 3 by 3 by 3 volume surrounding each contiguous block. The configuration is illustrated in Figure 5-5. Bulk flows across several blocks will depend on the correlation and variability of properties between blocks.

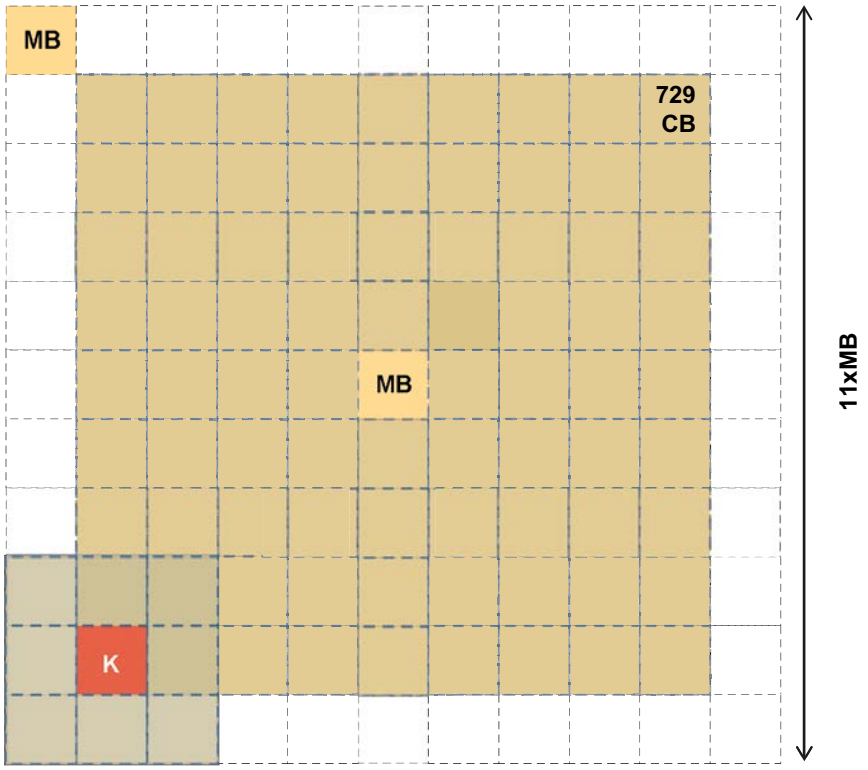

Figure 5-5. *Schematic illustration of arrangement of measurement blocks (MB) used in upscaling of a notional volume of fractured rock to obtain statistics of ECPM properties. The 11×11 blocks illustrate the total domain considered. The 9×9 central blocks are the ones for which ECPM properties calculated. The grey highlighted 3×3 blocks illustrates the window of blocks considered in calculating flow through each block to infer ECPM properties, here the red one.*

The computational cost of the calculations could be reduced significantly by neglecting the smaller fractures. Although the density of fractures increases with decreasing fracture size, the smaller fractures tend to be less well-connected and, for the semi-correlated and correlated models, tend to be less transmissive. The uncorrelated model can be more sensitive to size truncation since large transmissivities can be generated at any scale, although higher flow-rates still tend to be focussed toward fractures of larger size simply due to their increased probability to form connections. Therefore neglecting the smaller fractures potentially only involves a small approximation. A study of the effect of the minimum fracture size considered in the calculations was carried out for the 20 m and 100 m blocks in Rhén et al. (2008) for Laxemar, and is demonstrated for the Forsmark site in Figure 5-6. Due to the scarcity of the network some blocks have essentially zero conductivity as there is no network connecting between opposite faces of the blocks, and this proportion is a function of scale with a higher proportion of 'active' blocks for larger blocks. Here, in order to compare between the scales, the geometric mean conductivities for the active blocks are normalised by the fraction of blocks that are active.

Figure 5-6 suggests that the fracture size truncation limit of 5.64 m used in subsequent simulations of hydraulic conductivities for 100 m blocks is adequate, with the mean hydraulic conductivity, the percentage of active blocks and the standard deviation of the logarithm of hydraulic conductivity over the set of active blocks all remaining stable when the fracture size truncation limit is reduced. Here, an active block is defined as one which contains at least one fracture or network of fractures spanning at least one axis of the central contiguous 20 m block that is connected on the scale of surrounding 3 by 3 by volume, i.e. a 60 m cube. Figure 5-6 suggests that the fracture size truncation limit of 2.26 m used in subsequent simulations of hydraulic conductivities for 20 m blocks might slightly under-estimate the percentage of active blocks, based on 12% active for a 2.26 m truncation versus 20% for a 1.13 m truncation. However, the figure demonstrates that the calculation of the mean hydraulic conductivity and the standard deviation of the logarithm of hydraulic conductivity over the set of active blocks are less sensitive to the fracture size truncation limit.

Upscaled values of kinematic porosity were observed to show less scale dependence, but be considerably more sensitive to the fracture size truncation limits. Results in Appendix 6 of Rhén et al. (2008) show that the connected fracture porosity can increase by more than one order of magnitude when fractures smaller than radius c 0.1-5 m are included. There is also up to an order of magnitude variation between different transmissivity models when such small scale fractures are included, with the uncorrelated model having highest kinematic porosity since in that case small fracture can have high transport apertures. Hence, the effect of fracture truncation with size on kinematic porosity had to be considered in the regional-scale groundwater flow modelling (Rhén et al. 2009). The connected fracture surface area is also sensitive to fracture size truncation, being calculated in a similar way to the kinematic porosity.

By diagonalising the hydraulic conductivity tensor into the three principal components the effective hydraulic conductivity, K_{eff}, was calculated as the geometric mean of these eigenvalues. A summary of the effective hydraulic conductivities for FFM01/FFM06, Forsmark is shown in Figure 5-7. The percentages at the base of the columns for the model predictions indicate the fraction of blocks which are active, that is, contained a fracture network which formed a percolating cluster across the block (in at least one direction). In order to compare between scales when many block have essentially zero conductivity, the geometric mean hydraulic conductivity is taken over the active blocks, and scaled by the percentage of active blocks. Data from PSS and PFL-f hydraulic tests are also displayed in this figure for comparison. It should be noted that the model results are for the effective hydraulic conductivities of blocks of various scales. For the PSS data the percentages at the base of each column indicate measurements above the detection limit of the PSS method (outside deformation zones). Note that if a test at the 100 m/20 m scale reported no flow, a test at the 20 m/5 m scale would not be attempted. The percentages displayed correct for this bias, to give estimates over the total borehole length tested. The mean hydraulic conductivity is scaled by the percentage of measurements above the detection limit. For the PFL-f data, $<T>\cdot P_{10PFL}$ means the geometric mean specific capacity (Q/s; m^2/s), multiplied by the Terzaghi corrected frequency of PFL-f fractures (m^{-1}). *Sum(T)/L* means the sum of all specific capacities measured divided by the length of borehole tested. For the model variants, the error bars indicate one standard deviation in $Log_{10}\, K_{eff}$ for active bocks. For the PSS data, the error bars indicate one standard deviation over the set of observations where a value above the detection limit was reported. For the 100 m PSS data above –200 m there was insufficient data to provide an estimate of the standard deviation.

The data from the PSS tests give estimates for the effective hydraulic conductivity of borehole sections under injection conditions; and the PFL-f tests can also be used to estimate effective hydraulic conductivity to a given borehole length by summing the interpreted transmissivities and dividing by the length of the interval. It should be noted that these tests measured flow conditions resulting from injection or abstraction at a borehole (see Follin et al. 2011) compared to the linear flow boundary conditions across the blocks considered in the upscaling.

Some of the key trends in the data, such as the scale dependence of the hydraulic conductivity and the percentage of observation sections above the detection limit are reproduced in the simulations. It is thought that the apparent lower modelled effective permeability below –400 m by approximately one order of magnitude, compared to the estimates derived from PSS and PFL-f tests, arises from the following details of the modelling methodology. In the Hydro-DFN calibration methodology, inflows to the boreholes are calculated with all three depth zones modelled in the same simulation, and hence fractures between depth zones overlap on another (as illustrated in Figure 4-9 and Figure 4-19). In the case of Forsmark where this a sharp decrease in fracture intensity and the size of open fractures at –400 m it results in a transitional zone around this depth in the connectivity of the network, such that most of the modelled inflows below –400 m result from connections to fractures generated in the depth zone above that extend down and enhance the local connectivity. Hence, the model calibration below –400 m is sensitive to assumptions to the representation of the observed depth trend and the approach used to calibrate the sparse network and database of PFL-f fractures below this depth. In the block upscaling calculations, properties are calculated for fracture networks corresponding to each depth zone in isolation. This issue is particularly apparent at Forsmark because of the sharp reduction in PFL-f intensity with depth resulting in a very sparse system below –400 m. The reduction in PFL-f intensity with depth at Laxemar is more gradual and the scarcity of PFL-f fractures seen at Forsmark is only approach below c –650 m.

As noted the method used in the block modelling involved generated only fractures which originate in a particular depth zone. Regional-scale simulations and calculations of repository performance measures used a method similar to the calibration methodology, where fractures from higher depth zones can extent in to lower depth zones. Therefore it is not thought that there is necessarily any underestimate of hydraulic conductivity at depth in resulting upscaled regional-scale ECPM models.

Upscaling results for HRD_C, Laxemar are shown for depth zone 3 for a Hydro-DFN model based on OPO fractures, with a power-law fracture size model with r_0 fixed at 0.038 m and semi-correlated transmissivity model, in Figure 5-8. This figure shows the scale dependency of the hydraulic conductivity predicted by the underlying Hydro-DFN model, and the anisotropy introduced by the influence of the WNW and Sub-Horizontal fracture sets. It exemplifies how the mean conductivity increases with block size, while the variability decreases. The number of blocks without a value, i.e. do not contain a connected network, also reduces with block size.

A summary of the effective hydraulic conductivities for HRD_C, Laxemar within Depth Zone 3 calculated for different Hydro-DFN model variants is shown in Figure 5-9 presenting model results and data in a similar way to Figure 5-7 for Forsmark, but here illustrating differences between different model variants rather than depth zones. This figure reveals that the different model variants give similar effective hydraulic conductivity on the 100 m scale, within the range $2 \cdot 10^{-10}$–$2 \cdot 10^{-9}$ m/s.

A comparison between the three SDM-Site transmissivity variants (labelled OPO, $r_0 = 0.038$, in Figure 5-9) shows that the uncorrelated model gives greater spatial variability and less scale dependence in hydraulic conductivity than the other two transmissivity variants. This is thought to be because the uncorrelated model can assign high transmissivity to small fractures, resulting in an increased frequency of high hydraulic conductivity 5 m intervals compared to a correlated model. Each transmissivity model yields quite similar 100 m scale hydraulic conductivity, suggesting that this property might be reasonably well constrained by the calibration methodology of simulating the inflows measured during PFL-f tests, for a given fracture intensity-size distribution.

The case with fracture intensity based on OPO-CP fractures gives similar hydraulic conductivity, with a factor 2 lower in the mean and less variability on the 100 m scale compared to the OPO case, and a factor 3 lower on the 20 m scale. The Elaborated Hydro-DFN variant also predicted lower hydraulic conductivities at the 20 m and 100 m scale. The model variant was designed explicitly to reduce the hydraulic conductivities in response to indications that the hydraulic conductivities predicted by the OPO, $r_0 = 0.038$, semi-correlated variant were around a factor of three too high for consistency with the hydrochemistry data (see Section 6.6).

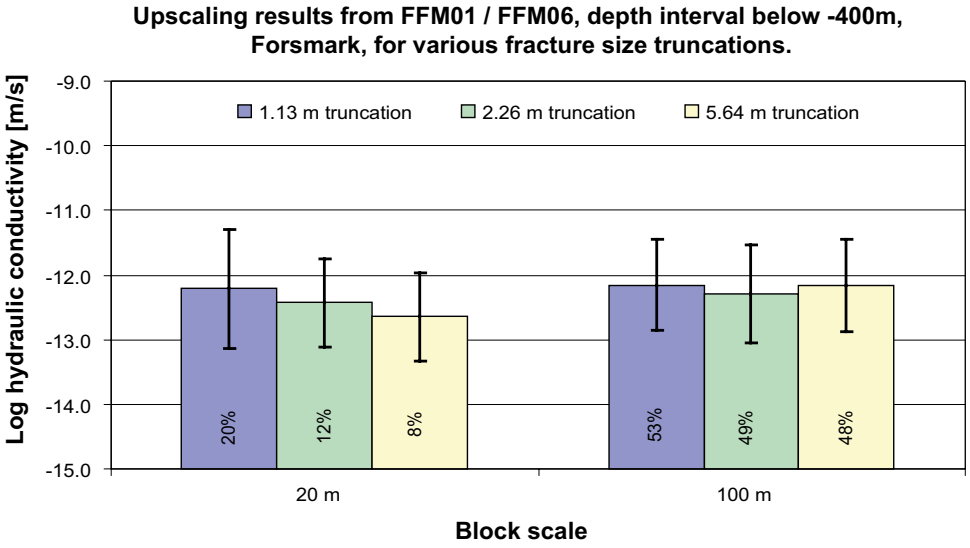

Figure 5-6. *Upscaled mean hydraulic conductivities for 20 m and 100 m blocks predicted by the Hydro-DFN model of FFM01/FFM06 with a semi-correlated transmissivity relationship, for the depth interval below –400 m, Forsmark, using different minimum fracture sizes. The percentages at the base of the columns indicate the fraction of blocks which are active, i.e. for 20 m block with 5.64 m truncation 8% are active, 92% inactive. The geometric mean hydraulic conductivity is taken over the active blocks, and is scaled by the percentage of active blocks. The error bars indicate one standard deviation in Log10 K_{eff} for active bocks. (Based on parameters from Follin et al. 2007a, Table 11-20.)*

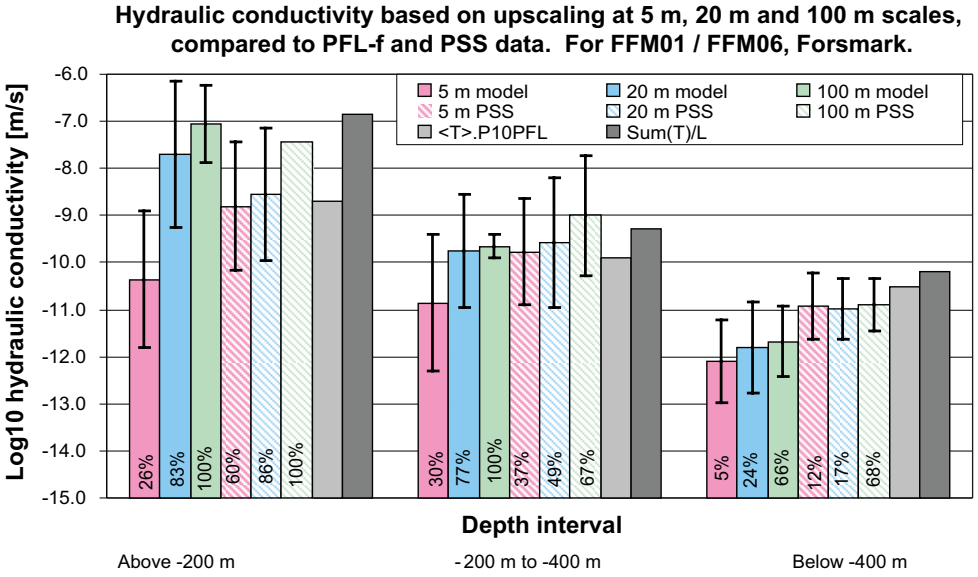

Figure 5-7. *A comparison upscaled mean hydraulic conductivities for 5 m 20 m and 100 m blocks predicted by the DFN model with a semi-correlated transmissivity function and hydraulic conductivities measured by the PSS method with 5 m 20 m and 100 m borehole sections and PFL-f data. The comparison is for FFM01/FFM06, Forsmark. (Based on parameters from Follin et al. 2007a, Table 11-20.)*

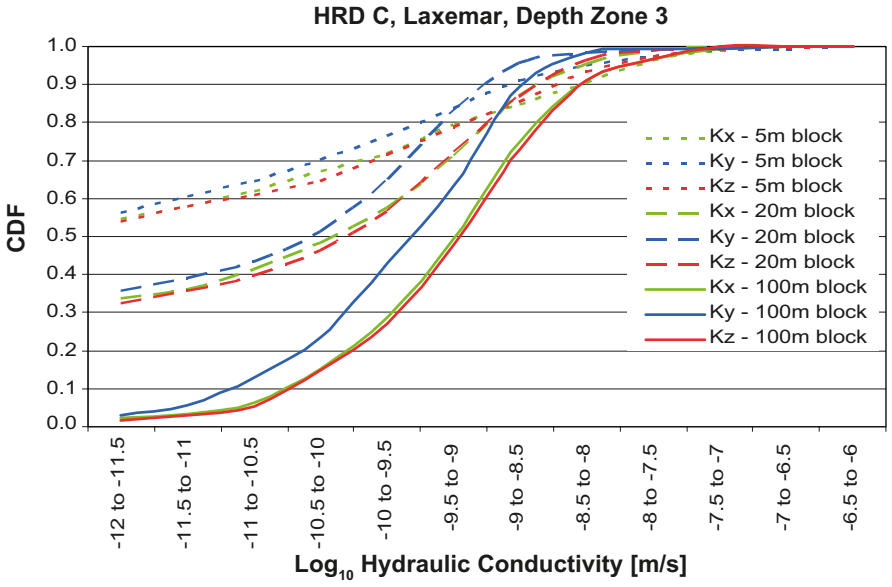

Figure 5-8. *Ensemble statistics for the upscaled hydraulic conductivities for the HRD_C, Laxemar, for elevations –150 m to –400 m for the Elaborated SR-Site Hydro-DFN model. A comparison of the cumulative distribution of Kx (E-W), Ky (N-S) and Kz (vertical) hydraulic conductivity for block scales of 5 m 20 m and 100 m. (Based on Joyce et al. 2010b, parameters in Table E-1 and results in Table E-5 therein.)*

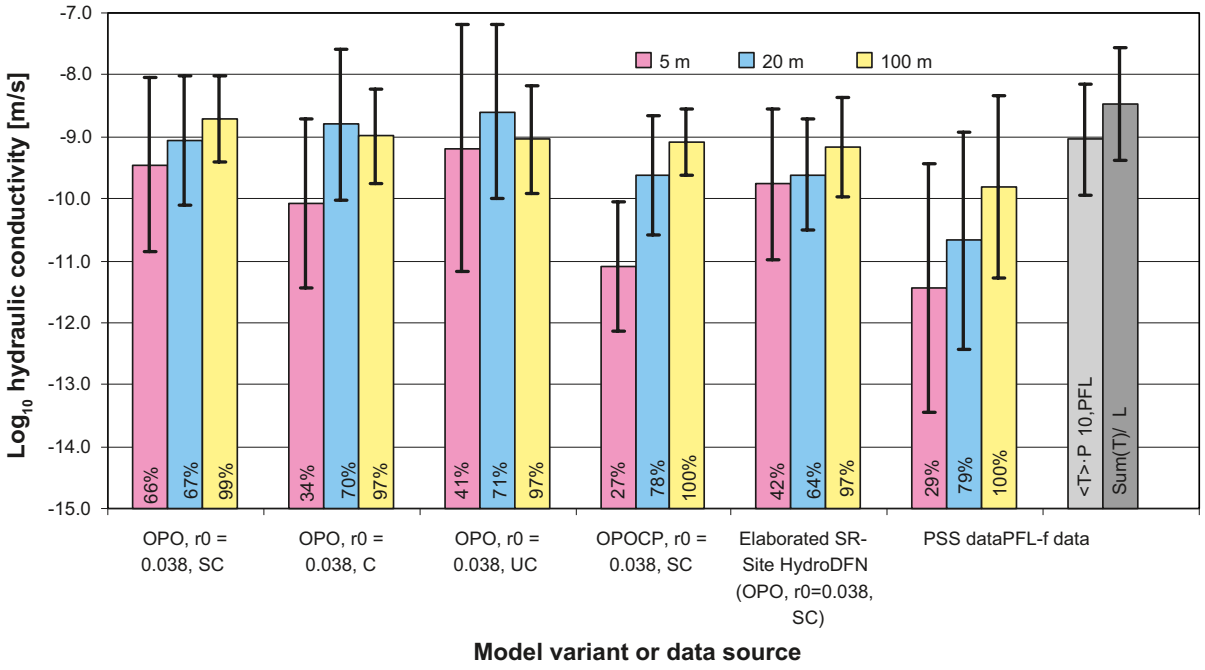

Figure 5-9. *A comparison between model variants of upscaled mean hydraulic conductivities for 5 m 20 m and 100 m blocks and hydraulic conductivities measured by the PSS method with 5 m 20 m and 100 m borehole sections and PFL-f data. The data are for HRD_C, depth zone 3, Laxemar. For PSS data, the error bars indicate one standard deviation based on the assumption of a lognormal distribution where censored data are accounted to give distributions that fit values above the measurement limit in an appropriate way (Rhén et al. 2008). (Based on Rhén et al. 2008, Table 10-21 and Appendix 6, Joyce et al. 2010b, Table E-5.)*

6 Regional model calibration and confidence assessment

6.1 Use of regional-scale models for calibration and confirmatory testing

The Hydro-DFN models developed for SDM-Site Forsmark and Laxemar have been applied on a regional-scale to a variety of modelling tasks with the aims of confirming that the hydraulic properties derived from the PFL-f single-hole measurements are representative of wider hydrogeological behaviour as indicated by cross-hole tests and the evolution of natural tracers, for example. Such tests also provide a basis for further conditioning of properties or choosing between alternative models. Confirming the conceptual hydrogeological model then provides a corroborated description of the groundwater system that is appropriate for regional-scale simulations of flow and transport, and thereby builds confidence that the groundwater flow models are also appropriate for calculations of the repository performance statistics which are used in the repository safety assessment. The details of the modelling described in this section are taken mainly from Follin et al. (2007b, 2008a) for Forsmark and Rhén et al. (2009) and Joyce et al. (2010b) for Laxemar.

The aims of the regional-scale calibration and confirmatory testing for the SDM were considered in five categories:

1. To perform local conditioning of hydraulic properties to single-hole hydraulic tests that intersect the HCD (deformation zones).
2. Simulation of groundwater levels.
3. Simulation of cross-hole (interference) hydraulic tests.
4. Simulation of drawdowns caused by the Äspö HRL (at Laxemar).
5. Simulation of the palaeo-climatic evolution of the groundwater in the bedrock.

If necessary, aspects of the HSD, HRD or HCD models were re-assessed, or re-calibrated, based on comparisons between simulated and measured values. In most cases an ECPM representation was used to simulate these tests, although a DFN representation was used to simulate some interference tests also, the choice depended on practical considerations. It should be noted that details of the predictions of the models depend on:

- The stochastic realisation used for the HRD, either directly or as the basis for an upscaled ECPM model.
- The stochastic realisation used for the HCD, either directly or as the basis for an upscaled ECPM model.

The base case models for the regional-scale ECPM simulations used a single upscaled stochastic realisation of the HRD, based on a semi-correlated transmissivity model and fracture intensity-size relationship derived for open fractures. The base case models used a deterministic model of the HCD. Variability between different stochastic realisations was studied as part of sensitivity studies. This kind of stochastic uncertainty reflects both the variability in the magnitude of hydraulic properties and also how those variations are distributed in space as a result of e.g. fracture spacing and size distribution.

Each of the five types of confirmatory tests were performed independently of the others. However, it was found that changes made to some parameters might improve the match of the model predictions to data in one situation, whilst making the match worse in another. The aim at the end of the regional modelling process was to have a model which predicted a reasonable match in all of the situations considered. This model was then used for the calculations relating to safety assessment.

For the Forsmark modelling, it was possible to perform groundwater flow calculations that produced satisfactory results for the tests 1-3 and 5 listed above (test 4 is specific to Laxemar) with only minor changes to the initial hydraulic parameters as derived from the DFN model for the HRD and

interpretation of the HCD provided in Follin et al. (2007a). The initial prescription of hydrogeological properties was refined through the regional-scale model simulations in order to improve the calibration of the model, as well as identifying preferred alternatives that are presented in Follin et al. (2007b). Other model elements such as HSD and solute transport properties were defined to produce a satisfactory calibration to the hydraulic single-hole and interference tests, as well as the groundwater levels.

For the Laxemar modelling, a reasonable match was achieved between simulated and measured natural groundwater levels in the regolith and percussion boreholes, with the discrepancy between the steady-state model results and the average measurements less than the measured seasonal variations. Similarly, the match of estimated environmental-water heads in the core-drilled boreholes was also acceptable. Modelling of the palaeo-climatic evolution of the Laxemar site and interference tests undertaken as part of SDM-Site (Rhén et al. 2009), produced a relatively poor match to data when using the initial model in that it predicted that more extensive flushing by meteoric water should have taken place than observed. This initial model was derived from upscaling the SDM-Site Hydro-DFN model (Rhén et al. 2008). Some improvements were gained by increasing the fracture surface area within volumes coincident with HCD to reflect the observed higher intensity in borehole intervals within such structures. Adjustments made to the hydraulic properties of the HCD to improve the match to confirmatory test 1-4 also improved the match to natural chemical tracers, suggesting a strong structural control and the palaeo-climatic evolution at the site. Ultimately, a reasonable match to both the various chemical tracers and interference test data was achieved by reducing the hydraulic conductivities of the initial ECPM model at elevations below –150 m by a factor of three. This suggested the values of the ECPM derived from upscaling the SDM-Site Hydro-DFN could be too high. It was considered that such an adjustment could be explained by aspects of the assumptions and methodology used in calibration of the underlying Hydro-DFN model.

To explore whether such changes could be explained by making the Hydro-DFN calibration methodology more elaborate in honouring more characteristics of the site in the model calibration, the so-called ‘Elaborated Hydro-DFN’ was developed (Joyce et al. 2010b) with some methodological changes as detailed in Section 4.1.1. The most significant changes being to calibrate the stochastic DFN model in the context of the hydro-structural framework of the HCD, and to capture in more detail the anisotropy in hydraulic properties between different fracture sets. The resulting model improved the match to the hydrochemical data from boreholes.

6.2 Local conditioning of the HCD model to single-hole (PSS) hydraulic tests

As part of SDM-Site Forsmark (Follin et al. 2007b) the properties of the ECPM model on a 20 m grid were first defined in terms of the upscaled Hydro-DFN model of the HRD. The interpreted deformation zones were then superimposed implicitly by altering the properties of the finite elements that they intersected according to the initial HCD model. The consistency of the resulting spatial distribution of hydraulic conductivity on a 20 m grid was compared with the measured PSS transmissivity data from 20 m long borehole sections in twenty core-drilled boreholes. This comparison was intended to provide both a check of the parameter settings of the HRD and HCD models, but also on the methods used to upscale the DFN and represent the deformation zones in an ECPM representation. An example of such a comparison is shown in Figure 6-1. For modelling stage F2.2 (Follin et al. 2007b), the properties of individual deformation zones in the HCD model was made by adjusting the hydraulic conductivity value of deformation zone within the relevant 100 m depth interval (i.e. the entire depth interval intercepted in that zone). For Modelling stage F2.3 (Follin et al. 2008a, Section 5.2.2), the adjustments were made by adjusting the HCD conductivity locally within a triangle of a defined side length 200 m was used, intersected by the borehole. The equivalent comparison was not made for SDM-Site Laxemar, although the same local conditioning method as used in F2.3 was applied in the modelling of HCD (Rhén et al. 2009).

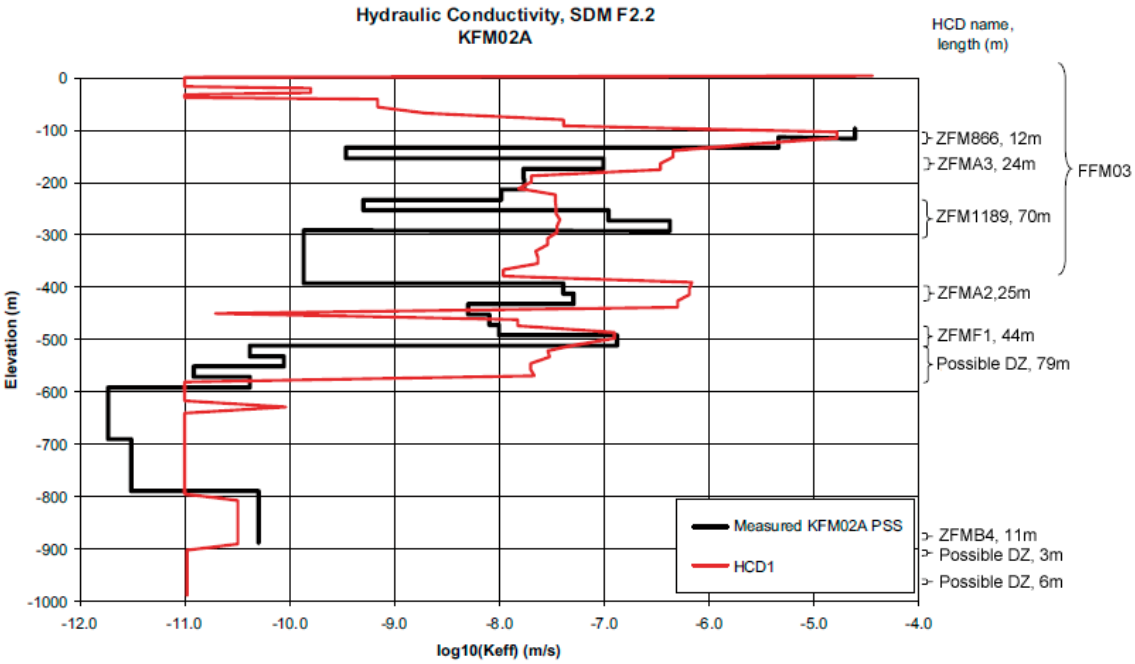

Figure 6-1. *Example profiles of ECPM hydraulic conductivity in borehole KFM02A after conditioning against 20 m section PSS transmissivity measurements. The red line shows the geometric mean horizontal hydraulic conductivity in the model, while the black lines show the measurements. The intercept by deformation zones is indicated on the right axis. Note there is no data to compare with above –100 m. (After Follin et al. 2007b, Figure 5-2).*

6.3 Matching natural groundwater levels

Calibrating against the natural groundwater levels observed in the regolith and in the uppermost part of the bedrock provides information on the interaction between the groundwater in the HSD and HRD. For this reason, this aspect of calibration focused on the hydraulic properties of the regolith and the upper bedrock, as well as providing confirmatory testing of the hydraulic boundary conditions which were used in subsequent regional-scale models. The models of the regolith were based on those developed in Johansson (2008) and Bosson et al. (2008) for Forsmark and Bosson et al. (2009) for Laxemar.

Groundwater levels in packed-off sections within the deep, core-drilled boreholes were also used for comparison. Groundwater density increases with depth due to increasing salinity. The groundwater levels measured in deep boreholes are therefore perceived as representing point-water heads. In order to understand vertical head gradients in a variable-density groundwater flow system, measured groundwater levels (point-water heads) were transformed into environmental-water heads, so that vertical flows are linearly proportional to the estimated environmental-water head gradient.

An example of the match between the simulated and measured groundwater levels in near-surface boreholes at Forsmark is shown in Figure 6-2. This figure indicates that that groundwater levels in the Quaternary deposits are generally closer to the ground surface than the groundwater levels in the bedrock, suggesting recharge conditions.

Examples of the match between the simulated and measured groundwater heads in deep boreholes at Laxemar are shown in Figure 6-3. Most of the core drilled boreholes in the Laxemar subarea display a gradual decrease in environmental-water head with depth, i.e. recharge conditions. The models predicted the correct magnitude of environmental-water head and the gradual decrease in environmental-water head with depth was also reproduced.

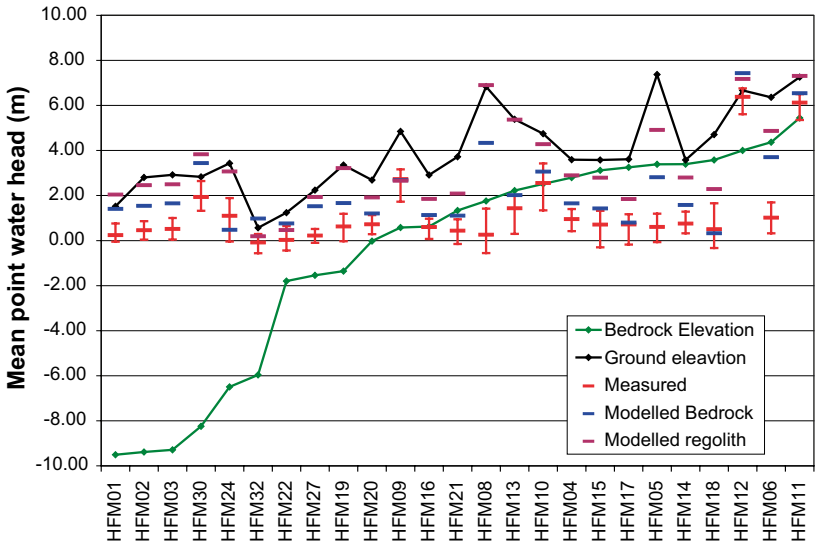

Figure 6-2. *Comparison of measured heads in percussion drilled near-surface boreholes (HFM) at Forsmark and stage 2.3 base model simulation. Modelled values are given for the regolith and as an average over the borehole section in the bedrock. Field data is plotted as mean groundwater levels in the bedrock with error bars to show the variation over time. Boreholes are ordered by bedrock elevation. (After Follin et al. 2008a, Figure 5-13).*

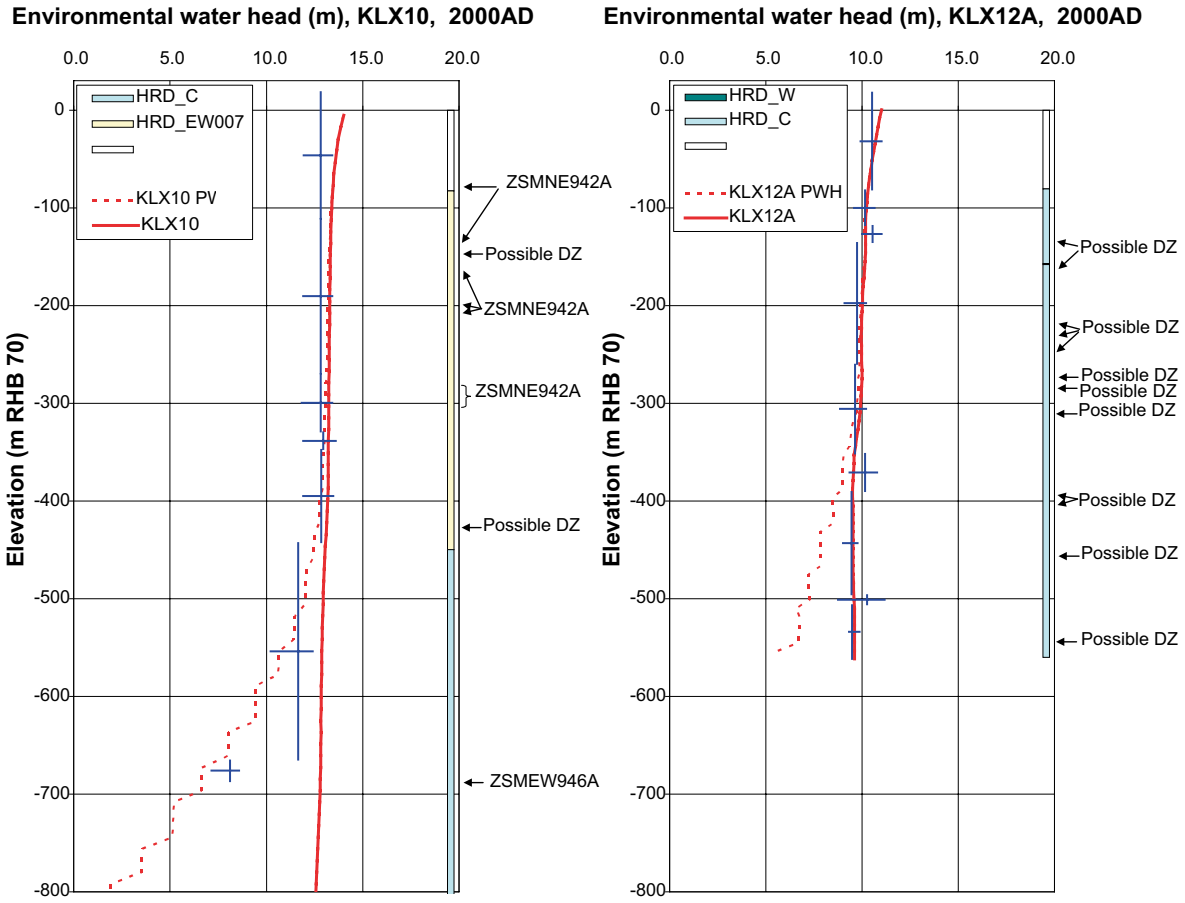

Figure 6-3. *Examples of modelled environmental-water head (solid red line) and point-water head (dotted red line) in KLX10 and KLX12A in HRD_C, Laxemar compared with estimated environmental-water heads (blue crossed lines, centre showing midpoint of the section, vertical line showing the extent of the section and horizontal line showing the temporal variation of the measured head) calculated from measured point-water head data in sections along the borehole. At the right hand side, the prevailing hydraulic rock domains are shown as coloured bars along the borehole. Detected deformation zones are indicated at the intersection depth in the borehole. (After Rhén et al. 2009, Figure 8-4).*

6.4 Cross-hole (interference) hydraulic tests

6.4.1 Interference test in HFM14, Forsmark

Simulation of the drawdowns produced during the 2006 interference test in borehole HFM14 were intended to test model predictions of hydraulic communications on scales up to approximately two kilometres (see Figure 6-4). Sub-horizontal to gently dipping sheet joints of high transmissivity were thought to dominate the hydraulic responses, and so simulation of the interference test acted as a confirmation of the structural model and hydraulic property assignment. Several boreholes were monitored at different depths; which showed different responses at different depths, the data provided a way of understanding distinctions in the hydraulic properties of the deformation zones, the fracture domains and regolith.

Transient calculations were performed using an ECPM approach with a 20 m local-scale grid embedded within a 60 m regional-scale grid. Some example comparisons of simulated and measured responses are given in Figure 6-5 (showing an overall comparison of all monitored intervals at the end of pumping) and Figure 6-6 for a particular borehole. The drawdown for the nearest monitoring intervals was found to be controlled by the hydraulic properties close to HFM14 (Follin et al. 2007b), specifically the transmissivity of the outcropping extensive sub-horizontal deformation zone A2 and the features used to represent the near-surface sheet joints in the upper bedrock. Sensitivity studies indicated that these are the key controls for most intervals up to about 500–600 m distant from HFM14. Beyond this, the responses were controlled by parameters relating to the hydraulic properties of the more distant deformation zones, the sheet joint features and the regolith. The calibration required an increase in the transmissivity of A2 in the top 400 m to 2.8×10^{-4} m^2/s and a reduction in the hydraulic thickness of zones A2, A8, ENE0401 and ENE0060 to 5 m thick to give more discrete responses, and provided the basis for deciding amongst possible implementations of the depth trends in HCD proposed in Follin et al. (2007a).

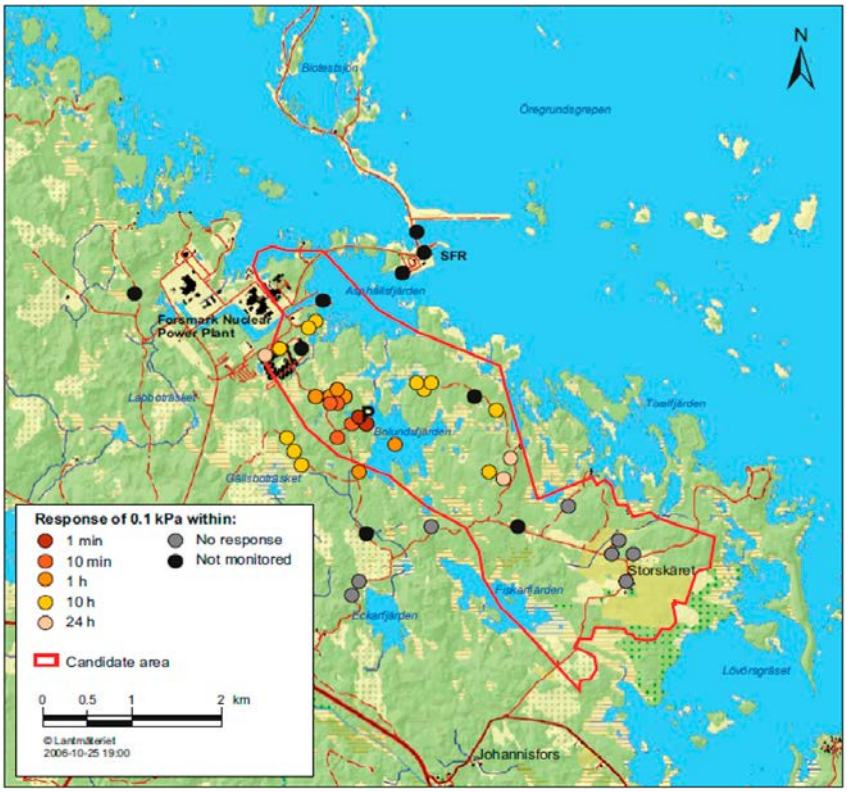

Figure 6-4. *Response times in the bedrock to the 3 weeks long interference test conducted at HFM14 (P) in 2006. Clear responses were observed in 71 out of a total of 110 monitoring sections. The maximum radius of influence was about 1.8 km. Reproduced from Follin et al. (2007a, b).*

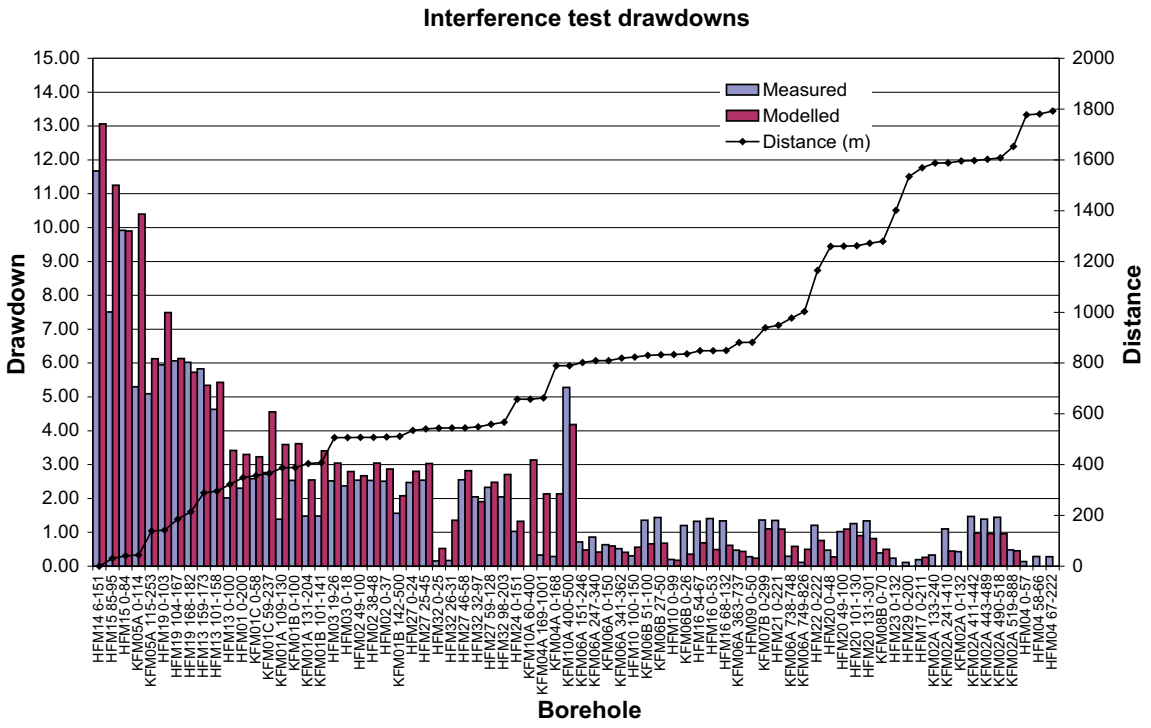

Figure 6-5. Comparison of measured (blue) and modelled (red) drawdown at the end of pumping (21 days) for all monitored borehole intervals for the Forsmark Stage 2.2 base case model. The borehole intervals are ordered according to the three-dimensional distance (the right axis) of the monitoring intervals to the abstraction borehole HFM14. (After Follin et al. 2007b, Figure 5-5.)

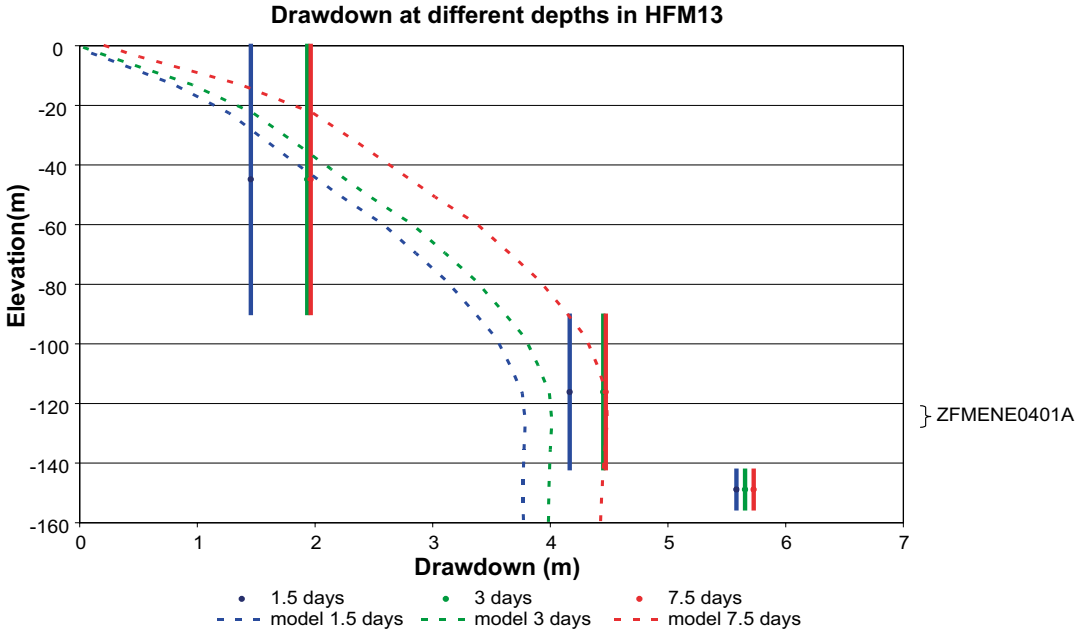

Figure 6-6. Comparison of measured (solid) and Forsmark Stage 2.2 base case model (dashed) drawdown at 3 times for the HFM13 monitoring hole. For the data, a vertical line shows the extent of the monitoring section with the drawdown representing an average within the interval, while the simulated spatial variation in drawdown in the borehole is shown for the model. (After Follin et al. 2007b, Figure 5-7.)

6.4.2 Interference test in HLX28, Laxemar

The HLX28 interference test was performed in April 2007, with pumping in HLX28 for 4.75 days. Hydraulic observations were made in surrounding boreholes (Harrström et al. 2007). HLX28 was interpreted to be hydraulically well connected to deformation zone ZSMNW042A, although not directly intersecting this zone since it dips slightly to the south (see Figure 6-8). The deformation zones ZSMNS001C and ZSMNS059A, located near to HLX28, were interpreted from discontinuities in observed heads to be dolerite dykes. They were thought to act as hydraulic barriers to flow across the deformation zones, due to the low-permeable characteristics of the dolerite. However, it was thought that the rock bordering the dolerite dykes could be quite permeable.

The measured responses to the interference test could not be adequately approximated by a simple radial flow fit. This is thought to be because the responses are governed by a complex network of predominantly steeply dipping fractures in the HCD and the barrier effects of the dolerite dykes. Because of the very discrete nature of the responses seen in this test, two simulation approaches were tried: The first using an ECPM model for the calibrated base case; the second was to use the underlying DFN model directly to simulate the test. For this second approach, the full regional HCD model was used, but only the stochastic fractures in a region about 1.5 km by 1.5 km centred on HLX28 were considered in order to make the simulations tractable. The results for the calibrated base case ECPM model predicted the responses in the closer monitoring boreholes reasonably well, but further away the magnitudes of responses could not be reproduced by the ECPM model for a number of variants. The problem was considered to be a result of the limitations of using a relatively coarse 40 m grid used, and the continuum method which tends to allow a hydraulic signal to diffuse outside of the network of deformation zones. Therefore, the underlying DFN model, without upscaling, was used directly to simulate the transient pumping in HLX28. It should be noted however that anisotropy of the dolerite dykes could not be implemented in the DFN model with the functionality available at that time. As a result, the model tended to predict some responses propagating across ZSMNS001C and ZSMNS0059A via stochastic fractures crossing these two dolerite dykes. By using a DFN model it was possible to simulate the correct levels of drawdown in the system even at large distances from HLX28. To achieve this, it was necessary to increase the transmissivities of three deformation zones by factors of 3 to 4 from those used in the calibrated base case ECPM model. The results of this best case DFN model are given in Figure 6-7.

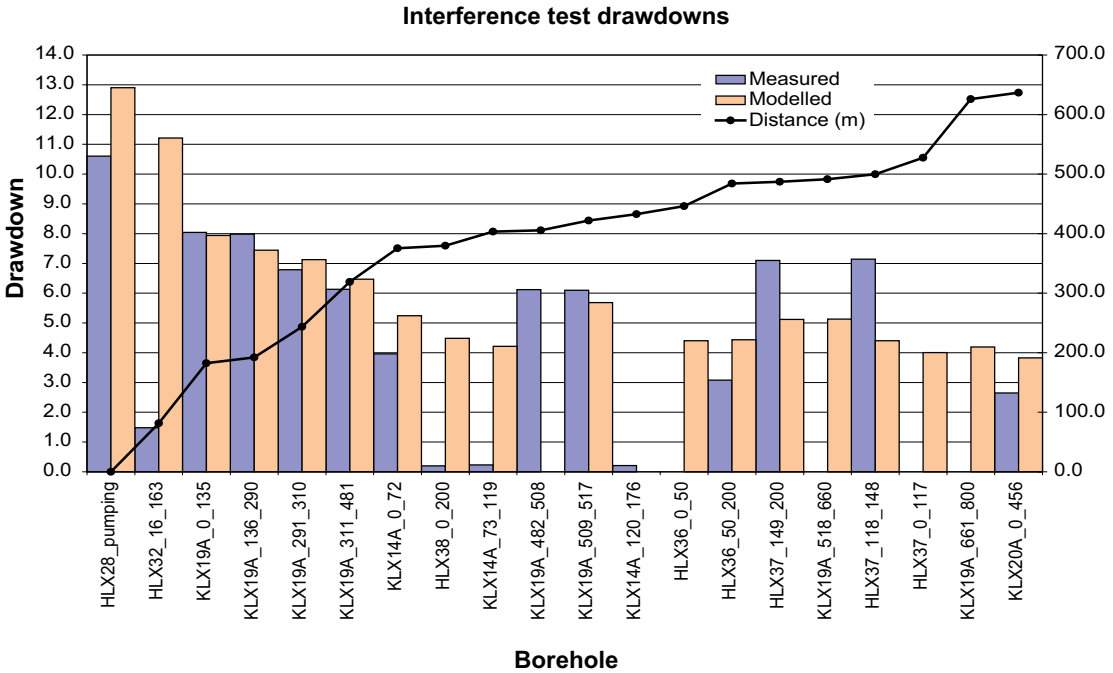

Figure 6-7. *Comparison of measured (blue) and modelled (orange) drawdown (m) at the end of pumping (5 days) in HLX28 at Laxemar for all monitored borehole intervals for the SDM-Site Hydro-DFN model. The borehole intervals are ordered according to the Euclidian distance (m), on the right axis, of the monitoring intervals from HLX28. (After Rhén et al. 2009, Figure 8-28.)*

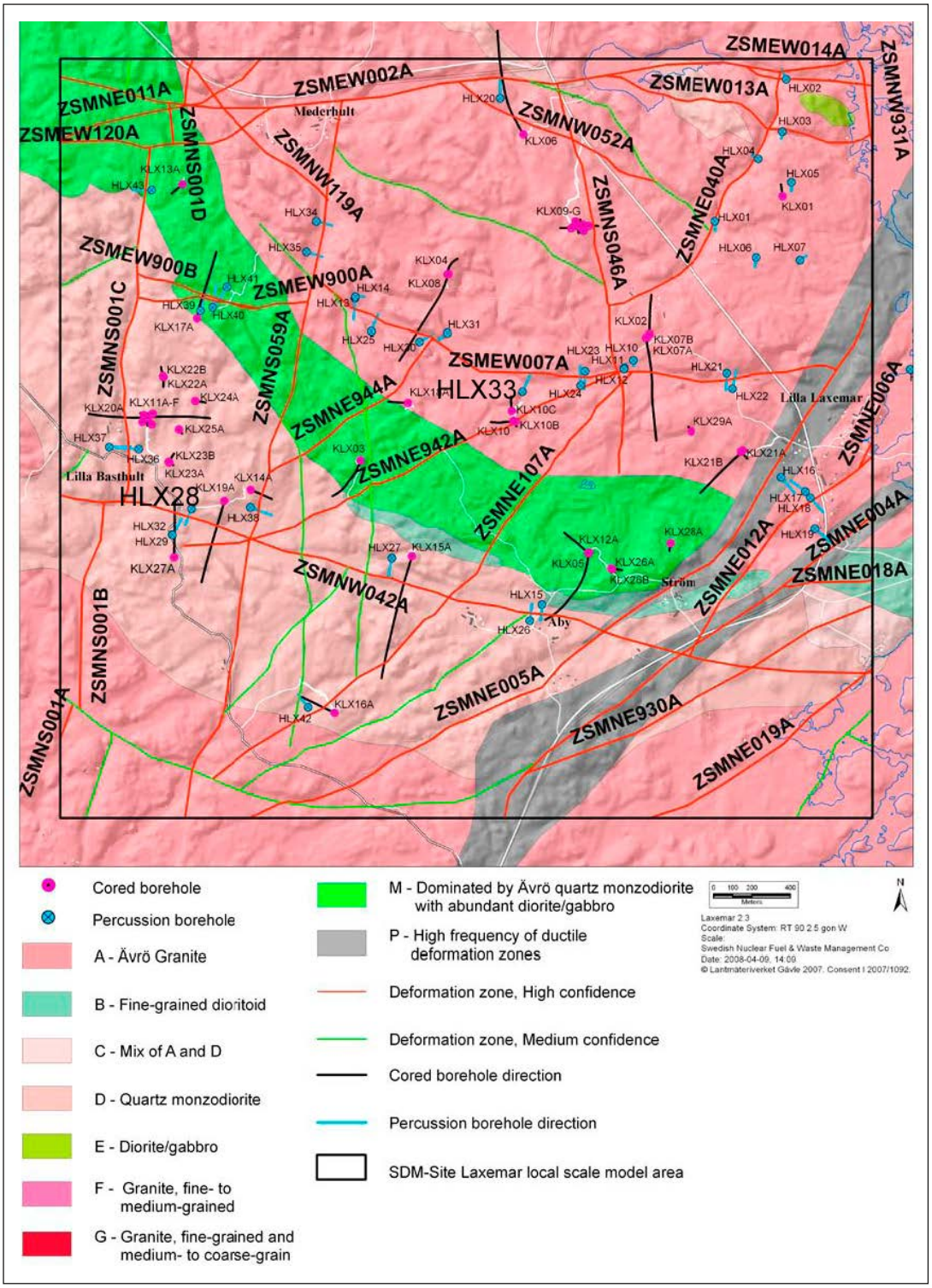

Figure 6-8. *Interpreted deterministic deformation zones and rock domains at Laxemar, showing the location of the HLX33 and HLX28 boreholes. (After Rhen et al. 2008, Figure 3-8).*

The storativity model used in these transient DFN calculations was based on a preliminary relationship $S = aT^b$, with a = 0.001, and b = 0.5. The relationship recommended in Section 7 of Rhén et al. (2008 (has a = 0.01 and b = 0.71, which gives similar storativities for transmissivities around 10^{-5} m^2/s that are characteristic of the deformations zones in the superficial bedrock. There was a notable difference in the hydraulic diffusivity interpreted from interference tests performed at Forsmark, where diffusivities in the range 10–1,000 m^2/s were obtained for tests dominated by sub-horizontal or gently dipping features within the superficial bedrock, to those performed at Laxemar, where values in the range 1–10 m^2/s resulted from tests typically dominated by sub-vertical deformation zones.

6.4.3 Interference test in HLX33, Laxemar

The HLX33 interference test used for calibration was performed between June 2006 and August 2006 (for around 40 days) with HLX33 as the pumping well (see Figure 6-8). The test was affected by some simultaneous pumping in HLX14 for water supply that started before the HLX33 pumping in addition to natural processes such as precipitation and evapotranspiration. Hydraulic observations were made in surrounding boreholes (Morosini et al. 2009). HLX33 was judged to be well connected to the steeply dipping deformation zone ZSMEW007A. The HLX33 interference test therefore focused on testing the properties of this deformation zone.

Simulation results using an ECPM model for the base case show reasonable agreement with both the observed values and also the predictions of Thiem's radial flow solution based on the pump-rate, an assumed constant transmissivity in ZSMNEW007A and the distance from HLX33, as measured in 3D. An example of transient simulation results for responses in various packed-off intervals in the deep cored KLX04 borehole intervals 700–1,000 m away from pumping in HLX33 is shown in Figure 6-9, agreeing with measurements that the responses are largest in zone ZSMEW007A. The drawdown responses to pumping in HLX33 are modest (up to a maximum of 1 m in HLX24 c 300 m away) and appear to vary fairly predictably with distance from HLX33 (i.e. reasonably well approximated by Thiem's equation for radial flow), since assignment of an appropriate value to the transmissivity of ZSMEW007A and assuming radial flow within this deformation zone seems sufficient to gain a qualitative understanding of the hydraulic test.

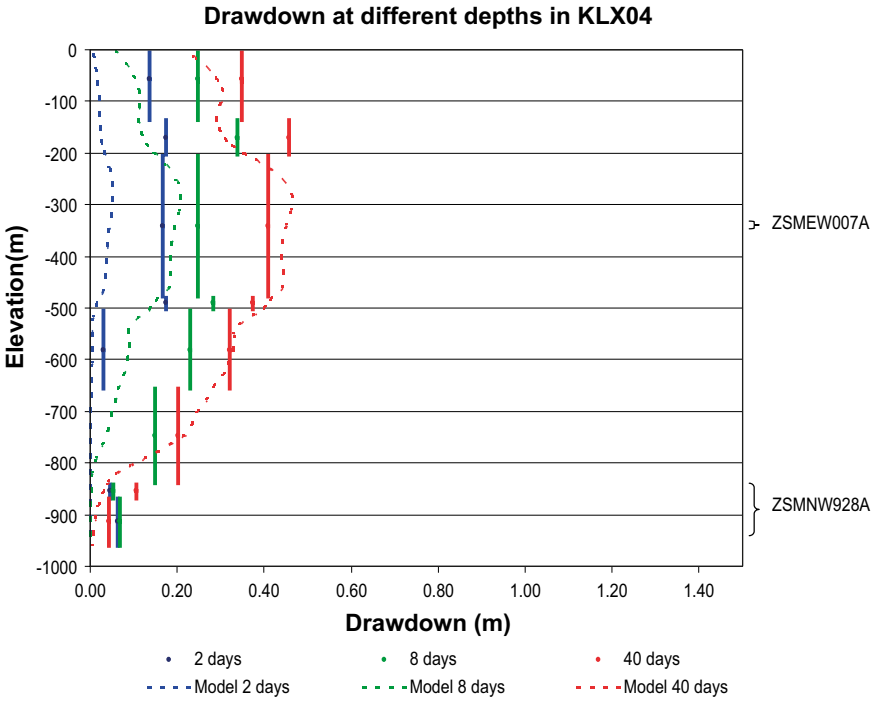

Figure 6-9. *A comparison of measured and simulated drawdown in KLX04, Laxemar, caused by pumping in the HLX33 interference test. (After Rhén et al. 2009, Figure 8-22.)*

The main changes made in calibrating the base case model to match the HLX33 test were:

- An increase in the transmissivity of ZSMEW007A (having thickness 80 m) in the top depth zones by a factor 50 above –150 m, to give a value c 10^{-4} m^2/s, and a factor of 10 below –150 m to give a value c 10^{-5} m^2/s.
- Low specific storage coefficients of around 10^{-7} m^{-1} for the bedrock and 10^{-3} m^{-1} for the soil were required to obtain the correct timescales for transmitting the responses. The storage coefficient above suggests a storativity of about 10^{-5} for ZSMEW007A or diffusivity around 10 m^2/s, which is within the range of values interpreted for HCD at Laxemar and Äspö (Rhén et al. 2008).
- The lowering of the hydraulic conductivity of the hydraulic domain HRD_EW007 (see Figure 3-6) by a factor 0.3 below –150 m to match point-water heads resulted in significantly increased drawdowns, which improved the calibration boreholes KLX04 and KLX07A/B. However, increased drawdowns were less consistent with observations at other boreholes such as HLX25 and HLX30. Hence, the tightening of HRD_EW007 suggested by point-water heads is only partially confirmed by the HLX33 interference test. This may be because heterogeneity in the rock near some of the boreholes is not well represented in the models.

6.5 Drawdown at Äspö Hard Rock Laboratory

There are presently two underground facilities in the Laxemar site: The Äspö Hard Rock Laboratory (Äspö HRL) situated below the Äspö island in the north-east of the Laxemar local model area, and the interim storage facility (Clab) on the Simpevarp peninsula. Inflows to these facilities cause disturbances to the natural hydrogeological situation.

The influence of the Äspö HRL has been simulated using the Hydro-DFN models developed during SDM-Site Laxemar (Rhén et al. 2009), and the model predictions of drawdowns in local boreholes compared to measured values. It is expected that the interim storage facility on the Simpevarp peninsula will have only a very local effect on the groundwater flow pattern given its superficial depth and the fairly low inflow-rate compared with that to the Äspö HRL.

The methodology for the simulations was to import the reference water and pressure distributions from the palaeo-climatic simulations (see Section 6.6) predicted at 1980, and then restart the simulations with a time dependent pump-rate specified in the tunnels of the Äspö HRL (Follin et al. 2007b). In order to quantify sensitivities of the drawdowns to changes to model parameters, a number of different variants were constructed. The following conclusions were drawn from the modelling:

- A reasonable match to the observed drawdowns resulting from the Äspö HRL could be obtained by modifying the HSD on the seabed in the bays around Äspö to be of gyttja clay type with vertical hydraulic conductivity of around $5 \cdot 10^{-9}$ m/s (reduced from an initial isotropic value of 10^{-8} m/s).
- The drawdowns at depth were mainly controlled by the hydraulic conductivities of the local HRD. They had a lesser, but significant, dependence on the HCD and HSD.
- The drawdowns in the percussion boreholes were most sensitive to the hydraulic conductivity of the HSD below the sea around Äspö. The HSD here separates the fracture system from the sea.

6.6 Palaeo-climatic simulation

6.6.1 Aims of the modelling

Changes in the chemical composition of groundwater in the Forsmark and Laxemar sites are driven by the infiltration of waters with glacial, marine and meteoric origins, as determined by the topographic and climatic evolution of the sites. This evolution can therefore be thought of as a natural tracer experiment (see Follin et al. 2008b, Hunter et al. 2008).

The chemical composition of the groundwater measured in the present-day, by analysis of groundwater samples from packed-off borehole sections, have been compared to simulations of regional-scale transient, coupled groundwater flow and solute transport models. This comparison was intended as a confirmatory test of the current models, in particular of the upscaled properties of the Hydro-DFN.

The inclusion of hydrochemistry data provides an additional data set to assess the groundwater flow model, and provides a way to improve our integrated understanding of the groundwater system. It gives an indication of natural solute transport processes on the timescales of thousands of years.

6.6.2 Understanding of the groundwater evolution of the sites

Up to around 50,000 years ago the Weichselian glaciation covered most of Scandinavia with ice sheets, depressing the bedrock elevation significantly (see SKB 2010d, Lund and Näslund 2009). A marked warming in climate took place about 18,000 years ago, shortly after the latest glacial maximum, and the ice started to retreat, a process that was completed after some 10,000 years. There was a major standstill and, in some areas, a re-advance of the ice front during a cold period c 13,000–11,500 years ago. The end of this period marked the onset of the present interglacial (Söderbäck 2008).

Forsmark is thought to have emerged from ice cover approximately 11,500 years ago. It is not clear whether the site spent any time beneath the Yoldia Sea shortly after de-glaciation. Between 13,000 and 9,500 years ago the Laxemar site was covered by the Baltic Ice Lake. Small areas in Laxemar might have been above lake level at the end of the period. Between 9,500 and 8,800 years ago the Laxemar site was covered by the Yoldia Sea. The mildly saline Yoldia Sea stage was succeeded after a few hundred years by the fresh water Ancylus Lake stage (which lasted between 10,800 and 9,500 years ago at Forsmark, or between 8,800 and 7,500 years ago at Laxemar). The Littorina Sea stage, followed by the Baltic Sea stage, began 9,500 years ago at Forsmark and 7,500 years ago at Laxemar. This evolution is summarised in Figure 6-10.

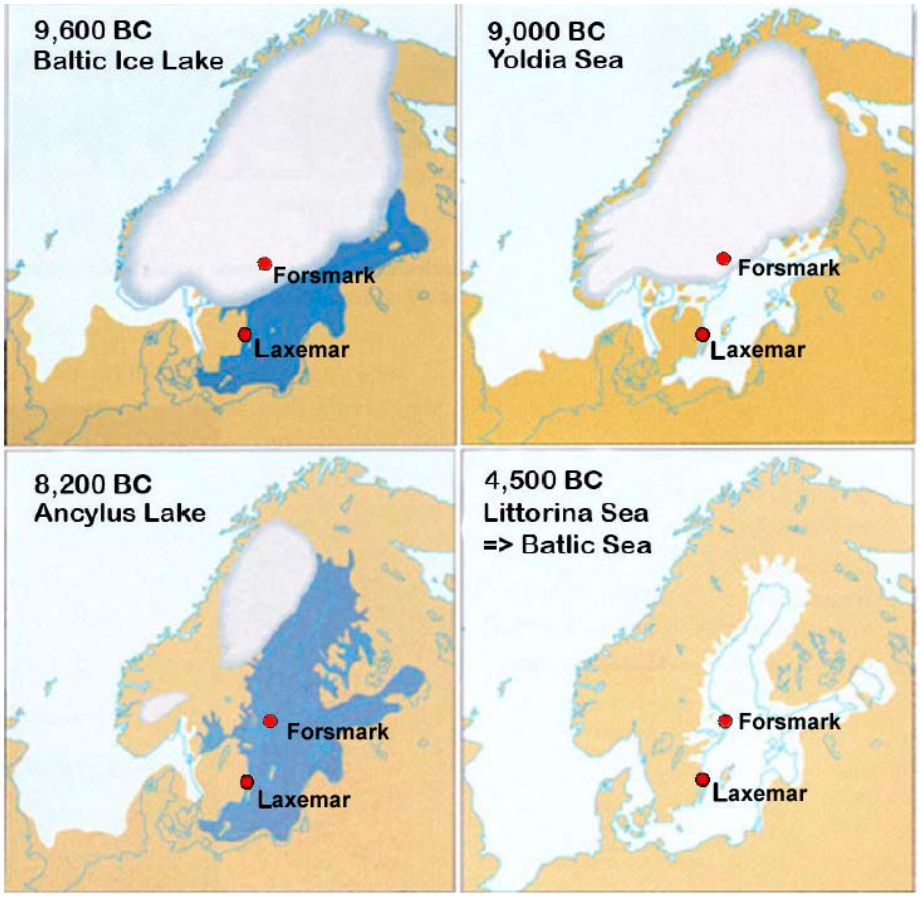

Figure 6-10. *Map of Fennoscandia with some important stages during the Holocene. Four main stages characterise the development of the aquatic systems in the Baltic basin since the latest de-glaciation: the Baltic Ice Lake (13,000–9500 BC), the Yoldia Sea (9500–8800 BC), the Ancylus Lake (8800–7500 BC) and the Littorina Sea, leading to the Baltic Sea (7500 BC–present). Fresh water is symbolised with dark blue and marine/brackish water with light blue. (After Follin et al. 2007b, Figure 3-56, Rhén et al. 2009, Figure 4-23).*

The peak salinity of the Littorina Sea has been estimated to be about 12 g/L (Westman et al. 1999). Since then the salinity of the seawater has been reduced steadily to its current value of c. 6 g/L. As a result of land-rise and sea level changes, the shorelines at both Forsmark and Laxemar have advanced. The shore level displacement started before the final de-glaciation and is still an active process throughout Sweden. A summary of the shoreline displacement and salinity of the Littorina/ Baltic Seas assumed in the modelling is given in Figure 6-11.

6.6.3 Reference waters

In the palaeo-climatic modelling it has been assumed that chemically conservative mixing of several so-called reference water (or end-member) types provides a reasonable estimation of the chemical composition of the groundwater (SKB 2007, Laaksoharju et al. 2009). Conceptually, each reference water type represents an important aspect of the changes in the climate and the evolution of the hydrological conditions. Each reference water type is described by its chemical composition in terms of concentrations of various solutes. The major ions considered in the groundwater flow model are Br, Ca, Cl, HCO_3, Mg, Na, K and SO_4. Two isotopes ratios of interest to hydrogeology are δ^2H and $\delta^{18}O$.

The following references waters have been defined in order to model the palaeo-climatic evolution of the groundwater at Forsmark and Laxemar, although the precise chemical compositions of each reference water varies between the sites:

- 8n-saline source implies low chloride content (< 8 mg/L). A non-marine origin implies low magnesium content (< 8 mg/L).

An additional reference water type was used in the palaeo-climatic modelling at Laxemar:

- Inter-glacial: Representing ancient water, it is composed of meteoric and brackish waters from periods before the Weichselian glaciation, implying high chloride content (> 20,000 mg/L). Its non-marine origin implies low magnesium content (< 50 mg/L). It has intermediate $\delta^{18}O$ concentrations (–12 to –11‰ VSMOW).

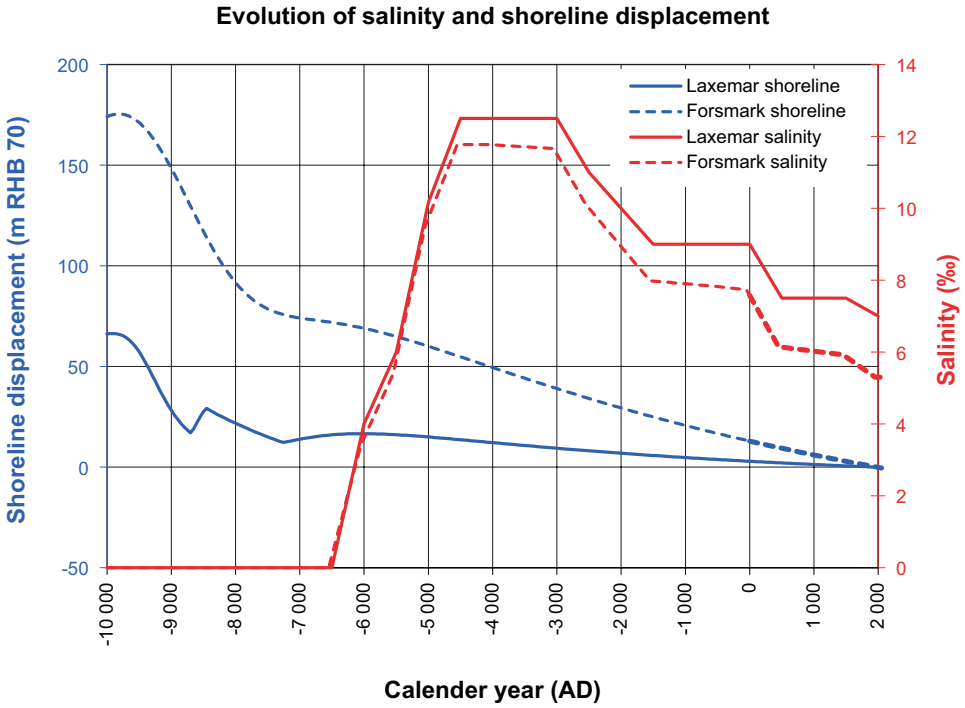

Figure 6-11. Shoreline displacements (relative to the year 2000 AD) and the range in the salinity of the aquatic systems in the Baltic basin specified in Rhén et al. (2009) and Follin et al. (2007b) for Forsmark and Laxemar.

In the borehole data, chemical signatures were interpreted to indicate the presence of various reference waters:

- Cl is used as an indicator of saline groundwater, which could be Littorina Sea Water or Deep Saline Water.
- the Br/Cl ratio is used to indicate the position of the transition in the origin of salinity from Deep Saline Water at depth to Littorina Sea Water above.
- $\delta^{18}O$ is used to indicate any remaining pockets of Holocene Glacial Melt Water.
- HCO_3 indicates the penetration of modern Meteoric Water.

In the palaeo-climatic modelling it has been assumed fracture groundwater chemistry can be adequately represented by chemically conservative mixing, that is, no chemical reaction takes place during transport. Hydrochemical evolution is modelled as mixing by advection and dispersion of fractions of reference waters. For some chemical constituents, such as Cl, Br and $\delta^{18}O$, it is thought that chemically conservative transport simulation is appropriate. For other chemical constituents, such as HCO_3 and SO_4, transport can be affected by chemical and microbial processes. Mg is not a conservative tracer either, due to ion exchange mechanisms. However, it is a useful indicator to differentiate between Deep Saline Water at depth and shallower Littorina Sea Water near the top surface of the model domain. Caution was exercised when using these non-conservative tracers for model calibration purposes. The Br/Cl ratio was used as an alternative to indicate the transition zone from Littorina Water to Deep Saline Water, because it was considered that both Br and Cl are transported conservatively. The environmental isotopes δ^2H and $\delta^{18}O$ provide guidance to differentiate between Glacial Melt Water and meteoric reference waters such as Old Meteoric Waters (from periods before latest glaciation) and Inter-glacial Porewater. Reactive solute transport is discussed in Laaksoharju et al. (2009) and Molinero et al. (2009).

6.6.4 The conceptual model of changes in groundwater composition

Groundwater chemistry can affect groundwater movement by changing the density and the viscosity of the groundwater. The density changes are likely to be dominated by the presence of dissolved salt. Since hydraulic gradients at both Forsmark and Laxemar are expected to be relatively low because of the gentle topography, the buoyancy forces arising from density variations in the groundwater are significant.

The conceptual model of the evolution of the groundwater can be expressed in terms of the reference waters as follows: It is thought that, at depth, Saline water (and at Laxemar, Inter-glacial water) have remained undisturbed for long time periods, due to the predicted low flow-rates at depth. Above this elevation groundwater mixing can take place driven through a combination of buoyancy forces and pressure differences arising from changes in the ground surface elevation.

Immediately after the Weichselian de-glaciation, it is thought that the glacial melt water associated with the retreating ice sheet was able to infiltrate the bedrock under pressure. Hence, an initial condition (at 8000 BC) for subsequent modelling was that that, above the Saline water, the groundwater was composed of Glacial and Inter-glacial waters. During the Littorina and Baltic Sea stages the denser sea waters were expected to displace the less dense Glacial and Inter-glacial waters as they infiltrate the bedrock. For the parts of the Forsmark and Laxemar sites that are submerged this flow is purely density driven. The infiltration to depth stops only when the Littorina and Baltic Sea waters encounter the more dense Saline water at depth. The variation in salinity of the Littorina and Baltic seas over time is represented by using a variable mixture of the Littorina and Meteoric reference waters. When land emerges from the sea, Meteoric water starts to infiltrate and mix with the pre-existing groundwater. Meteoric water is less dense than the predominately Littorina water that it encounters, therefore in order to displace this water the driving heads must be sufficient to overcome the opposing buoyancy forces.

6.6.5 Physical processes modelled and modelling strategy

The process of rock-matrix diffusion (RMD) is thought to be important in understanding the chemical evolution of the groundwater at Forsmark and Laxemar. In fractured rocks, most of the groundwater flow takes place through a network of interconnected fractures, which for an ECPM representation is

characterised by a hydraulic conductivity tensor and a kinematic porosity associated with the volume contained within the connected open fracture system. In addition to the kinematic porosity, the rock matrix is itself porous. Solutes can be transported by diffusion from the water in the kinematic porosity into the relatively immobile water in the low permeability rock matrix, which is controlled by the additional parameters for the fracture surface area per unit volume, the effective diffusivity of the matrix and the matrix porosity. In the modelling hydraulic conductivity, kinematic porosity and connected fracture surface area are determined by upscaling the underlying fracture system as represented by the Hydro-DFN model. The hydraulic conductivity is determined by the most connected and transmissive fractures in the fracture system which have been characterised by the PFL-f and PSS hydraulic tests.

The fracture surface area per unit volume is determined by the connectivity of the open fracture system, which is characterised by the intensity of PFL-f fractures, but as such is sensitive to the detection limit and configuration of the PFL-f tests since there may be significant connected fracture surface area in which there is either no circulation under the particular test conditions or below the detection limit. The kinematic porosity is affected by the connected fracture surface area and the transport aperture, and so is subject to similar detection limit and test configuration issues. The significance of the truncation of fracture sizes in calculating upscaled kinematic porosity was studied in Rhén et al. (2009) (e.g. Table 10-21) where it was demonstrated that kinematic porosity can be enhanced by up to a factor 10 when the volume associated with all small connected fractures is considered rather just the large fractures responsible for bulk flow. Hence, small fractures may provide significant additional porosity in which either slow rate advection takes place, or free-water diffusion unencumbered by tortuous pathways through the matrix structure, as well as providing additional extra surface area for exchange with the matrix. For these reasons the sensitivity to kinematic porosity and fracture surface area were tested in the palaeo-climatic simulations (Follin et al. 2007b, 2008a, Rhén et al. 2009), and the fracture surface area per unit volumes was found to be of particular importance. It should also be noted that assignment of matrix porosity also has to consider the effects of fractures. For example, Crawford (2008) notes altered core samples characterised by high porosities on the order of several percent due to micro-fractures.

Rock matrix diffusion is a retardation mechanism, because solutes would otherwise be transported at a velocity determined by the Darcy flux and the accessible kinematic porosity. Rock matrix diffusion also acts as an additional dispersive process, since solutes that have diffused into the rock matrix can diffuse back out over a period of time, increasing the range of travel times between early and late arrivals. The ECPM models use an RMD approach reported in Hoch and Jackson (2004).

The parameters used in the RMD model are:

- The effective (or intrinsic) diffusion coefficient (for diffusion in the diffusion accessible porosity).
- The diffusion accessible porosity.
- The maximum distance available for diffusion into the diffusion accessible porosity.
- The area of fracture surface per unit volume (the flow-wetted fracture surface per unit volume) over which there may be diffusion between the groundwater flowing in the fractures and the diffusion accessible porosity.
- The kinematic porosity formed by interconnected fractures.

Estimates of the effective diffusion coefficient and the diffusion accessible porosity are available from in-diffusion experiments, although it is recognised that these are based on small-scale experiments and there may be important scaling issues (e.g. sensitivity to altered volumes of rock with high intra-granular porosity) when considering transport on the scale of the blocks between connected fractures.

Parameters relating to the fracture surface area per unit volume for diffusive exchange between the fractures and matrix have been derived from information about the spacing of hydraulic fractures. They have been derived based on the intensity of flow-conducting fractures mapped using the PFL-f method. The rate of exchange of solutes between the fractures and matrix is determined by the effective diffusion coefficient, which is then multiplied by the surface area per volume to determine the total solute flux into the matrix. The diffusion accessible porosity of the matrix determines the rate of change of solute concentration in the matrix to this flux from the fractures.

The kinematic porosity has been derived by upscaling the underlying Hydro-DFN calculated element-by-element as the total interconnected fracture volume divided by the element volume. The fracture volume for an individual fracture is calculated as the fracture area within an element multiplied by the transport aperture. The flow wetted fracture surface area per unit volume of rock, a_r, used to parameterise RMD of solutes in the palaeo-climatic modelling task was derived from the intensity of flow-conducting features identified in the PFL-f tests as $a_r \approx 2\, P_{10,PFL,corr}$, where $P_{10,PFL,corr}$ is the Terzaghi corrected intensity of flowing fractures detected with the PFL-f method.

6.6.6 Illustrative results and conclusions

Regional hydrogeological simulations were carried out from 8000 BC until 2000 AD. The results were compared against measured hydrochemical information. The steps taken in matching against hydrochemical profiles in deep boreholes followed many common themes with the calibration on hydraulic and hydrological data, such as the importance of the deformation zones and the effective hydraulic conductivity of the HRD. The changes made to hydraulic parameters to calibrate against the interference test and natural groundwater levels were also tested in the palaeo-climatic simulations and generally found to have either beneficial or neutral effects on the calibration on hydrochemical data. However, other factors affecting solute transport had also to be considered, such as the kinematic porosity, the flow wetted fracture surface area per unit volume of rock and the initial distribution of groundwater chemistry. These transport related factors did not affect the calibration against the interference tests or the natural groundwater levels.

Having obtained satisfactory simulations of groundwater composition by calibration of model parameters, the sensitivity of the model was illustrated by running a series of single parameter variants about the calibrated model, see Section 6.1.4 of Follin et al. (2007b) for Forsmark, and Section 9.1.4 of Rhén et al. (2009).

The performance of the base model simulation of Forsmark in predicting salinity was assessed to be generally good. The predictions of transitions from Littorina Sea Water to Deep Saline Water shown by Br/Cl, and from present-day Meteoric Water to Littorina Sea Water shown by HCO_3 are both at the correct depths. Examples of the predications of the models and a comparison to data are given in Figure 6-12. Simulations are compared for both fracture water from groundwater samples and also pore water extracted by diffusion experiments on fresh core samples collected in KFM01D. Sensitivity studies were made by changing parameters relative to those used in the base model. Sensitivities to the hydraulic properties of the HCD, the effective vertical permeability of the HRD, the values of the kinematic porosity used, the flow wetted surface per unit volume, and hydrochemical initial conditions were considered.

At Laxemar it was found that the initial SDM-Site model parameterisation did not produce a satisfactory match to the hydrochemical data without significant changes to the hydraulic properties of the HRD, for example predicted flushing with altered meteoric water to greater depth than was observed. It was found that the match could be improved overall by reducing the hydraulic conductivity by a factor of three below –150 m elevation. Simulation results of two groundwater components and a reference water fraction for meteoric water after making these changes are exemplified in Figure 6-13. Such changes did not have a traceable origin in the calibration of the Hydro-DFN model beyond being possibly within the margin uncertainty of hydraulic properties predicted by the Hydro-DFN methodology. For this reason, the Hydro-DFN model methodology was reassessed and elaborated, to produce the Elaborated Hydro-DFN (Joyce et al. 2010b) based on several methodological changes (described in Chapter 4). The Elaborated Hydro-DFN model of Laxemar gave ECPM properties that produced a reasonable match to the hydrochemistry data without any adjustments to values obtained by upscaling. The degree of match to hydrochemical data achieved was comparable to that obtained in the SDM-Site (Rhén et al. 2009) after lowering the hydraulic conductivities derived from the upscaled SDM-Site Hydro-DFN by a factor of one-third below –150 m elevation. Figure 6-14 (after Joyce et al. 2010b, Appendix E.6) gives two examples of a comparison between the simulated and measured groundwater compositions for the Elaborated Hydro-DFN model (unmodified) and the upscaled SDM-Site Hydro-DFN (after being multiplied by a factor of one-third below –150 m elevation to get an acceptable match). Hence, the Elaborated Hydro-DFN model provided the basis for deriving hydraulic properties shown to simulate groundwater composition under palaeo-climatic evolution consistent with hydrogeochemical data and based on an underlying site Hydro-DFN model.

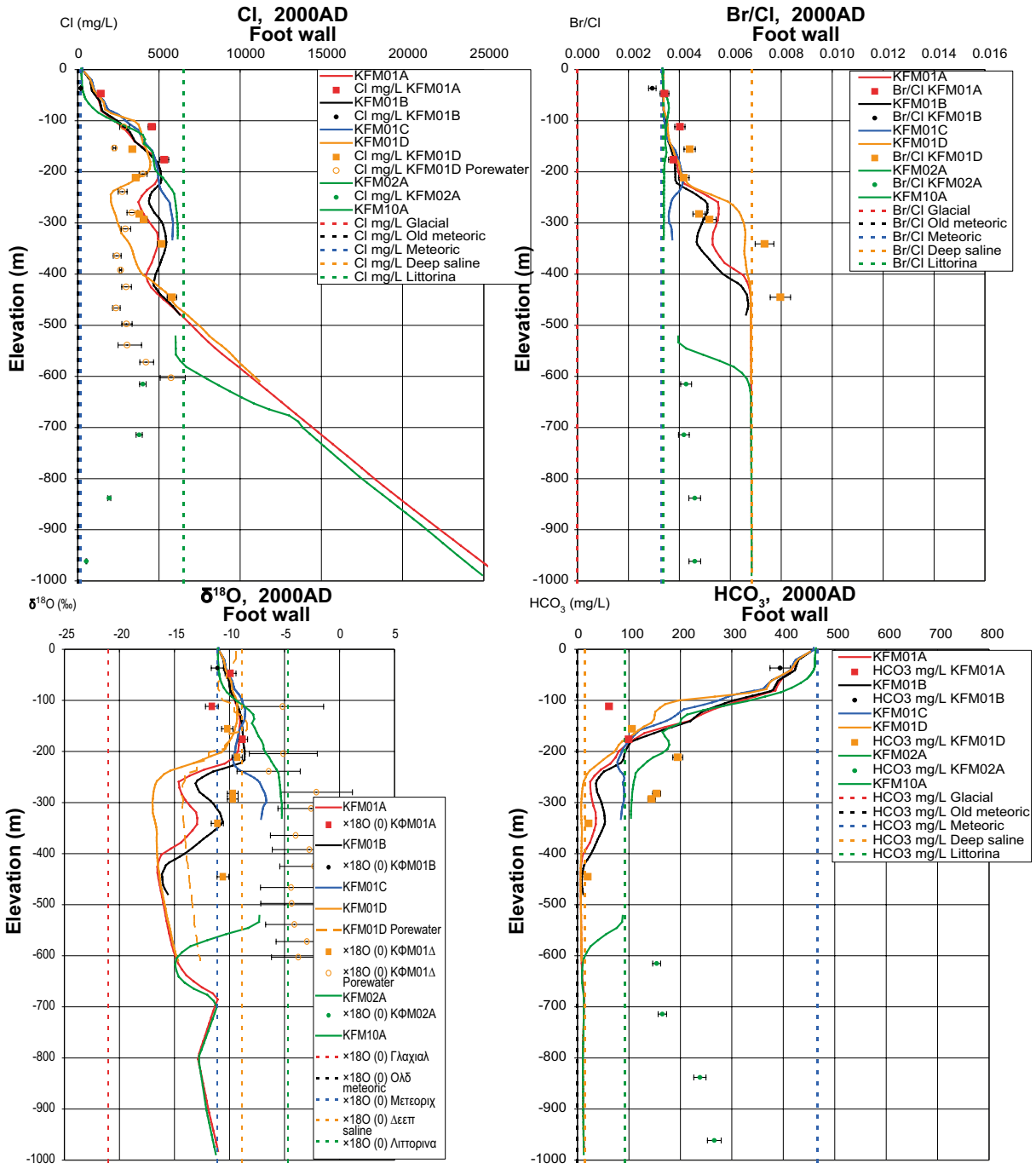

Figure 6-12. *Comparison between the deterministic base model simulation (solid lines) and measured concentrations of Cl, Br/Cl, $\delta^{18}O$ and HCO_3 in the fracture system (filled squares) for the first set of boreholes in the footwall of A2, Forsmark. The error bars on the measured data indicate the laboratory analytical error. The dashed lines show the specified concentration of Cl, Br/Cl, $\delta^{18}O$ and HCO_3 in the reference waters. (After Follin et al. 2008a, Figure 5-17).*

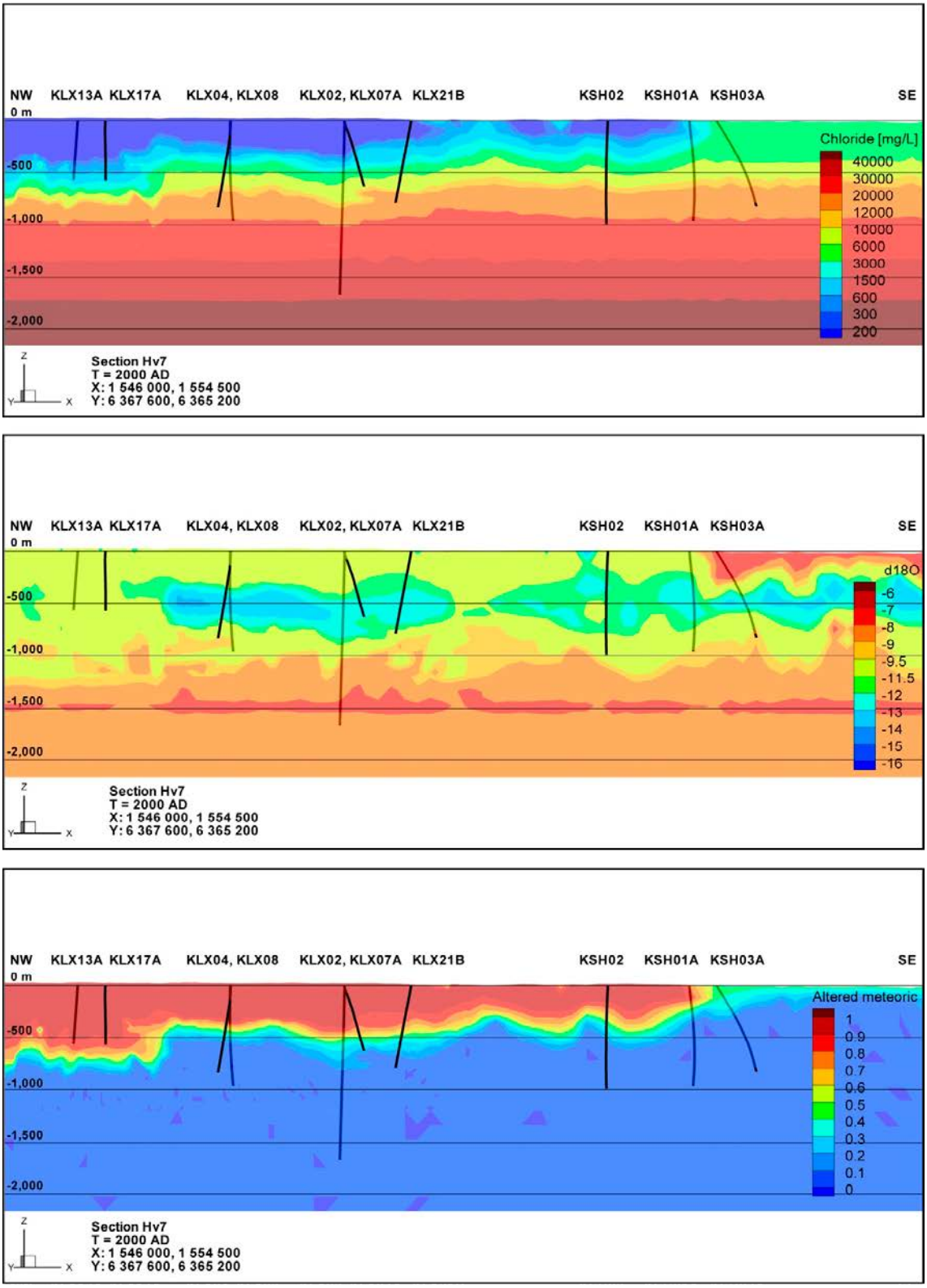

Figure 6-13. *Distribution of Cl (top) and $\delta^{18}O$ (middle) and Altered meteoric reference water fraction (bottom) predicted on a vertical slice covering the Laxemar site. (After Rhén et al. 2009, Figure 9-15.)*

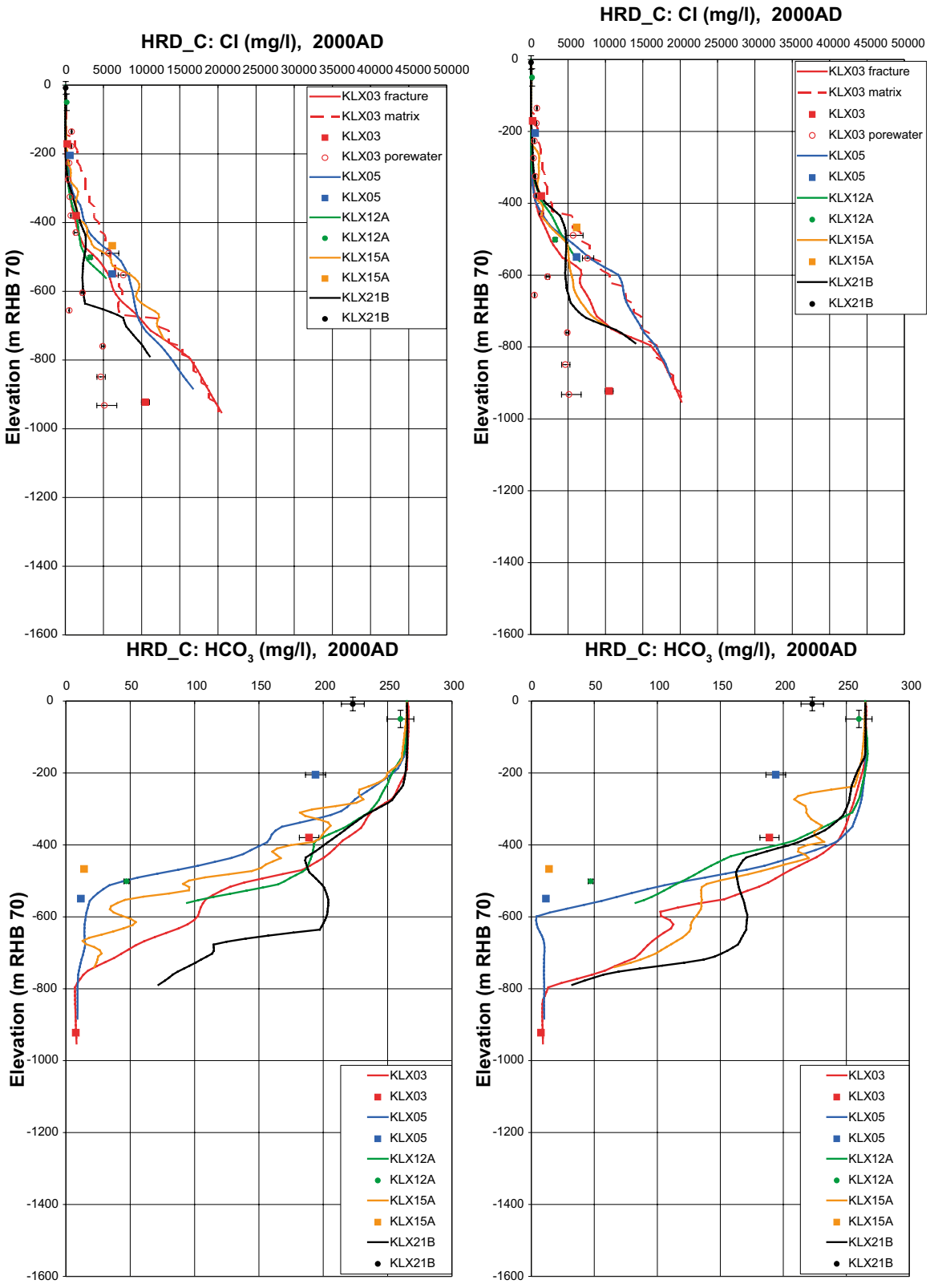

Figure 6-14. *A comparison of the modelled and measured Cl (top) and HCO_3 (bottom) concentrations in the fracture system for boreholes in boreholes in hydraulic domain HRD_C for the Elaborated Hydro-DFN (left) and the SDM-Site Hydro-DFN (right). Square symbols are used for category 1-3 data, circles are used for the pore water data, and small diamond symbols are used for category 4 data. The error bars on the data indicate the laboratory analytical error. The solid lines show the distribution in the borehole simulated in the fracture system, and the dashed lines are for the matrix.*

6.7 Remaining uncertainties

The regional-scale groundwater flow and solute transport simulation tests of palaeo-climatic evolution, natural head measurements, hydraulic interference test data and drawdowns due to the Äspö HRL at Laxemar have confirmed that hydrogeological properties, as given by the base case models developed during SDM-Site hydrogeological DFN model (Follin et al. 2007a, Rhén et al. 2008), together with the HCD parameterisations, provide appropriate descriptions of the hydrogeological situation in the bedrock at both Forsmark and Laxemar. Sensitivities to various features and parameters were considered in the regional-scale modelling, but prompted relatively few changes to the initial implementation of the model based on calibration against PFL-f borehole test data. These changes where considered to be within the reasonable ranges of parameter uncertainty. At Laxemar it was found that the match to the hydrochemical data could be improved through the use of an Elaborated Hydro-DFN (Joyce et al. 2010b).

The relatively good matches obtained to the available data covering a fairly extensive range of situations and modelling tasks builds confidence that the conceptual hydrogeological models provide a reasonable description of the hydrogeological conditions at both Forsmark and Laxemar. However, at both sites the conceptual models recognised the inherent spatial variability of the bedrock by characterising the HCD in terms of the variability in transmissivity about a mean depth trend and in describing the HRD in terms of a stochastic DFN concept. Initial model testing was performed using the mean depth trends interpreted for the transmissivity of each HCD and a single realisation of the Hydro-DFN model of the HRD. The significance of spatial variability was quantified for each type of modelling task by generating multiple realisations of the HRD (based on a realisation of the Hydro-DFN) and the HCD with spatial variability with each deformation zone (as represented by triangulation of side 200 m with the transmissivity in triangle independently sampled). These stochastic sensitivity tests are reported in Follin et al. (2008a, Chapter 7) and Rhén et al. (2009, Sections 8.1.4, 9.1.4). Some of uncertainties recognised in the conceptual model and tested in the numerical model are discussed below.

6.7.1 HCD

It was observed that there is a large variability of hydraulic properties within some of the deformation zones, indicating that heterogeneity is likely to be large within the HCD. In general, even within the focussed areas, the number of borehole intercepts with deformation zones is limited, particularly at depth. As a consequence, most assessments of hydraulic properties for an individual HCD in the present models must be considered very uncertain, although the general conceptual depth trends of mean transmissivity seem to be supported by the simulations made with the regional groundwater flow models. Some specific deformation zones, such as those of significance for the interference tests, had their effective hydraulic properties further constrained by the regional-scale modelling. As there are no hydraulic data for parts of the regional model volume, the assessed properties within the regional volume outside the focussed volume are uncertain. The sensitivity of simulations of confirmatory tests and inputs to safety calculations were quantified based on a stochastic approach to describing heterogeneity with zones based on hydraulic data.

The existence of dolerite dykes at Laxemar and their possible function as hydraulic barriers have been suggested by interference test results and pressure measurements. The geological description also indicates that possibly other dolerite dykes than those observed in boreholes may exist, but they are perhaps relatively thin and may act as highly localised hydraulic barriers. The regional-scale flow modelling has not addressed the effect of possible dolerite dykes on the groundwater flow at Laxemar.

6.7.2 HRD

At both Forsmark and Laxemar, all of the regional-scale simulations were based on Hydro-DFN models which used an intensity derived from open fractures, a power-law fracture size distribution with $r_0 = 0.038$, and a semi-correlated transmissivity model. Based on the similarity between the block upscaling results described in Section 5.2, it seems plausible that other Hydro-DFN variants, for example with channelling or spatial variability on fracture planes, would also allow reasonable matches to data in regional-scale simulations. The significance of some modelling assumptions such as fracture size-transmissivity relationships for the calculation repository performance measure

statistics was explored in SR-Site, as summarised here in Chapter 7. How sensitivities to assumptions about intensity-size-transmissivity might be further explored is discussed in Section 8.3.

6.7.3 Transport properties

Transport apertures used in the modelling were determined from tracer tests, based on earlier work at Äspö (Dershowitz et al. 2003) or more recent collations of experiments (Hjerne et al. 2010). The only way the transport aperture affects the regional-scale simulations is with respect to kinematic porosity values derived from upscaling. The palaeo-climatic simulations were found to be moderately sensitive to the kinematic porosity used for both HRD and HCD (see Follin et al. 2007b for Forsmark, Section 6.1.2 and Rhén et al. 2009 for Laxemar, Section 9.1.3).

Flow wetted surface area per unit volume was found to be an important parameter in the palaeo-climatic simulations, as it determines the area available for diffusion between the flowing groundwater and the rock matrix. This was particularly apparent at Laxemar, where assigning a flow wetted surface area per unit volume to the HCD according to the observed fracture intensity improved the match to hydrochemical data in those boreholes intersected the HCD.

The effect of uncertainty in transport aperture and effective diffusivity on repository performance measures such as advective travel times are addressed in Crawford (2008) and Crawford and Sidborn (2009).

7 Use of hydrogeological DFN models in safety evaluation

Having been fully calibrated and demonstrated to produce reasonable matches to data of different types in a regional-scale context, the hydrogeological models developed of Forsmark Laxemar were applied to the estimation of repository performance measures. The overall objective was to allow assessment of repository safety (Joyce et al. 2010a, b, Selroos and Follin 2010).

The hydrogeological evolution during the temperate period after repository closure involves two distinct time intervals. The first time period involve re-saturation of the repository volume once pumping of the open tunnels has stopped. The subsequent time interval deals with the evolution of the saturated repository up till the start of the next glacial period. At Forsmark and Laxemar, the primary hydraulic driving force for groundwater flow during the temperate period is the recharge flushing due to precipitation. The ongoing shoreline displacement implies a continuous change in the flushing pattern and evolution of the hydrochemical conditions. In order to assess the magnitude of these impacts, groundwater flow simulations have been performed. The time period 2000 AD to 12,000 AD was used at Forsmark to represent the interval following the closure, backfilling and saturation of the repository, while up to 15,000 AD was considered at the more southerly Laxemar. An illustration of the DFN models used for ring the detailed flow around the repository for the safety assessment at Forsmark is shown in Figure 7-1.

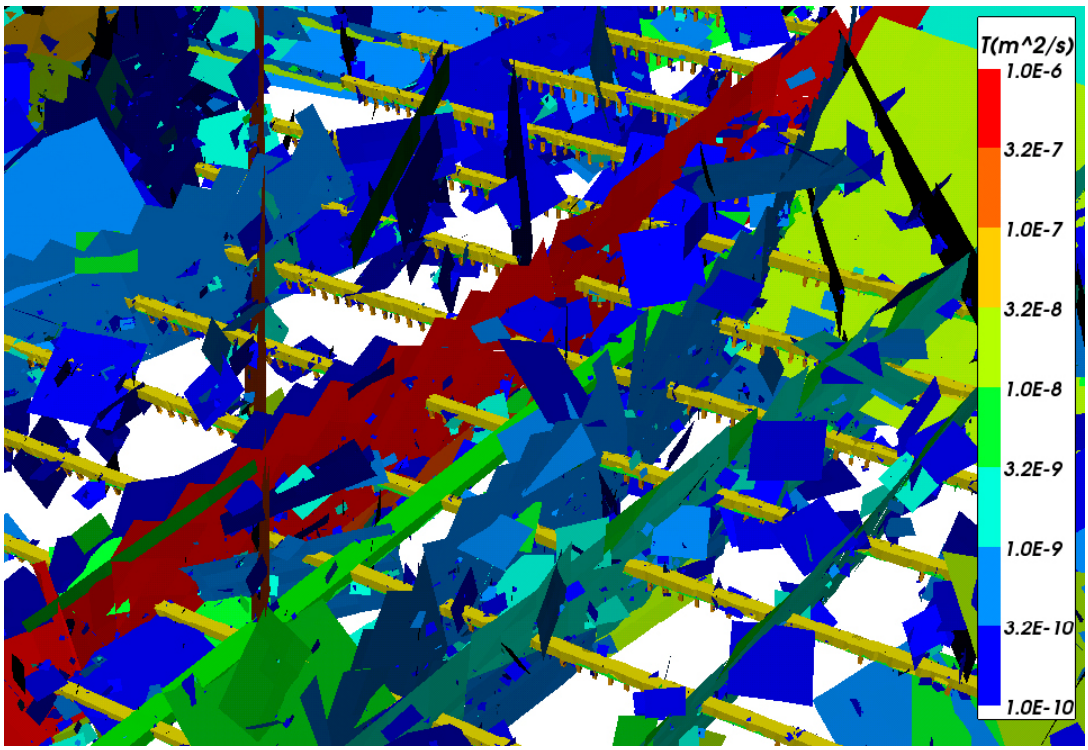

Figure 7-1. *An example of a DFN/CPM ConnectFlow model of Forsmark using a CPM sub-model of deposition and main tunnels embedded within a DFN sub-model. Some fractures have been removed to reveal the tunnels. The interface between the two sub-models is on the boundary of the CPM model.*

In the modelling work, transport was understood to occur along advective flow-paths. A particle tracking algorithm was used to represent the advective transport of radionuclides. In CPM models, particles are tracked in a deterministic way by moving along a discretised path within the local finite-element velocity field. In DFN models, a stochastic 'pipe' network type algorithm was used. Particles were moved between pairs of fracture intersections stepping from one intersection to another. At any intersection there may be several possible destinations that the particle may move to, as flow follows different channels through a fracture according the differences in pressure between intersections. A random process, weighted by the mass flux between pairs of intersections, was used to select which path was followed for any particular particle. The stochastic nature of this algorithm implies an explicit hydrodynamic dispersion process if more than one particle is released per start point as a consequence of the physical mixing that takes place at fracture intersection. The amount of mixing at fracture intersection can be controlled by increasing the spatial discretisation of the fractures (by sub-dividing them). The consequences of models used for mixing at intersection are discussed by Berkowitz et al. (1994).

7.1 Repository performance measures

The output from the models consisted of two types of performance measures of relevance to the safety assessments (Joyce et al. 2010a, b):

1) Characteristics of the flow-paths from the deposition holes to surface discharge, such as cumulative advective travel times (t_r [T]) and flow-related transport resistances (F_r [TL^{-1}]) of the released particles in the rock.
2) Characteristics of the flows around deposition holes, such as equivalent flux (U_r [LT^{-1}]) and equivalent flow-rates (Q_{eq} [L^3T^{-1}]) at the particle release points.

The advective transport time for the network of fractures forming conductive flow-paths from the repository to the top of the bedrock is also referred to as the water "residence time". The advective travel times and flow-related transport resistances are used as input for the far-field radionuclide transport calculations (SKB 2011).

Radionuclide migration through the bedrock is retarded by the processes of sorption and rock matrix diffusion. Flow-related transport resistance (sometimes called the "F-factor"), expresses the relation between flow wetted surface and groundwater flow, and describes the hydrodynamic control of retention of nuclides in the bedrock (Moreno and Neretnieks 1993, Cvetkovic et al. 1999). The flow-related transport resistance of a fracture is equated to $2WL/Q$ [TL^{-1}], where W is the width of the flow-path within the fracture, L is the length of the flow-path within the fracture and Q is the flow-rate. The greater the surface area in contact with flowing water for a given flow-rate, the greater the interaction will be with both the fracture surface itself and the rock matrix. The flow-related transport resistance is therefore a key parameter governing the retardation of radionuclides within fractured rock (Andersson et al. 1998). Coupling of the flow-related transport resistance estimated from hydrogeological modelling with a retardation model allows for the prediction of transport times for key radionuclides (SKB 2010c). The estimated flow-related transport resistances and advective travel times were used as the basis for calculations where the transport times of representative (sorbing) radionuclides were estimated for site specific conditions in Crawford (2008) and Crawford and Sidborn (2009). Additional analyses for Laxemar data are given in Frampton and Cvetkovic (2011) and Cvetkovic and Frampton (2012).

Flow-related transport resistance can be formulated as twice the advective travel time through a fracture divided by the effective transport aperture of the fracture. However, since travel time scales linearly with transport aperture, then in fact flow-related transport resistance does not depend on transport aperture. Quantifying flow-related transport resistance as twice the flow wetted area (flow width times length) divided by flow-rate allows it be related to measurements made by the PFL-f tests, since they measure the magnitude of flow-rate (albeit under disturbed pumped conditions) and the intensity (based on Terzaghi correction) of measured flow is used to estimate the flowing fracture surface area per unit volume. Details of how the flowing fracture surface area is distributed in space and how the variation in flow-rates is distributed over this surface area as well as any correlations cannot be determined directly from the field data. Such details emerged in the Hydro-DFN modelling

as a function of the assumptions made about spatial distribution, fracture intensity-size-transmissivity distributions. Still, any models calibrated on the PFL-f data following the process described in Section 4.1 will share common characteristics of distributions of flow-rate and surface area intensity of flowing fracture surface area per unit volume, and so might be expected to predict relatively similar distributions of flow-related transport resistance. If for example, a conceptual model were considered with narrow flow channels, then the calibration process would require sufficient numbers of numbers of channels to meet the observed intensity of flow channels, and sufficient variability in flow-rate either between or along channels. Some effects of channels width explored in SKB (2005b).

The detection limit of the PFL-f measurement of specific capacity c 10^{-9} m^2/s implies that the developed Hydro-DFN models do not represent any connected open fractures with lower specific capacity. This would imply there may be deposition holes with initial fluxes and transport pathways to the surface with performance measures controlled by fractures with transmissivity of order 10^{-9} m^2/s or less. The initial equivalent flux for such a deposition hole can be estimated from $U_r = T\nabla h/d$, where T=1 10^{-9} m^2/s, the hydraulic gradient is set to a characteristic value for Forsmark of about ∇h =0.005, and d=5 m is the canister height, implying a truncation on U_r of about $3 \cdot 10^{-5}$ m/y. The flow-related transport resistance truncation can be estimated as $2L/T\nabla h$ with the path distance L=1,000 m to give about $1 \cdot 10^{7}$ y/m, which are relatively low compared to values presented in Section 7.5.

In summary, the flow-related transport resistance is considered to be well constrained by the calibration to match the results of the PFL-f tests, although it is recognised than many assumptions have to be made in constructing a Hydro-DFN to essentially extrapolate the fracture characterisation performed primarily in boreholes to details of flow-paths in three-dimensions. This assertion was in part substantiated in SR-Site for model variants considering the sensitivity to size-transmissivity relationship for Forsmark (Joyce et al. 2010a, Section 6.3.2), while in the safety assessment calculations for Laxemar (Joyce et al. 2010b, Section 6.3) the sensitivity to Hydro-DFN calibration methodology was tested by comparing results for the SDM-Site Hydro-DFN (Rhén et al. 2008) with the Elaborated Hydro-DFN (Joyce et al. 2010b). At both sites the difference in flow-related transport resistance between model variants was less than a factor of about 2. It is recognised that a wider range of conceptual models would be need to be examined to further substantiate these arguments (see Chapter 8).

The equivalent fluxes at the release points and equivalent flow-rates at the release points are used as input to buffer erosion-corrosion analyses as well as input for the near-field radionuclide transport calculations. In addition, the spatial distribution of exit (discharge) locations, and how this distribution changes over time, is calculated. Furthermore, the palaeo-climatic evolution of the sites was modelled at the regional-scale to simulate groundwater composition at future times, albeit based transport and mixing of conserved fractions of reference waters.

Although the modelling studies discussed here focused on the temperate period between glacial periods, additional modelling was undertaken to understand the excavation and operational phases (Svensson and Follin 2010) and during glacial and periglacial periods (Vidstrand et al. 2010a). Temporal changes in groundwater conditions are expected during a glaciation cycle, with periods of recharge of glacial meltwater that imply a gradual dilution of the originally more saline water that may penetrate to repository depth. Arguments have been put forward that if glacial melt waters were rich in dissolved atmospheric gases, reducing conditions might no longer prevail at repository depth, infringing the safety function indicator criterion (Puigdomenech 2001). Studies reported in Sidborn and Neretnieks (2008), Spiessl et al. (2010), and Sidborn et al. (2010) agree that the flow-related transport resistance is a key parameter when studying the interaction between dissolved oxygen in the flow-conducting water and minerals in the rock.

7.2 Repository structures

The repository itself, along with structures such as the transport tunnels, shafts, and their associated excavation damaged zones (EDZs), have a potentially significant impact on the local groundwater flow, in particular if the fracture intensity is low. In order to account for these effects, it is necessary to represent the repository appropriately in the model. The potential conduits for flow within the repository are the deposition tunnels, main tunnels, transport tunnels, ramp and shafts, together with the EDZ around the tunnels created during construction of the repository. The operational and resaturation phases were not considered in the models of the temperate period. The unsaturated conditions

during the excavation and operation phases were described in Svensson and Follin (2010) based on simulations using the DarcyTools software (Svensson and Ferry 2010) using the same underlying realisations of the fracture network as used for the temperate period, but represented by a continuous porous medium in DarcyTools derived from a geometrical upscaling approach (Svensson et al. 2010). All tunnels were assumed to have been backfilled and represented by homogeneous CPM properties. For the EDZ, a conservative assumption was that it will be continuous and the transmissivity will be $1.0 \cdot 10^{-8}$ m^2/s over a thickness of 0.3 m (SKB 2010a). Although this was the scenario adopted by the base case model used in SR-Site as a conservative approach, data suggests that a continuous EDZ would not form at all (SKB 2010a). An illustration of the repository structures as implemented in the ConnectFlow models, along with results from stochastic particle tracking through the DFN model is shown in Figure 7-3.

In the transport calculations, three release paths for radionuclide release were considered:

1) A fracture intersecting the deposition hole.
2) The excavation damaged zone (EDZ), if such a zone exists, located below the floor of the deposition tunnel that runs above the deposition holes.
3) A path through the backfilled tunnel and into a fracture intersecting the deposition tunnel.

7.3 Modelling strategy

Here, we summarise the methodology used in the temperate period modelling for SR-Site (Forsmark) (Joyce et al. 2010a). In order to simulate the evolution of regional-scale (scale of c 10 km) groundwater flow and composition as well as details of flow-rates around individual deposition holes (scale of metres) three different scales of model were used in the temperate period modelling, called repository-scale, site-scale and regional-scale, see Figure 7-2. The same underlying discrete fracture network (DFN), which was derived from the interpretation of site data (Follin 2008), provides the basis for parameterization of all three scales. Where the models use a porous medium representation of the bedrock, the underlying DFN is upscaled to provide an equivalent continuous porous medium (ECPM) representation, whose hydraulic properties are consistent with the DFN on the scale of the model discretisation.

7.3.1 Regional-scale model

The evolution of the groundwater composition is an important consideration and this is modelled as transient coupled flow and solute transport of multiple reference waters at the regional-scale from 8000 BC to 12,000 AD. The regional-scale model extends about 15 km north to south, about 10 km east to west and extends from groundsurface to an elevation of –1,200 m. A refined local model area of side about 3 km is represented by ECPM properties on finite-elements of side 20 m embedded inside a coarser grid of side 100 m extending to the boundaries of present and expected future surface water catchments.. Simulations include density variation as a function of temperature and salinity, and viscosity variation as a function of temperature, with the temperature varying according to a geothermal gradient. It is also important to consider the density-dependent flow on a local scale and this is achieved in a computationally feasible manner by passing pressure and density values from the regional-scale model and interpolating them on to the corresponding site-scale and repository-scale models for particular time slices of interest, as depicted in Figure 7-2. The density values are then held fixed and the pressure values are used as boundary conditions to calculate a consistent steady-state pressure and flow field. The time slices chosen are 2000 AD, 3000 AD, 5000 AD and 9000 AD, typifying different periods in the evolution of the site through the temperate climate period. This approach is justified by the slow changes that occur in the evolution of the site driven by land uplift relative to the expected hydraulic diffusivity of the fracture system.

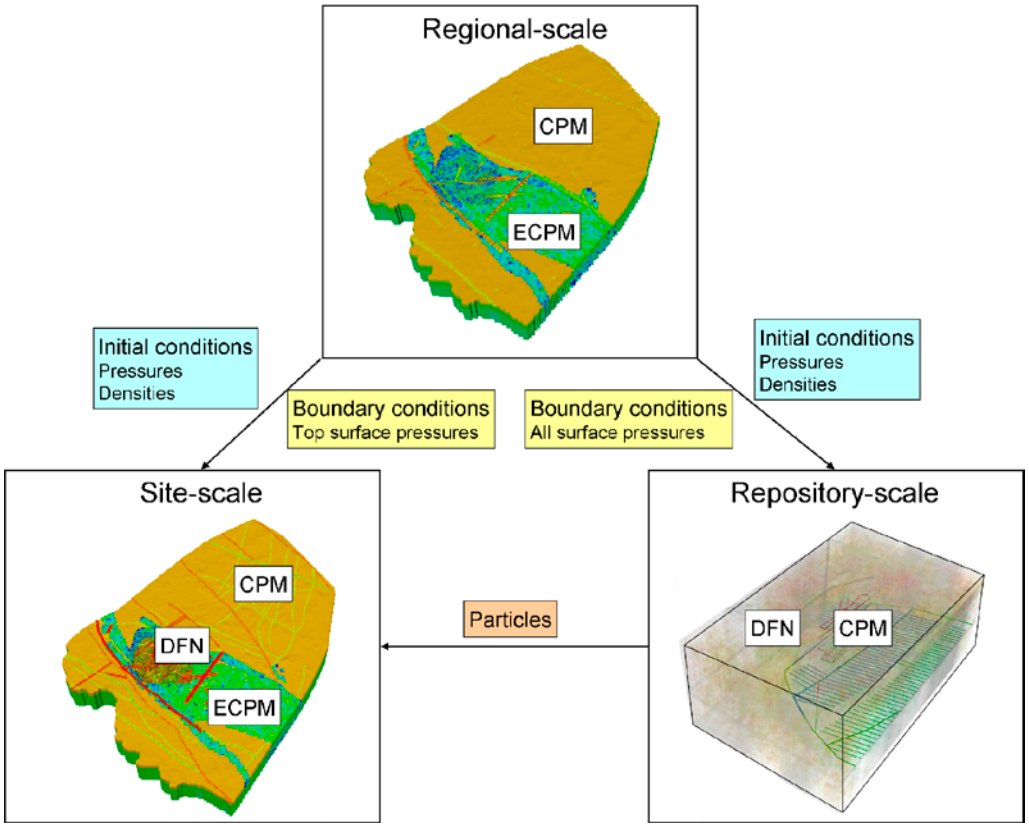

Figure 7-2. *Illustration of the concepts of model scales, embedding, and the transfer of data between scales used in the temperate period modelling of SR-Site (Forsmark) (Joyce et al. 2010a, Figure 3-9).*

7.3.2 Repository-scale model

The repository-scale model was concerned with calculating the detailed flows around the repository structures, particularly the deposition holes. Due to the detailed nature of the model it was necessary to divide it into three blocks, each corresponding to a section of the repository, for computational efficiency. Within each block, main tunnels, deposition tunnels and deposition holes were modelled as a CPM, with hydraulic properties that represented the porous medium backfill. The other repository structures and excavation damaged zones (EDZ) were represented by fractures with properties that were hydraulically equivalent to the backfilled structures. Surrounding the repository structures was a DFN representing the deformation zones and background fractures. The smallest fractures (between 0.4 m and 5.6 m radius) were only included close to the repository structures. The model blocks extend about 3 km southwest to northeast and 1 km wide and from the bottom of the regolith down to an elevation of –800 m, i.e. more than 300 m below the repository depth and extending into the deep saline zone. The regional-scale model provided pressure and density values that were interpolated onto the fractures and repository at representative time slices as described above to provide a basis for calculating density-dependent flow and transport. For each time slice a steady-state flow solution was calculated that was consistent with the pressure values at the model boundaries and the interpolated density values. A coupling of the flow equations between the DFN and CPM parts of the model ensured the continuity of pressure and flow at the interface between these rock concepts (AMEC 2012a).

Particle pathways for each time slice were calculated from each deposition hole location within a block to an external boundary of the block. Performance measure values were calculated for each segment in the pathway. Particles were continued from the boundary of each block to the ground surface within the site-scale model, as described in the following section. Three particles were started from each deposition hole location, corresponding to three release types, denoted Q1, Q2 and Q3. The Q1 release type was into a fracture that intersected the deposition hole. The Q2 release type was into the deposition tunnel EDZ above the deposition hole. The Q3 release type was into the deposition tunnel 1 m above the top of the deposition hole.

7.3.3 Site-scale model

The site-scale model replaces part of the local area about 3 km by 3 km of the regional-scale model with a DFN to better represent the detailed discrete flows and transport pathways within the repository region, whilst maintaining the overall size of the regional-scale model. Thus the model contains a DFN embedded within an ECPM/CPM with the flow equations formulated to ensure conservation of mass at the boundaries between the two regions (AMEC 2012a). The DFN includes both the deformation zones and background fractures within the repository area. These are the same fractures that were used for the repository-scale model. Additionally, the repository structures (tunnels, ramp, shafts and associated EDZ) themselves are represented by fractures with properties that are hydraulically equivalent to the backfilled structures.

The groundwater densities and pressures for the selected time slices are imported from the regional-scale model and interpolated on to the site-scale model. For each time slice, a steady-state density-dependent flow solution is calculated that is consistent with the pressure values at the model top surface and the interpolated density values in the fractures and porous medium. No flow boundary conditions are applied on the model sides and bottom, as in the regional-scale model.

The primary purpose of the site-scale model is to continue the particle pathway calculations from the locations where the particles exit the repository-scale model. Each particle is re-started in the fracture with the greatest flow within a specified distance of the exit location from the repository-scale model. The particle pathways are then calculated within the DFN or CPM parts of the model, as appropriate, until they reach the top surface of the model. Performance measures are calculated for each segment in each particle pathway and merged with the corresponding segment data for the portion of the pathway within the repository-scale model. The merged data thus represents the full pathway from a deposition hole to the ground surface.

Figure 7-3 shows an example of stochastic pathways calculated first in the repository-scale model and then continued in the site-scale model. Ensemble statistics of performance measures were calculated over the 6916 possible deposition hole locations (although not all would be required for canister deposition). With these number of start locations it was generally found that even with only particle released per deposition hole, then ensemble statistics over all holes were adequately converged. Releasing 10 particles per start location gave a distribution of flow-related transport resistance very similar to that for 1 particle. The main difference being slightly more dispersion of exit locations on the top surface with 10 particles compared to 1 particle, but centred on the same locations as for the 1 particle case.

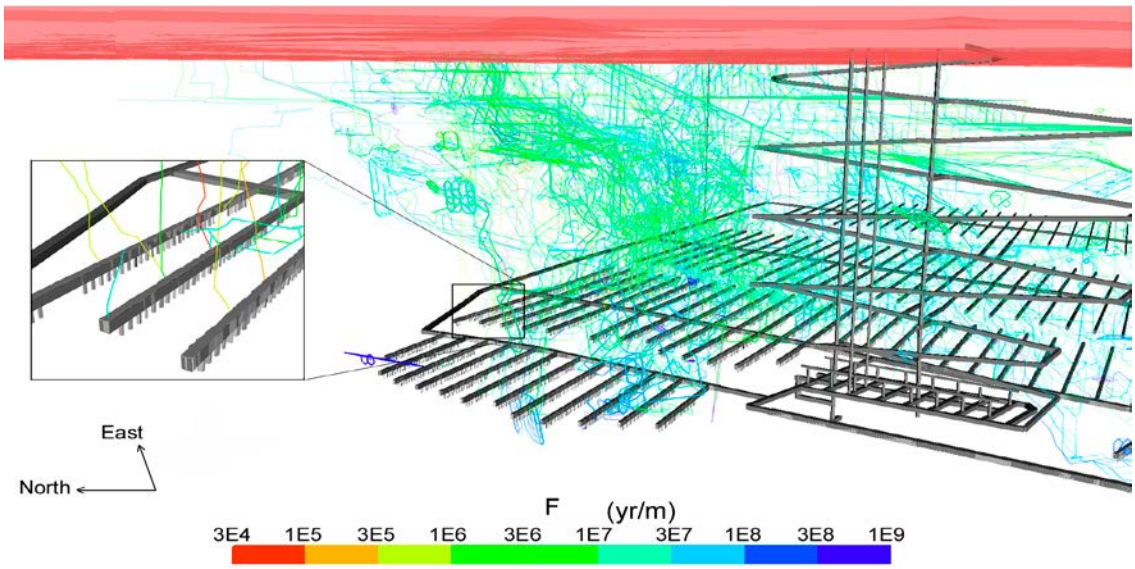

Figure 7-3. *Examples of stochastic pathways for particles released from 6916 deposition holes used in the SR-Site safety assessment calculations, coloured by flow-related transport resistance for the total path. The ground surface is coloured pink, and the repository structures are shown in grey. The fractures are not displayed in this figure. (A visualisation of pathways generated in Joyce et al. 2010a.)*

When carrying out particle tracking calculations not all released particles successfully reach the top surface of the model. Some are discarded before they start, either because there is not a water conducting fracture connecting to the deposition hole to start in or because the initial flow is below a numerical threshold. Some particles fail to reach the model boundary because of numerical issues, such as local mass balance problems in stagnant areas, and some exit from the sides or bottom of the model.

7.4 Recognised uncertainties and how they were quantified by modelling

For the hydrogeological modelling performed to support SR-Site (Selroos and Follin 2010) a set of reference results and performance measures were calculated using the so-called "hydrogeological base case", which is essentially a numerical implementation of the current understanding of the system based on the available data and the conceptual understanding of the site (Follin 2008). As with all models, this understanding is based on incomplete data and a number of simplifying assumptions, leading to a set of uncertainties about the system. In order to understand the impact of the recognised uncertainties on the performance measures, a series of model variants were used to assess the sensitivity of the results to following four categories of uncertainty. The actual model variants used to explore each of these categories of uncertainties from the safety assessment studies for the temperate period at Forsmark (Joyce et al. 2010a) and Laxemar (Joyce et al. 2010b).

1. Uncertainty due to spatial variability is examined by determining the variation in outcomes due to differences in fracture geometries and properties between different stochastic realizations of the bedrock fractures.
   a. The effect of stochastically varying the hydraulic discrete fracture network by generating multiple realisation of the fracture locations and their properties as well as sampling spatial variability within each deformation zone (Forsmark and Laxemar).
   b. Extended spatial variability. In the base model, the volume outside the repository site area the rock is modelled as a CPM with homogeneous and isotropic properties for each depth zone. Limited additional data from the ongoing investigations at SFR (Öhman and Follin 2010) allowed for a tentative parameterisation of a DFN in this area (Forsmark).
2. Uncertainties in the interpretation of the fracture data and the parameterization of the DFN are examined using models with alternative assumptions or parameterizations of the DFN and scoping the variation in outcomes.
   a. Alternative DFN size-transmissivity relationships (Forsmark).
   b. Inclusion of additional possible deformation zones (Forsmark).
   c. The effect of excluding minor deformation zones (Laxemar).
   d. Using an unmodified (compared to the initial Hydro-DFN) vertical hydraulic conductivity (Forsmark).
   e. The effect of an alternative methodology for deriving the Hydro-DFN model for Laxemar – the Elaborated Hydro-DFN (see Section 4.1.1).
   f. Using a stochastic continuum approach, rather than a DFN approach. The statistical properties of the hydraulic conductivities in the HRDs of this variant are derived from 20 m and 100 m PSS measurements (Laxemar).
   g. Alternative model for transport aperture (Forsmark).
3. Uncertainties in the properties of the engineered structures and their future evolution are examined using models with alternative properties for these structures and determining the impact on outcomes.
   a. Tunnel variants including cases with a crown space included, and other variants which consider changes to the assumed EDZ transmissivity (Forsmark).
   b. Effect of boreholes. Future human intrusion may lead to the creation of boreholes that could intersect the repository volume. These boreholes could provide additional flow-pathways for particles (Forsmark).
4. Uncertainties in future hydrogeological conditions
   a. Consideration of glacial conditions (Forsmark).

7.5 Results & sensitivities

Some of the key results and observations derived from the hydrogeological modelling to support repository performance assessment are summarised below. Important statistics estimated from the modelling are the equivalent fluxes (sum of flow-rates per unit length in fractures intersecting the deposition hole divide by the canister height) at the release points, U_r, and the flow-related transport resistance, F_r. The high U_r part of the distribution has implications for potential buffer erosion and subsequent corrosion of deposition canisters. The low F_r part of the distribution is of most concern regarding the transport of radionuclides from the repository to the surface or the penetration of dilute water from the surface to the repository potentially affecting reducing conditions around the deposition holes.

The distributions of the performance measures, U_r and F_r, calculated for SR-Site (Forsmark) (Joyce et al. 2010a) are reproduced in Figure 7-4 and Figure 7-5 comparing results for the hydrogeological base case (Hydro base case, r0, semi-correlated) and some of the model variants to scope the sensitivity to uncertainty described above. In Figure 7-4 it shows that the high-end initial flux distribution is slightly sensitive to stochastic realisation and moderate sensitivity to the relationship between size and transmissivity with a correlated relationship having the highest high-end values and uncorrelated the highest median. Figure 7-5 shows there is moderate sensitivity of flow-related transport resistance to each of the uncertainties considered with low-end values (i.e. less retardation) for some realisations, correlated size-transmissivity and EDZ and the formation of a crown space in the tunnels. The plots are referred to as "normalised" correspond to ensemble plots over those deposition holes for which the entity plotted is non-zero. There are for example, deposition holes that are not intersected by a connected fracture, and hence no particles could be tracked from these locations.

The distributions of the performance measures, U_r and F_r, calculated for calculations to support a safety evaluation of Laxemar (Joyce et al. 2010b) are reproduced in Figure 7-6 and Figure 7-7 comparing results between the DFN model derived in the SDM and the Elaborated Hydro-DFN and with results for an alternative model based on a stochastic continuum approach. There is little sensitivity to realisation, but the re-interpretation of the Hydro-DFN for the Elaborated Hydro-DFN (see Section 4.1.1) improves performance measures by a factor of 2-3. Initial flux and flow-related transport resistance are both affected by a factor of around 5 (lower flux and high F_r) when a stochastic continuum model is used instead of a Hydro-DFN, although for a DFN there are deposition holes with no flow (or below the PFL-f detection limit).

Deposition holes will be rejected if intersected by large fractures. While awaiting results from the on-going programme for detailed investigations, SKB made use of a proxy for large fractures; the so called FPCI (Full perimeter criterion). From this proxy, two rejection criteria (see Figure 7-8) were defined for SR-Site (Munier 2010):

1) Full perimeter criteria (FPC) – a deposition hole is excluded if it is intersected by the hypothetical extension of a fracture that intersects the full perimeter of the corresponding deposition tunnel.
2) Extended full perimeter criteria (EFPC) – a deposition hole is excluded if its full perimeter is intersected by a fracture that also intersects the full perimeter of four or more neighbouring deposition holes in the same deposition tunnel.

For the hydrogeological modelling, an algorithm for analysing the deposition holes according to the FPC and EFPC was used to indicate deposition holes that may be excluded due to these criteria (it should be noted than the criterion used in hydrogeology consider the whole deposition hole height, not just the canister height, as considered elsewhere in SR-Site). The models were then used to estimate how many deposition holes might be excluded, and how the distributions of repository performance measures would change as a result. The predictions of the models (see Figure 7-9) suggest that using these criteria could reduce the incidence of the higher values of equivalent flux at the release point, but had limited affect on the flow-related transport resistance distribution.

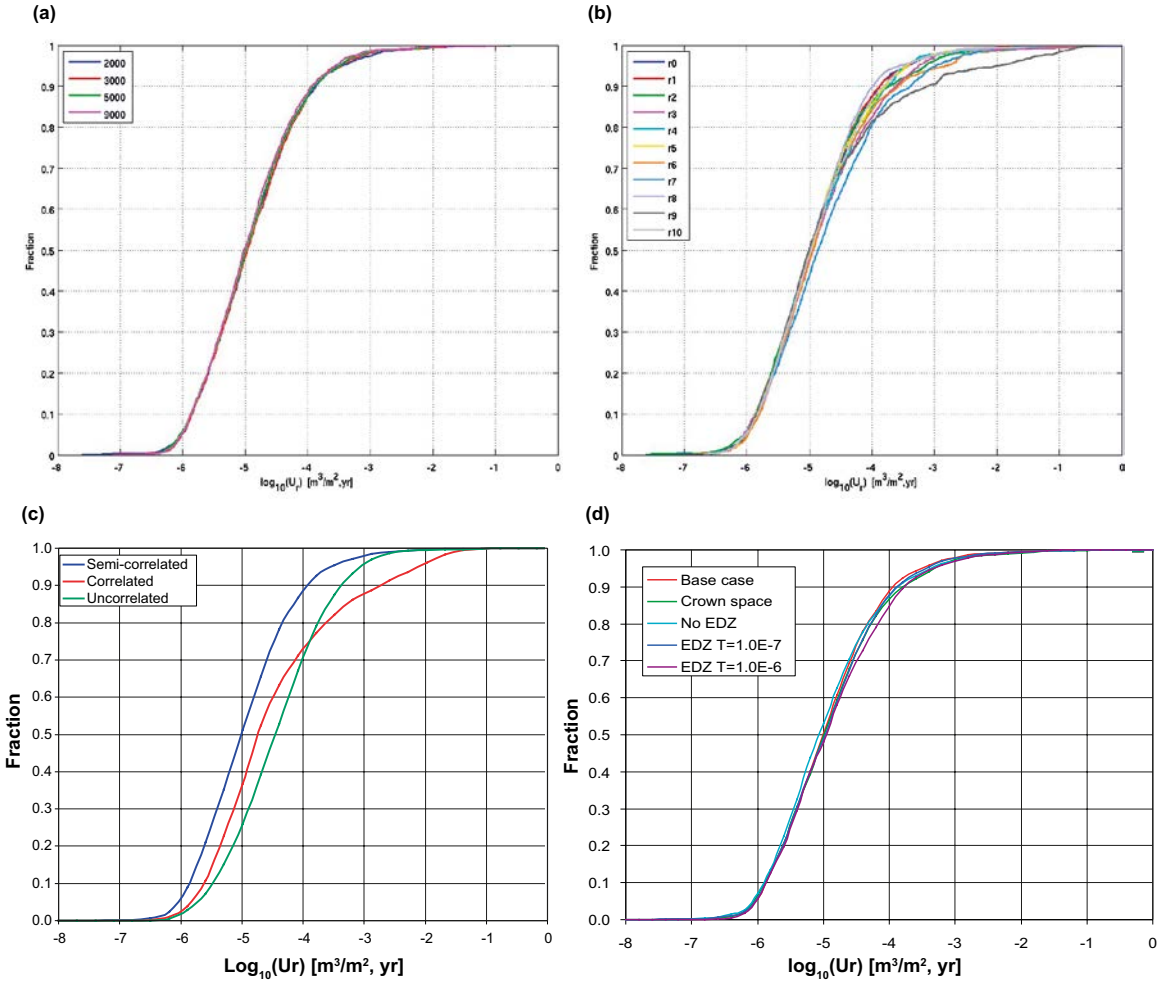

Figure 7-4. *Normalised CDF plots of the equivalent initial flux, U_r, from SR-Site (Forsmark), where variations in particle release time, stochastic realisation, size-transmissivity model and tunnel representation are considered for the release from fracture adjacent to a deposition hole (Q1). (a) The hydrogeological base case for different release times. (b) The hydrogeological base case (r0) and 10 stochastic realisations of the HCD and HRD (r1 to r10), for particles released at 2000 AD. (c) Realisation r0 of the correlated and uncorrelated size-transmissivity relationships compared to the hydrogeological base case (semi-correlated) for particles released at 2000 AD. (d) The hydrogeological base case model, the crown space case, the EDZ $T = 1{\cdot}10^{-7}$ m^2/s case, the EDZ $T = 1{\cdot}10^{-6}$ m^2/s case and the no EDZ case for the particles released at 2000 AD.). (After Joyce et al. 2010a, Figures 6-8, 6-17, 6-28, 6-36.)*

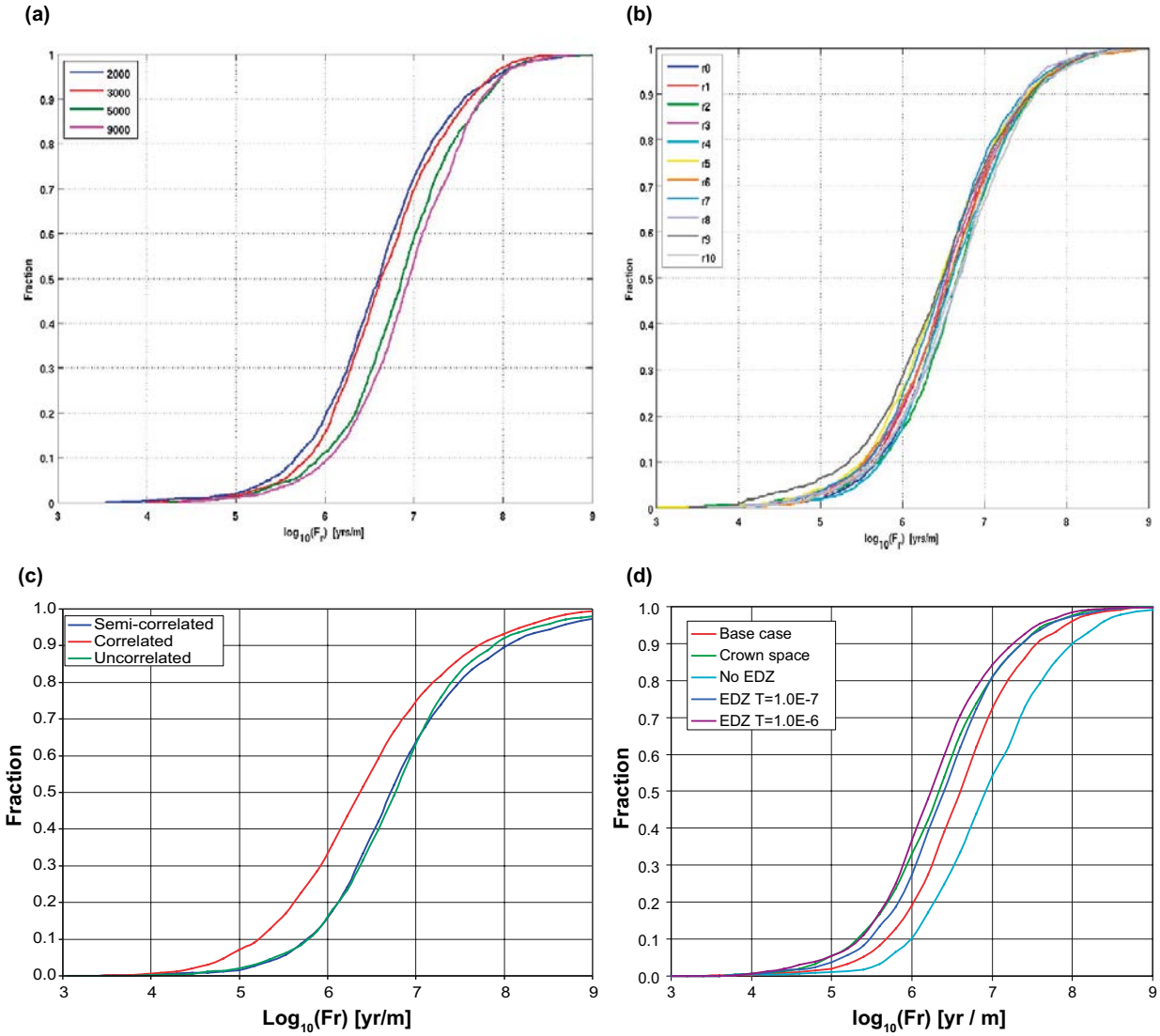

Figure 7-5. *Normalised CDF plots of the flow-related transport resistance, F_r, from SR-Site (Forsmark), where variations in particle release time, stochastic realisation, size-transmissivity model and tunnel representation are considered are considered for the release from fracture adjacent to a deposition hole (Q1). (a) The hydrogeological base case. Particles successfully reaching the model top boundary (24%), released at 2000 AD, 3000 AD, 5000 AD and 9000 AD. (b) The hydrogeological base case model (r0) and 10 stochastic realisations of the HCD and HRD (r1 to r10) for particles successfully reaching the model top boundary (24%–27%), released at 2000 AD. (c) Realisation r0 of the correlated and uncorrelated size-transmissivity relationships compared to the hydrogeological base case (semi-correlated) for particles successfully reaching the model top boundary (24% semi-correlated, 32% correlated, 27% uncorrelated), released at 2000 AD. (d) The hydrogeological base case model, the crown space case, the EDZ T = $1 \cdot 10^{-7}$ m^2/s case, the EDZ T = $1 \cdot 10^{-6}$ m^2/s case and the no EDZ case for the particles successfully reaching the model top boundary, released at 2000 AD. (14% no EDZ, 23%–24% others). (After Joyce et al. 2010a, Figures 6-9, 6-17, 6-28, 6-36.)*

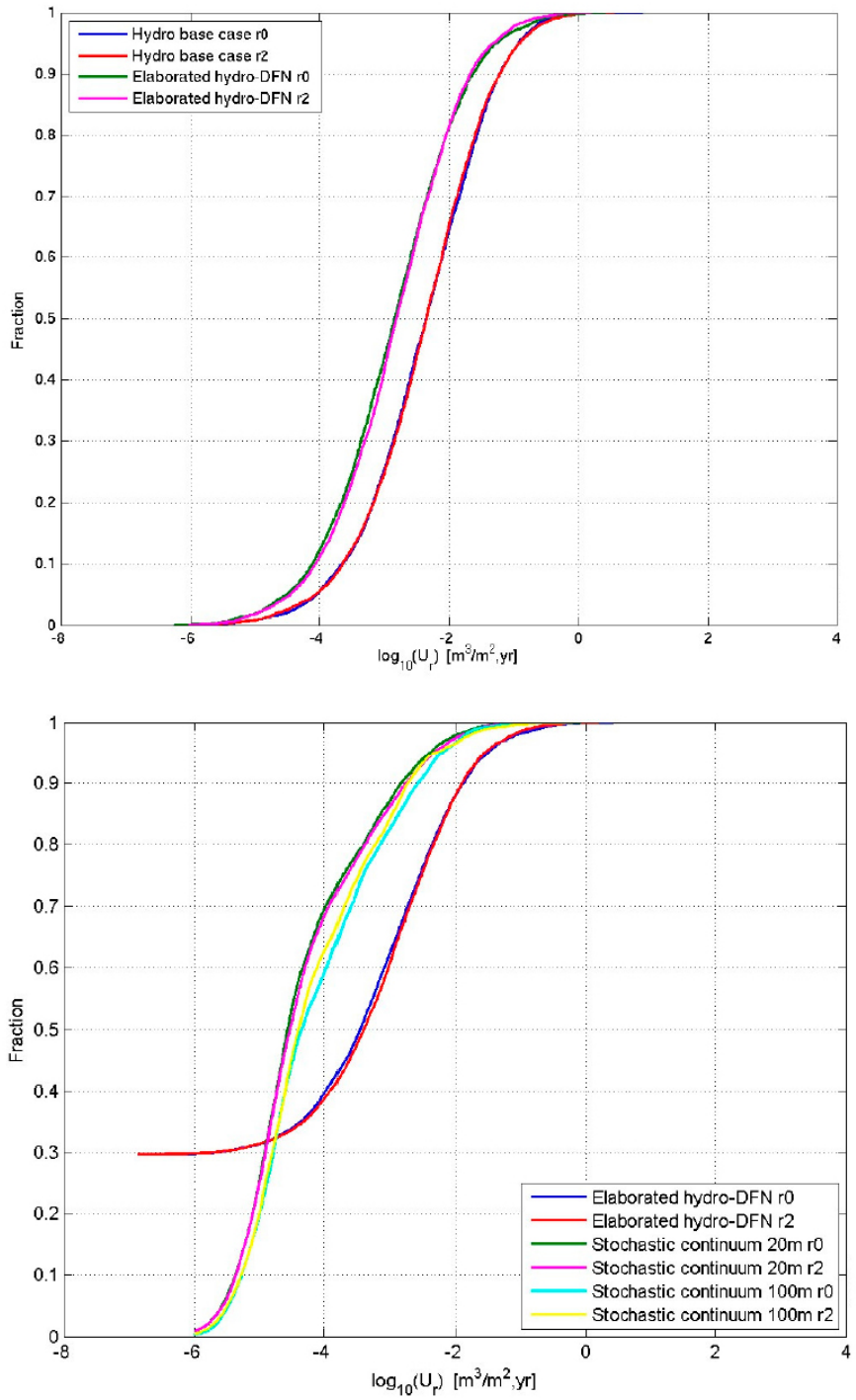

Figure 7-6. *CDF plots of the equivalent flux at the release point, U_r, at Laxemar (Joyce et al. 2010b), where variations in the Hydro-DFN model are considered for the release from fracture adjacent to a deposition hole (Q1). (Top) Normalised CDF plots of U_r in the hydrogeological base case model and the Elaborated Hydro-DFN model, including one additional realisation of each, for the particles successfully reaching the model top boundary (60%-69%) released at 2000 AD. (Bottom) Non-normalised CDF plots of U_r in a comparison of two realisations of the Elaborated Hydro-DFN model and the Stochastic continuum models on 20 m and 100 m scales for particles released at 2000 AD. (After Joyce et al. 2010b, Figures 6-26, 6-39.)*

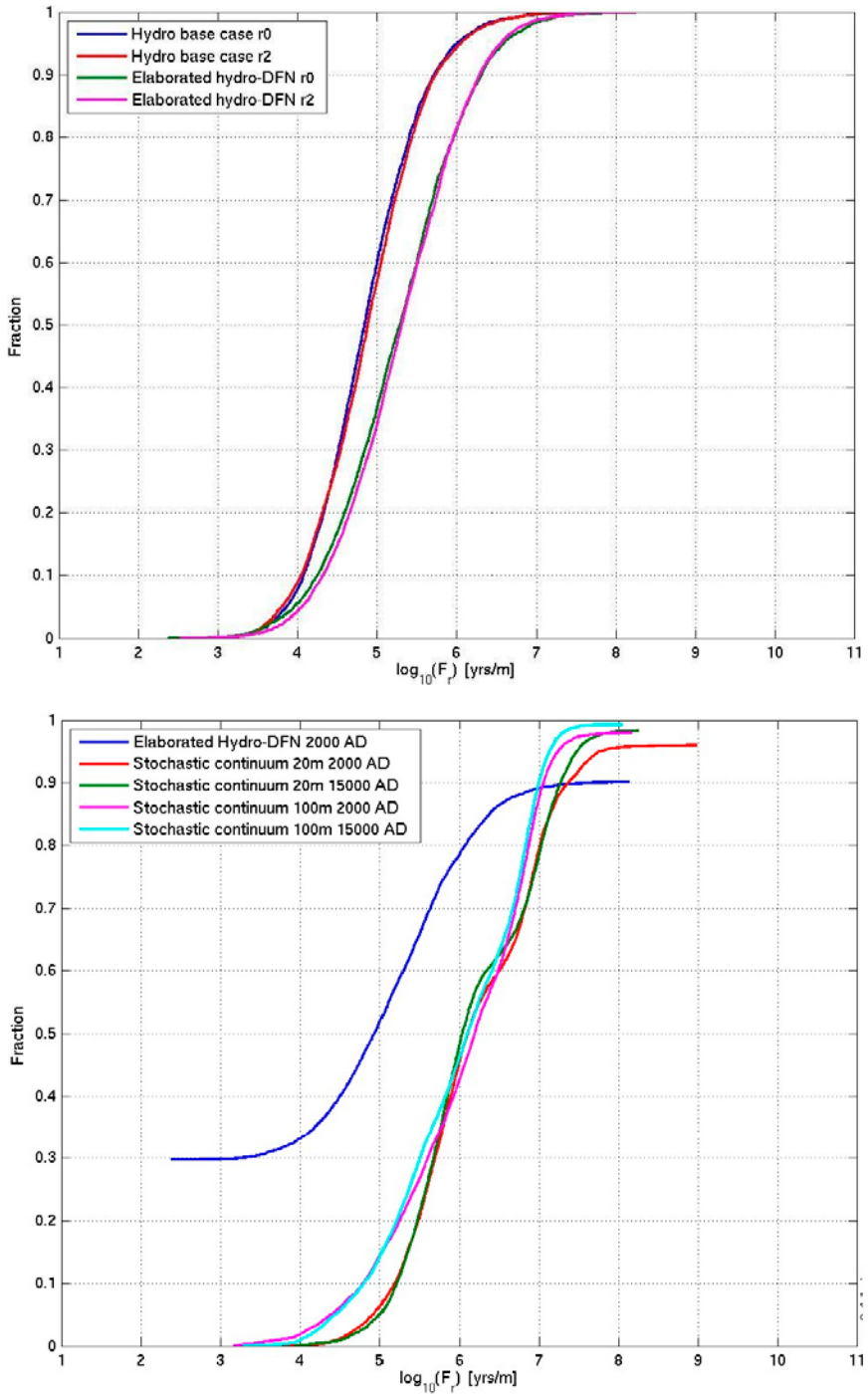

Figure 7-7. *CDF plots of the flow-related transport resistance, F_r, at Laxemar (Joyce et al. 2010b), where variations in the Hydro-DFN model are considered for the release from fracture adjacent to a deposition hole (Q1). (Top) Normalised CDF plots of F_r in the hydrogeological base case model and the Elaborated Hydro-DFN model, including one additional realisation of each, for the particles successfully reaching the model top boundary (60%-69%) released at 2000 AD. (Bottom) Non-normalised CDF plots of F_r in a comparison of two realisations of the Elaborated Hydro-DFN model and the Stochastic continuum models on 20 m and 100 m scales for particles released at 2000 AD. (After Joyce et al. 2010b, Figures 6-27, 6-39.)*

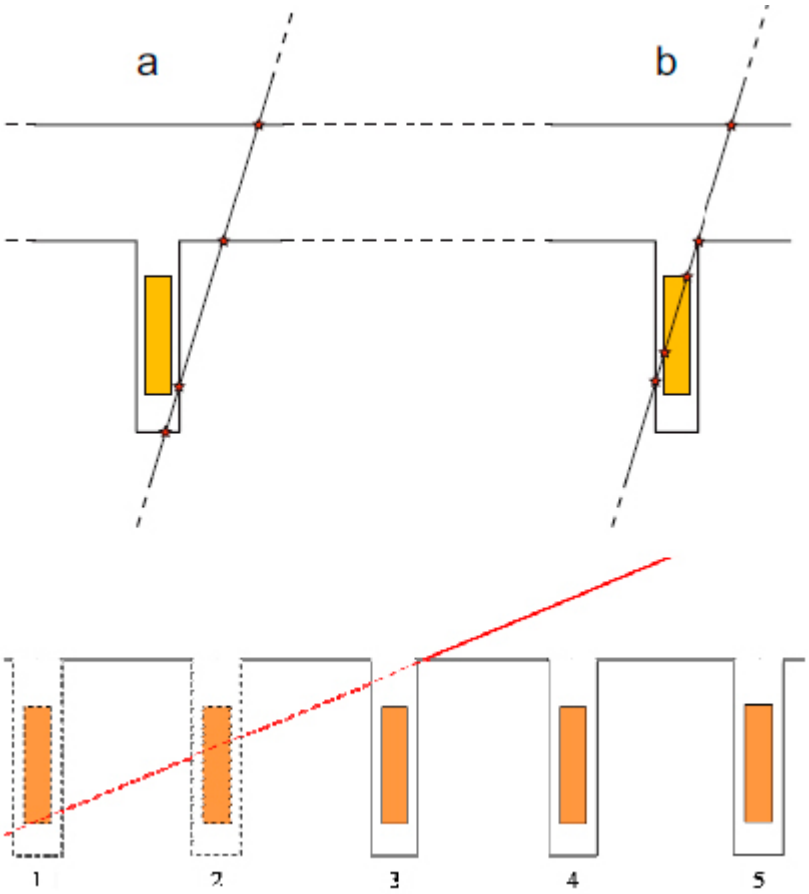

Figure 7-8. *The two rejection criteria defined for SR-Site (Munier 2010). (Top) The FPC criterion for a fracture that intersects the full tunnel perimeter and deposition hole below – the hydrogeological modelling considered an intersection with the any part of the whole deposition hole, while the rest of the SR-Site analysis considered only the part adjacent to the canister. (Bottom) The EFPC criterion based on an intersection with full tunnel perimeter and four or more deposition holes. (After Munier 2010, Figure 3-1, and SKB 2011, Figure 5-4.)*

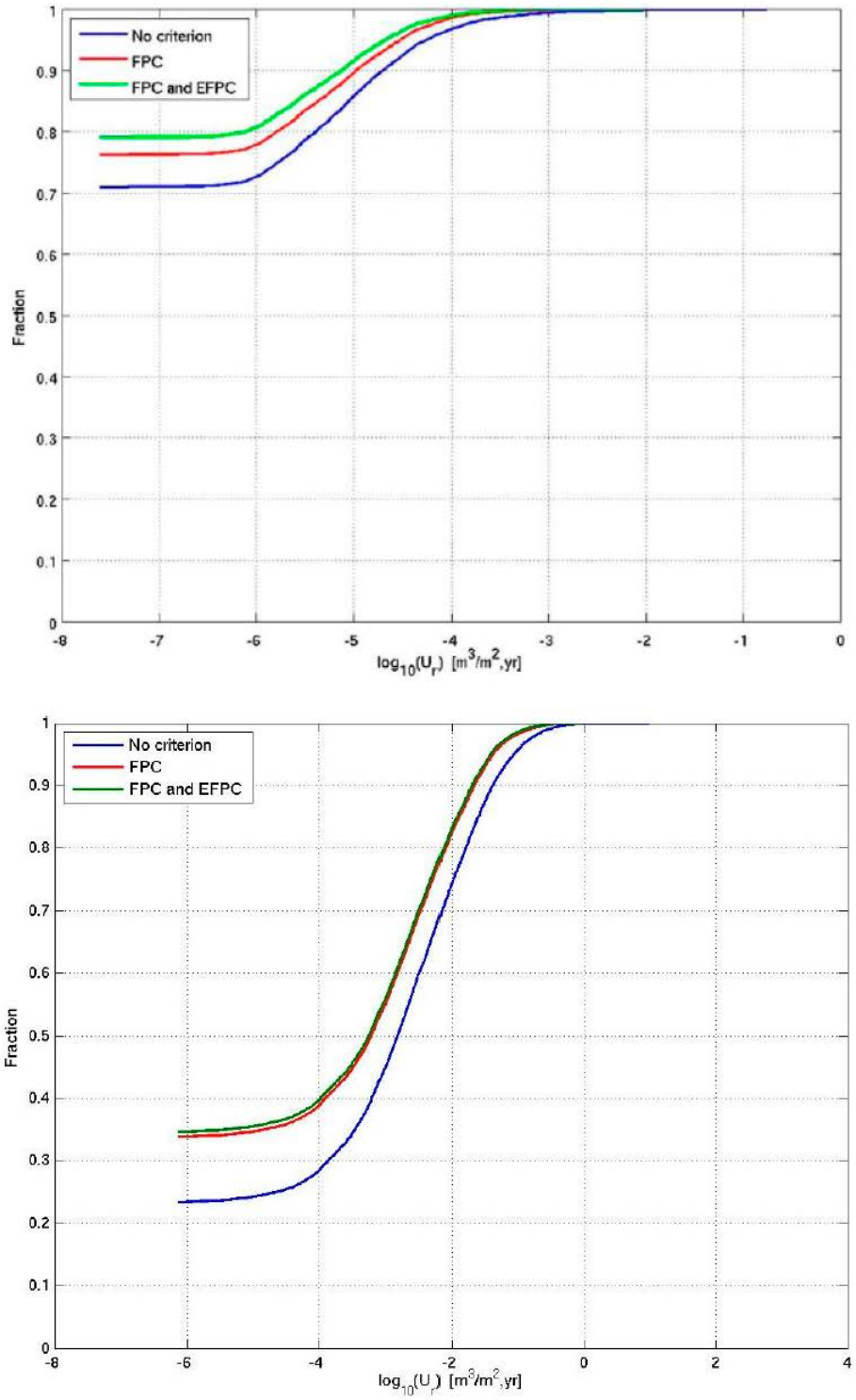

Figure 7-9. *Non-normalised (i.e. the fraction of deposition holes not intersected by a flowing fracture are plotted as a vertical offset of the plot) CDF plots of U_r in the hydrogeological base case models for particles released at 2000 AD, according to the application of FPC and EFPC criteria for Forsmark (top) and Laxemar (bottom). (After Joyce et al. 2010a, Figure 6-15, and Joyce et al. 2010b, Figure 6-22.)*

7.6 Sensitivities to flow channelling within fractures

In Section 3.3.8, flow channelling phenomena within fractures were considered to potentially influence the validity of the DFN modelling by:

(1) Biasing the observed measurements of flow-conducting fractures (a Type 1 flow censoring effect).

(2) If hydraulic testing successfully detects the nearby presence of a flow conduit, the borehole is unlikely to intersect it directly and therefore the transmissivity of the structure may be underestimated (a Type 2 flow censoring effect).

(3) Even assuming the above points are not significant, it is possible that the Hydro-DFN model predictions of distributions related to the safety assessment, such as advective travel time, flow-related transport resistance, and equivalent flux at the release point might still be biased by neglecting in-plane heterogeneity or fracture intersection zones.

Points 1 and 2 were discussed in Section 3.3.8. In this section the modelling work to address point (3) is reviewed. Modelling simulations were undertaken to scope the influence of both in-plane heterogeneity in transmissivity within a fracture (Painter 2006) and the effect of enhanced transmissivity at the intersections between fractures (Crawford 2008).

Simulations of the transport effects of flow channelling in variable aperture fractures sometimes consider a single fracture isolated from any wider network. Although these studies yield insights into the process, the unrealistic boundary conditions for flow limit the usefulness of the results for larger-scale applications. This is because flow in an individual fracture is controlled not only by the aperture variability, but also by the boundary conditions that are determined by connections with other fractures in the network. This limited connection to other fractures introduces a certain degree of flow channelling independent of that caused by aperture variability. The relative importance of the two channelling mechanisms – heterogeneity-induced or geometry-induced – cannot be investigated without considering heterogeneous fractures embedded in a three-dimensional network.

Painter (2006) addresses the importance of internal variability of the in-plane fracture aperture in determining field-scale transport in fractured rock. The internal fracture aperture variability assumed was empirical (due to lack of field data) and based on a multi-gaussian model for aperture variability. Under such assumptions, the study concluded based on numerical simulations that internal transmissivity variability can decrease the flow-related transport resistance, but only when the internal variability equals or exceeds the fracture to fracture variability, and that the decrease in flow-related transport resistance caused by internal variability is modest. At the leading edge of the distribution, internal variability reduced the flow-related transport resistance by approximately 50%. The reduction was found to be smaller (c. 15%) in the centre of the distribution.

Crawford (2008) performed scoping calculations based upon solution of the Navier-Stokes equations for flow to indicate that enhanced transmissivity at zones where fractures intersect should not contribute significantly to flow channelling phenomena in the rock at Forsmark. The impact of highly conductive fracture intersection zones was demonstrated using the Hydro-DFN model for FFM01/FFM06 (below –400 m) (Follin et al. 2007a) and assumed fracture traces with negligible flow resistance. Simulations were used to show that even if highly conductive features associated with fracture intersection zones comprise up to 50% of the typical flow-paths in the HRD, they should not have a significant effect on the flow-related transport resistance for the transport of solutes.

8 Possible areas of research and development in the future

8.1 The requirement for further development

The programme of work which involved the development of Hydro-DFN models of the crystalline bedrock at Laxemar and Forsmark reached a milestone in 2009 with the selection of Forsmark as the proposed location of the final repository for spent nuclear fuel. In 2011 the SR-Site report (SKB 2011) describing the safety assessment for the proposed repository was submitted to the regulatory authorities as part of the license application to begin construction of a repository. It is proposed that the Hydro-DFN methodology continue to be developed whilst the license application is assessed.

The regulatory authority, SSM, is responsible for the oversight of SKB's programme related to the engineering and implementation of the repository to meet operational and post-closure safety requirements. In order to help them with this work, an independent team of earth scientists, called the "INSITE" (INdependent Site Investigation Tracking and Evaluation) group, were employed to review the SKB investigations continuously, and in detail, and provide SSM with advice for the Site Investigations phase. Their report (Chapman et al. 2010) includes criticism of some aspects of the Hydro-DFN methodology, particularly with respect to how uncertainty and alternative conceptual model concepts were considered. SKB responded with suggestions for future developments to address these concerns in their report describing their programme for research, development and demonstration (RD&D) in 2010 (SKB 2010b). These reports provide motivation for some of the suggestions in this section.

The proposed developments might be categorised as having the following aims:

1) To integrate both geological and hydrogeological aspects of the DFN model so as to produce a single description of the fracture network, sufficiently parameterised to fulfil all aspects of safety assessment.
2) To ensure that the description of the bedrock at Forsmark, and the quantification of uncertainties, are as comprehensive as possible given the presently available data and DFN methodology, prior to the start of any repository construction and underground investigations.
3) To estimate the effect of further recognised uncertainties as listed in Section 4.7 that have has yet not be quantified by DFN models.
4) To develop a systematic approach to comparing different model variants in terms of their predictions of quantities which might be measured during underground construction and their predictions of statistics used for the repository safety assessment.
5) To understand how additional data and different types of data from any underground investigations should be used to validate the DFN models or allow the development of new DFN models by further reducing conceptual and other uncertainties, and the implications for the safety assessment that such exercises might reveal.
6) To develop the framework necessary to create local-scale DFN models conditioned to match observations at particular deposition locations.

Points (1), (2), (3) and (4) should be considered independent of how the proposed repository might be constructed. However, the processes described in points (5) and (6) depend on the specific details of underground data collection, repository construction and monitoring. In particular, at the time of writing, it is not clear what data will be collected during the construction of the repository, or how data freezes and model development will be managed. The suggestions made with respect to (5) and (6) should therefore be interpreted as contingent on these details being finalised. Suggested tasks which would address each of these points are described below.

8.2 Review of the hydrogeological DFN models of Forsmark

It is proposed that a review of the DFN models of Forsmark be undertaken in order to assess if they have made sufficient use of the available information from the relevant disciplines (geology, hydrogeology, hydrochemistry and rock mechanics) to fulfil all aspects of safety assessment. The Hydro-DFN model of Forsmark described in SR-Site was developed by 2007 (Follin et al. 2007b, a) in parallel. It is worthwhile to consider if additional understanding, models or information developed by other disciplines in a parallel could provide additional input to the hydrogeological understanding and modelling, particularly as it provides a forum for the integration of other disciplines and 3D numerical models, for example. Such a review would allow these issues to be considered, and if necessary new models developed, as described in subsequent sections, to provide an updated description of the site prior to underground investigations beginning. The following topics could be considered in such a review.

The Hydro-DFN was developed by pooling the data obtained from several boreholes. This was required to create a database at Forsmark due to the scarcity of data. At Laxemar, pooling was needed to homogenise the significant spatial variability. The locations of boreholes used to derive the Hydro-DFN and the resulting density of data should be reviewed in light of the proposed location of the repository. This would allow assessment of the uncertainties in applying the predictions of the Hydro-DFN to this volume. Any long-term monitoring data which becomes available at the Forsmark site, such as groundwater levels, should be incorporated into the data sets used for either model calibration or further confirmatory tests.

Use of data acquired recently during the SFR programmes (Öhman and Follin 2010) should be considered. A check should be made that the data measured as part of this programme is consistent with the understanding of the site developed in SDM-Forsmark. It might be possible to update or elaborate the Hydro-DFN models for the area affected, and certainly the disturbance to the hydraulic system around Forsmark caused by SFR provides an additional confirmatory test. Hydrochemical data gathered from the investigation for the extension of the SFR facility could also provide a means to confirm the regional setting for groundwater evolution simulated by the Forsmark regional-model.

If alternative Hydro-DFN models are developed for the Forsmark site (as discussed in Section 8.3), it will be necessary to devise a systematic methodology to compare any different model variants in terms of their predictions of quantities used in repository safety assessment. This model comparison might involve a standardised model domain and set of boundary conditions used to predict distributions of: equivalent continuous porous medium permeability; percolation fractions; flow-related transport resistance; other performance measures such as equivalent flux at the release point, equivalent flow-rate at the release point and flow-related transport resistance.

8.3 Alternative models and conceptual uncertainty

8.3.1 Alternative intensity-size-transmissivity distributions

For the Forsmark Hydro-DFN, only one intensity-size distribution model was considered, i.e. the Pareto (power-law) distribution. Subsequent development of the modelling methodology, as applied to the Laxemar (Joyce et al. 2010b) and Olkiluoto (Hartley et al. 2011) sites, has suggested that different assumptions for the size intensity distribution compared to those used at Forsmark are capable of reproducing the inflow statistics derived through borehole flow logging with equal accuracy, e.g. the log-normal distribution. The possibility of alternative intensity-size-transmissivity distributions is therefore thought to be an area of the Forsmark SDM where these types of uncertainties have not been addressed as fully as they now could be.

As well as addressing conceptual uncertainties, such alternative intensity-size-transmissivity distributions potentially allow closer integration with the Geo-DFN, by using certain Geo-DFN parameters explicitly within the Hydro-DFN models. Furthermore, alternative intensity-size-transmissivity distributions could be developed specifically to understand other uncertainties such as in-plane fracture heterogeneity or the potential impact of fractures flow-conducting below the PFL-f detection limit, see e.g. the work made for Posiva at the Olkiluoto site (Hartley et al. 2011).

Previously we have assumed that potentially flow-conducting fractures could be equated with open and partly open fractures, but generalisation allows us to consider different types of model. For example, we might assume that the flow-conducting fractures detected by the PFL-f method in fact equate to the majority of PFL fractures, which is a clear lower limit for the intensity of potential flow-conducting fractures ($P_{10,all} \geq P_{10,open} \geq P_{10,cof} \geq P_{10,PFL}$). This was tested for DFN modelling Olkiluoto (Hartley et al. 2011) applying a log-normal distribution of the size of open fractures and adjusting the mean and variance to obtain sufficient connectivity while remaining consistent with the power-law size distribution used in the Geo-DFN for the super-set of all fractures. At the other extreme, an upper limit is to assume all fractures are potentially flow-conducting fractures, but restrict the fraction of area available for flow (again this concept was tested in Hartley et al. (2011)).

Each conception of the definition of potentially flow-conducting fractures must be paired with a corresponding conception of flow-conducting fractures. Clearly the intensity of PFL-f fractures is a lower bound on the intensity of flow-conducting features, but if the detection limit of the system was lower, a higher intensity of flow-conducting features might be inferred. A plausible upper bound on the intensity of flow-conducting fractures is the intensity of all fractures.

The intensity of potentially flow-conducting fractures combined with the intensity of flow-conducting fractures could then be used within a geometric simulation of fracture connectivity to calibrate the parameters for the intensity-size model. The intensity of potentially flow-conducting fractures is further constrained to be less than or equal to the intensity of all fractures, as determined by the Geo-DFN. In the modelling used in the SDM, a power-law size intensity distribution has been assumed. Alternative models might assume different size intensity distributions, such as the log-normal fracture size distribution (Munier 2004). The suitability of a log-normal distribution for connected open fractures in sparsely fracture rock is suggested by Figure 4-16 and Figure 4-17, for example. This distribution, measured in terms of fracture radius r, is based on the mean m and standard deviation s of the common logarithm ($\log_{10}$) of r. The distribution $f(r)$ is only defined within the truncated range between r_{min} and r_{max}.

$$f(r) = \frac{1}{r \ln(10) s (2\pi)^{1/2}} \exp\left(\frac{-(\log r - m)^2}{2s^2} \right) \qquad (8\text{-}1)$$

where $r_{max} \geq r \geq r_{min}$; $s \geq 0$. Using a log-normal distribution for flowing fractures requires that the majority of modelled fractures need to be connected to give the correct intensity of flowing fractures at boreholes. Therefore, all generated fractures need to be relatively large fractures requiring a log-normal with mean and spread chosen to ensure most fractures are connected, but remaining consistent with the observed intensity of lineaments and deformation zones. The fracture transmissivity model would be calibrated by matching simulation predictions to the measured distributions of specific capacity once the intensity-size distribution has been established (see the Case B model used in Hartley et al. (2011)).

An intensity-size model could be developed to mimic one form of in-plane heterogeneity within fractures. For example, the prescription for such a model might start with simulating the intensity and size of all fractures, but then restrict the openings on these fractures to only occupy a sub-area of each fracture according to some size dependent probability function. A power-law size model might be appropriate based on the Geo-DFN tectonic continuum. The parameters determining the amount of fracture area that is hydraulically open for a given fracture size could then be adjusted to give sufficient connectivity for consistency with the intensity of PFL features, or some other calibration target as appropriate. Such a model was used to model the Olkiluoto site in Hartley et al. (2011) (where this model variant was referred to as 'Case C').

One aspect of uncertainty that alternative intensity-size-transmissivity distributions could assess is the potential influence of flow-conducting fractures with inflow-rates below the PFL-f method's detection limit. PFL-f testing in pilot holes drilled ahead of the ONKALO access tunnels at Olkiluoto performed with much lower drawdowns (c 100-400 m) have provided an indication that the intensity of detected PFL-f fractures can be 2-3 times higher under such conditions, essentially due to a lowering of the detection limit on specific capacity to less than 10^{-10} m^2/s (see Hartley et al. 2011, Chapter 10). At both Forsmark and Laxemar, the observed intensity of open fractures recorded in core-drilled boreholes is much larger (even when restricted to certain and probable classifications) than the observed intensity of fractures carrying flow above the detection limit of the PFL-f method.

The reasons that a hydraulically open part of a fracture might not carry flow above the PFL-f method detection (see Follin et al. 2011) include that:

- It is not connected to the percolating network, and so can not carry flow.
- It has such low transmissivity that it can not carry flow above the detection limit of the PFL-f method.
- Although the intersecting fracture itself might be highly transmissive locally, the percolating network that it is connected to has an effective transmissivity that is so low that it can not supply the intersecting fracture with enough groundwater to allow an inflow above the detection limit of the FPL-f method.

Each option above describes a constraint on groundwater flow, or flow bottleneck. The first option describes a constraint based on fracture network connectivity; the last two options describe different types of transmissivity bottlenecks. For any individual hydraulically open fracture intersecting with a borehole which does not result in a detectable inflow, it is not practically possible to decide which of the three options above is the correct description of the processes involved.

The conceptual models of Forsmark and Laxemar consider constraints of flow to be caused predominately by connectivity issues. This conceptual model is implemented by equating the intensity of connected open fractures simulated, with the intensity of PFL-f fractures measured, that is, by equating the measured intensity of PFL-f fractures with a quantity simulated by purely geometrical specifications. As discussed in Section 3.3.8, it is thought that this is a suitable approach since the connectivity of openings is probably the major control on the hydraulic system. However, the distribution of transmissivity can also cause hydraulic chokes (see Öhman and Follin 2010) having a strong control on the apparent flow characteristics of a network as mean transmissivity approaches the PFL detection limit. This is particularly apparent at depth where measurements of flowing fracture intensity become sensitive to the PFL detection limit (Hartley et al. 2011) due in part to an increased in vertical stress (Mattila and Tammisto 2012). It may therefore be suitable to considered alternative assumptions about fracture intensity-size-transmissivity that consider the hydraulic choking effect as well as geometrical percolation, and quantify the implications for safety assessment. If such alternative models are calibrated to the same existing hydraulic data, they should display similar characteristics as observed for the apparent network above the PFL detection limit and the Hydro-DFN model developed for SDM-Site. However, they will display more connectivity at low flow magnitudes which could have some implications for safety assessment, such as the number of deposition holes connected to a flowing fracture and resaturation of the buffer.

As part of the underground investigation stage it will be possible to test such concepts against PFL-f tests performed using a lower effective detection limit from the access tunnel, for example by using a higher drawdown (see Section 8.5), then it should be possible address some of the uncertainties associated with the detection limit and the significance of small flows at repository depth. However, such measurements will be made under conditions in which the hydraulic system and stress field are disturbed, and so the possible effects of these will need to be considered.

8.3.2 Treatment of in-plane heterogeneity and flow channelling

It is generally thought that flow in crystalline rock is heterogeneously distributed within fractures, and is concentrated along preferential flow-paths within fractures and deformation zones. Within the hydrogeological DFN modelling for SDM-Site, fractures have been represented as planar structures, with constant transmissivity within a fracture. This description reasons that flow at the scales of interest can be adequately represented by the assignment of an effective transmissivity value for a single fracture. This approach is used because flow channelling can not be adequately quantified from surface investigations, and models of flow within fractures would therefore be highly speculative. The potential bias introduced to the predictions of the models due to the absence of flow channelling within factures has been assessed, as described in Sections 3.3.8 and 7.6.

Painter (2006) addressed the importance of internal variability of the in-plane fracture aperture in determining field-scale transport in fractured rock. The work undertaken by Painter (2006) was based on a synthetic fracture network model which does not represent the bedrock at Forsmark. Its use to justify the limited influence of in-plane fracture heterogeneity on repository performance statistics at Forsmark might be criticised for this reason.

Crawford (2008) performed scoping calculations based upon solution of the Navier-Stokes equations for flow in crossing or terminating fracture intersections to indicate that fracture intersection zones should not contribute significantly to flow channelling phenomena. The work undertaken by Crawford (2008) was based on the Forsmark SDM Hydro-DFN, but the model was not re-calibrated to maintain an accurate representation of the measured inflows PFL tests as it was altered for each of the variant calculations. There may be some bias introduced by the assumptions made therefore that have not been constrained by available data.

Conceptual models for internal fracture variability/fracture textures need to be studied and evaluated, as the internal flow structure of fractures is generally unknown. This is an area for basic research. It might involve considering how concepts for internal fracture variability might be linked to relevant field data, e.g. use of aperture roughness information from SKB's or other similar sites. Such concepts for in-plane heterogeneity and fracture intersection zones could be investigated in the context of the models of the Forsmark site which are calibrated to the flow logging data, and based on the Hydro-DFN used in SDM-Site Forsmark (Follin et al. 2007a). Fracture intersection zones could be simulated by modifying hydraulic aperture at nodes corresponding to fracture intersections. In all cases, the geometric parameters for the Hydro-DFN would be taken from Follin et al. (2007a), but the transmissivity distributions re-calibrated for each model variant to ensure that the PFL-f inflow statistics are reproduced accurately. The differences between model variants could be compared in terms of their effects on repository performance statistics.

8.3.3 Models of fracture transport aperture

Advective travel time depends on the transport apertures of the fractures. Empirical relationships between fracture transport aperture and transmissivity were used in SDM-Site and SR-Site modelling (see Section 3.3.10). By compilation of tracer tests performed by SKB, Hjerne et al. (2010) derived relationships with typically an order of magnitude higher aperture. The sensitivity of travel times for the Forsmark safety assessment calculations are quantified in Section 5.3.8 of Selroos and Follin (2009) showing about an order of magnitude increase in advective travel time, but consider this to be an upper bound based on the bias in tracer tests toward more conductive open fractures and site-specific estimates of apertures based on electrical resistivity measurements. Further investigations of this issue may be appropriate.

8.3.4 Models of fracture termination behaviour

Fracture termination relationships are not represented in the hydrogeological modelling used in SR-Site Forsmark (Joyce et al. 2010a). The influence on connectivity characteristics or anisotropic flow properties due to termination behaviour therefore has not been quantified. It is suggested that models might be developed which simulate fracture termination relationships as defined in Fox et al. (2007), for example. The implications for termination on fracture size distribution are wider issues that require an approach to DFN modelling integrated with geology. From a hydrogeological perspective, these models would need to be calibrated to the PFL-f data, and the differences between the resulting models examined in terms of their network connectivity characteristics, repository performance statistics and equivalent continuous porous medium permeability distributions. Fracture termination behaviour could be simulated in a variety of different ways, with details of how the centres of fractures are distributed and how the specified intensity-size distribution is reproduced varying.

8.3.5 Fractal clustering of open fractures

The SDM-Site Forsmark DFN assumes that the spatial distribution of open fracture centres is Poissonian (see Section 3.3.6). A dimensional analysis of open fractures in addition to the group of all fracture considered by Fox et al. (2007) could be undertaken to determine if there is evidence for fractal clustering using the boremap data at Forsmark. Alternative spatial models of open fractures could be developed depending on the results of the above analysis. Introducing fractal clustering of fracture centres could potentially change the connectivity and percolation characteristics of the Hydro-DFN models. Dershowitz et al. (1992) simulated synthetic fracture networks with a specified log-normal fracture size intensity distribution for various fracture intensities and fractal dimensions using a Levy-Lee spatial model of fracture centres. They found that various connectivity measures, such as the number of fracture intersections in a unit volume and the total length of fracture intersections per unit volume, increase with fractal dimension.

8.3.6 Consideration of alternative fracture shapes

There influence of fracture shape on the connection characteristics of fracture networks has not been studied as part of the site modelling. Some results for elliptical fractures are presented in Black et al. (2007) for uniform fracture size distributions and in de Dreuzy et al. (2000) for power-law fracture size distributions. Black et al. (2007) were motivated by the hypothesis that a network based on ellipses with high aspect ratios, of around 5:1 to 10:1, might provide a better approximation of sparse flow channels than networks of omni-dimensional fractures. The work by de Dreuzy et al. (2000) studied the percolation threshold for the fracture surface area per unit volume required for a network to become connected for a wide variety of power-law shape parameters and eccentricities. It was found that the percolation threshold was relatively insensitive to the eccentricity of fracture ellipses, varying by around a factor 2-3 for fixed shape parameter. The percolation threshold was highest when the eccentricity was between 0.1-0.2. Similar conclusions were also made by Mourzenko et al. (2004, 2005).

Modelling fractures with length:width ratios greater than one might change the percolation and connectivity characteristics of fracture networks. This uncertainty could be bounded by assuming a range of different length:width ratios and comparing the consequences on percolation thresholds and the number of fracture intersections in a unit volume. However, of more relevance is to illustrate the constraint implied by matching the observed intensity of PFL-f fractures and distributions of specific discharge measured on models with non-unity aspect ratio using the described in Sections 4.5 and 4.6. This might work by assuming length:width ratios of say 0.1 and 0.3 and calibrating the shape parameter required to reproduce the observed intensity of connected open fractures. The resulting models could then be further calibrated for distribution of specific discharge and then used to simulate distributions of performance measures.

8.3.7 Elaborated model of the HCD

Deformation zones comprising the HCD have been modelled as tessellated planar structures featuring a decreasing average transmissivity with increasing depth. In reality there is likely to be a complex system of preferential flow-paths that follow a convoluted path in three-dimensional space. For example, the groundwater flow could be through a swarm of fractures within a zone of finite thickness. Although the models assume a simplified geometrical description, it is conservative in the sense that it will tend to overestimate flow-path connectivity and possibly underestimate the available flow wetted surface for a given flow-rate through the zone. This could result in lower flow-related transport resistance estimates than what would be obtained with a more detailed three-dimensional model of a deformation zone where the same flow is distributed over a larger flow wetted surface area. However, the accuracy of this argument depends upon whether the transmissivities of individual flow channels within a deformation zone are properly assessed from borehole data.

Since the HCD play a very important role in both recharge and discharge to depth at Forsmark it is proposed that models of the HCD could be developed which incorporate a degree of internal structure to quantify whether some aspects of safety assessment are sensitive to details of transport characteristics with a deformation zone. This should take the form of clusters of smaller fractures gathered around the central plane of the HCD. The properties of the clustered fractures should be justified from borehole data that have been gathered from the HCDs. For example, the orientation and intensity of PFL-f fractures could be used. At the very least the calculation of flow-related transport resistance as calculated along sections of pathways within HCD using DFN models should be more carefully considered.

8.4 Confirmatory tests using data from underground investigations

Each of the variant Hydro-DFN models could be used to make predictions which can subsequently be assessed against observations of new data acquired during underground investigations. The methodology should be standardised to allow comparisons between the different variants to assess which of the models best simulate new data as it becomes available. Criteria for a ‘good fit’ should be quantified before new data is analysed, possibly motivated by potential consequences for repository

performance statistics. This process of comparing the models with data which has not been used in the calibration process is particularly important for the Hydro-DFN model used in SR-Site, as it influences the confidence which might be associated with the transport models used in the safety assessment calculations.

Possible statistics for comparison include:

- Distributions of counts of PFL-f fractures with specific capacity in various bins per length of pilot hole. This should be interpreted in part as an indication of the clustering behaviour of PFL-f fractures.
- Distributions of total Inflows to lengths of tunnel (The details depend on the strategy adopted for the construction of the repository).
- Distribution of trace lengths on tunnel walls taking account of the censoring effect due to the dimensions of the tunnel.
- Predictions of inflow distributions and salinity of inflowing water during tunnel construction, and predictions of drawdown and changes in groundwater chemistry in monitoring boreholes.

The methodology for the model comparison and confidence assessment could be developed in part using data from investigations at Äspö HRL (accepting the different geological and hydrogeological environment though), in lieu of data becoming available from Forsmark.

8.5 Model development using data from underground investigations

Underground investigations at Forsmark will lead to more geological and hydraulic data and potentially more types of data. In this section, the issue of how different types of data might influence development of the Hydro-DFN models is considered.

Tunnel wall mapping potentially allows the fracture intensity-size distribution to be assessed at the depths of interest and on a important scale between those available from boreholes (decimetres) and from deformation zone modelling (kilometres). Interpreting trace lengths on tunnel walls is subject to considerable uncertainty relating to the size of the sample area relative to the size distribution, surface roughness and fracture segmentation. It is not clear at the time of writing what type of information relating to fracture aperture might be available; such information could allow some equivalent concept to that of the open fracture, as used in the boremap classifications, to be developed. The intensity-size distribution of the open fractures is probably the most significant source of uncertainty in the Hydro-DFN models in terms of consequence for safety assessment.

Tunnel wall mapping of fracture traces potentially also allows fracture termination behaviour at depth to be quantified. Furthermore, evidence of flow channelling could become apparent during tunnel construction, although quantifying this behaviour systematically might be practically difficult due to the disturbed flow condition around the tunnel. Measurements of fracture aperture made through recently developed techniques using electrical resistance logging could be used to motivate Hydro-DFN models which incorporate in-plane fracture heterogeneity, although it is noted that the apertures measured using this method are not directly linked to transport aperture or hydraulic aperture.

Using the PFL-f tool in pilot holes extending from tunnels at atmospheric pressure effectively increases the sensitivity of the device, and potentially allows more flow-conducting fractures to be detected. In order to simulate the smallest inflows measured under these circumstances it might be necessary to re-calibrate the Hydro-DFN models. De-watering caused by construction of the tunnels might reduce the sensitivity of the PFL-f method near the tunnel face, and potentially perturbations to the groundwater chemistry nearby. Both drawdowns caused by construction of tunnels and changes to salinity in fracture water in a long-term monitoring system could provide a valuable confirmatory tests of developed models.

It is thought that local-scale Hydro-DFN models will be required to predict inflows to lengths of tunnel using pilot-hole data (see Hartley et al. 2011, for example). The specification for the local scale DFN models is still to be defined precisely. For example, it remains to be determined whether it is required that fracture intersections and inflows are simulated exactly or statistically.

9 Conclusions

This report presents a summary of the development of hydrogeological DFN models used to model the Laxemar and Forsmark sites selected by SKB as potential sites for a geological repository of nuclear waste. The overall aims of the modelling were to:

- Provide inputs to safety assessment calculations relating to radionuclide transport from a repository to the accessible environment.
- Provide an understanding of the uncertainty associated with these inputs.
- Provide a method of combining the various types of geoscientific data such as borehole fracture logs, structural models interpreted from geophysical surveys, hydraulic test data and groundwater chemistry data into a self consistent "Site Descriptive Model" which describes to reasonable accuracy the present-day conditions observed at the sites. Such models build confidence that the calculated inputs to the safety assessment are justified.

The crystalline bedrock at Forsmark and Laxemar indicated that a DFN approach was more likely to accurately simulate flows on length scales comparable to those of the repository structures, compared to a CPM approach. However, there were practical constraints on the use of DFN models due to significant simulation run times and the fact that some physical processes are not implemented within the DFN framework. These issues were addressed in some circumstances by using a DFN model to derive an ECPM model through the process of upscaling.

Field observations suggest that fracture surfaces are often uneven and mineralised, with the result that groundwater flow and contaminant concentrations are distributed non-uniformly across the fracture in preferential paths, or channels. This phenomenon is commonly referred to as flow channelling. Within most of the DFN models reported here, fractures have been represented as planar structures, with constant transmissivity within a fracture. This description reasons that flow at the scales of interest can be adequately represented by the assignment of an effective transmissivity value for an entire fracture. Scoping calculations which account for some aspects of heterogeneity in transmissivity within fractures suggest that this heterogeneity does not lead to significant differences in the calculated repository performance measures compared to the case where a single effective transmissivity value is assigned to each feature (Crawford 2008, Painter 2006), as discussed in Section 3.3.8.

Considerable amounts of geoscientific data have been collected in order to characterise the Forsmark and Laxemar sites. This includes geophysical data (magnetic, reflection seismic and refraction seismic data), data from percussion and core-drilled boreholes, solute tracer tests, single-borehole hydraulic tests, multiple-borehole (interference) hydraulic tests, outcrop and lineament trace maps and chemical samples of groundwater and matrix porewater. This data has been synthesised in to a Site Descriptive Model of each site (SKB 2008, 2009). These site-specific data have been used to justify and inform the conceptual model of the geology and hydrogeology of each site and directly parameterise parts of the DFN model; the description of which starts with the identification of fracture domains that provide a large-scale conceptual framework for describing spatial heterogeneity in rock fracturing. A Geo-DFN model is then developed for each fracture domain that provides a framework on which to overlay the hydrogeological description. Site hydraulic and hydrochemical data provides both calibration for the parameterisation of Hydro-DFN models as well as a basis for confirmatory testing and confidence assessment of the Hydro-DFN models.

A key role in the development of the Hydro-DFN models is given to the so called "Posiva Flow Logging" method (PFL-f) applied to core-drilled boreholes. This technique allows inflows to a borehole from continuously flow-conducting fractures to be measured by means of difference flow logging. Flows measured by the PFL-f method have been assigned to individual fractures identified by analysis of the borehole core and the data produced by down-borehole imaging techniques. A modelling methodology has been developed which calibrates key aspects of the Hydro-DFN using statistics recorded for all fractures, flow-conducting fractures, and those fractures identified as hydraulically open in the borehole core data.

The PFL-f hydraulic tests were used to estimate the intensity of flow-conducting fractures and the distributions of inflow to boreholes from individual fractures. The quantities of interest in evaluated

long-term safety, particularly the flow-related transport resistance and the flow characteristics at deposition holes, are closely related to the inflow distributions measured by the PFL-f tests. Quantifying flow-related transport resistance as twice the flow wetted area (flow width times length) divided by flow-rate allows it be related to measurements made by the PFL-f tests, since they measure the magnitude of flow-rate (albeit under disturbed pumped conditions) and the intensity (based on Terzaghi correction) of measured flow is used to estimate the flowing fracture surface area per unit volume. Details of how the flowing fracture surface area is distributed in space and how the variation in flow-rates is distributed over this surface area as well as any correlations cannot be determined directly from the field data. In the modelling such details emerge as a function of the assumptions made about fracture spatial distribution, fracture intensity-size-transmissivity distributions. Still, any models calibrated on the PFL-f data following the process described in Section 4.1 will share common characteristics of distributions of flow-rate and surface area intensity of flowing fracture surface area per unit volume, and so might be expected to predict relatively similar distributions of flow-related transport resistance. Hence, although some conceptual and parameter uncertainties in the Hydro-DFN models remain, the predictions of the Hydro-DFN model variants, in terms of quantities of significance to long-term safety, are thought to be well constrained by the requirement that the Hydro-DFN models simulate the PFL-f tests accurately (as measured by the calibration targets defined in.

A stochastic DFN representation of the rock mass between mapped deformation zones was calibrated using fracture intensity data, and inflow data from the single-hole hydraulic tests. The resulting models were refined in a series of confirmatory tests where the prediction by regional-scale models were compared with data from multiple borehole hydraulic interference tests, groundwater heads in boreholes, and drawdowns caused by the Äspö HRL at Laxemar. In addition, the palaeo-climatic evolution of the groundwater since the Weichselian de-glaciation was simulated and the predictions of groundwater chemistry compared to measurements of present-day groundwater chemical composition. It was found that the regional-scale simulations were also sensitive to boundary conditions, the properties of local deformation zones and, for the palaeo-climatic modelling, parameters relating to rock matrix diffusion.

Uncertainties associated with the groundwater flow and transport modelling in the HRD can be considered in three categories; conceptual uncertainty; parameter and distribution uncertainty; and stochastic uncertainty. Conceptual uncertainty is understood to concern issues such as the validity of the DFN concept to the bedrock of interest, the influence of flow channelling phenomena, and decisions in the DFN modelling methodology such as the assumption that inflows measured by the PFL-f tests are primarily limited by network connectivity. Stochastic uncertainty might correspond to a lack of knowledge of the real fracture geometry at scales smaller than that of the mapped deformation zones, and therefore represents some aspects of spatial variability. It has been considered by presenting results for multiply realisations of the Hydro-DFN models. It is thought that the more significant uncertainties which might be categorised as parameter and distribution uncertainties are in the intensity of open fractures, the fracture intensity-size distribution and the fracture size-transmissivity distribution. The approach to these uncertainties has been to develop model variants which each use different assumptions.

Each of the model variants considered during the Hydro-DFN calibration process was able to simulate the PFL-f tests to a similar degree of accuracy. Furthermore, calculations of effective (upscaled) hydraulic properties on 100 m scales suggest limited differences between the model variants. It is therefore unlikely that the regional-scale confirmatory testing would be capable of conclusively categorising any model variant as implausible in light of other uncertainties. The differences between the predicted distributions of repository performance measures between model variants were used to give an indication of the uncertainties in these distributions.

The programme of work which resulted in the development of Hydro-DFN models of the crystalline bedrock at Laxemar and Forsmark reached a milestone in 2009 with the selection of Forsmark as the proposed location of the final repository for spent nuclear fuel. As part of this report (Section 8) a review the Hydro-DFN methodology, and its application at the Forsmark and Laxemar sites, has been undertaken in order to suggest future developments. These developments relate to: reviewing the Hydro-DFN models of Forsmark in light of any new data or methodological improvements developed during other modelling work; consideration of a wider range of alternative models in order to better understand conceptual and other uncertainties; consideration of how new types of data obtained during underground investigations might be used to validate the existing Hydro-DFN models, reduce uncertainty, or develop new Hydro-DFN models; and development of methods to apply local conditioning for use during repository construction.

References

SKB's (Svensk Kärnbränslehantering AB) publications can be found at www.skb.se/publications.

Abelin H, Birgersson L, Widén H, Ågren T, Moreno L, Neretnieks I, 1990. Channeling experiment. SKB Stripa Project Technical Report 90-13, Svensk Kärnbränslehantering AB.

Abelin H, Birgersson L, Moreno L, Widén H, Ågren T, Neretnieks I, 1991. A large scale flow and tracer experiment in granite: 2. Results and interpretation. Water Resourses Research 27, 3119–3135.

Abelin H, Birgersson L, Widén H, Ågren T, Moreno L, Neretnieks I, 1994. Channeling experiments in crystalline fractured rocks. Journal of Contaminant Hydrology 15, 129–158.

AMEC, 2012a. ConnectFlow technical summary. Release 10.4 AMEC/ENV/CONNECTFLOW/15, AMEC, UK.

AMEC, 2012b. NAMMU technical summary. Release 10.4. AMEC/ENV/CONNECTFLOW/8, AMEC, UK.

AMEC, 2012c. NAPSAC technical summary. Release 10.4. AMEC/ENV/CONNECTFLOW/12, AMEC, UK.

AMEC, 2012d. ConnectFlow verification. Release 10.4. AMEC/ENV/CONNECTFLOW/16, AMEC, UK.

Andersson J, 2003. Site descriptive modelling – strategy for integrated evaluation. SKB R-03-05, Svensk Kärnbränslehantering AB.

Andersson J, Almén K-E, Ericsson L O, Fredriksson A, Karlsson F, Stanfors R, Ström A, 1998. Parameters of importance to determine during geoscientific site investigation. SKB TR 98-02, Svensk Kärnbränslehantering AB.

Bath A, Lalieux P, 1999. Technical summary of the SEDE Workshop on the use of hydrochemical information in testing groundwater flow models. In Use of hydrochemical information in testing groundwater flow models: technical summary and proceedings of a workshop organised by the NEA Co-ordinating Group on Site Evaluation and Design of Experiments for Radioactive Waste Disposal (SEDE) and hosted by the Swedish Nuclear Fuel and Waste Management Company (SKB), Borgholm, Sweden, 1-3 September 1997. Paris: OECD/NEA, 13–30. (Radioactive Waste Management 8)

Berglund S, Selroos J-O, 2004. Transport properties site descriptive model. Guidelines for evaluation and modelling. SKB R-03-09, Svensk Kärnbränslehantering AB.

Bergman B, Juhlin C, Palm H, 2001. Reflektionsseismiska studier inom Laxemarområdet. SKB R-01-07, Svensk Kärnbränslehantering AB. (In Swedish.)

Berkowitz B, Naumann C, Smith L, 1994. Mass transfer at fracture intersections: an evaluation of mixing models. Water Resources Research 30, 1765–1773.

Bingham C, 1974. An antipodally symmetric distribution on the sphere. Annals of Statistics 2, 1201–1225.

Black J H, Barker J A, Woodman N D, 2007. An investigation of 'sparse channel networks'. Characteristic behaviours and their causes. SKB R-07-35, Svensk Kärnbränslehantering AB.

Bosson E, Gustafsson L-G, Sassner M, 2008. Numerical modelling of surface hydrology and near-surface hydrogeology at Forsmark. Site descriptive modelling, SDM-Site Forsmark. SKB R-08-09, Svensk Kärnbränslehantering AB.

Bosson E, Sassner M, Gustafsson L-G, 2009. Numerical modelling of hydrology and near-surface hydrogeology at Laxemar-Simpevarp. Site descriptive modelling, SDM-Site Laxemar. SKB R-08-72, Svensk Kärnbränslehantering AB.

Bour O, Davy P, 1998. On the connectivity of three-dimensional fault networks. Water Resources Research 34, 2611–2622.

Cacas M-C, 1989. Développement d'un modèle tridimensionnel stochastique discret pour la simulation de l'écoulement et des transferts de masse et de chaleur en milieu fracturé. PhD thesis. ENMP, Paris.

Carlsson A, Ohsson T, 1977. Water leakage in the Forsmark tunnel, Uppland, Sweden. Uppsala: SGU. (Serie C 734)

Crawford J, 2008. Bedrock transport properties Forsmark. Site descriptive modelling, SDM-Site Forsmark. SKB R-08-48, Svensk Kärnbränslehantering AB.

Crawford J, Sidborn M, 2009. Bedrock transport properties Laxemar. Site descriptive modelling, SDM-Site Laxemar. SKB R-08-94, Svensk Kärnbränslehantering AB.

Chapman N, Bath A, Geier J, Stephansson O, Tirén S, Tsang C-F, 2010. INSITE Summary Report. SSM 2010:30, Strålsäkerhetsmyndigheten (Swedish Radiation Safety Authority).

Cvetkovic V, Frampton A, 2012. Solute transport and retention in three-dimensional fracture networks. Water Resourses Research 48, W02509. doi:10.1029/2011WR011086

Cvetkovic V, Selroos J-O, Cheng H, 1999. Transport of reactive tracers in rock fractures. Journal of Fluid Mechanics 378, 335–356.

Darcel C, Davy P, Bour O, de Dreuzy J-R, 2004. Alternative DFN model based on initial site investigations at Simpevarp. SKB R-04-76, Svensk Kärnbränslehantering AB.

Darcel C, Davy P, Le Goc R, de Dreuzy J R, Bour O, 2009. Statistical methodology for discrete fracture model – including fracture size, orientation uncertainty together with intensity uncertainty and variability. SKB R-09-38, Svensk Kärnbränslehantering AB.

Davy P, Darcel C, Bour O, Munier R, de Dreuzy J-R, 2006. A note on the angular correction applied to fracture intensity profiles along drill core. Journal of Geophysical Research 111, B11408. doi:10.1029/2005JB004121

Davy P, Le Goc R, Darcel C, Bour O, de Dreuzy J R, Munier R, 2010. A likely universal model of fracture scaling and its consequence for crustal hydromechanics. Journal of Geophysical Research 115. doi:10.1029/2009JB007043

de Dreuzy J R, Davy P, Bour O, 2000. Percolation parameter and percolation-threshold estimates for three-dimensional random ellipses with widely scattered distributions of eccentricity and size. Physical Review E 62, 5948–5952.

de Marsily G, 1986. Quantitative hydrogeology: groundwater hydrology for engineers. Orlando: Academic Press.

Dershowitz W S, 1979. A probabilistic model for the deformability of jointed rock masses. M.S. thesis. MIT, Cambridge, MA.

Dershowitz W S, Herda H H, 1992. Interpretation of fracture spacing and intensity. In: Tillerson J A, Wawersik W R (eds). Proceedings of 33rd U.S. Rock Mechanics Symposium, Sante Fe, NM, 3–5 June 1992. Rotterdam: Balkema, 757–766.

Dershowitz W, Redus K, Wallmann P, La Pointe P, Axelsson C-L, 1992. The implication of fractal dimension in hydrogeology and rock mechanics. Version 1.1. SKB TR 92-17, Svensk Kärnbränslehantering AB.

Dershowitz W, La Pointe P, Cladouhos T, 1998. Derivation of fracture spatial pattern parameters from borehole data. International Journal of Rock Mechanics & Mining Sciences 35, 508.

Dershowitz W, Winberg A, Hermanson J, Byegård J, Tullborg E-L, Andersson P, Mazurek M, 2003. Äspö Hard Rock Laboratory. Äspö Task Force on modelling of groundwater flow and transport of solutes. Task 6C. A semi-synthetic model of block scale conductive structures at the Äspö HRL. SKB IPR-03-13, Svensk Kärnbränslehantering AB.

Enachescu C, Rahm N, 2007. Oskarshamn site investigation. Method evaluation of single hole hydraulic injection tests at site investigations Oskarshamn. SKB P-07-79, Svensk Kärnbränslehantering AB.

Fisher R, 1953. Dispersion on a sphere. Proceedings of the Royal Society of London. Series A, Mathematical and Physical Sciences 217, 295–305.

Follin S, 1992. Numerical calculations on heterogeneity of groundwater flow. SKB TR 92-14, Svensk Kärnbränslehantering AB.

Follin S, 2008. Bedrock hydrogeology Forsmark. Site descriptive modelling, SDM-Site Forsmark. SKB R-08-95, Svensk Kärnbränslehantering AB.

Follin S, Stigsson M, Svensson U, 2005. Regional hydrogeological simulations for Forsmark – numerical modelling using DarcyTools. Preliminary site description Forsmark area – version 1.2. SKB R-05-60, Svensk Kärnbränslehantering AB.

Follin S, Stigsson M, Svensson U, 2006. Hydrogeological DFN modelling using structural and hydraulic data from KLX04. Preliminary site description Laxemar subarea – version 1.2. SKB R-06-24, Svensk Kärnbränslehantering AB.

Follin S, Levén J, Hartley L, Jackson P, Joyce S, Roberts D, Swift B, 2007a. Hydrogeological characterisation and modelling of deformation zones and fracture domains, Forsmark modelling stage 2.2. SKB R-07-48, Svensk Kärnbränslehantering AB.

Follin S, Johansson P-O, Hartley L, Jackson P, Roberts D, Marsic N, 2007b. Hydrogeological conceptual model development and numerical modelling using CONNECTFLOW, Forsmark modelling stage 2.2. SKB R-07-49, Svensk Kärnbränslehantering AB.

Follin S, Hartley L, Jackson P, Roberts D, Marsic N, 2008a. Hydrogeological conceptual model development and numerical modelling using CONNECTFLOW, Forsmark modelling stage 2.3. SKB R-08-23, Svensk Kärnbränslehantering AB.

Follin S, Stephens M B, Laaksoharju M, Nilsson A-C, Smellie J, Tullborg E-L, 2008b. Modelling the evolution of hydrochemical conditions in the Fennoscandian Shield during Holocene time using multidisciplinary information. Applied Geochemistry 23, 2004–2020.

Follin S, Ludvigson J-E, Levén J, 2011. A comparison between standard well test evaluationmethods used in SKB's site investigations and the generalised radial flow concept. SKB P-06-54, Svensk Kärnbränslehantering AB.

Forsmark T, Wikström M, Forssman I, Rhén I, 2008. Oskarshamn site investigation. Correlation of Posiva Flow Log anomalies to core mapped features in KLX17A, KLX18A, KLX19A, KLX20A and KLX21B. SKB P-07-215, Svensk Kärnbränslehantering AB.

Fox A, La Pointe P, Hermanson J, Öhman J, 2007. Statistical geological discrete fracture network model Forsmark modelling stage 2.2. SKB R-07-46, Svensk Kärnbränslehantering AB.

Fox A, Forchhammer K, Pettersson A, La Pointe P, Lim D-H, 2012. Geological discrete fracture network model for the Olkiluoto Site, Eurajoki, Finland, Version 2.0. Posiva 2012-27, Posiva Oy, Finland.

Frampton A, Cvetkovic V, 2010. Inference of field-scale fracture transmissivities in crystalline rock using flow log measurements. Water Resources Research 46, W11502. doi: 10.1029/2009WR008367.

Frampton A, Cvetkovic V, 2011. Numerical and analytical modeling of advective travel times in realistic three-dimensional fracture networks. Water Resourses Research 47, W02506. doi:10.1029/2010WR009290

Glamheden R, Fredriksson A, Röshoff K, Karlsson J, Hakami H, Christiansson R, 2007. Rock mechanics Forsmark. Site descriptive modelling Forsmark stage 2.2. SKB R-07-31, Svensk Kärnbränslehantering AB.

Goblet P, de Lope L F, Gomit J M, 1994. Study of coupling between 'fractured medium' and 'porous medium' flow models. Report EUR 15033 EN, European Commission.

Gustafson G, Franson Å, 2006. The use of the Pareto distribution for fracture transmissivity assessment. Hydrogeology Journal 14, 15–20.

Gustafsson E, Ludvigson J-E, 2005. Oskarshamn site investigation. Combined interference test and tracer test between KLX02 and HLX10. SKB P-05-20, Svensk Kärnbränslehantering AB.

Gylling B, Marsic N, Hartley L, Holton D, 2004. Applications of hydrogeological modelling methodology using NAMMU and CONNECTFLOW. Task 1, 2, 3 and 4. SKB R-04-45, Svensk Kärnbränslehantering AB.

Harrström J, Walger E, Ludvigson J-E, Morosini M, 2007. Oskarshamn site investigation. Hydraulic interference tests of HLX27, HLX28, HLX32 and single hole pumping test of KLX27A. Subarea Laxemar. SKB P-07-186, Svensk Kärnbränslehantering AB.

Hartley L, Cox I, Hunter F, Jackson P, Joyce S, Swift B, Gylling B, Marsic N, 2005. Regional hydrogeological simulations for Forsmark – numerical modelling using CONNECTFLOW. Preliminary site description Forsmark area – version 1.2. SKB R-05-32, Svensk Kärnbränslehantering AB.

Hartley L, Hunter F, Jackson P, McCarthy R, Gylling B, Marsic N, 2006a. Regional hydrogeological simulations using CONNECTFLOW. Preliminary site description Laxemar subarea – version 1.2. SKB R-06-23, Svensk Kärnbränslehantering AB.

Hartley L, Hoch A, Jackson P, Joyce S, McCarthy R, Rodwell W, Swift B, Marsic N, 2006b. Groundwater flow and transport modelling during the temperate period for the SR-Can assessment. Forsmark area – version 1.2. SKB R-06-98, Svensk Kärnbränslehantering AB.

Hartley L, Jackson P, Joyce S, Roberts D, Shevelan J, Swift B, Gylling B, Marsic N, Hermanson J, Öhman J. 2007. Hydrogeological pre-modelling exercises. Assessment of impact of the Äspö Hard Rock Laboratory. Sensitivities of palaeo-hydrogeology. Development of a local near-surface Hydro-DFN for KLX09B–F. Site descriptive modelling, SDM-Site Laxemar. SKB R-07-57, Svensk Kärnbränslehantering AB.

Hartley L, Appleyard P, Baxter S, Hoek J, Roberts D, Swan S, 2011. Development of a hydrogeological discrete fracture network model for the Olkiluoto site descriptive model 2011. Posiva Working Report 2012-32, Posiva Oy, Finland.

Hermanson J, Forssberg O, Fox A, La Pointe P, 2005. Statistical model of fractures and deformation zones. Preliminary site description, Laxemar subarea, version 1.2. SKB R-05-45, Svensk Kärnbränslehantering AB.

Hjerne C, Nordqvist R, Harrström J, 2010. Compilation and analyses of results from cross-hole tracer tests with conservative tracers. SKB R-09-28, Svensk Kärnbränslehantering AB.

Hoch A R, Jackson C P, 2004. Rock-matrix diffusion in transport of salinity. Implementation in CONNECTFLOW. SKB R-04-78, Svensk Kärnbränslehantering AB.

Hunter F M I, Hartley L J, Hoch A, Jackson C P, McCarthy R, Marsic N, Gylling B, 2008. Calibration of regional palaeohydrogeology and sensitivity analysis using hydrochemistry data in site investigations. Applied Geochemistry 23, 1982–2003.

Jackson C P, Hoch A R, Todman S, 2000. Self-consistency of a heterogeneous continuum porous medium representation of a fractured medium. Water Resources Research 36, 189– 202.

Johansson P-O, 2008. Description of surface hydrology and near-surface hydrogeology at Forsmark. Site descriptive modelling, SDM-Site Forsmark. SKB R-08-08, Svensk Kärnbränslehantering AB.

Joyce S, Simpson T, Hartley L, Applegate D, Hoek J, Jackson P, Swan D, Marsic N, Follin S, 2010a. Groundwater flow modelling of periods with temperate climate conditions – Forsmark. SKB R-09-20, Svensk Kärnbränslehantering AB.

Joyce S, Simpson T, Hartley L, Applegate D, Hoek J, Jackson P, Roberts D, Swan D, Gylling B, Marsic N, Rhén I, 2010b. Groundwater flow modelling of periods with temperate climate conditions – Laxemar. SKB R-09-24, Svensk Kärnbränslehantering AB.

Juhlin C, Bergman B, Palm H, Tryggvason A, 2004. Oskarshamn site investigation. Reflection seismic studies on Ävrö and Simpevarpshalvön, 2003. SKB P-04-52, Svensk Kärnbränslehantering AB.

Kesten H, 1980. The critical probability of bond percolation on the square lattice equals ½. Communications in Mathematical Physics 74, 41–59.

Laaksoharju M, Smellie J, Tullborg E-L, Gimeno M, Hallbeck L, Molinero J, Waber N, 2008. Bedrock hydrogeochemistry Forsmark. Site descriptive modelling, SDM-Site Forsmark. SKB R-08-47, Svensk Kärnbränslehantering AB.

Laaksoharju M, Smellie J, Tullborg E-L, Wallin B, Drake H, Gascoyne M, Gimeno M, Gurban I, Hallbeck L, Molinero J, Nilsson A-C, Waber N, 2009. Bedrock hydrochemistry Laxemar. Site descriptive modelling, SDM-Site Laxemar. SKB R-08-93, Svensk Kärnbränslehantering AB.

La Pointe P R, 2002. Derivation of parent fracture population statistics from trace length measurements for fractal fracture populations. International Journal of Rock Mechanics & Mining Sciences 39, 381–388.

La Pointe P R, Wallmann P, Follin S, 1995. Estimation of effective block conductivities based on discrete network analyses using data from the Äspö Site. SKB TR 95-15, Svensk Kärnbränslehantering AB.

La Pointe P R, Olofsson I, Hermanson J, 2005. Statistical model of fractures and deformation zones for Forsmark. Preliminary site description Forsmark area – version 1.2. SKB R-05-26, Svensk Kärnbränslehantering AB.

La Pointe P, Fox A, Hermanson J, Öhman J, 2008. Geological discrete fracture network model for the Laxemar site. Site descriptive modelling, SDM-Site Laxemar. SKB R-08-55, Svensk Kärnbränslehantering AB.

Lindquist A, Hjerne C, Nordqvist R, Wass E, 2008. Forsmark site investigation. Large-scale confirmatory multiple-hole tracer test. SKB P-08-59, Svensk Kärnbränslehantering AB.

Long J C S, Remer J S, Wilson C R, Witherspoon P A, 1982. Porous media equivalents for networks of discontinuous fractures. Water Resourses Research 18, 645–658.

Ludvigson J-E, Hansson K, Hjerne C, 2007. Forsmark site investigation. Method evaluation of single-hole hydraulic injection tests at site investigations in Forsmark. SKB P-07-80, Svensk Kärnbränslehantering AB.

Lund B, Näslund J-O, 2009. Glacial isostatic adjustment: implications for glacially induced faulting and nuclear waste repositories. In Connor C B, Chapman N A, Connor L J (eds). Volcanic and tectonic hazard assessment for nuclear facilities. Cambridge: Cambridge University Press, 142–155.

Löfgren M, Crawford J, Elert M, 2007. Tracer tests – possibilities and limitations. Experience from SKB fieldwork: 1977–2007. SKB R-07-39, Svensk Kärnbränslehantering AB.

Marsic N, Hartley L, Jacskon P, Poole M, Morvik A, 2001. Development of hydrogeological modelling tools based on NAMMU. SKB R-01-49, Svensk Kärnbränslehantering AB.

Martin D, 2007. Quantifying in situ stress magnitudes and orientations for Forsmark. Forsmark stage 2.2. SKB R-07-26, Svensk Kärnbränslehantering AB.

Mattila J, Tammisto E, 2012. Stress-controlled fluid flow in fractures at the site of a potential nuclear waste repository, Finland. Geology. doi:10.1130/G32832.1

Molinero J, Salas J, Arcos D, Duro L, 2009. Integrated hydrogeological and hydrochemical modelling of the Laxemar-Simpevarp area during the recent Holocene (last 8000 years). In Kalinowski B (ed). Background complementary hydrochemical studies. Site descriptive modelling, SDM-Site Laxemar. SKB R-08-111, Svensk Kärnbränslehantering AB, 47–78.

Moreno L, Neretnieks I, 1991. Fluid and solute transport in a network of channels. SKB TR 91-44, Svensk Kärnbränslehantering AB.

Moreno L, Neretnieks I, 1993. Flow and nuclide transport in fractured media: the importance of the flow-wetted surface for radionuclide migration. Journal of Contaminant Hydrology13, 49–71.

Morosini M, Ludvigson J-E, Walger E, 2009. Oskarshamn site investigation. Hydraulic characterisation of deformation zone EW007. Subarea Laxemar. SKB P-05-193, Svensk Kärnbränslehantering AB.

Mourzenko V V, Thovert J-F, Adler P M, 2004. Macroscopic permeability of three-dimensional fracture networks with a power-law size distribution. Physical Review E 69. doi:10.1103/PhysRevE.69.066307.

Mourzenko V V, Thovert J-F, Adler P M, 2005. Percolation of three-dimensional fracture networks with power-law size distribution. Physical Review E 72. doi:10.1103/PhysRevE.72.036103.

Moye D G, 1967. Diamond drilling for foundation exploration. Civil Engineering Transactions, Institute of Engineers (Australia), 95–100.

Munier R, 2004. Statistical analysis of fracture data, adapted for modelling discrete fracture networks – Version 2. SKB R-04-66, Svensk Kärnbränslehantering AB.

Munier R, 2010. Full perimeter intersection criteria. Definitions and implementations in SR-Site. SKB TR-10-21, Svensk Kärnbränslehantering AB.

Munier R, Hökmark H, 2004. Respect distances: rationale and means of computation. SKB R-04-17, Svensk Kärnbränslehantering AB.

Munier R, Stenberg L, Stanfors R, Milnes A G, Hermanson J, Triumf C-A, 2003. Geological Site Descriptive Model. A strategy for the model development during site investigations. SKB R-03-07, Svensk Kärnbränslehantering AB.

Neretnieks I, 1994. Nuclear waste repositories in crystalline rock – an overview of flow and nuclide transport mechanisms. In Murakami T, Ewing R C (eds). Scientific basis for nuclear waste management XVIII: symposium held in Kyoto, Japan, 23–27 October 1994. Pittsburgh, PA: Materials Research Society. (Materials Research Society Symposium Proceedings 353), 7–20.

NRC, 1996. Rock fractures and fluid flow: contemporary understanding and applications. Washington, DC: National Academy Press.

OECD/NEA, 1993. Proceedings of a SEDE workshop on palaeohydrogeological methods and their applications for radioactive waste disposal, Paris, 9–10 November 1992. Paris: OECD/NEA.

Olofsson I, Simeonov A, Stephens M, Follin S, Nilsson A-C, Röshoff K, Lindberg U, Lanaro F, Fredriksson A, Persson L, 2007. Site descriptive modelling Forsmark, stage 2.2. A fracture domain concept as a basis for the statistical modelling of fractures and minor deformation zones, and interdisciplinary coordination. SKB R-07-15, Svensk Kärnbränslehantering AB.

Painter S, 2006. Effect of single-fracture aperture variability on field-scale transport. SKB R-06-25, Svensk Kärnbränslehantering AB.

Puigdomenech I (ed), 2001. Hydrochemical stability of groundwaters surrounding a spent nuclear fuel repository in a 100,000 year perspective. SKB TR-01-28, Svensk Kärnbränslehantering AB.

Pöllänen J, Sokolnicki M, Väisäsvaara J, 2007. Oskarshamn site investigation. Difference flow logging in borehole KLX15A. Subarea Laxemar. SKB P-07-176, Svensk Kärnbränslehantering AB.

Renard P, de Marsily G, 1997. Calculating equivalent permeability: a review. Advances in Water Resources 20, 253–278.

Rhén I, Hartley L, 2009. Bedrock hydrogeology Laxemar. Site descriptive modelling, SDM-Site Laxemar. SKB R-08-92, Svensk Kärnbränslehantering AB.

Rhén I (ed), Gustafson G, Stanfors R, Wikberg P, 1997. Äspö HRL – Geoscientific evaluation 1997/5. Models based on site characterization 1986–1995. SKB TR 97-06, Svensk Kärnbränslehantering AB.

Rhén I, Follin S, Hermanson J, 2003. Hydrological Site Descriptive Model – a strategy for its development during Site Investigations. SKB R-03-08, Svensk Kärnbränslehantering AB.

Rhén I, Thunehed H, Triumf C-A, Follin S, Hartley L, Hermansson J, Wahlgren C-H, 2006. Development of a hydrogeological model description of intrusive rock at different investigation scales: an example from south-eastern Sweden. Hydrogeology Journal 15, 47–69.

Rhén I, Forsmark T, Hartley L, Jackson P, Roberts D, Swan D, Gylling B, 2008. Hydrogeological conceptualisation and parameterisation. Site descriptive modelling, SDM-Site Laxemar. SKB R-08-78, Svensk Kärnbränslehantering AB.

Rhén I, Forsmark T, Hartley L, Joyce S, Roberts D, Gylling B, Marsic N, 2009. Bedrock hydrogeolology. Model testing and synthesis. Site descriptive modelling, SDM-Site Laxemar. SKB R-08-91, Svensk Kärnbränslehantering AB.

Robinson P C, 1984. Connectivity, flow and transport in network of fractured media. PhD thesis. Oxford University.

Selroos J-O, Follin S, 2010. SR-Site groundwater flow modelling methodology, setup and results. SKB R-09-22, Svensk Kärnbränslehantering AB.

Selroos J-O, Walker D, Ström A, Gylling B, Follin S, 2002. Comparison of alternative modeling approaches for groundwater flow in fractured rock. Journal of Hydrology 257, 174–188.

Sidborn M, Neretnieks I, 2008. Long-term oxygen depletion from infiltrating groundwaters: model development and application to intra-glaciation and glaciation conditions. Journal of Contaminant Hydrology 100, 72–89.

Sidborn M, Sandström B, Tullborg E-L, Salas J, Maia F, Delos A, Molinero J, Hallbeck L, Pedersen K, 2010. SR-Site: Oxygen ingress in the rock at Forsmark during a glacial cycle. SKB TR-10-57, Svensk Kärnbränslehantering AB.

SKB, 2005a. Preliminary site description. Forsmark area – version 1.2. SKB R-05-18, Svensk Kärnbränslehantering AB.

SKB, 2005b. Preliminary safety evaluation for the Forsmark area. Based on data and site descriptions after the initial site investigation stage. SKB TR-05-16, Svensk Kärnbränslehantering AB.

SKB, 2006a. Site descriptive modelling Forsmark stage 2.1. Feedback for completion of the site investigation including input from safety assessment and repository engineering. SKB R-06-38, Svensk Kärnbränslehantering AB.

SKB, 2006b. Data report for the safety assessment SR-Can. SKB TR-06-25, Svensk Kärnbränslehantering AB.

SKB, 2007. Hydrochemical evaluation of the Forsmark site, modelling stage 2.1 – issue report. SKB R-06-69, Svensk Kärnbränslehantering AB.

SKB, 2008. Site description of Forsmark at completion of the site investigation phase. SDM-Site Forsmark. SKB TR-08-05, Svensk Kärnbränslehantering AB.

SKB, 2009. Site description of Laxemar at completion of the site investigation phase SDM-Site Laxemar. SKB TR-09-01, Svensk Kärnbränslehantering AB.

SKB, 2010a. Data report for the safety assessment SR-Site. SKB TR-10-52, Svensk Kärnbränslehantering AB.

SKB, 2010b. Fud-program 2010. Program för forskning, utveckling och demonstration av metoder för hantering och slutförvaring av kärnavfall. Svensk Kärnbränslehantering AB.

SKB, 2010c. Radionuclide transport report for the safety assessment SR-Site. SKB TR-10-50, Svensk Kärnbränslehantering AB.

SKB, 2010d. Climate and climate-related issues for the safety assessment SR-Site. SKB TR-10-49, Svensk Kärnbränslehantering AB.

SKB, 2011. Long-term safety for the final repository for spent nuclear fuel at Forsmark. Main report of the SR-Site project. SKB TR-11-01, Svensk Kärnbränslehantering AB.

Spiessl S M, MacQuarrie K T, Mayer K U, 2008. Identification of key parameters controlling dissolved oxygen migration and attenuation in fractured crystalline rocks. Journal of Contaminant Hydrology 95, 141–153.

Stephens M B, Fox A, La Pointe P, Simeonov A, Isaksson H, Hermanson J, Öhman J, 2007. Geology Forsmark. Site descriptive modelling Forsmark stage 2.2. SKB R-07-45, Svensk Kärnbränslehantering AB.

Stephens M B, Simeonov A, Isaksson H, 2008. Bedrock geology Forsmark. Modelling stage 2.3. Implications for and verification of the deterministic geological models based on complementary data. SKB R-08-64, Svensk Kärnbränslehantering AB.

Svensson U, Ferry M, 2010. Darcy Tools version 3.4. User's guide. SKB R-10-72, Svensk Kärnbränslehantering AB.

Svensson U, Follin S, 2010. Groundwater flow modelling of the excavation and operational phases – Forsmark. SKB R-09-19, Svensk Kärnbränslehantering AB.

Svensson U, Rhén I, 2010. Groundwater flow modelling of the excavation and operational phases – Laxemar. SKB R-09-23, Svensk Kärnbränslehantering AB.

Svensson U, Ferry M, Kuylenstierna, H-O, 2010. DarcyTools version 3.4 – Concepts, Methods and Equations. SKB R-07-38, Svensk Kärnbränslehantering AB.

Söderbäck B (ed), 2008. Geological evolution, palaeoclimate and historical development of the Forsmark and Laxemar-Simpevarp areas. Site descriptive modelling, SDM-Site. SKB R-08-19, Svensk Kärnbränslehantering AB.

Terzaghi R D, 1965. Sources of error in joint surveys. Geotechnique 15, 287–304.

Thiem G, 1906. Hydrologische Methoden. Leipzig: Gebhardt.

Tröjbom M, Söderbäck B, Kalinowski B, 2008. Hydrochemistry of surface water and shallow groundwater. Site descriptive modelling, SDM-Site Laxemar. SKB R-08-46, Svensk Kärnbränslehantering AB.

Uchida M, Doe T, Dershowitz W, Andrew T, Wallmann P, Sawada A, 1994. Discrete-fracture modeling of the Äspö LPT-2, large scale pumping and tracer test. SKB ICR-94-09, Svensk Kärnbränslehantering AB.

Vidstrand P, Follin S, Zugec N, 2010a. Groundwater flow modelling of periods with periglacial and glacial climate conditions – Forsmark. SKB R-09-21, Svensk Kärnbränslehantering AB.

Vidstrand P, Rhén I, Zugec N, 2010b. Groundwater flow modelling of periods with periglacial and glacial climate conditions – Laxemar. SKB R-09-25, Svensk Kärnbränslehantering AB.

Wahlgren C-H, Curtis P, Hermanson J, Forssberg O, Öhman J, Fox A, La Pointe P, Drake H, Triumf C-A, Mattsson H, Thunehed H, Juhlin C, 2008. Geology Laxemar. Site descriptive modelling, SDM-Site Laxemar. SKB R-08-54, Svensk Kärnbränslehantering AB.

Wass E, Andersson P, 2006. Forsmark site investigation. Groundwater flow measurements and tracer tests at drill site 1. SKB P-06-125, Svensk Kärnbränslehantering AB.

Wei L, Chakrabarty C, 1996. Evaluation of a self-consistent approach to fractured crystalline rock characterization. Nuclear Science and Technology Report EUR 16926, European Commission.

Westman P, Wastegård Stefan, Schoning K, Gustafsson B, Omstedt A, 1999. Salinity change in the Baltic Sea during the last 8,500 years: evidence, causes and models. SKB TR-99-38, Svensk Kärnbränslehantering AB.

Wikström M, Forsmark T, Teurneau B, Forssman I, Rhén I, 2008. Oskarshamn site investigation. Correlation of Posiva Flow Log anomalies to core mapped features in KLX09, KLX09B–G. KLX10, KLX10B–C and KLX11A–F. SKB P-07-213, Svensk Kärnbränslehantering AB.

Yi Y B, Tawerghi E, 2009. Geometric percolation thresholds of interpenetrating plates in three-dimensional space. Physical Review E 79, 041134. doi:10.1103/PhysRevE.79.041134

Öhman J, Follin S, 2010. Site investigation SFR. Hydrogeological modelling of SFR. Model version 0.2. SKB R-10-03, Svensk Kärnbränslehantering AB.